UNIVERSITAT JAUME I

Departamento de Química Inorgánica y Orgánica

Área de Química Inorgánica

NHC-based multifunctional catalysts of Ru, Ir and Rh in C-H bond activation processes

Doctoral Thesis

Amparo Prades Ferrer

PhD. supervisors: Eduardo Peris and Macarena Poyatos

Castellón de la Plana, June 2012

Prof. Eduardo Peris Fajarnés, Catedrático del área de Química Inorgánica y Macarena Poyatos de Lorenzo, contratada Ramón y Cajal de la misma área, perteneciente al Departamento de Química Inorgánica y Orgánica de la Universitat Jaume I,

Certifican: Que la Tesis Doctoral con el título 'NHC-based multifuctional catalysts of Ru, Ir and Rh in C-H bond activation processes' ha sido desarrollada bajo su dirección, en el área de Química Inorgánica del Departamento de Química Inorgánica y Orgánica de la Universitat Jaume I, por Amparo Prades Ferrer.

Castellón de la Plana, a

Fdo. Prof. Eduardo Peris Fajarnés Fdo. Dra. Macarena Poyatos de Lorenzo

Acknowledgements/Agradecimientos

Son muchas las personas a las que tengo que agradecer esta Tesis, ¡espero no olvidarme de nadie!

En primer lugar me gustaría agradecer a mis directores de tesis, Eduardo Peris y Macarena Poyatos, la oportunidad que me han dado al permitirme formar parte de este gran grupo de investigación. Gracias Eduardo, por estar siempre pendiente, tanto en lo profesional como en lo personal, por la gran confianza que has depositado en mí, por las felicitaciones cuando las cosas salían bien y por tus consejos y ánimos cuando no salían tan bien. Maca, volviste al laboratorio después de unos años de *postdoc* con muchas ideas y muchas ganas, gracias por transmitirme ambas cosas; muchas gracias por todas tu explicaciones sobre química y lo que no es química, por todas las correcciones de abstracts, partes experimentales, capítulos interminables, etc., ¡gracias por ser como eres!

A todos mis compañeros de laboratorio, al Dr. Jose Mata, por muchas de las estructuras que se presentan en esta Tesis, por los experimentos de CV, por su ligando JM y por alguna que otra fiestecita (y resaquita). A la Dr. E+ porque gran parte de esto es por su culpa. A Cande y Sara, por las risas y confidencias compartidas, sin ellas no sé qué sería de mí! os echaré mucho de menos guapas. A Sergio porque, ya sabes, eres una más, me quito el sombrero! A mi wei (Arturo) por esos ánimos en estos últimos meses. A los que acaban de llegar, Roberto, Sara y Sheila, espero que os vaya muy bien y que hagáis grandes tesis.

A Rouse, Monix y Alex, ahora ya doctores, con los que empecé y de los que aprendí muchísimo. A los también doctores Andre, Miriam y Sergio S que pasaron por el laboratorio y de los que guardo grandes recuerdos. Al Profesor Fernando Godoy, que pasó una temporada con nosotros. Thanks Prof. Dmitri Gusev for the DFT calculations, your stay in the group was a pleasure.

I would like to thank to Prof. Martin Albrecht for giving me the opportunity to work in his group. I want to thank to his group, specially Puia, Seva and Manuel for the help offered during my stay, and to Fiona, it was nice to meet you.

I would like to thank also to Dr. Manuel Alcarazo for three amazing months, thanks for the talks about orbitals and I'm sorry if I revolutionized your wonderful group. Thanks all of them, Blanca, Javi, Agnes, Shabana, Sigrid… and, of course…gracias mi arma!

Gracias al Dr. Eduardo Sola y a todo su grupo por acogerme tan bien las tres semanas que pasé en Zaragoza, en especial a Janeth, porque no me separé de ella en un solo momento, a la Dr Marta Martín por esa estructura del dihidruro que creía imposible.

A Mercedes Sanaú por su ayuda en la resolución de algunas de las estructuras de RX.

A mis compañeros de *qio*, en especial a los de la planta 0. Gracias al grupo de Floren y Santiago por todos los reactivos que me han dejado, aunque me sigue dando miedo entrar en esa cueva. Al grupo de Juan y Bea, por las risas en las comidas de la salita. Gracias también a Mª José y a las técnicos de *qio*, Silvia, Inma y Alicia.

A Purificación Escribano porque fuiste una gran profesora. A Bea Julián porque siempre es un placer hablar contigo.

Al grupo de Rosa Llusar porque siempre están dispuestos a ayudar, especialmente a Iván y Tomás a quienes siempre acudo con millones de preguntas.

A los técnicos de Servicios Centrales, Cristian, José Miguel y Gabriel, porque, aunque quede mal decirlo, a veces, me han dado un trato especial (es decir, me han colado) y a Laura por los análisis elementales que tantas veces hemos repetido.

A Bancaixa por las becas de investigación que me han ofrecido y al Ministerio de Ciencia e Innovación por la beca FPI de la que actualmente disfruto.

A mis amigas de la infancia, que aunque aún no tiene muy claro que es esto de la investigación, siempre están ahí cuando las necesito, por todos los momentos vividos juntas ¡y los que nos quedan por vivir! A Cris porque sin ella todo sería diferente. Als meus amics, tant als de CS team com als exiliats, per les discussions que tenim per arreglar el món i les 'posades de crestes'. A mis compis de carrera, especialmente a Cris y Ramón, con los que sigo compartiendo grandes momentazos.

Y por último, siempre lo más importante, a mi familia. A mis tíos y primos y a mi abu, que me siguen preguntando cuando voy a acabar de estudiar. A Marc, por estar siempre a mi lado, por la paciencia que ha tenido conmigo durante estos últimos meses, porque junto a él es todo más fácil. A mi hermana, Mariajo, y a Fer porque siempre han estado y estarán ahí, por esas llamadas de ánimo y porque me quieren tal y como soy. A mis padres, por lo valores que me han enseñado, la educación que me han dado, por su apoyo incondicional y porque, realmente, es gracias a ellos por lo que he llegado hasta aquí.

Nomenclature

The nomenclature employed to name the compounds described in this work is:

Ligands: letters of the alphabet (**A**-**J**).

Precursor salts of the ligands: the ligand letter with the acidic protons and its counterion. For example, [**A**H]I is the precursor salt of the ligand **A** which contains a acidic proton and iodide as counterion.

Metallic complexes with NHC ligands: the number followed by the letter of the coordinated ligand. The complexes have been sorted in order to appearance.

List of abbreviations

Δ	refluxing temperature
η	ligand hapticity
μ	bridge ligand
AcO	acetate
*a*NHC	*abnormal* N-heterocyclic carbene
BIAN	bis(imino)acenaphthene
Bu	butyl
cat.	catalyst
COA	cyclooctane
COD	1,5-cyclooctadiene
COE	cyclooctene
Conv.	conversion
Cp*	1,2,3,4,5-pentamethylcyclopentadiene
Cy	Cyclohexyl
C_6Me_6	hexamethylbenzene
DFT	Density Functional Theory
dipp	diisopropylphenyl
DG	directing group
DMSO	dimethylsulfoxide
EA	elemental analysis
EtOH	ethanol
ESI-MS	Electrospray Ionization Mass Spectrometry
GC	Gas Chromatography

h	hour
HMBC	Heteronuclear Multiple Bond Correlation
HSQC	Heteronuclear Single Quantum Coherence
*i*PrOH	*Iso*-propanol
IR	infrared
KIE	kinetic isotopic effect
Me	methyl
MeOH	methanol
MIC	mesoionic carbene
NBD	2,5-norbornadiene
NBE	norbornene
NHC	N-heterocyclic carbene
NMP	N-methyl-2-pyrrolidone
NMR	nuclear magnetic resonance
	δ chemical shift
	br broad
	d doublet
	J coupling constant
	m multiplet
	ppm parts per million
	s singlet
	sp septuplet
	t triplet
Oct	octyl
OTf	triflate
Ph	phenyl
R.T.	room temperature
t	time
TBAB	*tert*butylaluminiumbromide
TBE	*tert*butylethene
*t*Bu	*tert*butyl
TEP	Tolman Electronic Parameter
TIP	tetrakis(imino)pyracene
TM	transition metal
trz	triazole

Chapter 1

General introduction and objectives

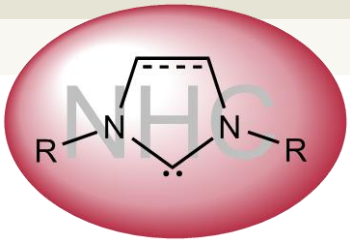

1.1 General introduction

1.1.1 Metal-carbenes

Carbenes are a family of organic molecules composed of a neutral divalent carbon atom with a sextet of electrons and two substituents ($:CR_2$). Two extreme types of coordinated carbenes can be distinguished, the Fischer and the Schrock type. Their different chemical behavior may be explained by a different bonding situation, in the singlet or triplet state.

Carbenes, L*n*M=CR_2, have Fischer character in complexes containing late transition metals with low oxidation states, having π-acceptor L ligands and π-donor R substituents (-OMe or $-NMe_2$). Such a carbene behaves as if it carries a $\partial+$ charge and is electrophilic. Schrock carbenes are bound to higher oxidation state, early transition metals, having non-π-acceptor L ligands and non-π-donor R groups. In this case, the carbene behaves as a nucleophile, having a $\partial-$ charge.

The charge on the carbon atom of the carbene is determined by the M(d_π) orbital energy. Late transition metals, more electronegative, have more stable M(d_π) orbitals than the early transition metals, which are more electropositive. In a Fischer (singlet-derived) carbene, a lone pair is donated from the singlet carbene [C(sp^2)] to an empty d_σ orbital on the metal, and a lone pair is back-donated from a filled M(d_π) to the empty C(p_z) orbital (**a**, Figure 1.1). Therefore, the CR_2 ligand in a Fisher carbene is considered to act as an L type ligand. The electrons remain on the metal because is more stable, and this leads to an electrophilic carbene carbon (direct C $\rightarrow$ M donation is only partly compensated by M $\rightarrow$ C back donation). The electron deficiency is compensated by π-donating substituents, which stabilize the carbene.

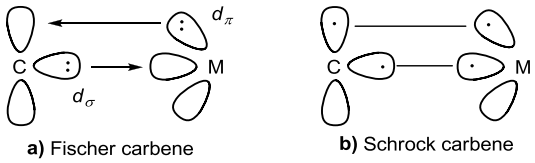

Figure 1.1 a) Fischer carbene and b) Schrock carbene

A Schrock carbene forms two covalent bonds via interaction of the triplet CR_2 fragment with a metal fragment having two unpaired electrons, thus acting as an X_2 ligand (**b**, Figure 1.1). Each M-C bond is polarized toward the carbon because, in this case, the carbon is more electronegative than the metal, leading to a nucleophilic carbene carbon.

1.1.2 N-Heterocyclic carbenes: electronic properties

N-heterocyclic carbenes (NHCs), as the imidazol-2-ylidene shown in Figure 1.2, can be considered as an extreme case of a Fischer carbene. The free NHC has a lone pair at C2 that can act as σ-donor to the metal. An empty *p* orbital at C2 acts as acceptor for the π lone pairs at N1 and N3. This π-bonding strongly disfavors the triplet carbene because the occupation of the C2 *p* orbital would interfere with the π bonding.[1]

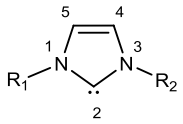

Figure 1.2 Imidazol-2-ylidene

On binding to a d^2 or higher d^n configuration metal, the d_π electron density at the metal can engage in back-bonding to the NHC. As common for most Fischer carbenes, the importance of back bonding is probably small, so the structure may be represented as **1.1** (Figure 1.3). Although **1.1** may provide a more exact representation, along this PhD. Thesis, the NHC-based complexes are represented as depicted in **1.2** (Figure 1.3), in order to avoid misunderstandings with the charge of the complex.

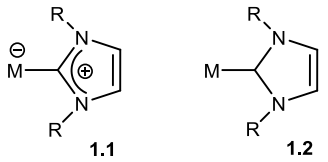

Figure 1.3 Different representations of the M-C bond in NHC-based transition metal complexes

Infrared spectroscopy proved to be a particularly useful technique for the evaluation of the ligand donor properties *via* CO stretching frequencies of metal carbonyls. Several systematic experimental and computational studies have compared the σ-donating abilities of NHCs and tertiary phosphines for a variety of transition-metal complexes.[2-3] The experimental or calculated frequencies may be scaled to represent the Tolman's electronic parameters (TEPs), which were originally developed for phosphines.[4] The ν(CO) data collected using FT-IR spectroscopy for nickel-carbonyl complexes, $Ni(CO)_3(NHC)$,[5] and iridium and rhodium-carbonyl complexes, $M(CO)_2X(NHC)$ (M = Ir or Rh; X = halide),[6] reveal that NHC ligands are more electron-donating than phosphines.

Prof. Gusev recently reported the electron-donor and steric properties of a diverse group of representative NHC ligands quantified with the help of DFT calculations.[2] This study allowed the representation of NHC ligands on the same stereoelectronic scale, in a similar way to the seminal work of Tolman.[4] The results found included also a better steric descriptor, which correlates the ease of CO loss from $Ni(CO)_3(NHC)$ complexes. The calculations provided reaction enthalpies for CO elimination from the $Ni(CO)_3(NHC)$ complexes and formation of the 16-electron $Ni(CO)_2(NHC)$ species. This reaction is largely under steric control, since the most stable tricarbonyl complexes possesses the smallest ligand. Prof. Gusev concluded that an increase of the size of the N-substituents promotes a decrease of the TEP (cm^{-1}), and an increase of the NHC ring size from 5 to 6 members makes them better σ-donor ligands. Also, substitution at C4 or C5 of the imidazole ring has a major effect on TEP (cm^{-1}); for example the donor power increases significantly in the order

NO_2 < CN < CF_3 < F ≈ Cl < CO_2Me < H OMe < Me. Figure 1.4 shows a plot of TEPs *vs* the averaged C-O bond distances in $Ni(CO)_3$(NHC) complexes, with added points for typical phosphines. The figure helps to visualize the differences observed between the different ligands. The author named the ligands using the following format: (parent heterocycle)(substituents)$_n$*N*(substituents)$_m$. For example, Im*N*Me$_2$ is an imidazole derivative and it has two methyl groups as N-substituents.

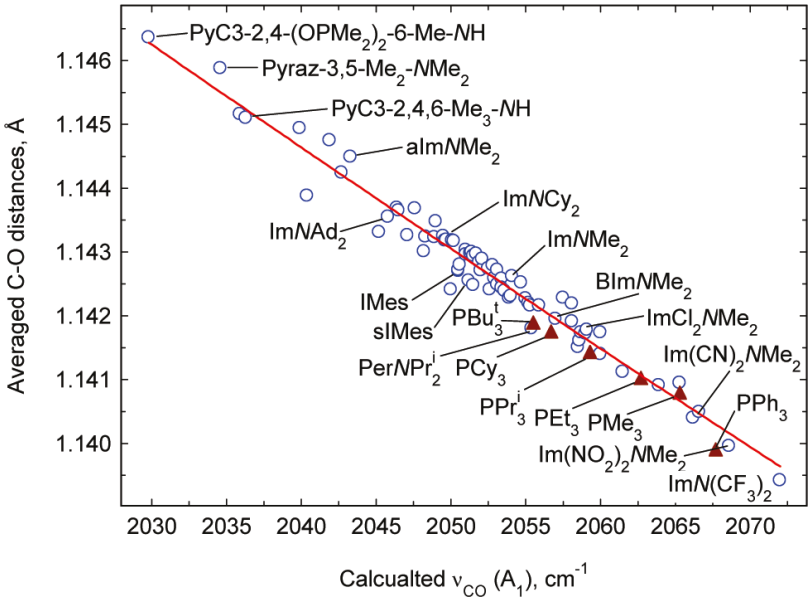

Figure 1.4 Plot of calculated TEPs *vs* averaged ν(CO) values for a series of $Ni(CO)_3L$ complexes[2]

1.1.3 N-Heterocyclic carbenes: background

In 1968, Öfele[7] and Wanzlick and Schönherr[8] independently published the first transition metal NHC complexes. Whereas Öfele reacted an imidazolium salt with a transition metal hydride, $[Cr(CO)_5H]^-$, to obtain complex **1.3** (Figure 1.5); Wanzlick and Schönherr reacted an imidazolium salt with a transition metal acetate, $Hg(OAc)_2$, obtaining complex **1.4** (Figure 1.5).

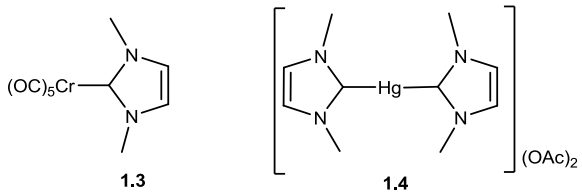

Figure 1.5 First transition metal NHC complexes described in the literature

With the exception of the studies by Lappert[9] on the coordination of NHC ligands to late transition metal complexes, the area remained dormant until 1991, when Arduengo isolated the first free carbene stable enough to be characterized by X-ray diffraction.[10] 1,3-Diadamantylimidazol-2-ylidene (**1.5**, Figure 1.6) was obtained by deprotonation of the corresponding imidazolium salt using NaH or *t*BuOK. The isolated N-heterocyclic carbene is electronically and sterically stabilized. First of all, the steric shielding of the carbene carbon by means of the sterically demanding adamantyl groups is an important factor. More generally, it can be said that the steric shielding of the carbene carbon atom increases the carbene's lifetime. Second and most importantly, the singlet carbene is stabilized by the orbital interaction of its empty *p*-orbital with the electron lone pairs of the two neighboring nitrogen atoms.

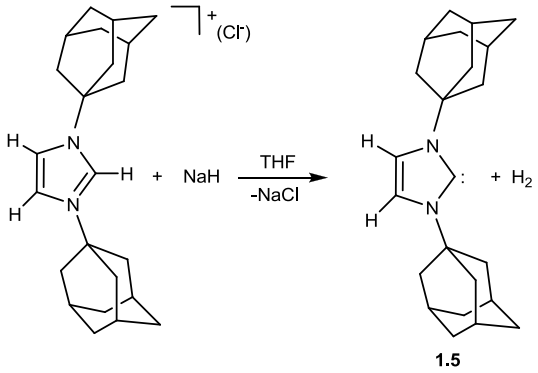

Figure 1.6 Isolation of the first free NHC ligand characterized by X-ray diffraction

Ever since, NHC ligands have attracted great interest due to their use in the design of homogeneous catalysts. In 1995, Herrmann described the first NHC-based Pd(II) complex,[11] which proved to be very effective in Heck[12] and Suzuki[13] C-C coupling

reactions. The catalyst (**1.6**, Scheme 1.1) demonstrated an activity comparable with other palladium complexes containing phosphine ligands, but possessed a greater thermal stability. The Pd(II) complex was obtained by reacting 1,3-dimethylimidazolium iodide with $Pd(OAc)_2$ in THF. In this case, the acetate group acts as internal base, facilitating of the deprotonation of the imidazolium salt with the consequent formation of two molecules of AcOH. The extraordinary stability of complex **1.6** was attributed to the strength of the Pd-$C_{carbene}$ bond.

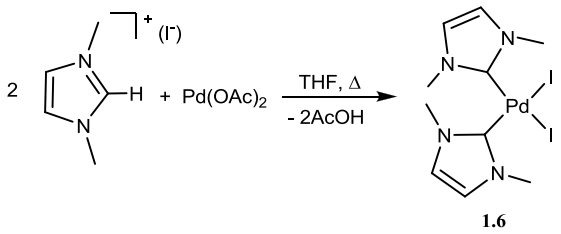

1.6

Scheme 1.1 Synthesis of the NHC-based Pd(II) complex employed by Herrmann in C-C coupling reactions

Besides the development of Pd(II)-NHC complexes for C-C coupling reactions, the coordination of NHC ligands to ruthenium has allowed the preparation of a new generation of catalysts for olefin metathesis. The substitution of a phosphine ligand in the complex $RuCl_2(=CHPh)(PCy_3)_2$ by a more electron donor N-heterocyclic carbene one stabilizes the compound and, also, increases its activity in metathesis reactions.[14] The fast development of this area is due, mainly, to the work of Grubbs[15] and Fürstner.[16] Figure 1.7 shows some examples of these Ru(II) catalysts for olefin metathesis, so-called second generation Grubb's catalysts.

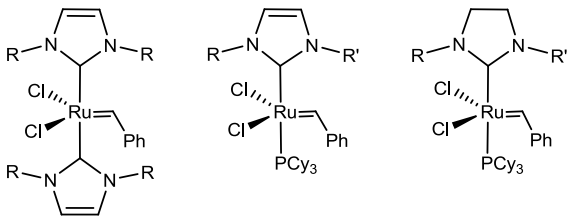

1.7 **1.8** **1.9**

Figure 1.7 Second generation Grubb's catalysts bearing saturated and unsaturated NHC ligands

1.1.4 N-heterocyclic carbenes: metallation strategies

The coordination of NHCs to a metal center usually requires the activation of a precursor. Some of the most widely used strategies are: [17]

1) Insertion of a metal into the C=C bond of bis(imidazolidin-2-ylidene) olefins

Lappert and co-workers proposed the use of electron-rich olefins as NHC precursors in the synthesis of carbene transition metal complexes.[18] This methodology can afford mono-, bis-, tris-, and even tetrakis-carbene complexes (Scheme 1.2). All the NHC complexes obtained by this method contain saturated NHCs.

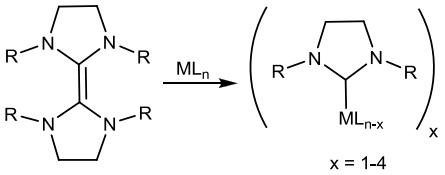

Scheme 1.2 Synthesis of a M-NHC complex by insertion of a metal into the C=C bond of an electron-rich olefin

2) Isolation of the free carbene

Deprotonation of an azolium salt with a strong base such as NaH or *t*BuOK renders the free carbene, which can then be reacted with a suitable transition metal complex to yield the transition metal carbene complex.[1, 19]

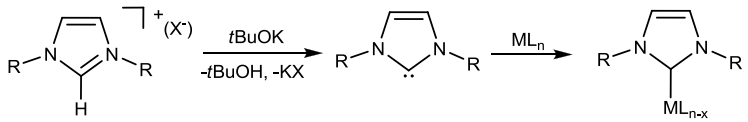

Scheme 1.3 Synthesis of a M-NHC complex by reaction of the isolated free carbene with a metal precursor

3) Use of carbene adducts or "protected" forms of free carbenes

The isolation of free carbenes is not always trivial, mainly due to difficulties with decomposition and the need to handle free NHCs under inert and moisture-free atmosphere conditions. In this context, the use of protected forms of free carbenes has

appeared as a useful alternative. N-heterocyclic rings containing alkoxide or trichloromethyl groups can be considered as NHC-adducts, in the sense that they can readily eliminate alcohol or chloroform to unmask the carbene, which would then coordinate to the metal.[20]

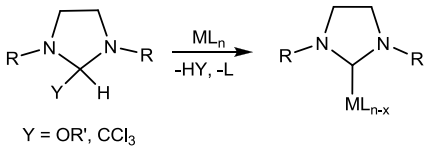

Scheme 1.4 Use of carbene adducts as route to M-NHC complexes

4) In situ deprotonation of azolium salts with an internal or external base

This method has the advantage that the carbene does not have to be isolated. Several strong bases such as NaH,[21] *n*BuLi,[22] *t*BuOK,[23] NaOEt[24] and KN(SiMe$_3$)$_2$[25] are among the most widely used. Also, weak bases such as NEt$_3$,[26] NaOAc[27] and Cs$_2$CO$_3$[28] usually provide very good results.

In situ deprotonation of the NHC precursors can be also achieved by basic ligands on the metal complexes. Commercially available or easy-to-prepare metal complexes with acetate,[29] alkoxide,[30] hydride[31] or acetylacetonate[32] ligands are frequently used.

5) Transmetallation from a Ag-NHC complex

The use of Ag-NHC complexes as carbene transfer reagents was described by Wang and Lin[33] and, in many cases, provides a convenient way to overcome the difficulties arising from using strong bases, inert atmosphere and complicated work-ups. In most cases, transmetallation reactions can be carried out under aerobic conditions, and the process has shown successful with a variety of metals such as Au, Cu, Ni, Pd, Pt, Rh, Ir and Ru.[34] The lability of the Ag-NHC bond and the low solubility of the generated silver halide can be considered as the driving forces of the reaction.

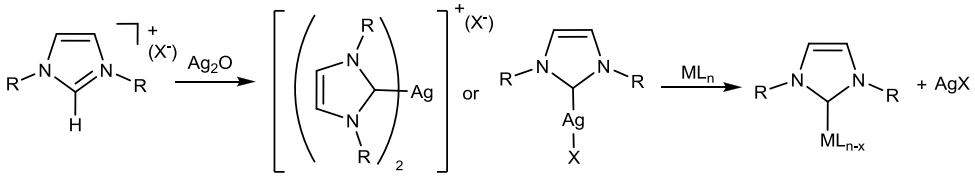

Scheme 1.5 Synthesis of a M-NHC complex by transmetallation from a Ag-NHC complex

6) Activation of the C2-X bond (X= Me, halogen, H) of an imidazolium cation

The oxidative addition of C-Cl bonds in azolium salts to generate carbene complexes has been known since 1974.[35] In 2001, Cavell and co-workers extended the method to 2-iodo-imidazolium salts, and studied the oxidative addition process to group 10 M(0) complexes.[36] Years later, our group of research proved that the C2-H oxidative addition of imidazolium salts to metal complexes can also be applied to other metals than low valent group 10, such as iridium[37] or rhodium.[38]

Although the latter strategies are among the most widely used, new methods to prepare carbene complexes have been reported in the last few years. In some cases, the NHC-based metal complexes are prepared from non-traditional precursors.

7) Synthesis of NHC complexes by decarboxylation of an imidazolium-2-carboxylate

In 2005, Crabtree and co-workers reported that an air- and moisture-stable N,N'-disubstituted imidazolium-2-carboxylate can act as a carbene transfer agent to yield Rh-, Ru-, Ir- and Pd-NHC complexes.[39]

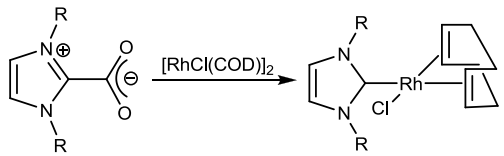

Scheme 1.6 Synthesis of a Rh(I)-NHC complex by decarboxylation of an imidazolium-2-carboxylate

8) Reactions of lithiated azoles with transition-metal complexes

Lithiated azoles are readily C2-metallated by transition metals. The alkylation or protonation of the remaining nitrogen atom leads to stable transition metal NHC complexes.[40]

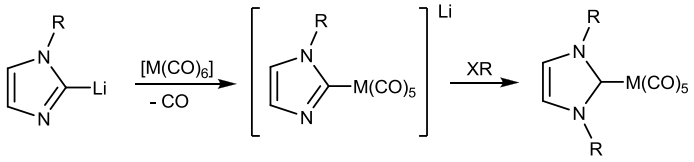

Scheme 1.7 Synthesis of M-NHC complexe from lithiated azole

9) Double C(sp^3)-H$_2$ dehydrogenation of a neutral N-heterocycle

Metallic carbenes can be generated by double C-H bond activation of C(sp^3)-H$_2$ groups.[41] Caulton and co-workers described the first example in which the double C(sp^3)-H$_2$ dehydrogenation of a saturated N-heterocycle (imidazolidine), afforded a Ru-NHC complex.[42] In chapter 4 of this Thesis, we will describe some other related examples described by us, together with a plausible mechanism proposal.[43]

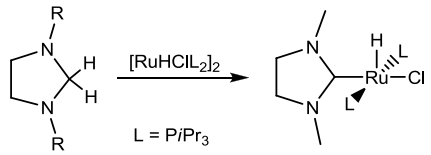

Scheme 1.8 Synthesis of a Ru(II)-NHC complex by double C-H bond activation of a C(sp^3)H$_2$ group

10) Template-controlled cyclization of β-functionalized isocyanides

Hahn and co-workers recently developed an innovative way of generating M-NHC complexes from nucleophile-functionalized isocyanides in metal-template-controlled reactions.[44]

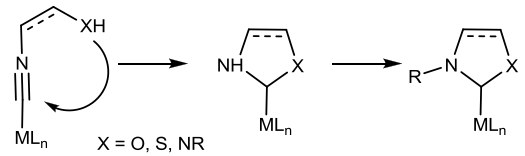

Scheme 1.9 Template-controlled cyclization of β-functionalized isocyanides

The cyclization reactions of isocyanides constitute an alternative and complementary method for the preparation of complexes bearing cyclic diaminocarbenes compared to the classic method starting from cyclic azolium salts.[45] This method is convenient when the azolium precursor is not readily available or is difficult to deprotonate. In addition, this method allows for the stepwise alkylation of the nitrogen atoms of the carbene heterocycle which gives access to complexes with unsymmetrically N,N'-substituted NHC ligands.

1.2 Objectives

During the last decade, our group of research has developed new synthetic strategies for the preparation of NHC-based homogeneous catalysts with novel stereoelectronic properties. Within this context, this work is focused on the synthesis and characterization of new metallic complexes containing different N-heterocyclic carbene ligands, the study of their reactivity and the exploration of their catalytic properties. This general objective can be divided in the following more specific objectives:

- Synthesis of a series of simple and easy-to-make N-heterocyclic monocarbene (imidazolylidene, pyrazolylidene and triazolylidene) ligands and their coordination to $[RuCl_2(\eta^6\text{-arene})]_2$ and $[IrCp^*Cl_2]_2$.
- Study of the catalytic properties of the new Ru(II) and Ir(III) complexes in **C-H bond activation processes**, such as those governed by a *borrowing-hydrogen* mechanism and functionalization of arenes. The main goal is to perform the catalytic reactions under the 'greenest' possible conditions, thus using non-toxic solvents under the highest atom-economic conditions and minimum waste of energy.
- Synthesis and characterization of new bimetallic complexes containing bis-NHC bridging ligands.
- Study of methods to generate NHC-complexes, which may provide access to sophisticated bimetallic architectures circumventing the use of the ubiquitous but not always accessible azolium salts.

1.3 References

(1) Herrmann, W. A. *Angew. Chem. Int. Ed.* **2002**, *41*, 1291; Weskamp, T.; Böhm, V. P. W.; Herrmann, W. A. *J. Organomet. Chem.* **2000**, *600*, 12.

(2) Gusev, D. G. *Organometallics* **2009**, *28*, 6458.

(3) Perrin, L.; Clot, E.; Eisenstein, O.; Loch, J.; Crabtree, R. H. *Inorg. Chem.* **2001**, *40*, 5806; Esteruelas, M. A.; Gomez, A. V.; Lahoz, F. J.; Lopez, A. M.; Onate, E.; Oro, L. A. *Organometallics* **1996**, *15*, 3423; Canac, Y.; Lepetit, C.; Abdalilah, M.; Duhayon, C.; Chauvin, R. *J. Am. Chem. Soc.* **2008**, *130*, 8406; Perez-Temprano, M. H.; Casares, J. A.; Espinet, P. *Chem.-Eur. J.* **2012**, *18*, 1864.

(4) Tolman, C. A. *Chem. Rev.* **1977**, *77*, 313.

(5) Dorta, R.; Stevens, E. D.; Scott, N. M.; Costabile, C.; Cavallo, L.; Hoff, C. D.; Nolan, S. P. *J. Am. Chem. Soc.* **2005**, *127*, 2485.

(6) Huang, J. K.; Stevens, E. D.; Nolan, S. P. *Organometallics* **2000**, *19*, 1194; Herrmann, W. A.; Schutz, J.; Frey, G. D.; Herdtweck, E. *Organometallics* **2006**, *25*, 2437; Leuthausser, S.; Schwarz, D.; Plenio, H. *Chem.-Eur. J.* **2007**, *13*, 7195; Chianese, A. R.; Li, X. W.; Janzen, M. C.; Faller, J. W.; Crabtree, R. H. *Organometallics* **2003**, *22*, 1663.

(7) Ofele, K. *J. Organomet. Chem.* **1968**, *12*, 42.

(8) Wanzlick, H. W.; Schönherr, H. J. *Angew. Chem. Int. Ed.* **1968**, *7*, 141.

(9) Lappert, M. F.; Pye, P. L. *J. Chem. Soc.-Dalton Trans.* **1977**, 2172.

(10) Arduengo, A. J.; Harlow, R. L.; Kline, M. *J. Am. Chem. Soc.* **1991**, *113*, 361.

(11) Herrmann, W. A.; Elison, M.; Fischer, J.; Kocher, C.; Artus, G. R. J. *Angew. Chem. Int. Edit. Engl.* **1995**, *34*, 2371.

(12) Herrmann, W. A.; Brossmer, C.; Ofele, K.; Reisinger, C. P.; Priermeier, T.; Beller, M.; Fischer, H. *Angew. Chem. Int. Edit. Engl.* **1995**, *34*, 1844.

(13) Beller, M.; Fischer, H.; Herrmann, W. A.; Ofele, K.; Brossmer, C. *Angew. Chem. Int. Edit. Engl.* **1995**, *34*, 1848.

(14) Arduengo, A. J.; Gamper, S. F.; Calabrese, J. C.; Davidson, F. *J. Am. Chem. Soc.* **1994**, *116*, 4391; Huang, J. K.; Schanz, H. J.; Stevens, E. D.; Nolan, S. P. *Organometallics* **1999**, *18*, 2370; Huang, J. K.; Stevens, E. D.; Nolan, S. P.; Petersen, J. L. *J. Am. Chem. Soc.* **1999**, *121*, 2674.

(15) Trnka, T. M.; Grubbs, R. H. *Acc. Chem. Res.* **2001**, *34*, 18; Bielawski, C. W.; Grubbs, R. H. *Angew. Chem. Int. Ed.* **2000**, *39*, 2903; Louie, J.; Grubbs, R. H. *Organometallics* **2002**, *21*, 2153.

(16) Furstner, A.; Ackermann, L.; Gabor, B.; Goddard, R.; Lehmann, C. W.; Mynott, R.; Stelzer, F.; Thiel, O. R. *Chem.-Eur. J.* **2001**, *7*, 3236.

(17) Peris, E. *Topics in Organometallic Chemistry* **2007**, *21*, 83.

(18) Lappert, M. F. *J. Organomet. Chem.* **1988**, *358*, 185.

(19) Bourissou, D.; Guerret, O.; Gabbai, F. P.; Bertrand, G. *Chem. Rev.* **2000**, *100*, 39.

(20) Enders, D.; Breuer, K.; Raabe, G.; Runsink, J.; Teles, J. H.; Melder, J. P.; Ebel, K.; Brode, S. *Angew. Chem. Int. Edit. Engl.* **1995**, *34*, 1021; Teles, J. H.; Melder, J. P.; Ebel, K.; Schneider, R.; Gehrer, E.; Harder, W.; Brode, S.; Enders, D.; Breuer, K.; Raabe, G. *Helv. Chim. Acta* **1996**, *79*, 61; Hoffmann, R. W. *Angew. Chem. Int. Ed.* **1968**, *7*, 754.

(21) Douthwaite, R. E.; Houghton, J.; Kariuki, B. M. *Chem. Commun.* **2004**, 698; Alcarazo, M.; Roseblade, S. J.; Alonso, E.; Fernandez, R.; Alvarez, E.; Lahoz, F. J.; Lassaletta, J. M. *J. Am. Chem. Soc.* **2004**, *126*, 13242.

(22) Wanzlick, H. W.; Schikora, E. *Chem. Ber.-Recl.* **1961**, *94*, 2389; Fehlhammer, W. P.; Bliss, T.; Kernbach, U.; Brudgam, I. *J. Organomet. Chem.* **1995**, *490*, 149.

(23) Baker, M. V.; Brayshaw, S. K.; Skelton, B. W.; White, A. H.; Williams, C. C. *J. Organomet. Chem.* **2005**, *690*, 2312; Herrmann, W. A.; Goossen, L. J.; Spiegler, M. *Organometallics* **1998**, *17*, 2162.

(24) Burling, S.; Field, L. D.; Li, H. L.; Messerle, B. A.; Turner, P. *Eur. J. Inorg. Chem.* **2003**, 3179; Kocher, C.; Herrmann, W. A. *J. Organomet. Chem.* **1997**, *532*, 261.

(25) Coleman, K. S.; Turberville, S.; Pascu, S. I.; Green, M. L. H. *J. Organomet. Chem.* **2005**, *690*, 653.

(26) Poyatos, M.; Sanau, M.; Peris, E. *Inorg. Chem.* **2003**, *42*, 2572; Poyatos, M.; Mata, J. A.; Falomir, E.; Crabtree, R. H.; Peris, E. *Organometallics* **2003**, *22*, 1110; Poyatos, M.; Mas-Marza, E.; Sanau, M.; Peris, E. *Inorg. Chem.* **2004**, *43*, 1793.

(27) Semeril, D.; Bruneau, C.; Dixneuf, P. H. *Adv. Synth. Catal.* **2002**, *344*, 585.

(28) Lee, H. M.; Chiu, P. L.; Zeng, J. Y. *Inorg. Chim. Acta* **2004**, *357*, 4313.

(29) Herrmann, W. A.; Schwarz, J.; Gardiner, M. G.; Spiegler, M. *J. Organomet. Chem.* **1999**, *575*, 80; Peris, E.; Loch, J. A.; Mata, J.; Crabtree, R. H. *Chem. Commun.* **2001**, 201.

(30) Baratta, W.; Herdtweck, E.; Herrmann, W. A.; Rigo, P.; Schwarz, J. D. *Organometallics* **2002**, *21*, 2101.

(31) Grundemann, S.; Kovacevic, A.; Albrecht, M.; Faller, J. W.; Crabtree, R. H. *Chem. Commun.* **2001**, 2274; Grundemann, S.; Kovacevic, A.; Albrecht, M.; Faller, J. W.; Crabtree, R. H. *J. Am. Chem. Soc.* **2002**, *124*, 10473.

(32) Clyne, D. S.; Jin, J.; Genest, E.; Gallucci, J. C.; RajanBabu, T. V. *Org. Lett.* **2000**, *2*, 1125.

(33) Wang, H. M. J.; Lin, I. J. B. *Organometallics* **1998**, *17*, 972.

(34) Garrison, J. C.; Youngs, W. J. *Chem. Rev.* **2005**, *105*, 3978; Lin, I. J. B.; Vasam, C. S. *Coord. Chem. Rev.* **2007**, *251*, 642.

(35) Fraser, P. J.; Roper, W. R.; Stone, F. G. A. *J. Chem. Soc.-Dalton Trans.* **1974**, 760; Fraser, P. J.; Roper, W. R.; Stone, F. G. A. *J. Chem. Soc.-Dalton Trans.* **1974**, 102.

(36) McGuinness, D. S.; Cavell, K. J.; Yates, B. F.; Skelton, B. W.; White, A. H. *J. Am. Chem. Soc.* **2001**, *123*, 8317; McGuinness, D. S.; Cavell, K. J.; Yates, B. F. *Chem. Commun.* **2001**, 355; Cavell, K. J.; McGuinness, D. S. *Coord. Chem. Rev.* **2004**, *248*, 671.

(37) Viciano, M.; Mas-Marza, E.; Poyatos, M.; Sanau, M.; Crabtree, R. H.; Peris, E. *Angew. Chem. Int. Ed.* **2005**, *44*, 444.

(38) Mas-Marza, E.; Sanau, M.; Peris, E. *Inorg. Chem.* **2005**, *44*, 9961.

(39) Voutchkova, A. M.; Appelhans, L. N.; Chianese, A. R.; Crabtree, R. H. *J. Am. Chem. Soc.* **2005**, *127*, 17624; Voutchkova, A. M.; Feliz, M.; Clot, E.; Eisenstein, O.; Crabtree, R. H. *J. Am. Chem. Soc.* **2007**, *129*, 12834.

(40) Raubenheimer, H. G.; Stander, Y.; Marais, E. K.; Thompson, C.; Kruger, G. J.; Cronje, S.; Deetlefs, M. *J. Organomet. Chem.* **1999**, *590*, 158; Raubenheimer, H. G.; Lindeque, L.; Cronje, S. *J. Organomet. Chem.* **1996**, *511*, 177; Raubenheimer, H. G.; Desmet, M.; Lindeque, L. *J. Chem. Res.-S* **1995**, 184; Raubenheimer, H. G.; Cronje, S. *J. Organomet. Chem.* **2001**, *617*, 170.

(41) Werner, H. *Angew. Chem. Int. Ed.* **2010**, *49*, 4714.

(42) Ho, V. M.; Watson, L. A.; Huffman, J. C.; Caulton, K. G. *New J. Chem.* **2003**, *27*, 1446; Coalter, J. N.; Ferrando, G.; Caulton, K. G. *New J. Chem.* **2000**, *24*, 835.

(43) Prades, A.; Poyatos, M.; Mata, J. A.; Peris, E. *Angew. Chem. Int. Ed.* **2011**, *50*, 7666.

(44) Hahn, F. E.; Jahnke, M. C. *Angew. Chem. Int. Ed.* **2008**, *47*, 3122.

(45) Hahn, F. E.; Tamm, M. *J. Organomet. Chem.* **1993**, *456*, C11; Flores-Figueroa, A.; Kaufhold, O.; Feldmann, K. O.; Hahn, F. E. *Dalton Trans.*

2009, 9334; Kaufhold, O.; Flores-Figueroa, A.; Pape, T.; Hahn, F. E. *Organometallics* **2009**, *28*, 896.

Chapter 2

Synthesis and characterization of *non-conventional* 'Ru(η^6-arene)(NHC)' and 'IrCp*(NHC)' complexes

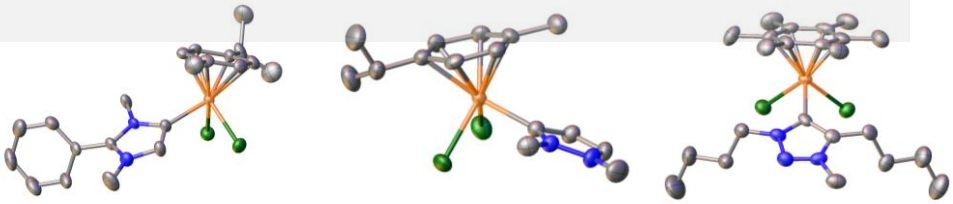

2.1 Introduction

2.1.1 Conventional and *non-conventional* N-heterocyclic carbene complexes

The coordination versatility of NHC ligands and the relatively easy preparation of their precursors, have allowed them to be obtained with a variety of topologies and coordination properties. Apart from the most widely used NHCs, imidazol-2-ylidenes and imidazolin-2-ylidenes (so-called *normal*-NHCs), a wide set of other N-heterocyclic frameworks has allowed the preparation of carbenes in which the electronic and steric parameters can be modified compared with the normal ones. This new set includes not only a variety of five-membered ring carbenes (*abnormal*-NHCs, pyrazolylidenes, triazolylidenes, benzoimidazolylidenes, etc.) but also four-, six- and seven-membered rings.[1] Scheme 2.1 depicts some of the most representative NHC frameworks.

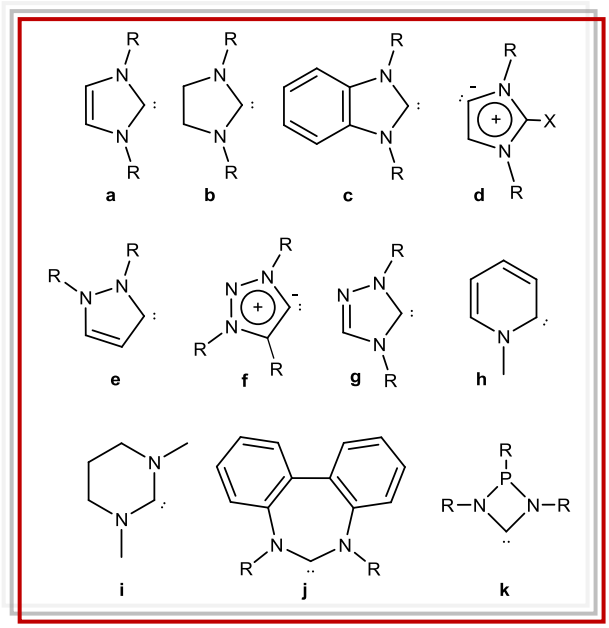

Scheme 2.1 Different NHC frameworks

This chapter describes the synthesis and characterization of Ru(II) and Ir(III) complexes bearing five-membered NHC ligands, particularly imidazolylidenes (**a** and **d**), pyrazolylidenes (**e**) and 1,2,3-triazolylidenes (**f**).

2.1.2 Complexes with C4(5)-bound or *abnormally*-bound imidazolylidenes

Until 2001, it was generally assumed that NHC ligands always bound to metals *via* the activation of the more acidic C2 position of the corresponding imidazolium precursors (Scheme 2.2).

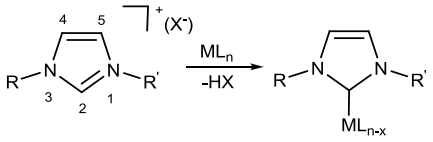

Scheme 2.2 Synthesis of an imidazol-2-ylidene-based complex

It is now known that, in some cases, the use of standard procedures to generate metal carbene complexes can lead to the formation of C4(5)-bound complexes. The term *abnormal*-NHC (*a*NHC) was given to this new type of coordination, referring to its unusual nature. Crabtree and co-workers were the first to observe this kind of C4(5)-bond complexes.[2]

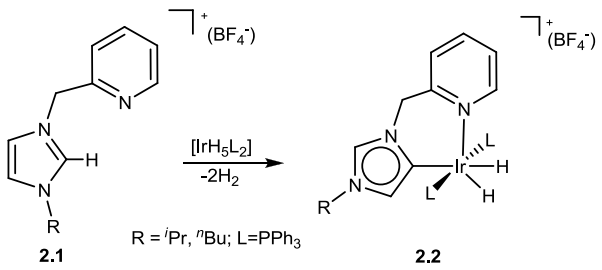

Scheme 2.3 Synthesis of the first *a*NHC-based complex

As depicted in Scheme 2.3, the reaction of a potentially C-N chelating pyridine-imidazolium salt **2.1** with $IrH_5(PPh_3)_2$, afforded the abnormal C4(5)-bound iridium(III) complex **2.2**. The selective formation of the C4(5)- or C2-bound carbene complexes depends on multiple factors, such as the steric bulk of the terminal N-

substituent,[3] the counterion[4] and the base used in the reaction.[5] Recently, it has been proposed that the solvent also has a significant effect on the formation of the abnormally bound carbene.[6]

A simple way to selectively obtain complexes with this type of coordination is to use NHC ligand precursors blocked at the C2 position by an appropriate group (alkyl or aryl group). Whit this in mind, Crabtree and co-workers described a series of Ir(I) complexes bearing an imidazol-4(5)-ylidene ligand. In this case, it was necessary to block the C2 and C4 positions to form a stable sterically protected C5-bound complex.[7] The disubstituted imidazolium salt **2.3** undergoes clean deprotonation in the presence of Ag_2O. Subsequent transmetallation of the presumably formed silver complex with $[IrCl(COD)]_2$ yields the *abnormal*-NHC-Ir(I) complex **2.4** (Scheme 2.4).

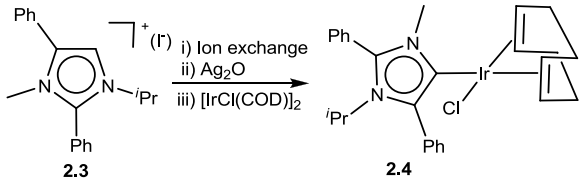

Scheme 2.4 Synthesis of *a*NHC-based Ir(I) complex

Since Crabtree and co-workers reported the first *a*NHC in 2001, the number and range of abnormally-bound (or C4(5)-bound) complexes largely increased.[8] A very interesting example was reported in 2007, by Whittlesey and co-workers, who prepared the first example of an *a*NHC ligand coordinated to Ru(II).[9] As shown in Scheme 2.5, 1,3-di-*tert*-butylimidazol-2-ylidene reacts with $[Ru_3(CO)_{12}]$ at room temperature to generate a Ru-*a*NHC complex (**2.5**), which under heating in THF forms the triruthenium cluster **2.6**. Complex **2.6** has many interesting features since a C-H activation at the C4 and the C5 positions of the NHC ligand has taken place. In this case, the C2 coordination is precluded by the bulky *tert*-butyl N-substituents.

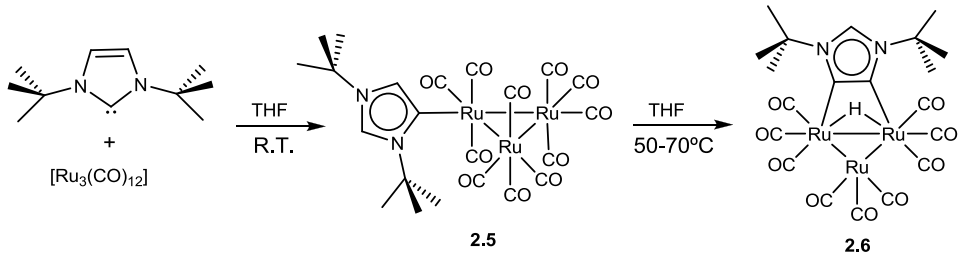

Scheme 2.5 Synthesis of the first *a*NHC-based ruthenium complex

On the other hand, Albrecht and co-workers described the interesting Rh(III) complex **2.7** shown in Figure 2.1.[10] The formation of this compound involves a triple C-H bond activation process, finally affording a species with both types of NHCs, *normal* and *abnormal*.

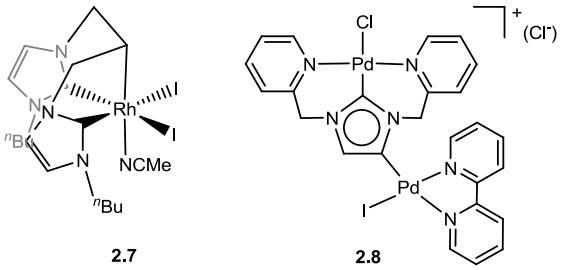

Figure 2.1

The same group of research described the unprecedented Pd(II) complex **2.8** (Figure 2.1).[11] As depicted in the figure, complex **2.8** is a dimetallic complex in which the two palladium centers are bridged by a single NHC ligand. Complex **2.8** was obtained by sequential metallation at the C2 position, by means of transmetallation, followed by a C4–I oxidative addition. The complex could not be isolated, although it was identified by NMR and ESI mass spectroscopy.

Infrared spectroscopy studies of carbonyl derivatives indicate that abnormally-bound N-heterocyclic carbenes are significantly more electron-donating than their C2-bound analogues,[7, 12] a fact that has been confirmed by means of DFT calculations.[13]

2.1.3 Pyrazolylidene-based complexes

Although the coordination of pyrazole-based NHC ligands is known since 1976,[14] only a few examples regarding Cr, Mo,[14] Rh,[15-16], Pd,[17], Cu,[18] Fe,[19] and Au-complexes[20] have been synthesized by different metallation strategies. Like imidazolium-derived carbenes, pyrazolium metallation may give either normal or abnormal (or remote) carbenes, as shown in Figure 2.2. While in *normal*-pyrazolylidenes (pyrazol-3-ylidenes), a single N atom is located in α-position to the carbenic carbon, in *abnormal*-pyrazolylidenes, only remotely located nitrogen atoms are available for carbene stabilization.

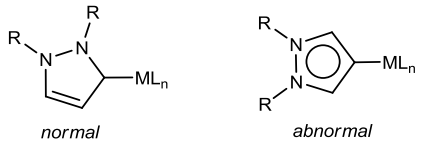

Figure 2.2 Pyrazolylidene-based metal complexes

In order to compare the relative donor strengths of the pyrazol-3-ylidenes with the imidazol-2-ylidenes, Öfele and co-workers observed the carbonyl stretching frequencies in $Mo(CO)_5$-NHC complexes.[14] They attributed stronger donor properties to pyrazol-3-ylidenes than to imidazol-2-ylidenes. Years later, the same conclusion was described by Herrmann and co-workers who reported the carbonyl IR stretching frequencies of a series of [*cis*-RhI(NHC)$(CO)_2$] type complexes. As stated earlier, when pyrazolylidenes are coordinated through the C3 position, a single N atom is located adjacent to the carbene carbon, thus increasing the donor properties of these ligands compared to those of normal-imidazolylidenes.[21]

2.1.4 Triazolylidene-based complexes. *Mesioionic* character of the carbene

The existence of two types of triazolylidene ligands (1,2,4-triazolylidenes[22] and 1,2,3-triazolylidenes[23]) may also give either normal- or abnormal- NHC complexes (Figure 2.3).

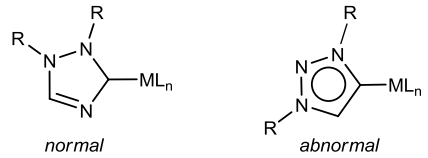

Figure 2.3 Triazolylidene-based metal complexes

Aiming to expand the family of abnormal N-heterocyclic carbene ligands, Albrecht and co-workers reported the preparation of 1,4-substituted 1,2,3-triazolium salts, which provided versatile ligand precursors for the synthesis of new 1,2,3-triazolylidene metal complexes.[24] The neutral triazole heterocycles can be prepared by [3 + 2] cycloaddition of azides and acetylenes ("click chemistry").[25] Copper-mediated cyclization allows for introducing functional groups into the triazole framework for diverse purposes (Scheme 2.6).

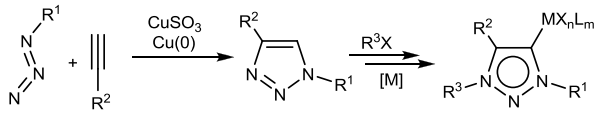

Scheme 2.6 1,2,3-Triazolylidene-based metal complexes

The same research group described the coordination of these new carbenes to several transition metals (Ag, Rh, Ir and Pd). [20] Since this seminal report, several examples have appeared of transition metal complexes containing these ligands.[24, 26, 27] The studies on the donor properties of 1,2,3-triazolylidene ligands concluded that they are stronger σ-donors than the most basic imidazol-2-ylidene ligands, although slightly less basic than other abnormally-bound carbenes.

The first time that the term *abnormal* term appeared, it was to refer to imidazolylidene type carbenes coordinated to the metal center by an unusual position (C4 or C5).[2] The rest of unusual carbenes, such as 1,2,3-triazol-5-ylidenes, have also been called *abnormal* carbenes, as a consequence of their lineage. Recently, it has been suggested that reasonable canonical resonance forms containing these carbenes cannot be drawn for the free ligands without additional charges (Scheme 2.7). [23, 27-28]

As they are, in fact, mesoionic compounds[29] Bertrand and co-workers proposed naming this family of compounds as mesoionic carbenes (MICs).[23]

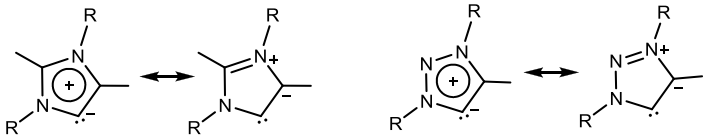

Scheme 2.7 Mesoionic carbene isomers

2.2 Results and Discussion

2.2.1 Synthesis and characterization of azolium salts

Aiming to prepare a systematic list of Ir and Ru simple, yet conventional and non-conventional, NHC metal complexes, a variety of five-membered NHC ligand precursors were synthesized (Scheme 2.8). The imidazolium salts [**A**H]I,[30] [**B**H]I[31] and [**D**H]I[32] and the pyrazolium salt [**F**H]I[15] were prepared from the known literature methods, while the imidazolium salts [**C**H]I, [**E**H]I and the triazolium salt [**G**H]I were synthesized and characterized during the development of this research work.

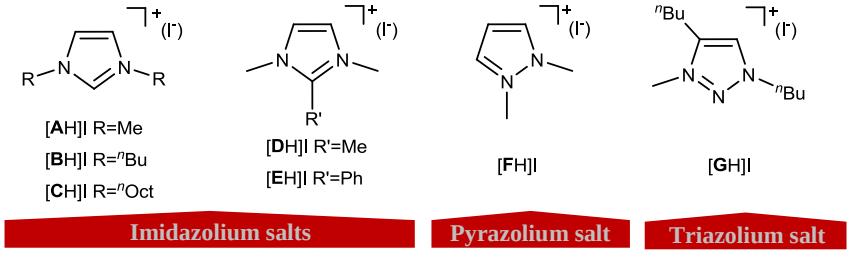

Scheme 2.8 NHC ligand precursors

The CO stretching frequencies observed by infrared spectroscopy provide valuable information about the electron donor strength of the coordinated ligands. In this sense, as stated in the Introduction of this Chapter, different research groups have concluded that abnormally-bound NHCs,[7] pyrazol[21] and triazol-based[24] NHCs are stronger σ-donors than imidazol-2-ylidenes. Besides, DFT calculations carried out by Prof. Gusev reported the electron-donor and steric properties of a diverse group of NHCs.[13] This study afforded the conventional TEP data [Tolman Electronic Parameter = ν_{CO} (A_1) of $Ni(CO)_3(NHC)$], which allowed ranking different NHC ligands in order of increasing donor power. As stated by Gusev and also other researchers as Fürstner,[33] the $Ni(CO)_3$-TEP-scale has been preferred over the use of other different metal carbonyl templates, in order 'to avoid meaningful results' upon comparison of the different scales. Calculated TEP (cm^{-1}) values for carbenes similar to ours are collected in Table 2.1. As shown in the table, imidazol-2-ylidenes present

higher TEP values, implying that their electron donor strength is lower than those of the others ligands shown in the table. The results are in agreement with the experimental data.

Table 2.1 Calculated TEP of $Ni(CO)_3(NHC)$

Carbene	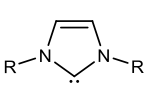	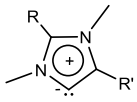	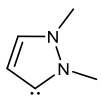	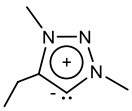
TEP (cm^{-1})	(R = Me) 2054.1 (R = ^{n}Bu) 2051.4	(R = R' =H) 2043.3 (R = Me, R'= Et) 2039.9	2049.0	2047.6

Taking all this into account, we believe that the azolium salts obtained ([**A**H]I - [**G**H]I) will provide NHC ligands with different electronic properties. This will allow to explore the effect of the σ-donor abilities of the chosen ligands on the catalytic activity of the generated metal complexes.

a) General protocol for the preparation of the imidazolium salts

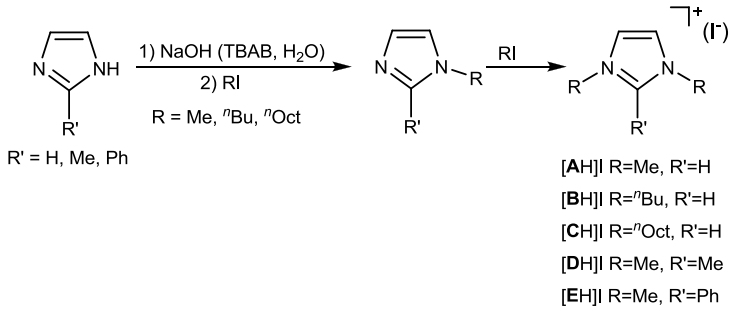

Scheme 2.9 General protocol for the preparation of the imidazolium salts

Scheme 2.9 shows the general protocol for the synthesis of the imidazolium salts employed in this research work, which involves two steps. First, the imidazole deprotonation is carried out using a strong base, and then a nucleophilic attack of the species formed to the corresponding alkyl halide leads to the formation of the desired neutral alkylimidazole. The second step of the synthesis involves the reaction of the

alkylimidazole with the corresponding alkyl halide to yield the desired imidazolium salt.

The preparation of [**A**H]I, [**B**H]I and [**D**H]I, only required the second step of the procedure, because the neutral alkylimidazole substrates are commercially available. The imidazolium salts [**C**H]I and [**E**H]I were synthesized for the first time in a 90% and 80% yield, respectively.

b) General protocol for the preparation of the pyrazolium salt

The synthesis of 1,2-dimethylpyrazolium iodide [**F**H]I was carried out following the above described procedures, as depicted in Scheme 2.10.

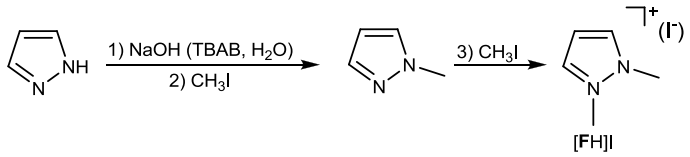

Scheme 2.10 Synthesis of [**F**H]I

c) General protocol for the preparation of the triazolium salt

The synthesis of 1,4-dibutyl-3-methyl-1,2,3-triazolium iodide [**G**H]I implies three steps (Scheme 2.11). First, the BuN_3 preparation is carried out by alkylation of the azide with *n*-butyliodide. Then, the BuN_3 cyclization with a solution of 1-hexyne and Cu(I) affords the neutral triazole. Finally, the N-quaternization with CH_3I gives the desired salt in 85% yield.

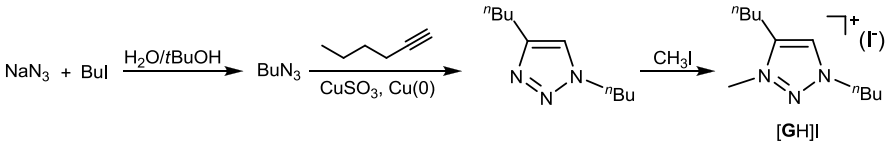

Scheme 2.11 Synthesis of [**G**H]I

The new salts, [**C**H]I, [**E**H]I and [**G**H]I were characterized by NMR and mass spectroscopy and elemental analysis. As an example, the spectroscopic characterization of [**G**H]I is discussed below in detail.

*^{1}H NMR spectrum of triazolium salt [**G**H]I*

Figure 2.4 shows the ^{1}H NMR spectrum of [**G**H]I. The signal due to the acidic proton, C5-H, appears at 9.09 ppm (a). The N-CH_3 protons display their resonance at 4.28 ppm (c). All the rest of the signals regarding the *n*-butyl groups, are conveniently assigned on the NMR spectrum shown in Figure 2.4.

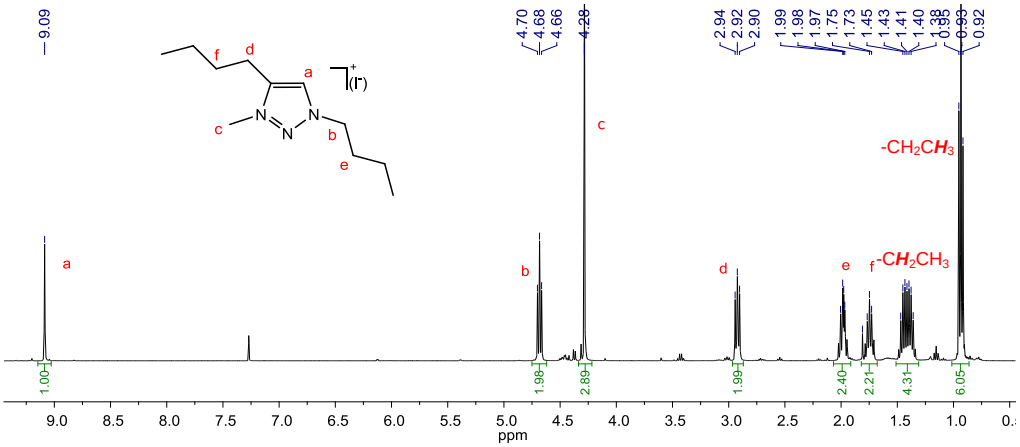

Figure 2.4 ^{1}H NMR spectrum of triazolium salt [**G**H]I in $CDCl_3$

*^{13}C {^{1}H} NMR spectrum of triazolium salt [**G**H]I*

Figure 2.5 shows the ^{13}C {^{1}H} NMR spectrum of [**G**H]I. The signal due to the quaternary carbon of the triazolium salt appears at 144.6 ppm (a). The signal corresponding to the C4 atom (b) appears at 129.2 ppm. All other signals attributed to the *n*-butyl and N-CH_3 groups are conveniently assigned on the NMR spectrum shown in Figure 2.5.

COSY and ^{13}C HSQC NMR experiments were carried out in order to confirm the assignation of the signals displayed on the ^{1}H and ^{13}C NMR spectra of [**G**H]I (see Experimental Section).

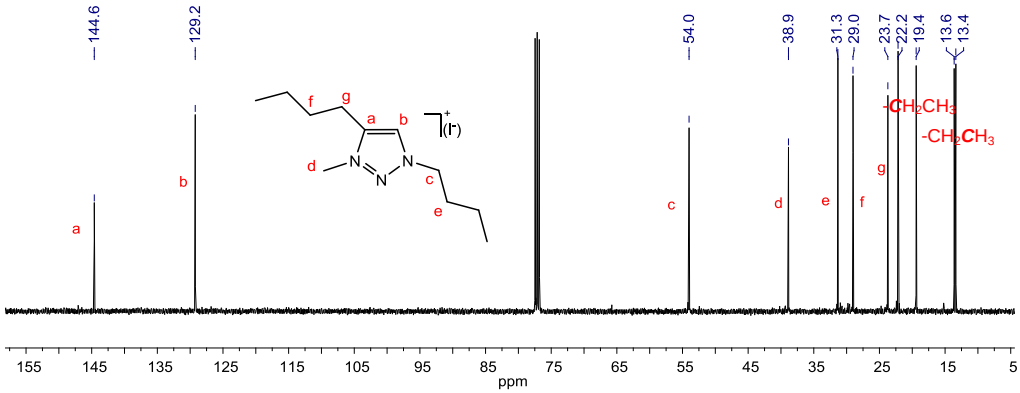

Figure 2.5 ^{13}C {^{1}H} NMR spectrum of triazolium salt [**G**H]I in $CDCl_3$

2.2.2 Synthesis and characterization of 'Ru(η^6-arene)(NHC)' complexes

Once the azolium salts were synthesized and fully characterized, a series of 'Ru(η^6-arene)(NHC)' complexes were obtained following different metallation strategies. The use of three different η^6-arene ligands (*p*-cymene, hexamethylbenzene and methyl benzoate), and different NHC ligands (imidazolylidene, pyrazolylidene and triazolylidene) seemed a good choice for the tuning of the electronic and steric properties of the metal centre, and the study of their influence on the catalytic outcomes in a series of standard reactions which will be discussed in Chapter 3.

2.2.2.1 Synthesis and characterization of 'Ru(η^6-arene)(imidazolylidene)' complexes

In this section the preparation of complexes **1A**, **2A**, **3B**, **4B**, **5B**, **6C**, **7D** and **8E** will be discussed. Complexes **2A**, **4B**, **5B**, **6C**, **7D** and **8E** are new and have been prepared during the development of the present work. Complexes **1A**[34] and **3B**[35] were previously described.

The synthesis of complex **1A** was previously reported[34] but we prepared it by a different methodology. The synthesis of **1A** and **2A** was carried out using the metallation strategy shown in Scheme 2.12. The reaction of [**A**H]I with [$RuCl_2$(*p*-

cymene)]$_2$ or [RuCl$_2$(CMe)$_6$]$_2$ in the presence of an excess of Cs_2CO_3 in refluxing acetonitrile, allowed the formation of complexes **1A** or **2A**, respectively. The mixture was filtered through Celite to eliminate the excess of Cs_2CO_3, and the solvent was removed under reduced pressure. The resulting crude solid was purified by column chromatography. Both complexes were precipitated from a mixture of dichloromethane/diethyl ether to give yellow solids in 80% (**1A**) and 62% (**2A**) yields. Both compounds were characterized by NMR spectroscopy and mass spectrometry and elemental analysis. The NMR spectra of **1A** were compared with those previously reported.[34]

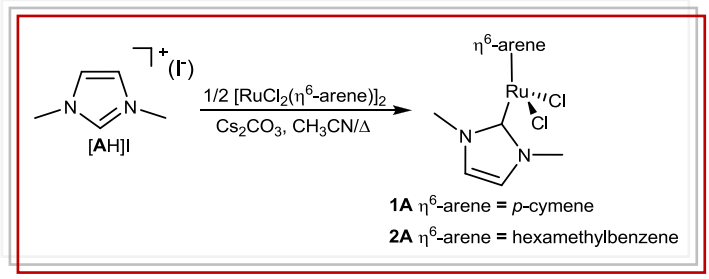

Scheme 2.12 Synthesis of **1A** and **2A**

The preparation of the rest of ruthenium-imidazol-2-ylidene complexes **3B**, **4B, 5B** and **6C** was carried out following a different coordination strategy. The complexes were synthesized following the procedure described for **3B**.[35] As depicted in Scheme 2.13, the coordination to Ru(II) was carried out by transmetallation from the corresponding pre-formed silver-NHC complexes, prepared by treatment of imidazolium salt [**B**H]I or [**C**H]I with Ag_2O. This methodology, first described by Wang and co-workers,[36] has been employed in the preparation of many of the complexes described in this Thesis.

The silver-NHC complexes were obtained by reaction of [**B**H]I or [**C**H]I with Ag_2O at room temperature during 1h in dichloromethane under the exclusion of light. After filtering through Celite to eliminate the excess of Ag_2O and other insoluble by-products, the corresponding Ru(II) precursor was added to the filtrate. The mixture was stirred for 3-12h at 25-45ºC. Compounds **4B** and **6C** were purified by column

chromatography. Both complexes were precipitated from a mixture of dichloromethane/diethyl ether to give orange solids in 78% (**4B**) and 53% (**6C**) yields. Pure compound **5B** was directly precipitated from a mixture of dichloromethane/diethyl ether as a red solid in 62% yield. Compounds **4B**, **5B** and **6C** were characterized by NMR and mass spectrometry and elemental analysis.

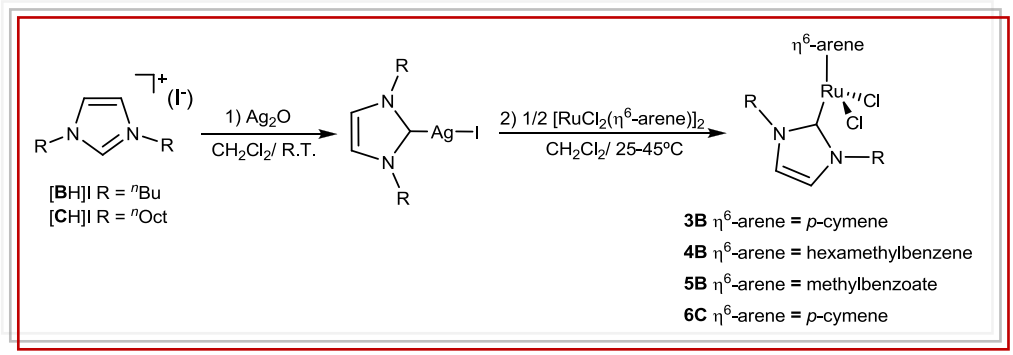

Scheme 2.13 Synthesis of **3B**, **4B**, **5B** and **6C**

One of the most widely used methods for the preparation of *a*NHC-based metal complexes, is to block the C2 position of the ligand precursor with an alkyl or aryl group.[7, 37] By following this procedure, [**D**H]I and [**E**H]I (in which the C2 position is blocked by a methyl and a phenyl group, respectively), were chosen in order to prepare the corresponding *a*NHC-based Ru-complexes.

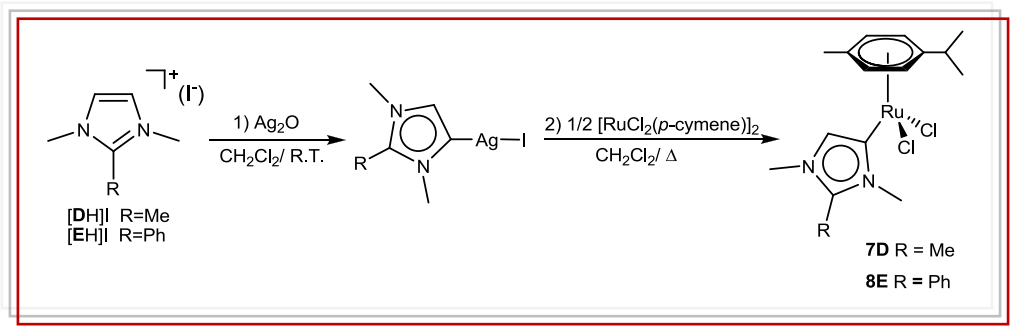

Scheme 2.14 Synthesis of **7D** and **8E**

As shown in Scheme 2.14, the coordination of [**D**H]I and [**E**H]I to $[RuCl_2(p\text{-cymene})]_2$ was performed by transmetallation of the pre-formed silver-NHC in dichloromethane at reflux. Both complexes were purified by column chromatography.

The pure complexes were precipitated from a mixture of dichloromethane/diethyl ether as brown solids in moderate yields [40% (**7D**) and 65% (**8E**)], and were characterized by NMR and mass spectrometry and elemental analysis.

Due to the similarity of these two compounds, only the spectroscopic characterization of **8E** is discussed in detail.

*^{1}H NMR spectrum of complex **8E***

Figure 2.6 shows the ^{1}H NMR spectrum of **8E**. The signals attributed to the phenyl aromatic protons appear between 7.61 and 7.37 ppm (a). The most significant signal is the one due to the proton of the abnormal coordinated azole, C5-H, at 6.91 ppm (b). The signals attributed to the aromatic protons of the *p*-cymene ligand are displayed as two doublets at 5.31 and 5.17 ppm. Due to the loss of the symmetry of the ligand precursor, the signals assigned to the protons of the N-CH_3 groups appear as two singlets at 3.81 and 3.51 ppm (c). The rest of the signals are conveniently displayed on the NMR spectrum shown in Figure 2.6.

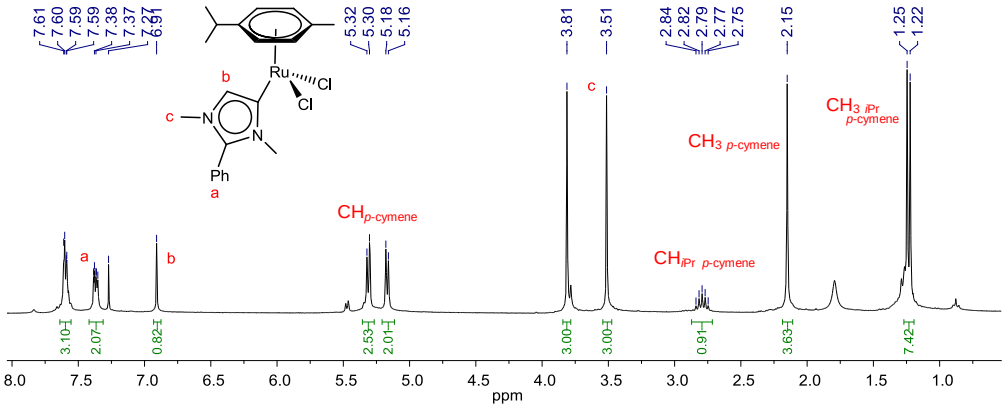

Figure 2.6 ^{1}H NMR spectrum of complex **8E** in $CDCl_3$

*^{13}C {^{1}H} NMR spectrum of complex **8E***

Figure 2.7 shows the ^{13}C {^{1}H} NMR spectrum of **8E**. The most characteristic signal is that attributed to the metallated carbon at 154.3 ppm (a). The signal corresponding to the quaternary carbon of the imidazole ring appears at 143.6 ppm (b). The resonance

due to the C5 atom is shown at 131.3 ppm (c). All the rest of the signals, including those due to the *p*-cymene, phenyl and N-CH_3 carbons, are conveniently displayed on the spectrum shown in Figure 2.7, and are consistent with the structure assigned to the complex.

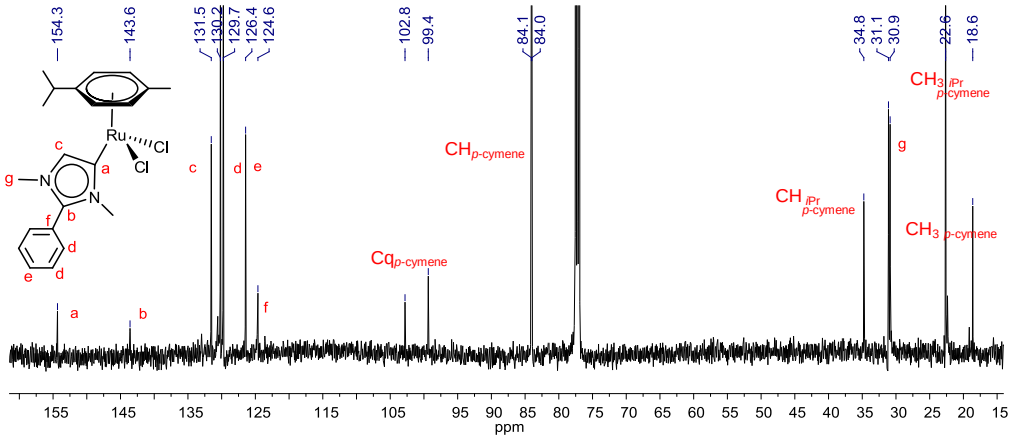

Figure 2.7 ^{13}C {^{1}H} NMR spectrum of complex **8E** in $CDCl_3$

*Molecular structure of **8E***

Crystals of **8E** suitable for X-ray diffraction analysis were obtained by slow diffusion of pentane in a concentrated solution of the compound in dichloromethane. The molecular structure of **8E** (Figure 2.8) confirms the *abnormal* coordination of the NHC ligand. The structure can be regarded as a three-legged piano stool. Along with the imidazolylidene ligand, two chloride ligands and a *p*-cymene ligand complete the coordination sphere about the ruthenium atom.

Table 2.2 shows the most representative bond lengths (Å) and angles (º) of complex **8E**. The Ru-$C_{carbene}$ distance is 2.084 Å, in the range of other 'Ru(*p*-cymene)(NHC)' complexes.[34, 38] The Ru-Cl and Ru-$C_{centroide}$ distances and the $C_{carbene}$-Ru-Cl angles lie in the expected range.

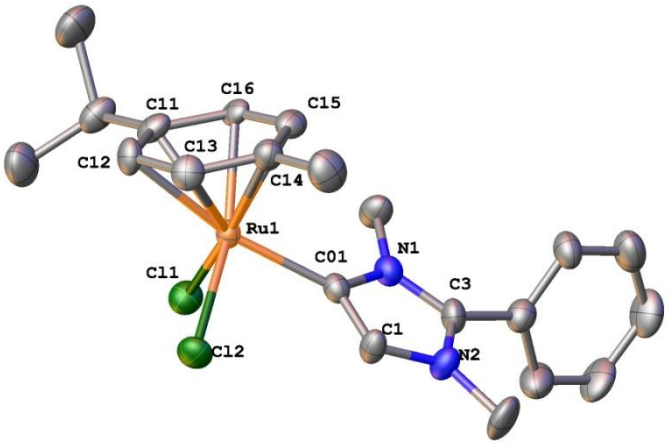

Figure 2.8 Molecular diagram of complex **8E**. Ellipsoids are at 30% probability. Hydrogen atoms have been omitted for clarity

Table 2.2 Selected bond lengths (Å) and angles (º) of complex **8E**

Bonds		Angles	
Ru(1)-C(01)	2.084(7)	C(01)-Ru(1)-Cl(1)	85.14(19)
Ru(1)-Cl(1)	2.4212(16)	C(01)-Ru(1)-Cl(2)	85.73(19)
Ru(1)-Cl(2)	2.4465(14)	Cl(1)-Ru(1)-Cl(2)	89.55(5)
Ru(1)-$C_{centroide}$	1.688		

2.2.2.2 Synthesis and characterization of 'Ru(η^6-arene)(pyrazolylidene)' complexes

In this section the preparation of complexes **9F** and **10F** will be discussed. Both complexes are new and have been prepared during the development of the present work.

The transmetallation from a pre-formed silver-NHC complex was also effective for the coordination of the pyrazolylidene ligand to $[RuCl_2(p\text{-cymene})]_2$ (Scheme 2.15). The reaction of [**F**H]I with Ag_2O in dichloromethane afforded the corresponding Ag-NHC complex, which was *in situ* transmetallated to $[RuCl_2(p\text{-cymene})]_2$. Depending on the Ru/pyrazolium molar ratio used, a monocarbene (**9F**) or a cationic bis-carbene complex (**10F**) were obtained. The complexes were purified by

column chromatography. In the case of complex **10F**, an amount of KPF_6 was added to the eluting solution in order to obtain complex with a PF_6 counteranion. Both complexes were precipitated from a mixture of dichloromethane/hexanes as a yellow solid in 60 % yield (**9F**) and as a green solid in 35% yield (**10F**). These new complexes were characterized by NMR and mass spectrometry and elemental analysis. Only the spectroscopic characterization of **9F** is discussed in detail. All the details of the spectroscopic data for compound **10F** can be found in the Experimental Section.

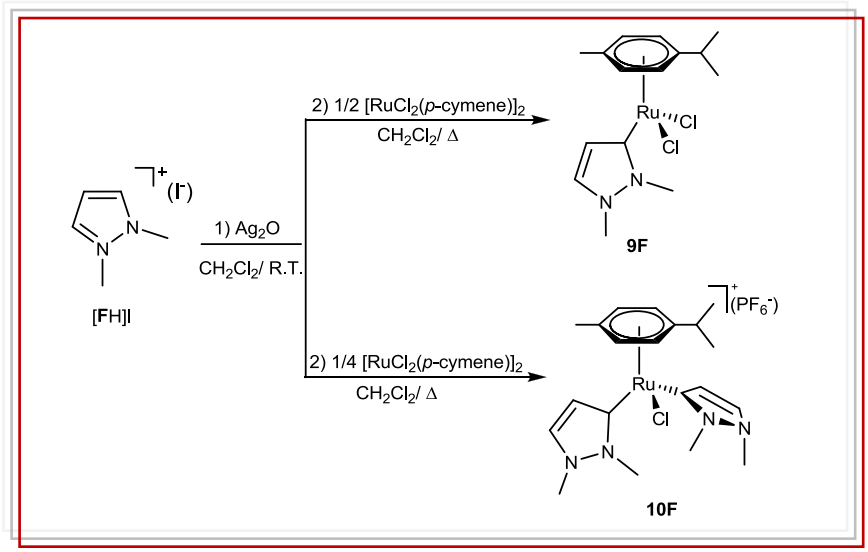

Scheme 2.15 Synthesis of **9F** and **10F**

*^{1}H NMR spectrum of complex **9F***

Figure 2.9 shows the ^{1}H NMR spectrum of **9F**. The signals attributted to the protons of the pyrazole ring are shown as two doublets at 7.34 ppm (a) and 6.58 ppm (b). Due to the loss of symmetry, the signals due to the protons of the methyl groups appear as two singlets at 4.09 and 3.85 ppm (c). The signals attributed to the protons of *p*-cymene ligand are displayed at similar chemical shifts as those shown for **8E** (Figure 2.6).

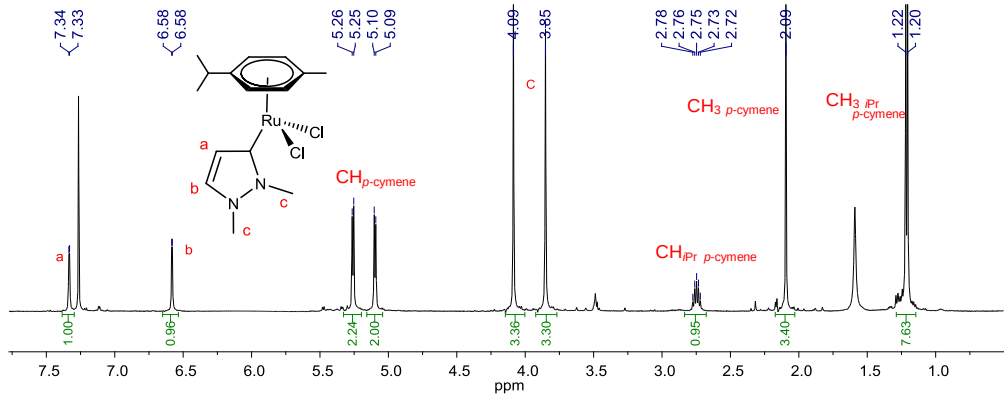

Figure 2.9 ^{1}H NMR spectrum of complex **9F** in $CDCl_3$

*$^{13}C\ \{^{1}H\}$ NMR spectrum of complex **9F***

Figure 2.10 shows the $^{13}C\ \{^{1}H\}$ NMR spectrum of **9F**. The most characteristic signal is the one attributed to the metallated carbene-carbon at 180.3 ppm (a). The signals due to the rest of the carbon atoms of the pyrazole ring are shown at 133.0 ppm (b) and 117.1 ppm (c). The rest of the signals are conveniently assigned on the spectrum and are consistent with the structure proposed.

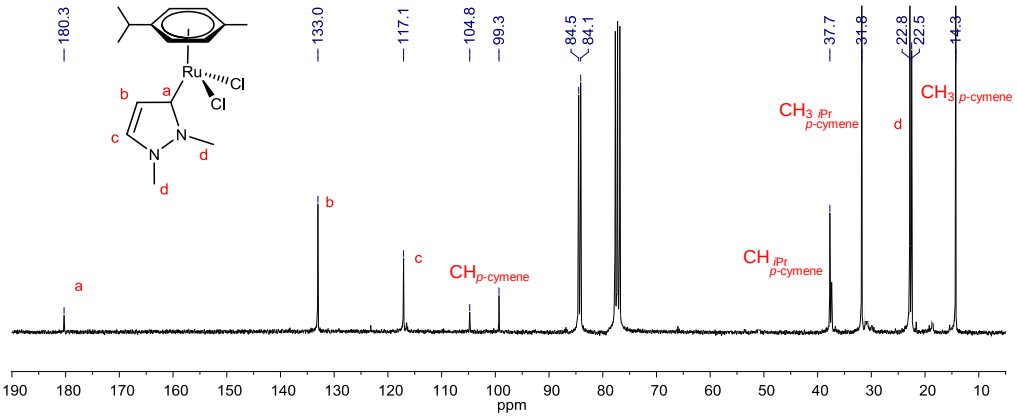

Figure 2.10 $^{13}C\ \{^{1}H\}$ NMR spectrum of complex **9F** in $CDCl_3$

*Molecular structure of **9F***

Crystals of **9F** suitable for X-ray diffraction analysis were obtained by slow diffusion of pentane into a dichloromethane solution of the compound.

The geometry of **9F** can be regarded as a three-legged piano stool similar to that of **8E**. The molecular structure (Figure 2.11) confirms the coordination of the NHC ligand through the C(1) of the pyrazole ring. Along with the pyrazolylidene ligand, two chloride ligands and a *p*-cymene complete the coordination sphere about the metal atom.

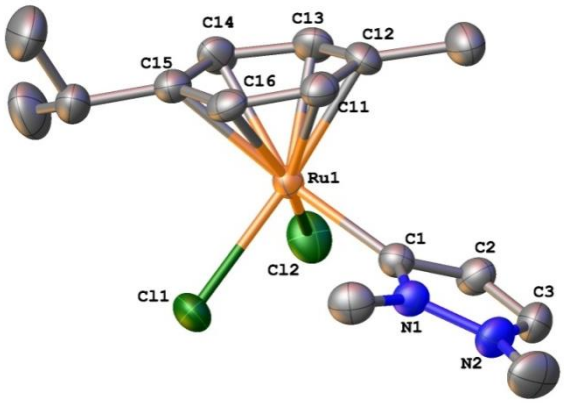

Figure 2.11 Molecular diagram of complex **9F**. Ellipsoids are at 30% probability. Hydrogen atoms have been omitted for clarity.

Table 2.3 Selected bond lengths (Å) and angles (º) of complex **9F**

Bonds		**Angles**	
Ru(1)-C(1)	2.044(5)	C(1)-Ru(1)-Cl(1)	88.54(13)
Ru(1)-Cl(1)	2.4295(13)	C(1)-Ru(1)-Cl(2)	86.47(14)
Ru(1)-Cl(2)	2.4201(14)	Cl(1)-Ru(1)-Cl(2)	87.31(5)
Ru(1)-$C_{centroide}$	1.695		

Table 2.3 shows the most representative bond distances (Å) and angles (º) of complex **9F**. The Ru-$C_{carbene}$ distance is 2.044 Å, in the range of other 'Ru(*p*-cymene)(NHC)'

complexes.[34, 38] The Ru-Cl and Ru-$C_{centroide}$ distances, and the $C_{carbene}$-Ru-Cl angles lie in the expected range.

2.2.2.3 Synthesis and characterization of 'Ru(η^6-arene)(triazolylidene)' complexes

Most of the experiments described in this section were carried out in the School of Chemistry & Chemical Biology at the University College of Dublin under the co-supervision of Prof. Martin Albrecht.

The syntheses of the triazolylidene-based complexes **11G** and **12G** (Scheme 2.16) were again carried out following the transmetallation coordination strategy using $[RuCl_2(p\text{-cymeme})]_2$ and $[RuCl_2(CMe)_6]_2$ as metal precursors. The silver-NHC complex was obtained by reaction of salt [**G**H]I with Ag_2O at room temperature in dichloromethane under the exclusion of light. The silver complex was filtered through Celite to eliminate the excess of Ag_2O and other insoluble by-products. The Ru(II) precursors were then added to the solution. The mixture was stirred for 3h at room temperature. The crude was filtered through Celite to eliminate AgI, and the solvent was removed under reduced pressure. Compounds **11G** and **12G** were purified by column chromatography and the pure complexes were precipitated from a mixture of dichloromethane/diethyl ether as orange solids in 71% (**11G**) and 62% (**12G**) yields. Both complexes were characterized by NMR and mass spectrometry and elemental analysis.

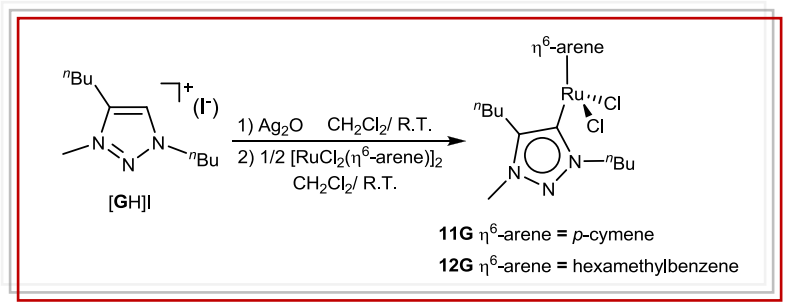

Scheme 2.16 Synthesis of **11G** and **12G**

*^{1}H NMR spectra of complexes **11G** and **12G***

There are significant chemical shift differences between **11G** and **12G**, which may reflect the stronger electron-donating power of the hexamethylbenzene ligand compared to that of the *p*-cymene one. Figure 2.12 and Figure 2.13 show the 0-5.5 ppm region of the ^{1}H NMR spectra of **11G** and **12G**, respectively. The resonances due to the diastereotopic protons of the R-CH_2 groups (N-CH_2 and C_{trz}-CH_2) of the heterocycle substituents are shown.

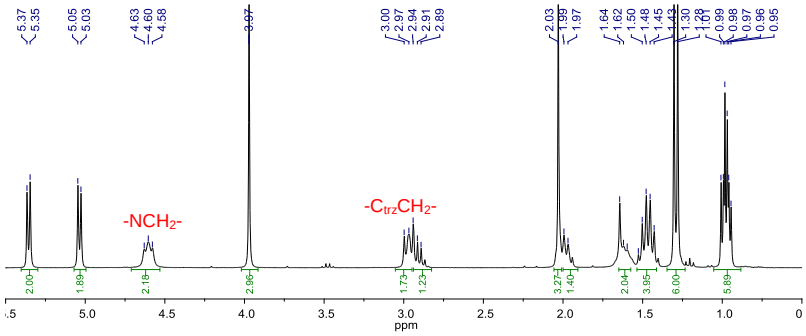

Figure 2.12 ^{1}H NMR spectrum of complex **11G** in $CDCl_3$

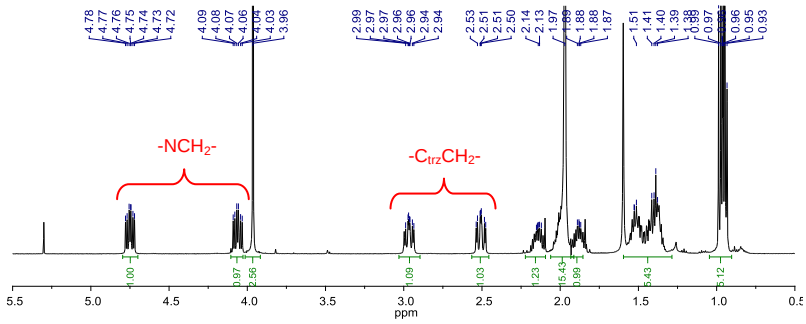

Figure 2.13 ^{1}H NMR spectrum of complex **12G** in $CDCl_3$

Due to the similarity of these two compounds, only the carbon spectroscopic characterization of **12G** is discussed in detail. All the details of the spectroscopic data for compound **11G** can be found in the Experimental Section.

*$^{13}C\ \{^1H\}$ NMR spectrum of complex **12G***

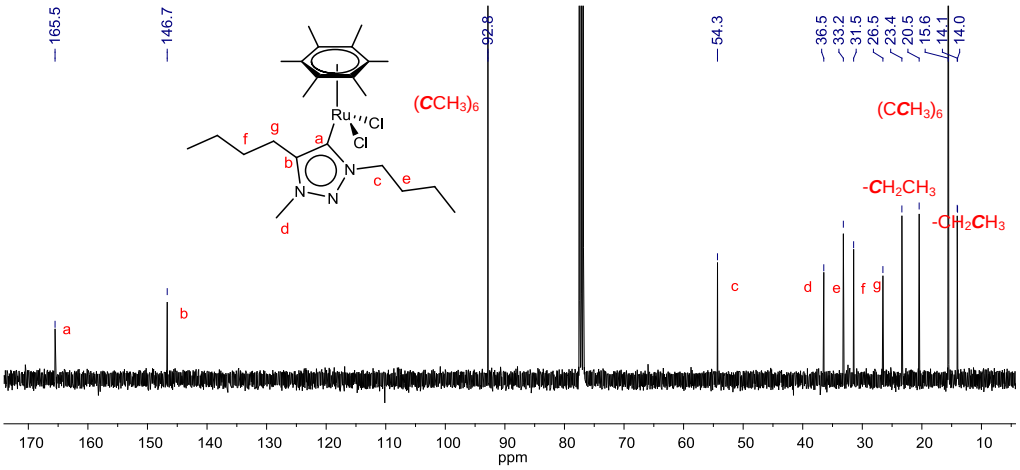

Figure 2.14 $^{13}C\ \{^1H\}$ NMR spectrum of complex **12G** in $CDCl_3$

Figure 2.14 shows the $^{13}C\ \{^1H\}$ NMR spectrum of **12G**. The most characteristic signal is the one attributed to the metallated carbene-carbon at 165.5 ppm (a). The signal due to the quaternary carbon of the triazole appears at 146.7 ppm (b). All other signals attributed to the *n*-butyl, N-CH_3 and hexamethylbenzene groups are conveniently assigned on the NMR spectrum and are consistent with the proposed structure of the complex.

*Molecular structure of **12G***

Crystals of **12G** suitable for X-ray diffraction analysis were obtained by slow diffusion of pentane into a dichloromethane solution of the compound. The geometry of **12G** can be regarded as a three-legged piano stool similar to that of **8E** and **9F**. The molecular structure (Figure 2.15) confirms the coordination of the NHC ligand throught the C(1) of the triazole ring. Along with the triazolylidene ligand, two chloride ligands and a hexamethylbenzene ligand complete the coordination sphere about the ruthenium atom.

Table 2.4 shows the most representative bond distances (Å) and angles (º) of complex **12G**. The Ru(1)-C(1) bond length is 2.093(6) Å, and hence slightly longer in

comparison to similar bonds in other 'Ru(η^6-arene)(NHC)' complexes.[34, 38] The long bond distance may be a consequence of the steric constraints imposed by the hexamethylbenzene, as suggested by ^{1}H NMR spectroscopy. The chloride and the triazolylidenes ligands occupy a regular face of the ruthenium center, with L-Ru-L' bond angles between 86.0 and 90.4º.

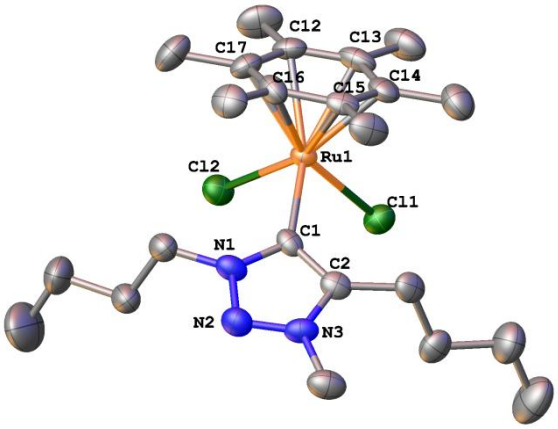

Figure 2.15 Molecular diagram of complex **12G**. Ellipsoids are at 50% probability. Hydrogen atoms have been omitted for clarity.

Table 2.4 Selected bond lengths (Å) and angles (º) of complex **12G**

Bonds		**Angles**	
Ru(1)-C(1)	2.093(6)	C(1)-Ru(1)-Cl(1)	87.11(19)
Ru(1)-Cl(1)	2.4386(19)	C(1)-Ru(1)-Cl(2)	90.44(18)
Ru(1)-Cl(2)	2.4377(19)	Cl(1)-Ru(1)-Cl(2)	86.08(7)
Ru(1)-$C_{centroide}$	1.718		

Anion metathesis with ethanolic Na_2CO_3 of **11G** and **12G** at room temperature during 3 h, allowed the formation of the Ru(II) carbonated species **13G** and **14G** (Scheme 2.17). The mixture was filtered through Celite and the solvent was removed under reduced pressure. The precipitation with cold Et_2O afforded both complexes as yellow solids in 45% (**13G**) and 75% (**14G**) yields.

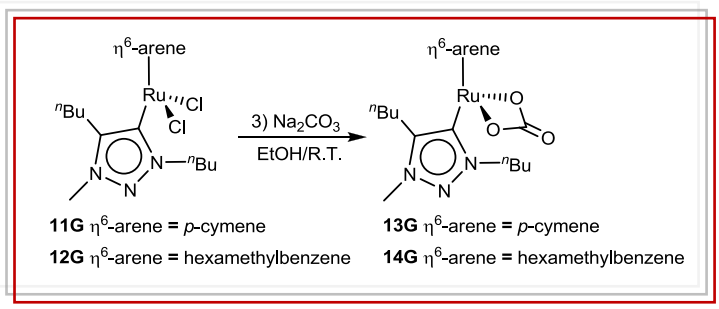

Scheme 2.17 Synthesis of **13G** and **14G**

*^{1}H NMR spectra of complexes **13G** and **14G***

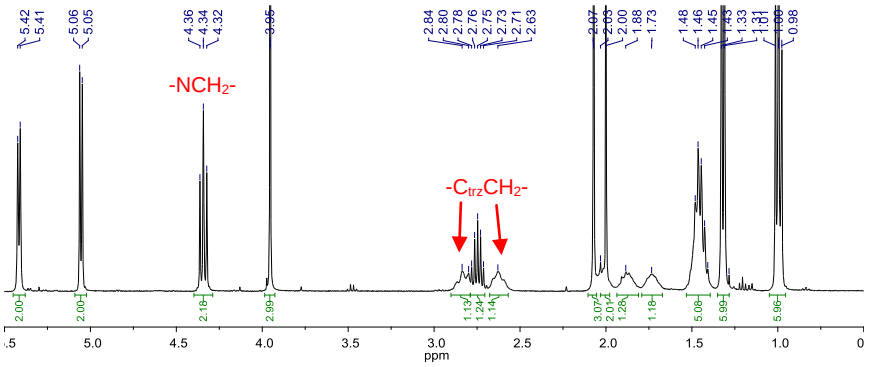

Figure 2.16 ^{1}H NMR spectrum of complex **13G** in $CDCl_3$

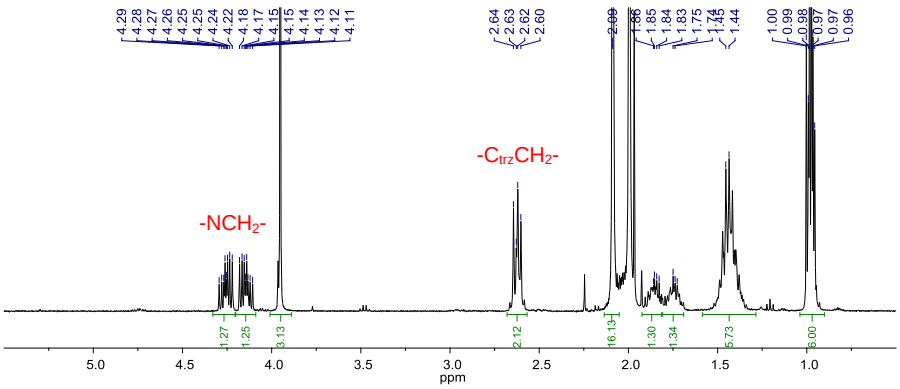

Figure 2.17 ^{1}H NMR spectrum of complex **14G** in $CDCl_3$

Figure 2.16 and Figure 2.17 show the ^{1}H NMR spectra of the new complexes. An upfield shift of the N-CH_2 resonance (from δ_H 4.61 in **11G** to δ_H 4.34 in **13G**) constitutes more evidence for successful chloride substitution. In addition, the

separation of the multiplets in **14G** is considerably less pronounced than in **12G**, which may be attributed to a substantial decrease of the X-Ru-X bond angle from 86.1º in **12G** (X=Cl) to an estimated 60º in **14G**. Accordingly, rotation should become less hindered and the chemical environment of the two hydrogens in each methylene group is more equivalent.

Direct evidence of the presence of the carbonate group was provided by the ^{13}C NMR resonance at 166.7 ppm (**13G**) and 169.0 ppm (**14G**), and by the strong IR absorption band at 1611 cm^{-1} (**13G**) and 1602 cm^{-1} (**14G**), as shown for other previously reported 'Ru(η^6-arene)(NHC)(CO_3)' complexes.[39]

2.2.3 Synthesis and characterization of 'IrCp*(NHC)' complexes

In this section the preparation of the iridium complex **17F** will be discussed. For comparative purposes, the previously described IrCp*(NHC) complexes **15B**[40] and **16D**[41] were also prepared, according to the literature methods.

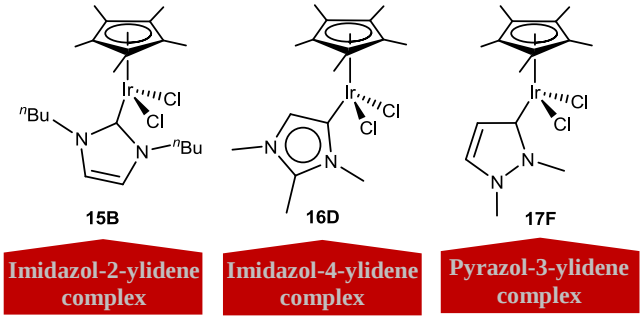

Figure 2.18 'IrCp*(NHC)' complexes

17F was prepared by transmetallation from the corresponding silver(I)-NHC complexes prepared by treatment of the pyrazolium salt [**F**H]I with Ag_2O (Scheme 2.18). Pure complex **17F** was obtained in a 40% yield, after being purified by column chromatography.

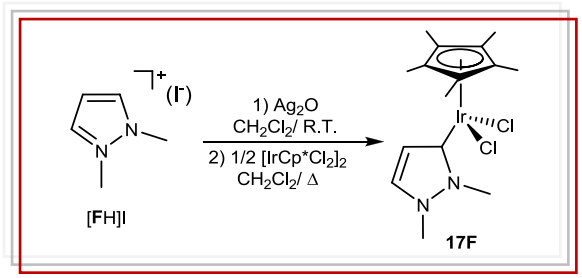

Scheme 2.18 Synthesis of **17F**

Compound **17F** was characterized by NMR and mass spectrometry and elemental analysis.

*^{1}H NMR spectrum of complex **17F***

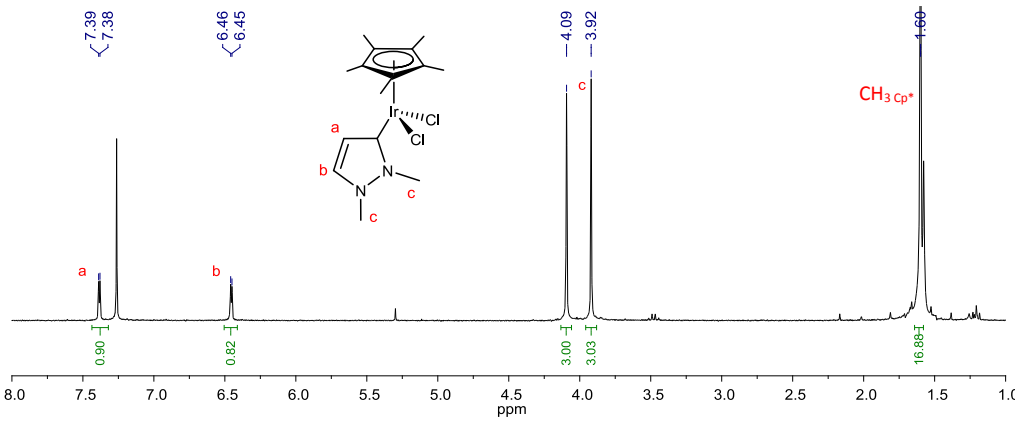

Figure 2.19 ^{1}H NMR spectrum of complex **17F** in $CDCl_3$

Figure 2.19 shows the ^{1}H NMR spectrum of **17F**. The signals due to the protons of the pyrazole ring are shown as two doublets at 7.39 ppm (a) and 6.46 ppm (b). Due to the loss of symmetry of the ligand precursor, the signals assigned to the protons of to the methyl groups appear as two singlets at 4.09 and 3.92 ppm (c). Finally, the resonance at 1.60 ppm is assigned to the protons of the Cp* methyl groups.

*^{13}C {^{1}H} NMR spectrum of complex **17F***

Figure 2.20 shows the ^{13}C {^{1}H} NMR spectrum of complex **17F**. The signal corresponding to the metallated carbene-carbon appears at 162.4 ppm (a). The carbons of the CH groups of the pyrazole display their resonances at 135.4 and 117.2

ppm (b and c, respectively). All other signals are conveniently assigned on the spectrum.

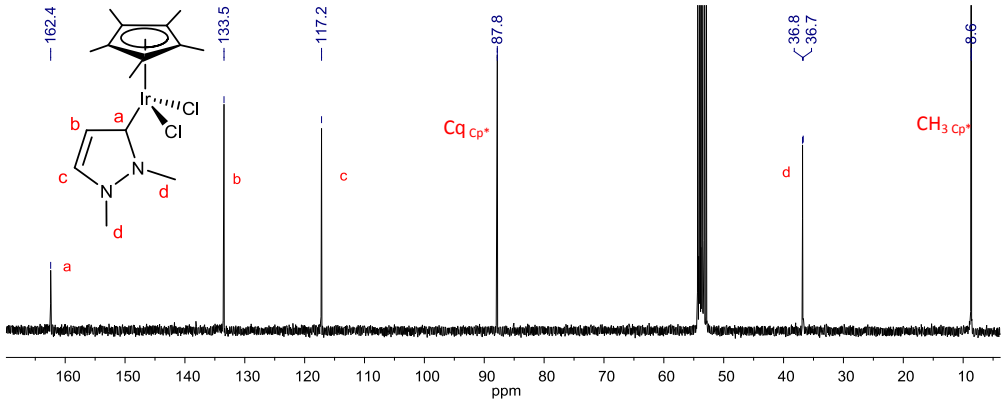

Figure 2.20 $^{13}C\{^{1}H\}$ NMR spectrum of complex **17F** in $CDCl_3$

2.3 Conclusions

A set of simple 'Ru(η^6-arene)(NHC)' and 'IrCp*(NHC) complexes with different NHC ligands have been prepared. The complexes were obtained using two methodologies, namely, transmetallation from the corresponding silver(I)-carbene pre-formed complexes and deprotonation of the azolium salt with a weak base. More precisely:

- First, a series of azolium salts, suitable precursors of mono-carbene N-heterocyclic ligands, has been synthesized by the usual methodologies. In principle, these ligands should provide different electronic and steric properties to the metal complexes, a fact that may have consequences in their catalytic outcomes (as will be described in Chapter 3).
- A series of 'Ru(η^6-arene)(NHC)' complexes have been obtained. Three different η^6-arene ligands (*p*-cymene, hexamethylbenzene and methylbenzoate), and different NHC ligands (imidazol-2-ylidene, imidazol-4-ylidene, pyrazol-3-ylidene and triazolylidene) were selected for the tuning of the electronic and steric properties of the isolated metal complexes. Ru-pyrazolylidene complexes **9F** and **10F** constitute the first examples of ruthenium complexes bearing pyrazolylidene-based ligands, and two of the very few examples known for transition metal complexes.
- Three 'IrCp*(NHC)' complexes containing imidazol-2-ylidene, imidazol-4-ylidene and pyrazol-3-ylidene ligands have also been synthesized. In particular, the pyrazol-3-ylidene Ir(I) complex constitutes one of the very few examples of metal complexes with this type of ligand.

2.4 References

(1) Poyatos, M.; Mata, J. A.; Peris, E. *Chem. Rev.* **2009**, *109*, 3677; Schuster, O.; Yang, L. R.; Raubenheimer, H. G.; Albrecht, M. *Chem. Rev.* **2009**, *109*, 3445; de Fremont, P.; Marion, N.; Nolan, S. P. *Coord. Chem. Rev.* **2009**, *253*, 862; Kruger, A.; Albrecht, M. *Aust. J. Chem.* **2011**, *64*, 1113; Poulain, A.; Iglesias, M.; Albrecht, M. *Curr. Org. Chem.* **2011**, *15*, 3325; Mata, J. A.; Poyatos, M.; Peris, E. *Coord. Chem. Rev.* **2007**, *251*, 841.

(2) Grundemann, S.; Kovacevic, A.; Albrecht, M.; Faller, J. W.; Crabtree, R. H. *Chem. Commun.* **2001**, 2274.

(3) Grundemann, S.; Kovacevic, A.; Albrecht, M.; Faller, J. W.; Crabtree, R. H. *J. Am. Chem. Soc.* **2002**, *124*, 10473; Eguillor, B.; Esteruelas, M. A.; Olivan, M.; Puerta, M. *Organometallics* **2008**, *27*, 445; Cavallo, L.; Correa, A.; Costabile, C.; Jacobsen, H. *J. Organomet. Chem.* **2005**, *690*, 5407.

(4) Kovacevic, A.; Grundemann, S.; Miecznikowski, J. R.; Clot, E.; Eisenstein, O.; Crabtree, R. H. *Chem. Commun.* **2002**, 2580; Appelhans, L. N.; Zuccaccia, D.; Kovacevic, A.; Chianese, A. R.; Miecznikowski, J. R.; Macchioni, A.; Clot, E.; Eisenstein, O.; Crabtree, R. H. *J. Am. Chem. Soc.* **2005**, *127*, 16299; Baya, M.; Eguillor, B.; Esteruelas, M. A.; Olivan, M.; Onate, E. *Organometallics* **2007**, *26*, 6556.

(5) Lebel, H.; Janes, M. K.; Charette, A. B.; Nolan, S. P. *J. Am. Chem. Soc.* **2004**, *126*, 5046.

(6) Kovacevic, A.; Meadows, K. R.; Counts, M.; Arthur, D. J. *Inorg. Chim. Acta* **2011**, *373*, 259.

(7) Chianese, A. R.; Kovacevic, A.; Zeglis, B. M.; Faller, J. W.; Crabtree, R. H. *Organometallics* **2004**, *23*, 2461.

(8) Arnold, P. L.; Pearson, S. *Coord. Chem. Rev.* **2007**, *251*, 596.

(9) Ellul, C. E.; Mahon, M. F.; Saker, O.; Whittlesey, M. K. *Angew. Chem. Int. Ed.* **2007**, *46*, 6343.

(10) Krueger, A.; Haeller, L. J. L.; Mueller-Bunz, H.; Serada, O.; Neels, A.; Macgregor, S. A.; Albrecht, M. *Dalton Trans.* **2011**, *40*, 9911.

(11) Krüger, A. K., E.; Müller-Bunz, H.; Neels, A.; Albrecht M. *Eur. J. Inorg. Chem.* **2012**, 1394.

(12) Song, G. Y.; Zhang, Y.; Li, X. W. *Organometallics* **2008**, *27*, 1936; Leuthausser, S.; Schwarz, D.; Plenio, H. *Chem.-Eur. J.* **2007**, *13*, 7195; Kelly, R. A.; Clavier, H.; Giudice, S.; Scott, N. M.; Stevens, E. D.; Bordner, J.;

Samardjiev, I.; Hoff, C. D.; Cavallo, L.; Nolan, S. P. *Organometallics* **2008**, *27*, 202.

(13) Gusev, D. G. *Organometallics* **2009**, *28*, 6458.

(14) Ofele, K.; Roos, E.; Herberhold, M. *Z.Naturforsch.(B)* **1976**, *31*, 1070.

(15) Kocher, C.; Herrmann, W. A. *J. Organomet. Chem.* **1997**, *532*, 261.

(16) Herrmann, W. A.; Schutz, J.; Frey, G. D.; Herdtweck, E. *Organometallics* **2006**, *25*, 2437.

(17) Han, Y.; Huynh, H. V.; Tan, G. K. *Organometallics* **2007**, *26*, 6581; Han, Y.; Huynh, H. V. *Chem. Commun.* **2007**, 1089.

(18) Raubenheimer, H. G.; Desmet, M.; Lindeque, L. *J. Chem. Res.-S* **1995**, 184.

(19) Raubenheimer, H. G.; Desmet, M.; Olivier, P.; Kruger, G. J. *J. Chem. Soc.-Dalton Trans.* **1996**, 4431.

(20) Kessler, F.; Szesni, N.; Maass, C.; Hohberger, C.; Weibert, B.; Fischer, H. *J. Organomet. Chem.* **2007**, *692*, 3005.

(21) Tafipolsky, M.; Scherer, W.; Ofele, K.; Artus, G.; Pedersen, B.; Herrmann, W. A.; McGrady, G. S. *J. Am. Chem. Soc.* **2002**, *124*, 5865.

(22) Enders, D.; Breuer, K.; Raabe, G.; Runsink, J.; Teles, J. H.; Melder, J. P.; Ebel, K.; Brode, S. *Angew. Chem. Int. Edit. Engl.* **1995**, *34*, 1021.

(23) Guisado-Barrios, G.; Bouffard, J.; Donnadieu, B.; Bertrand, G. *Angew. Chem. Int. Ed.* **2010**, *49*, 4759.

(24) Mathew, P.; Neels, A.; Albrecht, M. *J. Am. Chem. Soc.* **2008**, *130*, 13534.

(25) Kolb, H. C.; Finn, M. G.; Sharpless, K. B. *Angew. Chem. Int. Ed.* **2001**, *40*, 2004.

(26) Poulain, A.; Canseco-Gonzalez, D.; Hynes-Roche, R.; Muller-Bunz, H.; Schuster, O.; Stoeckli-Evans, H.; Neels, A.; Albrecht, M. *Organometallics* **2011**, *30*, 1021; Bernet, L.; Lalrempuia, R.; Ghattas, W.; Mueller-Bunz, H.; Vigara, L.; Llobet, A.; Albrecht, M. *Chem. Commun.* **2011**, *47*, 8058; Bouffard, J.; Keitz, B. K.; Tonner, R.; Guisado-Barrios, G.; Frenking, G.; Grubbs, R. H.; Bertrand, G. *Organometallics* **2011**, *30*, 2617; Yuan, D.; Huynh, H. V. *Organometallics* **2012**, *31*, 405.

(27) Keske, E. C.; Zenkina, O. V.; Wang, R.; Crudden, C. M. *Organometallics* **2012**, *31*, 456.

(28) Iglesias, M.; Albrecht, M. *Dalton Trans.* **2010**, *39*, 5213.

(29) Compendium of Chemical Terminology, (E. A. D. M., A. Wilkinson), Blackwell Scientific, Oxford, , 2007; XML online corrected version:

http://goldbook.iupac.org (2006) created by M. Nic, J. Jirat, B. Kosata; updates compiled by A. Jenkins [http://goldbook.iupac.org/M03842.html].

(30) Herrmann, W. A.; Kocher, C.; Goossen, L. J.; Artus, G. R. J. *Chem.-Eur. J.* **1996**, *2*, 1627.

(31) Sala, A.; Ferrario, F.; Rizzi, E.; Catinella, S.; Traldi, P. *Rapid Commun. Mass Spectrom.* **1992**, *6*, 388.

(32) Ricciardi, F.; Romanchick, W. A.; Joullie, M. M. *J. Polym. Sci. Pol. Chem.* **1983**, *21*, 1475.

(33) Fuerstner, A.; Alcarazo, M.; Krause, H.; Lehmann, C. W. *J. Am. Chem. Soc.* **2007**, *129*, 12676.

(34) Herrmann, W. A.; Elison, M.; Fischer, J.; Kocher, C.; Artus, G. R. J. *Chem.-Eur. J.* **1996**, *2*, 772.

(35) Mercs, L.; Neels, A.; Albrecht, M. *Dalton Trans.* **2008**, 5570.

(36) Wang, H. M. J.; Lin, I. J. B. *Organometallics* **1998**, *17*, 972.

(37) Chianese, A. R.; Zeglis, B. M.; Crabtree, R. H. *Chem. Commun.* **2004**, 2176; Bacciu, D.; Cavell, K. J.; Fallis, I. A.; Ooi, L. L. *Angew. Chem. Int. Ed.* **2005**, *44*, 5282; Alcarazo, M.; Roseblade, S. J.; Cowley, A. R.; Fernandez, R.; Brown, J. M.; Lassaletta, J. M. *J. Am. Chem. Soc.* **2005**, *127*, 3290.

(38) Cariou, R.; Fischmeister, C.; Toupet, L.; Dixneuf, P. H. *Organometallics* **2006**, *25*, 2126; Poyatos, M.; Mas-Marza, E.; Sanau, M.; Peris, E. *Inorg. Chem.* **2004**, *43*, 1793; Ozdemir, I.; Demir, S.; Cetinkaya, B.; Toupet, L.; Castarlenas, R.; Fischmeister, C.; Dixneuf, P. H. *Eur. J. Inorg. Chem.* **2007**, 2862.

(39) Azua, A.; Sanz, S.; Peris, E. *Organometallics* **2010**, *29*, 3661; Demerseman, B.; Mbaye, M. D.; Semeril, D.; Toupet, L.; Bruneau, C.; Dixneuf, P. H. *Eur. J. Inorg. Chem.* **2006**, 1174.

(40) Corberan, R.; Sanau, M.; Peris, E. *J. Am. Chem. Soc.* **2006**, *128*, 3974.

(41) Viciano, M.; Feliz, M.; Corberan, R.; Mata, J. A.; Clot, E.; Peris, E. *Organometallics* **2007**, *26*, 5304.

Chapter 3

Catalytic properties of Ru(II) and Ir(III) complexes in C-H bond activation processes

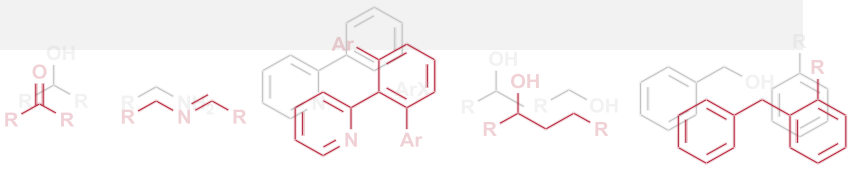

3.1 Introduction

In the last few years, an enormous number of catalytic applications of NHC-based metal complexes have been described and reviewed.[1]

It is now widely accepted that there is a connection between the activity of the catalyst in C-H bond activation processes and the electron-donor character of the ligands present in the catalyst.[2-3] With this in mind, and taking into account the strong electron-donor power of NHCs, this chapter deals with the evaluation of the catalytic properties of the complexes described in Chapter 2 in a series of *C-H bond activation processes*, especially those regarding *borrowing-hydrogen mechanisms* and arylation of arenes.

The following two introductory sections will try to give a short overview on these two types of general catalytic processes.

3.1.1 Catalytic reactions through borrowing-hydrogen mechanisms

The catalytic processes governed by a borrowing-hydrogen mechanism represent a range of reactions in which the catalyst serves as a hydrogen carrier between the substrates.[4-8] The search for efficient catalysts for borrowing-hydrogen processes is a challenging issue, mainly because this type of reactions provides access to a wide variety of highly valuable organic molecules under environmental-friendly workups.

The key to the catalytic cycle is the borrowing of hydrogen: dehydrogenation of an alcohol to aldehyde releases H_2, which would be stored by the catalyst and then returned in the final hydrogenation step. In a typical borrowing-hydrogen reaction, the first step implies the oxidation of a substrate, usually an alcohol, by a metal catalyst which 'borrows' two hydrogen atoms, thus forming a metal-hydride and an aldehyde or ketone. The carbonyl compound can react *in situ* to lead to a wide range of products, as depicted in Scheme 3.1. Indeed, the carbonyl compound can condensate with an amine, alkane or alcohol, to generate an imine, alkene or ketone, respectively. In the final step of the reaction, the metal-hydride 'returns' the two

hydrogen atoms to the generated compound, leading to the formation of amines (a), alkanes (b) or functionalized alcohols (c). In all cases there is, ideally, no net hydrogen loss or gain during the reaction sequence.

These reactions follow the highest atom-economic conditions, since all the atoms of the substrates appear in the products or, at most, the generated byproducts are H_2O or NH_3, so the process is considered to fit within the grounds of green chemistry.

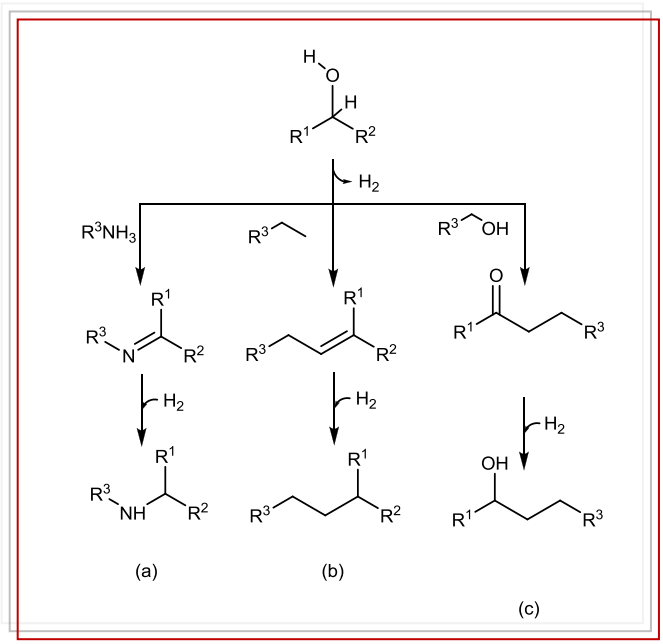

Scheme 3.1 Borrowing-hydrogen reactions

The principles governing hydrogen-transfer (or borrowing-hydrogen) processes are common to amines and alcohols. In this regard, the number of catalysts, capable of reacting with both types of substrates has grown considerably in the last few years, and most of them refer to Ru(II)[9-14] and Ir(III)-based[13, 15-17] catalysts. Specifically, Shvo's catalyst (Scheme 3.2) has exceptional features that make it one of the most effective catalysts for the transfer hydrogenation to alkenes, alkynes, carbonyl groups and imines from alcohols and other dihydrogen sources.[11, 18] As shown in Scheme 3.2, Shvo's catalyst is a dimeric pre-catalyst that forms monomeric oxidizing (**I**) and reducing (**II**) forms upon dissociation in solution. The concentrations of these active

forms are governed by equilibrium effects; compounds **I** and **II** interconvert through the gain or loss of hydrogen from donors (AH_2) and acceptors (A).

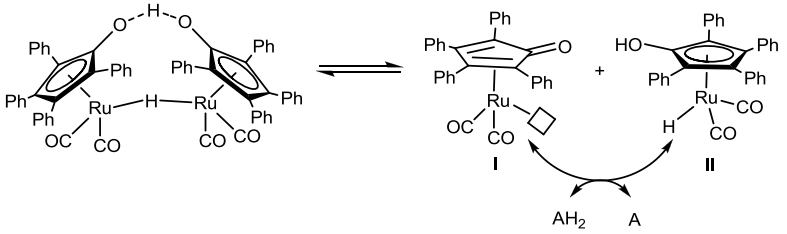

Scheme 3.2 Shvo's catalyst, **I** and **II** interconvert in the presence of a hydrogen acceptor (A) or donor (AH_2)

As will be discussed later, the catalytic properties of the Ru(II) and Ir(III) complexes described in Chapter 2 were studied in a wide set of reactions governed by the *borrowing-hydrogen* mechanism. The reactions studied imply a dehydrogenative activation of alcohols or amines. Our initial aim was to study a series of catalytic reactions under the 'greenest' possible conditions, thus using non-toxic solvents under the highest atom-economic conditions and minimum waste of energy.

3.1.2 C-H Activation/C-C bond formation processes

Metal-catalyzed cross-coupling reactions constitute the most useful method for C-C bond formation.[19] During recent years, transition metal-catalyzed C-H bond functionalizations have matured to being increasingly viable alternatives to traditional cross-coupling reactions, which avoid the use of organometallic reagents in stoichiometric quantities (Scheme 3.3).

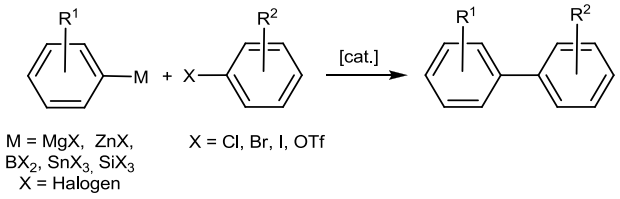

Scheme 3.3 Biaryl synthesis *via* traditional transition-metal-catalyzed cross-coupling reactions

The C-H bond activation allows the use of cheap and readily available starting materials, shortening reaction sequences, and providing compounds that are otherwise difficult to synthesize. In this context, various protocols for efficient catalytic direct arylations for versatile biaryl and heterocycle synthesis were established.[20, 21] The substrates are found from a wide range of important compounds, including natural products, pharmaceuticals, agrochemicals, and functional materials.[22] Although palladium catalysts have been the most widely employed in the direct arylation of arenes,[23] other metals have also been examined, including Ru,[24] Rh[25-26] and Cu,[27] albeit with different degrees of success.

During the development of this Ph. D. Thesis, we focused our interest on two types of C-H activation/C-C bond formation processes, namely, the benzylation of arenes catalyzed by 'IrCp*(NHC)' complexes, and the chelation-assisted arylation of arylpyridines catalyzed by 'Ru(η^6-arene)(NHC)' complexes.

Benzylation of arenes: 'Classical' well known C-C coupling reactions such as Friedel-Crafts alkylations are widely used for the functionalization of arenes.[28] In spite of their reliability, these methods have significant drawbacks. For example, the use of benzyl halides as benzylating agents is undesirable from an environmental point of view. Besides, this procedure not only requires to use acid catalysts, which are corrosive (e.g., H_2SO_4, $AlCl_3$, BF_3, etc.), but also generates a large amount of waste materials during the isolation of the products. These are the main reasons why the development of more environmentally friendly transformations of arenes is an important issue in organic chemistry and catalysis.[29] With this in mind, as will be described later in this chapter, we developed a set of catalysts for novel Friedel-Crafts type reactions of benzylation of arenes employing a set of simple benzylic alcohols or other reagents such styrenes, ethers or aldehydes/ketones, under mild conditions with high tolerance towards functional groups.

Chelation-assisted arylation of arylpyridines: traditionally, these reactions required the use of two functionalized starting materials, which are often expensive

and/or difficult to synthesize using conventional methods. In one of the first examples of catalytic C-H activation/C-C bond formation reactions, Murai proposed that the presence of a heteroatom in the substrate could function as a directing group (Scheme 3.4).[30] Ever since, many other examples have appeared that are based on this simple idea.[31] In general, the reactions using the chelation assistance of a directing group take place through a kinetically and thermodynamically favored five or six-membered metallacycle. The presence of a heteroatom (as directing group) in the substrate allows the metal to approach the C-H bond (that otherwise would be completely unreactive).

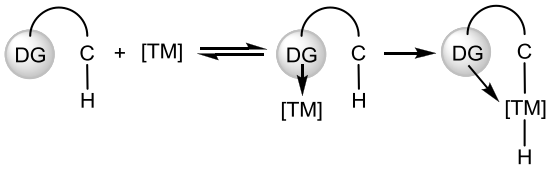

Scheme 3.4 C-H Bond functionalization through the use of directing groups (DG)

3.2 Results and Discussion

In the following sections, the catalytic results achieved with the NHC-based complexes described in Chapter 2 will be described. It is advisable to use the table containing the different complexes attached to the thesis in order to facilitate the reading of the chapter.

We have classified the different catalytic tests according to the metal fragment involved:

➢ **Catalytic activity of 'Ru(η^6-arene)(NHC)' complexes**:

Borrowing-hydrogen processes:

β-Alkylation of secondary alcohols with primary alcohols

Oxidation and oxidative coupling

Other *C-H activation processes*:

Dimerization of phehylacetylene

Chelation-assisted reactions: arylation and deuteration of arylpyridines

➢ **Catalytic activity of 'IrCp*(NHC)' complexes**:

Borrowing-hydrogen processes:

Dehydrogenation of alcohols

Homo-coupling of alcohols

Cross-coupling of alcohols and amines

Other *C-H activation processes*:

Functionalization of arenes

3.2.1 Catalytic activity of 'Ru(η^6-arene)(NHC)' complexes

When talking about Ru-NHC chemistry, it is inevitable to mention the enormous applications that these compounds have achieved in the development of highly effective catalysts for the metathesis of olefins.[32] Ruthenium complexes have also demonstrated a great potential in the development of metal-based drugs, and many

studies have shown their cytotoxicity against several cancer cell lines, including those cisplatin-resistant.[33]

In the last years, interesting catalytic non-metathetical applications of Ru-NHC complexes have been described.[3] The most frequently studied reactions are C=C and/or C=O hydrogenations[13, 34, 35] and C=C isomerizations.[36] In order to evaluate the catalytic properties of the 'Ru(η^6-arene)(NHC)' complexes described in Chapter 2, we decided to test them in typical non-metathetical reactions catalyzed by Ru(II) compounds implying C-H activation processes which are:

Borrowing-hydrogen processes:

3.2.1.1 *β*-Alkylation of secondary alcohols with primary alcohols

3.2.1.2 Oxidation and oxidative coupling:

a) Catalytic oxidation of alcohols

b) Oxidative homocoupling of amines to from imines

c) Catalytic formation of amides

Other *C-H activation processes*:

3.2.1.3 Dimerization of phehylacetylene

3.2.1.4 Chelation-assisted reactions: arylation and deuteration of arylpyridines

3.2.1.1 *β*-Alkylation of secondary alcohols with primary alcohols

We studied the catalytic activity of the Ru(II) complexes described in Chapter 2 in the *β*-alkylation of secondary alcohols with primary alcohols. We thought that the 'Ru(η^6-arene)(NHC)' complexes could be good candidates for this reaction, since Ru-NHC complexes have proven to be excellent catalysts for the transfer hydrogenation reactions between alcohols and ketones.[37]

Despite its important benefits, we found only a few pioneering examples of *β*-alkylation of secondary alcohols with primary alcohols, catalyzed by Ru(II)[5, 38, 39] and Ir(III)[40] complexes. In this context, the present work benefits from the experience of our research group, which has been interested in this transformation for a long time and achieved a series of remarkable results.[35, 41-42]

The simultaneous activation of two alcohols by a borrowing-hydrogen methodology, can lead to an interesting coupling process. Typically, a secondary alcohol reacts with a primary one establishing a new C-C bond that generates the new product. Mechanistically, as shown in Scheme 3.5, the reactions are believed to involve the oxidation of both alcohols to form a ketone (**I**), an aldehyde (**II**), together with the metal dihydride [M]-$(H)_2$. The presence of a base promotes an aldol condensation, giving an α,β-unsaturated ketone (**III**). The metal-dihydride reduces the C=C and C=O double bounds to give the saturated alcohol (**IV**) recovering the catalyst.[4, 40] The overall reaction consists of a *β*-alkylation of a secondary alcohol with a primary alcohol.

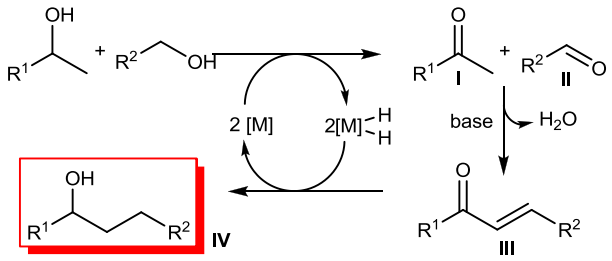

Scheme 3.5 Plausible mechanism for the *β*-alkylation of secondary alcohols with primary alcohols

We decided to test the catalytic performances of complexes **1A**, **7D**, **8E**, **9F** and **10F** bearing three different types of NHC ligands with similar topological features but different electron-donor power (Scheme 3.6). Our purpose was to check the influence of the electron-donating character of the ligand on the catalytic outcome.

In our experiments, the reactions were carried out under atom-economic conditions; this is, using an equimolecular amount of the primary and secondary alcohols. A fixed catalyst loading of 1 mol % was used in the presence of KOH in toluene at 110 °C.

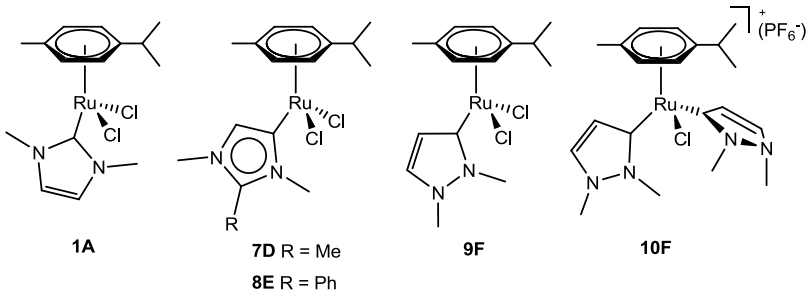

Scheme 3.6 'Ru(η^6-arene)(NHC)' catalysts used in *β*-alkylation of secondary alcohols with primary alcohols

The reactions were performed using 2-phenylethanol and 2-heptanol as secondary alcohols, and four different primary alcohols (*n*-butanol, benzylalcohol, 3-chlorobenzylalcohol and 4-chlorobenzylalcohol). The reaction can lead to two products, the alkylated alcohol or/and the alkylated ketone; the products ratio depends on the selectivity of the catalyst.

Table 3.1 shows the catalytic results for this process. The reaction times reflected in the table correspond to the maximum conversions achieved by each catalyst. As can be observed, all catalysts show good catalytic activities in this reaction, although significant differences are observed between them. The cationic compound **10F** invariably was the best catalyst; full conversions were achieved in short reaction times (8-10 h, entries 5, 10, 15, 20 and 25). The mono-pyrazolylidene complex **9F** also showed an excellent activity in all the reactions tested, although slightly longer reaction times were needed for completion (8-13 h, entries 4, 9, 14, 19 and 24). The *abnormal*-NHC complexes **7D** and **8E** showed good activity in terms of conversions, but longer reaction times were needed (8-24h, entries 2, 3, 7, 8, 12, 13, 17, 18, 22 and 23). The phenyl-substituted NHC complex (**8E**) showed lower efficiency than **7D**, probably due to the higher steric hindrance around the metal center. The *normal*-NHC complex **1A** showed lower activity than the rest of the

catalysts, providing only moderate yields in rather long reaction times (20-24 h, entries 1, 6, 11, 16 and 21).

Table 3.1 *β*-Alkylation of secondary alcohols with primary alcohols[a]

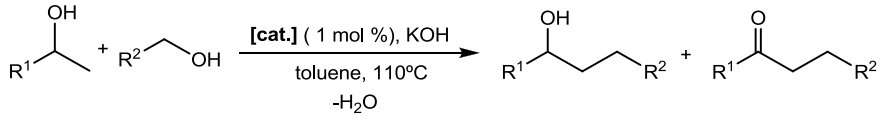

Entry	Cat.	R^1	R^2	t(h)	Conv.(%)[b]	alcohol:ketone[b]
1	**1A**			22	60	78:22
2	**7D**			22	>95	90:10
3	**8E**	Ph	Pr	22	86	91:9
4	**9F**			13	>95	90:10
5	**10F**			10	95	90:10
6	**1A**			24	95	92:8
7	**7D**			24	94	81:19
8	**8E**	Ph	3-Cl(C_6H_4)	24	86	100:0
9	**9F**			10	>95	100:0
10	**10F**			8	>95	85:15
11	**1A**			24	57	100:0
12	**7D**			24	>95	88:12
13	**8E**	Ph	Ph	8	>95	93:7
14	**9F**			8	>95	97:3
15	**10F**			8	>95	90:12
16	**1A**			24	87	92:8
17	**7D**			8	>95	90:10
18	**8E**	Ph	4-Cl(C_6H_4)	24	90	83:17
19	**9F**			8	>95	77:23
20	**10F**			8	>95	96:4
21	**1A**			20	>95	100:0
22	**7D**			14	>95	100:0
23	**8E**	C_5H_{11}	Ph	20	>95	100:0
24	**9F**			10	>95	100:0
25	**10F**			8	>95	100:0

[a]Reaction conditions: 1 mmol of primary alcohol, 1 mmol of secondary alcohol, 1 mmol of KOH and 1 mol % of catalyst in 0.3 mL of toluene at 110ºC. [b]Conversions and ratios were determined by ^{1}H NMR.

In general, the process is very selective in the production of the alkylated alcohols, although in some cases small amounts of the alkylated ketones were obtained as secondary products.

The evolution of the reactions was monitored by ^{1}H NMR. The progress of the reactions was evaluated by comparing the signals corresponding to the initial alcohol with the signals corresponding to the *β*-alkylated alcohol or ketone formed. As an example, Scheme 3.7 shows the signals selected as reference to determine the progress of the reaction between 1-phenylethanol and *n*-butanol. As the reaction evolves, the signals corresponding to the proton of the -CH group of 1-phenylethanol (1H, q, 4.90 ppm) and to the protons of the -C*H*$_2$OH group of *n*-butanol (2H, t, 3.62 ppm) disappear, while new signals due to the products appear. The reference signals for the new products were those corresponding to the proton of the -CH group of the generated alcohol (1H, t, 4.64) and to the protons of the -C*H*$_2$CO group of the generated ketone.

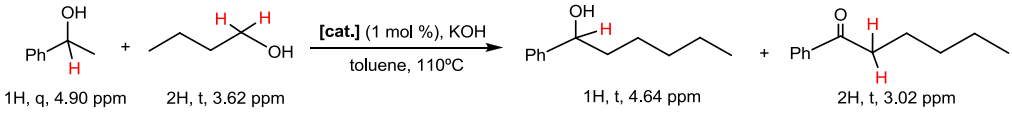

Scheme 3.7 Reference signals for the reaction between 1-phenylethanol and *n*-butanol

An interesting feature about the comparison of the results shown in Table 3.1 is that the different types of NHC ligands provided different activities in a quite rational way. It seems that the more *σ*-donating NHCs (*a*NHCs and pyrazolylidene) are providing the best activities and, among these, the pyrazole-based NHC complexes seem to be the most active ones. Until recently, there were no studies comparing the *σ*-donating capacity of *a*NHCs and pyrazolylidenes but, in a recent analysis of the *σ*-donating character of a wide set of NHCs, Gusev determined that pyrazolylidenes are less *σ*-donor than *a*NHCs.[43] This implies that our results do not fit to a simple assignation of the activities of the catalysts to the *σ*-donor character of their ligands. On the other hand, the pyrazolylidene complexes **9F** and **10F** benefits from a lower steric hindrance than the *a*NHCs-based analogues, as a consequence of the absence of

one of the methyl groups close to the coordination sphere of the metal (see Scheme 3.8), a factor that may be influencing the best catalytic outcome shown by **9F** and **10F.**

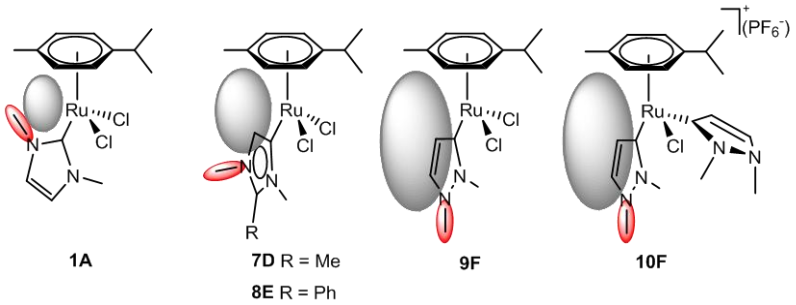

Scheme 3.8 Steric differences comparing the complex

It is worth mentioning that until the time of the publication of these results, compound **10F** was among the most efficient ruthenium catalysts for this type of reaction.[4, 38, 39, 44] For example, Yus and co-workers reported conversions around 90% in three days employing $RuCl_2(DMSO)_4$ under the same conditions used by us.[39] In 2008, our group reported a dinuclear and a tetranuclear compounds of Ru(II) containing the 1,2,4-trimethyltriazolylidene ligand. These complexes improved the reaction times reported by Prof. Yus (20h), demonstrating that the introduction of the basic NHC ligand has some implications in the yield of this C-H activation process.[44] In 2011, our research group reported two iridium complexes, **3.1** and **3.2** (Scheme 3.9), which were even more effective than **10F**.[42] The catalysts achieve complete conversions in shorter reaction times (3-6h). Catalyst **3.1** is also active at a catalyst loading of 0.1 mol%, especially when benzylalcohol and 4-chlorobenzylalcohol were used, although longer reaction times were needed (24 h).

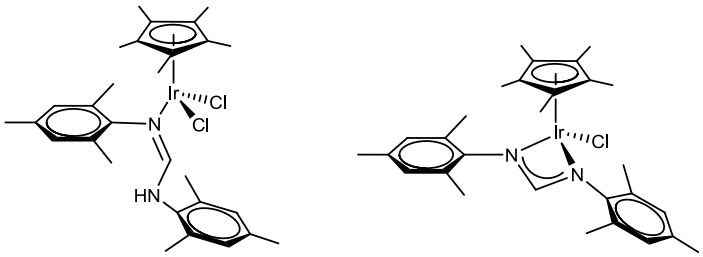

3.1 3.2

Scheme 3.9 Iridium complexes active in *β*-alkylation of secondary alcohols with primary alcohols

Summarizing, the catalytic activity of a series of '$RuCl_2$(*p*-cymene)(NHC)' complexes was tested in the *β*-alkylation of secondary alcohols with primary alcohols. The results obtained and presented were the best reported to the date of their publication and allowed a clear comparison of the activities provided by the different ligands, the pyrazolylidenes (**9F** and **10F**) being the best ones.

3.2.1.2 Oxidation and oxidative couplings

Most of the catalytic experiments described in this section were carried out at the School of Chemistry & Chemical Biology of the University College of Dublin under the co-supervision of Prof. Martin Albrecht.

a) Catalytic oxidation of alcohols

The oxidation of alcohols to carbonyl compounds is one of the most important reactions in organic chemistry. The process exploits the wider range of reactions available to carbonyl compounds.[8] The homogeneously catalyzed base-free dehydrogenation of alcohols should be ideal from the viewpoint of atom efficiency and safety of the reaction, constituting a much more benign methodology than other known Cr-mediated oxidations.[45-48] Moreover, this process generates molecular hydrogen as a more useful side-product.[7, 9, 49, 50]

Since oxidative couplings start from the oxidation of alcohols to aldehydes or ketones, we first studied the catalytic oxidation of alcohols using catalysts **3B**, **11G**, **12G**, **13G** and **14G** (Scheme 3.10). We chose this set of catalysts because ruthenium

complexes are among the best catalysts for this transformation.[45, 50-51] Since 1,2,3-triazolium-based NHCs are a new type of ligands that have been signaled with potential applications in nucleophilic organic transformations, we thought that the set of complexes **11G-14G** could be good candidates to promote these transformations. We decided to evaluate also the catalytic properties of compound **3B** because it is sterically similar to **11G**. Hence, the catalytic differences can be predominantly attributed to the different electronic properties imparted by the two different types of carbene ligands.

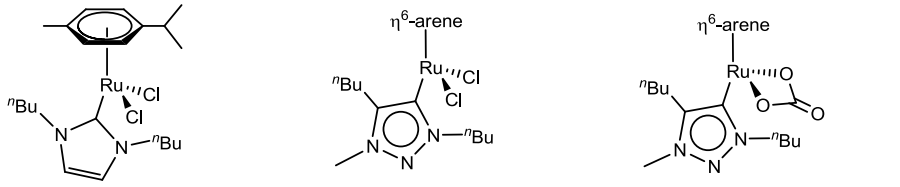

3B

11G η^6-arene = *p*-cymene
12G η^6-arene = hexamethylbenzene
13G η^6-arene = *p*-cymene
14G η^6-arene = hexamethylbenzene

Scheme 3.10 'Ru(η^6-arene)(NHC)' catalysts used in catalytic oxidation of alcohols

As a preliminary test, we chose the oxidation of benzylalcohol into benzylaldehyde, the reaction was carried out in refluxing toluene under base-free conditions, using a catalyst loading of 5 mol %.

Table 3.2 shows the catalytic results for this process. The data revealed the highest activity of complex **11G**. Full conversion to benzaldehyde was observed in 16 h using **11G**, while the analogue complex with the hexamethylbenzene ligand, **12G**, performed considerably worse (entries 2 and 3). The substitution of the chloride ligands in the catalyst for carbonate ligand had diverging effects. Whereas **13G** performed worse than **11G**, a significant increase from 55% (**12G**) to 85% (**14G**) conversion was noted for their hexamethylbenzene counterparts (entries 3 and 5). It seems that the different activity of the catalysts containing different η^6-arene ligands (*p*-cymene or hexamethylbenzene) depends not only on the σ-donor character of the ligand but also on the steric hindrance. The imidazolylidene complex **3B** is less efective than its analogue triazolylidene complex **11G** (entry 6). In this case, more σ-

donating NHCs (triazolylidenes) are providing the best activities. Lowering the temperature to 70ºC still provided high conversion, though increased catalyst loading (10 mol %) and reaction times were required (compare entries 7 and 8).

Table 3.2 Catalyst screening in the oxidation of benzylalcohol[a]

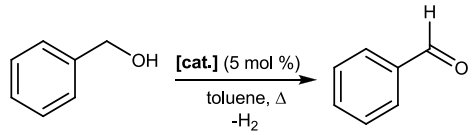

Entry	Cat.	t(h)	Yield (%)[b]
1	none	20	<2
2	**11G**	16	>95
3	**12G**	20	55
4	**13G**	16	82
5	**14G**	16	85
6	**3B**	20	60
7[c]	**11G**	24	32
8[d]	**11G**	24	95

[a]Reaction conditions: 0.2 mmol of benzylalcohol and 5 mol % of catalyst in toluene (2 mL) at reflux. [b]Yields determined by ^{1}H NMR (C_6Me_6 as internal standard). [c]At 70ºC. [d]At 70ºC using 10 mol % of catalyst.

Once complex **11G** was chosen as the best catalyst, the reaction was carried out under the same reaction conditions, with a wide variety of primary alcohols and a secondary alcohol (2-phenylethanol). As shown in Table 3.3, when benzylalcohol and 1-phenylethanol were used good conversions were achieved to benzaldehyde and acetophenone, respectively (entries 1 and 2). Aliphatic alcohols such as 2-phenylethanol and 1-octanol were not oxidized (entries 3 and 4). The electronic nature of the aryl group plays an important role. Electron-withdrawing substituents, regardless of their position, reduced the activity of the catalyst, although the conversions to the final benzylalcohols were still high (entries 5-7).

Table 3.3 Oxidation of different alcohols using **11G**[a]

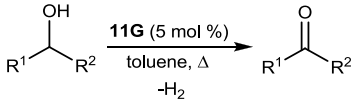

Entry	R^1	R^2	t(h)	Yield (%)[b]
1	C_6H_5	H	16	>95
2		CH_3	24	>95
3	$CH_2C_6H_5$	H	20	<5
4	C_7H_{15}		20	<5
5	4-C_6H_4-NO_2		22	65
6	4-C_6H_4-Cl		22	68
7	2-C_6H_4-Cl		22	70
8	4-C_6H_4-Br		16	91
9	4-C_6H_4-CH_3		16	>95
10	4-C_6H_4-OCH_3		16	90

[a]Reaction conditions: 0.2 mmol of alcohol and 5 mol% of catalyst in toluene (2 mL) at reflux. [b]Yields determined by ^{1}H NMR (C_6Me_6 as internal standard).

The evolution of the reactions described was followed by ^{1}H NMR. The progress of the reaction was evaluated adding hexamethylbenzene as an internal standard. As the reaction takes place, the signals corresponding to the initial substrates (alcohol) decrease while the signals due to the products (aldehyde) appear and increase.

b) Oxidative homocoupling of amines to form imines

In the last few years, considerable attention has been devoted to the oxidation of amines to imines. Imines can act as versatile synthetic intermediates, in particular, as electrophilic reagents in a large number of reactions, including reductions, additions, condensations, and cycloadditions.[52] Traditionally, imines are synthesized from the reaction of ketones or aldehydes with amines in the presence of an acid catalyst. Extensive efforts have been made to develop catalytic systems that use green oxidants for the synthesis of imines from primary amines.[53]

We have focused our interest on the synthesis of imines by self-condensation of aliphatic amines upon oxidation. A schematic mechanism for the reaction is shown in Scheme 3.11. The first step involves the oxidation of the amine to give the imine (**I**) and the metal dihydride [M]-$(H)_2$. The imine reacts with another equivalent of the substrate amine, giving the N-alkylated imine (**II**) and elimination of ammonia. The hydrogen can be liberated to regenerate the catalyst.

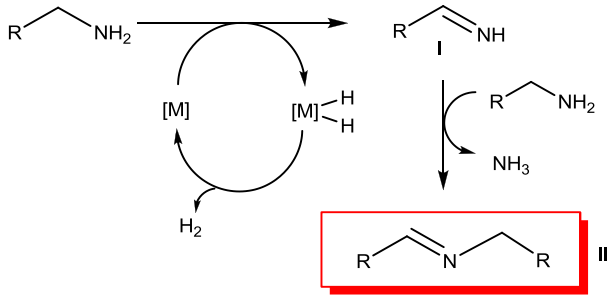

Scheme 3.11 Mechanism for the oxidative homo-coupling of amines to form imines

Due to the good catalytic behavior of complexes **11G-14G** and **3B** in the oxidation of alcohols, we were interested in seeing whether an extension of the catalytic activity to amines under oxidant-free conditions was accessible, hence contributing to the development of green methods for imine production. In principle, we can imagine that the good activity of the catalyst in alcohol oxidation is an indication that the complexes may also be active in the oxidation of amines to imines. The oxidation of amines is the first step in a wide variety of reactions.

For the catalytic tests, the reactions were carried out with different primary amines in toluene and a fixed catalyst amount (5 mol %), in the absence of an auxiliary base. As shown in Table 3.4, the oxidative homocoupling of aromatic amines was observed, cleanly affording the corresponding imines. The imidazolylidene-based complex **3B** was found more active than the triazolylidene-based ones **11G-14G** and reached full conversion after 12 h (entry 6). In contrast, the carbonate-containing complexes were inactive (entries 4 and 5), perhaps because the exchange of the carbonate ligand by an amine is thermodynamically unfavored.

Aliphatic amines were also effectively oxidized, albeit at a lower rate (entries 7 and 8). The substrates with electron-withdrawing substituent in *para*- position gave also high conversions (entry 9). The harsher conditions needed in amine oxidation (150ºC) as compared to those for alcohol oxidation (110ºC) may be a consequence of the slower β-elimination for the case of the amines. These observations insinuate that product release from the metal coordination sphere could be rate-limiting.

Table 3.4 Oxidative homocoupling of amines to imines[a]

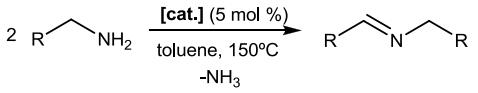

Entry	Cat.	R	t(h)	Yield (%)[b]
1	none	C_6H_5	20	<2
2	**11G**		20	>95
3	**12G**		20	>95
4	**13G**		20	<5
5	**14G**		20	<5
6	**3B**		12	>95
7	**3B**	C_5H_{11}	22	70
8	**3B**	C_3H_7	22	62
9	**3B**	4-C_6H_4-Cl	22	90

[a]Reaction conditions: 0.2 mmol of amine, 5 mol % of catalyst in toluene (2 mL) at 150 °C. [b]Yields determined by ^{1}H NMR (decane as internal standard).

The evolution of the reactions described was followed by ^{1}H NMR. The progress of the reactions was evaluated adding decane as an internal standard. As the reaction takes place, the signals corresponding to the initial substrates (amine) decrease while the signals due to the products (imine) appear and increase.

c) Catalytic formation of amides

Amides are among the most prevalent linkages in organic chemistry. They are the key functional groups in peptides and a number of polymers, and are also found in many pharmaceuticals and natural products.[54] One of the seminal works on the catalytic

amide formation was reported by Milstein and co-workers, who developed a Ru-based catalyst containing a hemilabile PNN pincer ligand.[55] By using this catalyst, primary amines can be directly acylated by equimolecular amounts of alcohols, affording amides and molecular hydrogen (as the only products) in high yield. More recently, several groups have reported direct amide synthesis from alcohols and amines using M-NHC-based catalyst systems.[56, 57]

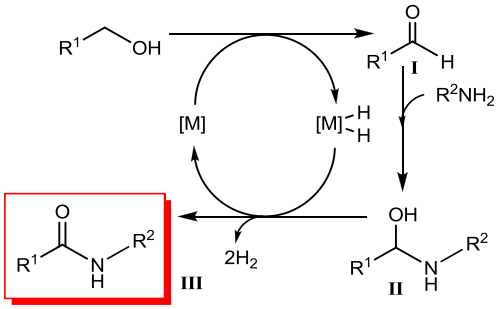

Scheme 3.12 Mechanism of the catalytic formation of amides

The reaction presumably occurs by initial dehydrogenation of the alcohol to the aldehyde (**I**), which then reacts with the amine to give the hemiaminal (**II**) (Scheme 3.12). The elimination of dihydrogen from the metal complex regenerates the catalyst, giving the amide (**III**) and completing the catalytic cycle. The dehydrogenation of the hemiaminal **II** to the amide prevails relative to the expected facile water elimination to give an imine, which on hydrogenation would provide a secondary amine.

As consequence of the catalytic activity of complexes **3B**, **11G** and **12G** in alcohol and amine oxidative dehydrogenation, a combination of these two processes will conceivably provide a convenient protocol for amide synthesis. The reactions were carried out with different primary alcohols and amines in toluene and a fixed amount of catalyst (5 mol %), in the presence of NaH.

The reaction of 2-phenylethanol with benzylamine in the presence of catalysts **11G**, **12G** or **3B** (5 mol %) and NaH in toluene at 150ºC gave the corresponding amide, N-benzylphenylacetamide (Table 3.5, entries 1-3). Again, the imidazolylidene-based complex **3B** was found to be more active than the

triazolylidene-based compounds **11G** and **12G,** and achieved full conversion after 15 h (entry 3). Complex **3B** was also able to convert aliphatic and benzylic substrates (both, amine or alcohol) to the corresponding amides (entries 4 and 5). Interestingly, 2-phenylethanol behaves as an excellent substrate for this type of coupling, contrary to what may be suggested by the results shown in Table 3.3 (entry 3, page 70), where the same substrate is inert toward oxidation under base-free conditions.

Table 3.5 Amide formation from alcohols and amines[a]

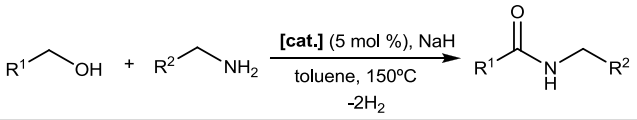

Entry	Cat.	R^1	R^2	t(h)	Yield (%)[b]
1	**11G**			15	68
2	**12G**	$CH_2C_6H_5$	C_6H_5	15	40
3	**3B**			15	>95
4	**3B**	C_6H_5	C_6H_5	20	>95
5	**3B**		C_5H_{11}	20	>95

[a]Reaction conditions: 0.2 mmol of alcohol , 0.8 mmol of amine, 0.4 mmol of NaH and 5 mol% catalyst in toluene (2 mL) at reflux. [b]Yields determined by ^{1}H NMR (C_6Me_6 as internal standard).

The evolution of the reactions described was followed by ^{1}H NMR. The progress of the reactions was evaluated adding hexamethylbenzene, (18H, s, 1.22 ppm), as an internal standard. As the reaction takes place, the signals corresponding to the initial substrates (alcohol and amine) decrease while the signals due to the products (amide) appear and increase. As an example, Scheme 3.13 shows the signals chosen to determine the progress of the reaction between 2-phenylethanol and benzylamine. As the reaction takes place, the signals corresponding to the protons of the -C*H*$_2$OH group of 2-phenylethanol (2H, d, 3.78 ppm) and to the protons of the -C*H*$_2$NH$_2$ group of benzylamine (2H, s, 3.84 ppm) disappear, while the signal corresponding to the products appear. The signals selected as reference for the generated amide were those corresponding to the protons of the -NHC*H*$_2$Ph (2H, d, 4.30) and PhC*H*$_2$CO- (2H, s, 3.51) groups.

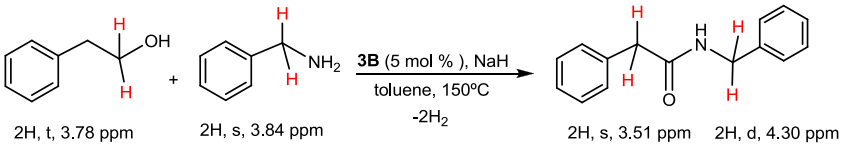

Scheme 3.13 Reference signals for the reaction between 2-phenylethanol and benzylamine

The imidazolylidene complex **3B** is more effective than triazolylidene complex **11G** in the coupling of amines and alcohols to form amides (Table 3.5) while this trend is inverted for the base-free oxidation of alcohols (see data shown in Table 3.2). The difference in behavior is probably due to the presence of base (not used in the oxidation of alcohols reaction) which should facilitate the oxidation of the primary alcohol to the aldehyde in the step preceding the coupling to the amine. The yields provided by the different catalysts seem to correlate with the activity in oxidative amine homocoupling reactions (see data shown in Table 3.4).

It is noteworthy mentioning that the absence of imine in the product mixture indicates efficient suppression of H_2O elimination from the postulated hemiaminal intermediate (**II,** Scheme 3.12). Presumably, the hemiaminal displays an enhanced stability when bound to the ruthenium carbene unit. We propose the formation of intermediate **A** (Figure 3.1), which is reminiscent of the carbonate complexes **13G-14G**. Subsequent β-hydrogen elimination to produce the amide in the metal coordination sphere is apparently more favorable than imine formation via water elimination. Hydrogen migration from the carbon in intermediate **A** to ruthenium is surmised to subsequently yield a ruthenium dihydride species that has been proposed as a further intermediate very recently by Hong and co-workers.[57-58]

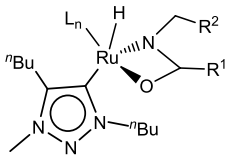

Figure 3.1 Intermediate **A**

Summarizing, we have explored the catalytic properties of the Ru(II) complexes in various oxidations of alcohols and amines. The catalytic activity of the triazolylidene-based Ru complexes **11G-14G** has been compared with that shown by the isostructural imidazolylidene analogue **3B**. The triazolylidene complexes are more effective than the imidazolylidene systems in the base-free oxidation of alcohols, while this trend is inverted for the oxidative homo-coupling of amines and the coupling of amines and alcohols to form amides. Only few catalysts have shown appreciable activity under such mild conditions for the oxidation of alcohols, and we are unaware of similar behavior toward amines.

3.2.1.3 Dimerization of phenylacetylene

The direct coupling of two terminal alkynes is an interesting route because enynes may serve as building blocks for the synthesis of natural products.[59] This reaction, of potential synthetic utility, involves C-H activation and satisfies the criteria of atom economy, where one substrate is converted into a dissymmetric species without waste products. One of the main challenges in dimerization of alkynes is the preparation of highly effective catalysts capable of affording good selectivity. There is a competition among *head-to-head* coupling to give 1,4-disubstituted *E* and *Z* enynes (**a** or **b**, Scheme 3.14) or *head-to-tail* coupling yielding 2,4-disubstituted enynes, cyclotrimerization (**c**, Scheme 3.14), or polymerization. Ruthenium complexes are the best choice for facilitating *head-to-head* couplings, normally affording good selectivities in the formation of *Z*-isomers.[60] However, *E*-selective dimerization has been achieved only in a few cases.[61-62]

The same compounds that we have previously used in the *β*-alkylation of alcohols, **1A**, **7D**, **8E**, **9F** and **10F** (see page 63, Section 3.2.1.1 in this chapter) were tested in the catalytic dimerization of phenylacetylene to provide the corresponding enynes. Our aim was to study the catalytic activity of these complexes containing different types of NHC ligands with similar topological features but different electron-donor power. The dimer $[RuCl_2(p\text{-cymene})]_2$ was also tested for comparative

purposes. The reactions were carried out with phenylacetylene and a fixed amount of catalyst (5 mol %) in deuterated acetonitrile at 70ºC and in the presence of NEt_3 (Scheme 3.14).

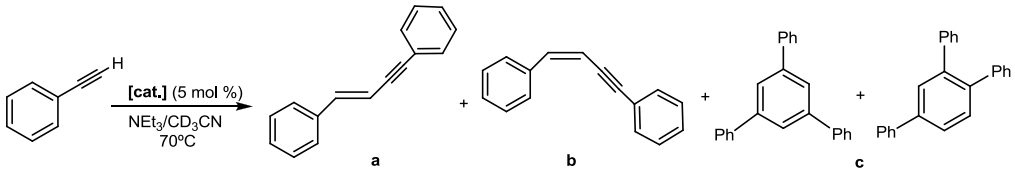

Scheme 3.14 Dimerization of alkynes

As we can observe from the data shown in Table 3.6, high conversions were achieved in all cases, although the dimerization competes with the trimerization of the acetylene, generating two possible trisubstituted benzenes. All Ru-NHC catalysts provided yields in the range 20-42% in the dimerization products with a moderate *E*-selectivity, while $[RuCl_2(p\text{-cymene})]_2$ afforded only the cyclotrimerization compounds under the same reaction conditions. **1A** showed the best catalytic activity and also gave the highest selectivity towards the *E*-isomer.

Table 3.6 Dimerization and cyclotrimerization reaction of phenylacetylene[a]

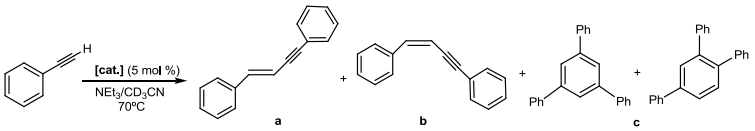

Entry	Cat.	Conv.(%)[b]	a:b:c[b]
1	**1A**	>95	33:9:58
2	**7D**	88	14:5:81
3	**8E**	79	26:10:64
4	**9F**	95	21:8:71
5	**10F**	81	28:9:63
6	$[RuCl_2(p\text{-cymene})]_2$	56	0:0:100

[a]Reaction conditions: 0.3 mmol of phenylacetylene; 25 mol % of NEt_3 and 5 mol % of catalyst in 0.3 mL of CD_3CN at 70ºC for 8h. [b]Conversions and ratios were determined by ^1H NMR.

The evolution of the reactions described was followed by ^{1}H NMR. The progress of the reactions was evaluated adding ferrocene as an internal standard. As the reaction takes place, the signals corresponding to the initial substrates decrease while the signals due to the products appear and increase.

The results obtained for compounds **1A**, **7D**, **8E**, **9F** and **10F** compare well with the activities shown by other ruthenium catalysts previously reported.[61, 63] For this reaction we did not find any substantial differences in the catalytic activities, although it becomes clear that the introduction of the basic NHC ligand provides an inversion of the selectivity compared to that shown by $[RuCl_2(p\text{-cymene})]_2$.

3.2.1.4 Chelation-assisted reactions: arylation and deuteration of arylpyridines

a) Arylation of arylpyridines

As stated in the introduction of this chapter, a new approach for direct arylation of arenes has been investigated, involving the reaction of aryl halides with non-functionalized arenes by C-H bond activation. Following the pioneering work of Oi and co-workers,[64] many efforts are currently being made to generate efficient ruthenium catalysts for such a challenging transformation.[21, 65-69, 70]

With this in mind, we thought that some of the 'Ru(η^6-arene)(NHC)' complexes described in Chapter 2, would be good candidates for this type of transformation.

We first optimized the reaction conditions for the arylation of 2-phenylpyridine using chlorobenzene. Complexes **1A**, **2A**, **3B**, **4B**, **5B** and **6**C were tested in this preliminary reaction (Scheme 3.15). The use of three different η^6-arene ligands (*p*-cymene, hexamethylbenzene, and methylbenzoate), different NHC ligands and one phosphine, seemed a good choice for the tuning of the electronic and steric properties of the metal centre. For comparative purposes, we also studied the activity of the metal precursors $[RuCl_2(p\text{-cymene})]_2$ and $[RuCl_2(CMe)_6]_2$.

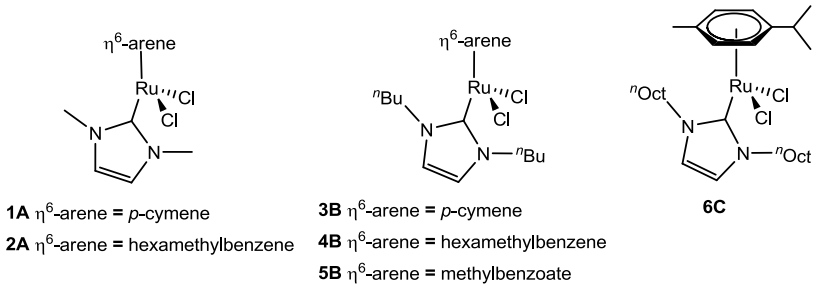

Scheme 3.15 'Ru(η^6-arene)(NHC)' catalysts used in arylation of arylpyridines

For this study, we used the previously described reaction conditions (120ºC in NMP, N-methyl-2-pyrrolidone)[64] and a catalyst loading of 5 mol%. 2-Phenylpyridine was treated with chlorobenzene in the presence of coordinating bases[71] to yield the monoarylated and/or the bisarylated compounds (Scheme 3.16). The catalytic reactions described in this section were followed by Gas Chromatography (GC). The progress of the reaction was evaluated adding to the reaction one equivalent of anisole as internal standard.

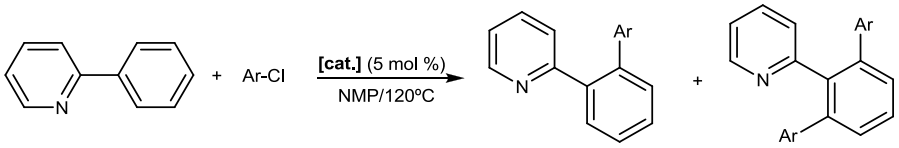

Scheme 3.16 Arylation of 2-phenylpyridine with chlorobenzene

As Table 3.7 shows, the best catalytic performances were found when using a mixture of KOAc and K_2CO_3 (entry 6). Once the reaction conditions were optimized, the different activities of the Ru-NHC complexes were studied (entries 6-17). As can be seen from the data, the best performances were provided by **3B**, which achieved full conversion to the bisarylated product in 5 h. In general, it is observed that the introduction of the NHC ligands provides better performances than those provided by the metal precursors without this type of ligand (entries 16 and 17) or with PPh_3 (entry 15).

The arene ligand has also a clear influence in the catalytic outcome of the system, with *p*-cymene providing the best results. This observation is difficult to

justify if we consider that the release of the coordinated arene ligand is necessary for the catalytic activity of these species, because this would imply that the complex containing methylbenzoate ligand (more weakly bound to the metal) should have provided the best outcomes.

Table 3.7 Optimization conditions and catalyst screening in the arylation of 2-phenylpyridine with chlorobenzene[a]

Entry	Cat.	Conditions	t(h)[b]	Mono[b]	Bis[b]
1	**3B**		20	15	1
2	None	$NaOAc/Na_2CO_3$	20	-	-
3	**4B**		20	-	-
4	**3B**	$NaOAc/K_2CO_3$	5	25	5
5	**3B**		18	-	>95(91)
6	**3B**		5	-	>95(92)
7	**3B**		3	25	70
8[c]	**3B**		7	60	22
9	**4B**		5	4	1
10	**5B**		5	25	40
11	**1A**		5	10	89
12	**2A**	$KOAc/K_2CO_3$	5	-	-
13	**6C**		5	-	>95
14	**6C**		3	25	60
15	$[RuCl_2(PPh_3)(p\text{-cymene})]$		5	68	10
16	$[RuCl_2(p\text{-cymene})]_2$		5	20	10
17	$[RuCl_2(CMe)_6]_2$		5	9	42
18	None		20	-	-

[a]Reaction Conditions: 0.05 mmol of NaOAc or KOAc, 0.025 mmol of catalyst in NMP (2 mL) at room temp. for 1h, then 0.5 mmol of 2-phenylpyridine, 1.25 mmol of PhCl and 1.5 mmol of Na_2CO_3 or K_2CO_3 at 120ºC. [b]Yields and ratios determined by GC (internal standard: anisole) and by ^1H NMR. [c]Using 2 mL of toluene as solvent instead of NMP. Isolated yields in parenthesis.

The change of the nature of the N-alkyl groups at the NHC ligand also provides changes in the catalytic activity of the complexes under study. Complex **1A** (N-Me), provided good activity, although the formation of the bisarylated product was rather

poor compared to the monoarylated one (entry 11), implying that the reaction may not have been fully completed after 5 h. In addition, complex **6C** (N-*n*Oct) showed similar activity to **3B** after 5 h (entry 13), but the outcome after 3 h was significantly lower (entry 14). The complexes **2A** and **4B**, containing hexametylbenzene as η^6-arene ligand, showed negligible activities (entries 9 and 12).

Once we confirmed that catalyst **3B** was the most active one in the arylation of 2-phenylpyridine, we decided to extend its use to other substrates.

Table 3.8 Arylation of pyridines using catalyst **3B**[a]

Entry	Pyridine	Ar-X	t(h)	Mono[b]	Bis[b]
1			4	-	>95(92)
2			4	1	90
3		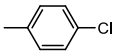	4	-	>95(90)
4		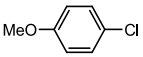	5	25	60
5	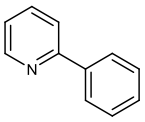	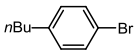	5	-	>95(91)
6			24	80	6
7			24	4	90
8			24	45	2
9			24	15	<5
10			24	15	5
11	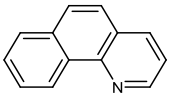		5	94(89)	-
12			12	50	-
13		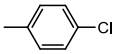	6	92	-
14	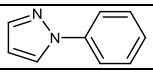		5	-	95(81)

[a]Reaction Conditions: 0.05 mmol of KOAc, 0.025 mmol of **3B** in NMP (2 mL) at room temp. for 1h. Then 0.5 mmol of substrate, 1.25 or 0.75 mmol of ArX and 1.5 mmol of K_2CO_3 at 120ºC. [b]Yields and ratios determined by GC (internal standard: anisole) and by ^{1}H NMR. Isolated yields in parenthesis.

Table 3.8 shows the catalytic results when compound **3B** was used in the arylation of 2-phenylpyridine, benzo[*h*]quinoline and N-phenylpyrazole with different arylating agents. Interestingly, the catalyst was capable of providing good results for all of them, a feature that illustrates its wide applicability. For the reactions with 2-phenylpyridine, **3B** provides higher activity than previously reported ruthenium catalysts that generally need longer reaction times (>10 h) to achieve lower product yields[64-66, 72] and compares well with the most efficient catalytic systems reported for this process.[73-74] In general, it seems that the use of chloroarenes provides higher conversions than iodo- and bromoarenes, a trend that is also observed in the arylation of benzo[*h*]quinoline (compare entries 11 and 12).

b) Deuteration of arylpyridines

Hydrogen/deuterium exchange processes are powerful methods to evaluate the potential of a catalyst for the cleavage and formation of C-H bonds. Since the mechanism of the arylation of arylpyridines implies the regioselective C-H activation at the 2-position of the aromatic rings of 2-substituted pyridines, we thought that it may be possible to use the same catalyst, **3B**, for the N-directed regioselective deuteration of C-H bonds of different pyridines. We found in the literature the description of the selective deuteration of benzo[*h*]quinoline at the C-10 position using a dirhodium(II) complex, although in this case the reaction needed a stoichiometric amount of the dimetallic species (the reaction is not catalytic) and base.[25] Table 3.9 shows the selective deuteration of six different pyridines, in the presence of MeOH-d_4 at 120ºC with 5 mol% of catalyst **3B**.

Catalyst **3B** provided good activity in the selective deuteration of arylpyridines. The addition of an additive such as a base, KOAc, was only necessary for the deuteration of two substrates (entries 5 and 6). Remarkably, the deuteration of the sp^3 C-H bonds at the methyl group of 8-methylquinoline was also almost quantitative. To the best of our knowledge, this is the first time that this selective deuteration of arylpyridines had been described. More recently, and based on this

work, our group of research has carried out the same catalytic reaction using a series of water-soluble Ir(III)-biscarbene complexes and D_2O as deuterium source, achieving good results.[75]

Table 3.9 Deuteration of pyridines in MeOH-d_4 using **3B**[a]

Entry	Substrate	Product	t(h)	Conv. (%)[b]
1	2-phenylpyridine	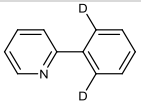	7	92(89)
2	benzo[*h*]quinoline	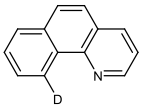	5	90(82)
3	1,2-bis(2-pyridyl)ethylene	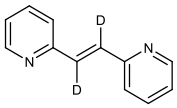	10	>95
4	N-phenylpyrazole	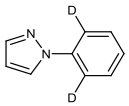	10	>95
5[c]	methylbenzylimine	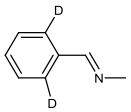	10	>95
6[c]	8-methylquinoline	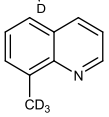	10	80

[a]Reaction Conditions: catalyst **3B** (0.025 mmol), substrate (0.5 mmol), 4mL of MeOH-d_4 at 120ºC. [b]Conversion determined by ^{1}H NMR. [c]Using KOAc (0.05 mmol). Isolated yields in parenthesis.

It is important to point out that this reaction can be easily monitored by ^{1}H NMR, for which a growth of the resonance due to the protons of the CH_3- group of CH_3OH is concomitant with the deuteration of the pyridine. This observation suggests a C-D rather than O-D activation in the functioning of the deuterium source in the catalytic cycle, a fact that is confirmed by the absence of reaction when CH_3OD is used instead of MeOH-d_4 (CD_3OD).

The catalytic tests described in this section were followed by ^{1}H NMR. The ^{1}H NMR spectra illustrates that the signal corresponding to the proton changed by the

deuterium disappears. As an example of the monitoring of the process, Figure 3.2 shows two ^{1}H NMR spectra of the deuteration of benzo[*h*]quinoline at t = 0 h and t = 5 h, which clearly illustrate that the signal due to the proton at the C-10 position of benzo[*h*]quinoline ring (9.31 ppm, d, 1H) disappears after 5 h of reaction.

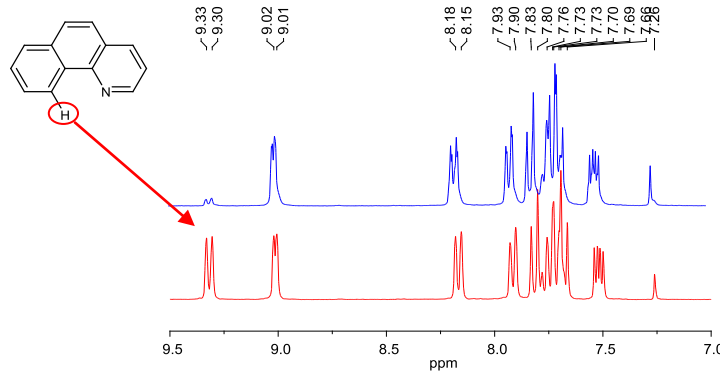

Figure 3.2 ^{1}H NMR spectrum of the deuteration of benzo[*h*]quinoline at 0h (red) and at 5h (blue)

In general, the search for catalysts able to selectively deuterate organic molecules is a matter of continuous interest because deuterium labeled compounds can be used in a wide range of applications such as the study of biologically active systems, solvents for NMR spectroscopy, and the study of reaction mechanisms.[76] In our case, the possibility to selectively deuterate pyridines provides an excellent opportunity for the experimental study of the reaction mechanism of the arylation of these substrates.

Kinetic isotope effect

One of the most common techniques for studying reaction mechanisms is the measurement of the kinetic isotope effect (KIE). This parameter is the ratio between reaction rates shown by two different isotopically labeled molecules in a chemical reaction. A KIE involving hydrogen and deuterium is represented as: KIE = k_H/k_D (where k_H and k_D are reaction rate constants).

For the interpretation of the KIE observed in our experiments, we first find convenient to explain the different kinetic isotope effects which can be found:

Primary kinetic isotope effect: when the isotopic change occurs in the bond which is being broken in the rate-limiting step, the reaction rate changes substantially. In this case, the kinetic isotope effect is expected to be greater that one (normal), because breaking the C-H bond is easier than breaking the C-D bond.

Secondary kinetic isotope effect: when the isotopic change does not occur in the bond which is being broken in the rate-limiting step, a smaller rate change is observed. In this case the kinetic isotope effect can be negligible or lower than one (inverse).

With this in mind, we monitored the time course of the arylation of benzo[*h*]quinoline and benzo[*h*]quinoline-*d* with chlorobenzene (Scheme 3.17). The reactions were carried out under the same conditions than those in the arylation of arylpyridines (section 3.2.1.4, a) KOAc/K_2CO_3 in NMP at 120ºC) using catalyst **3B**.

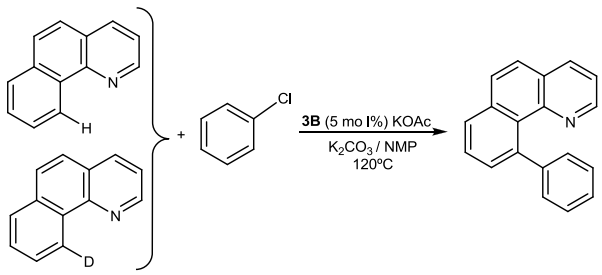

Scheme 3.17 Arylation of benzo[*h*]quinoline and benzo[*h*]quinoline-*d* with chlorobenzene

The catalytic tests were followed by Gas Chromatography (GC) using anisole as internal standard, taking samples at the desired times. As the reaction takes place, the signals corresponding to the initial substrates decreased and the signals due to the product obtained appeared.

Figure 3.3 represents the time-course for the arylation of benzo[*h*]quinoline (blue) and benzo[*h*]quinoline-*d* (red). As can be observed, the deuterared substrate reacts faster than the non-deuterated one, suggesting an inverse KIE of k_H/k_D = 0.43 (based on the determination of $t_{1/2}$ values at 120ºC).

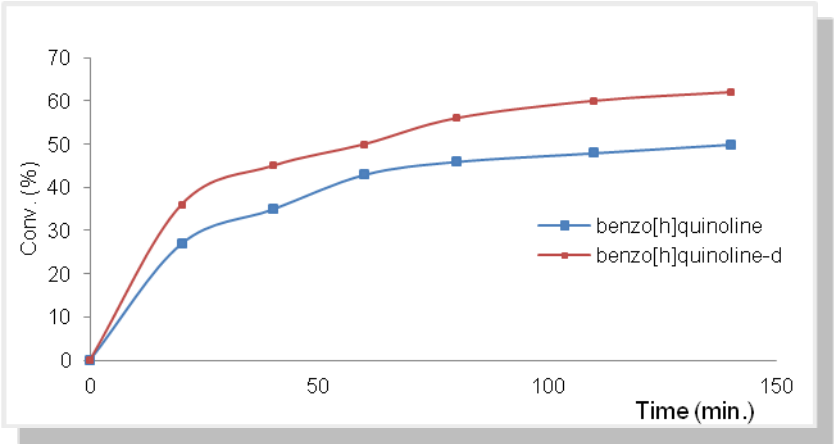

Figure 3.3 Time-course for the arylation of benzo[*h*]quinoline and benzo[*h*]quinoline-*d*

This inverse KIE is different from the normal KIEs found for other related hydrogen abstraction processes,[25, 77] thus indicating that a different mechanism should be at play or, at least that a different transition state is determining the kinetics of the process. It is important to recall that, for our Ru-catalyzed deuteration reactions, the results indicate that the C-H activation is a metal-mediated process that takes place in the absence of a base, which also supports the idea that the rate-limiting step of the catalytic reaction does not imply the proton abstraction from the phenyl ring of the arylpyridine compound.

Regarding the mechanism of the arylation of arylpyridines reaction, it was first believed that it proceeded through an oxidative addition of the aryl halide to the ruthenium complex to afford an arylruthenium intermediate.[64, 70] However, experimental observations[68, 74, 78] and DFT calculations[65] support that the reaction proceeds *via* proton abstraction from the substrate by the cooperative actions of the ruthenium(II) centre and the coordinated base (carbonate or acetate), leading to the crucial *ortho*-metallated intermediate (Scheme 3.18).

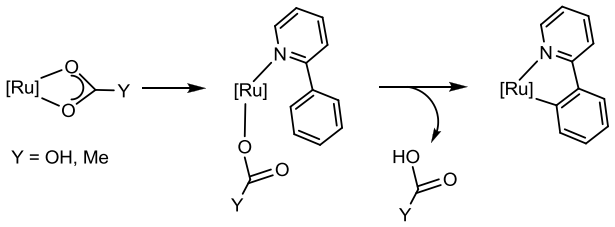

Scheme 3.18 *Ortho*-metallated intermediate by proton abstraction mechanism

The fact that the C-H cleavage is not the rate-determining step of the process can be explained as follows. The diagram sown in Figure 3.4 represents a qualitative reaction profile indicating the relative rates for the different steps of the reaction.

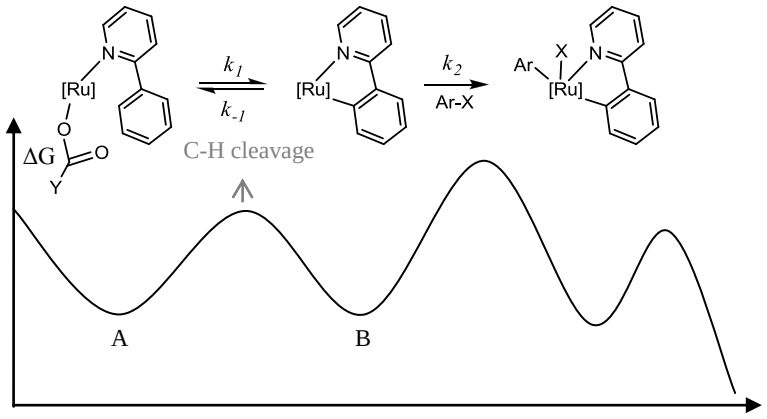

Figure 3.4 The relative rates for the different steps of the reaction

The C-H bond cleavage is reversible, and occurs before the rate-determining step, which is irreversible. The rate of the determining step is given by k_2[B], but the concentration of B depends on the rate constants k_1 and k_{-1}. Consequently the KIE is sensitive to H/D substitution.[79] This fact is in agreement with the studies carried out by Ackermann and co-workers, who suggested that ruthenium-catalyzed direct arylations proceed through reversible C-H bond activation and subsequent rate limiting oxidative addition with aryl halides.[67]

As can be seen in this section, the ruthenium catalysts were effective for the chelation-assisted direct arylation of a wide series of pyridines. **3B** was also an efficient catalyst for the N-directed regioselective deuteration of sp^2 and sp^3 C-H

bonds, a process that is unprecedented in the literature. The easy access to selective deuterated arylpyridines allowed the determination of the kinetic isotope effect in the direct arylation of arylpyridines, which being inverse, suggests that the reaction mechanism proceeds via a different mechanism than those proposed for other related hydrogen abstraction processes.

3.2.2 Catalytic activity of 'IrCp*(NHC)' complexes

In recent years, Fujita and Yamaguchi described a series of 'IrCp*(NHC)' compounds[46, 80, 81] and their application in Oppenauer-type oxidations of primary and secondary alcohols (Scheme 3.19).[46, 81]

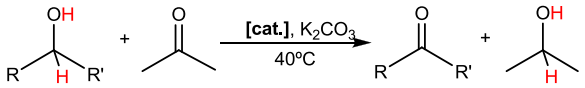

Scheme 3.19 Oppenauer-type oxidations of primary and secondary alcohols

At the same time, our group has developed a series of similar compounds with excellent catalytic activities in reactions implying C=O or C=N bond reduction by hydrogen transfer, some even in the absence of base.[41, 82-83] Some of these complexes also showed excellent activity in the deuteration of organic molecules.[84-85] Taking all this into account, we decided to explore the scope and limitations of 'IrCp*(NHC)' complexes in a wider range of catalytic processes, including:

Borrowing-hydrogen processes:

3.2.2.1 Dehydrogenation of alcohols

3.2.2.2 Homo-coupling of alcohols

3.2.2.3 Cross-coupling of alcohols and amines:

a) Etherification of benzylalcohol with primary and secondary alcohols

b) N-Alkylation of anilines with aliphatic amines

c) N-Alkylation of primary amines with primary and secondary alcohols

Other *C-H activation processes*:

3.2.2.4 Functionalization of arenes:

a) Benzylation of arenes with alcohols and ethers

b) Benzylation of arenes with styrenes

c) Benzylation of aniline derivates with styrene

3.2.2.5 Tandem reaction: Transfer hydrogenation and benzylation of arenes

3.2.2.1 Catalytic dehydrogenation of alcohols

As discussed in section 3.2.1.2, the dehydrogenation of alcohols is an interesting process, not only because it provides the more reactive carbonylated species, but also because it affords an easy way for the generation of hydrogen. Recently, much effort has been devoted to the transition-metal-catalyzed oxidation of alcohols using environmentally friendly oxidants. An example of an efficient catalytic system has been described by Profs. Yamaguchi and Fujita. The authors described an Ir(III)-based complex bearing a 2-hydroxypyridine ligand capable to catalyze the "ligand promoted" dehydrogenation of alcohols.[47]

In this sense, and because our group described that **15B** has shown an excellent catalytic activity in a large number of C-H activation processes,[83-84] we decided to study the activity of **15B** in the oxidation of alcohols. The reactions were carried out adding a catalyst loading of 5 mol % and 20 mol % of Cs_2CO_3 with respect to the substrate, using toluene as solvent at 110ºC for 24 hours. Under these reaction conditions, **15B** is capable of oxidising benzylalcohol and 1-phenylethanol (data shown in Table 3.10).

Table 3.10 Dehydrogenation of alcohols[a]

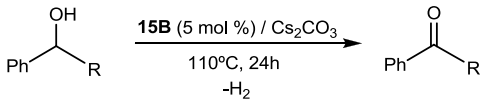

Entry	Alcohol	t(h)	Yield(%)[b]
1	benzylalcohol	24	50
2	1-phenylethanol	24	70

[a]Reaction conditions: 0.4 mmol of alcohol, 5 mol % of **15B** and 0.08 mmol of Cs_2CO_3. [b]Yields were determined and by ^{1}H NMR.

Although the yields obtained were moderate, this process establishes the basis for reactions governed by a borrowing-hydrogen mechanism, so it prompted us to study some other related reactions such as the homo-coupling of alcohols to afford ethers, and the cross-coupling of amines and alcohols.

3.2.2.2 Homo-coupling of alcohols

When the reaction with primary alcohols was carried out under base-free conditions, in the presence of **15B** and an excess of AgOTf, the homo-coupling of the alcohols to yield the corresponding ethers took place. Under these reaction conditions, we believe that the active species is that in which chloride ligands have been replaced by triflate ones (OTf^-) (See Scheme 3.20, on page 92). The reaction was carried out at 110ºC, using a catalyst loading of 1 mol % with respect to the aliphatic alcohol, and a small excess of AgOTf, so the active [Ir Cp*(NHC)$(OTf)_2$] species can be generated *in situ*.

The results for this reaction are shown in Table 3.11. Compound **15B** showed excellent activities in the homo-coupling of aliphatic alcohols. Remarkably, when *n*-butanol was used as substrate the yield was 95% (entry 1).

Table 3.11 Homo-coupling of alcohols[a]

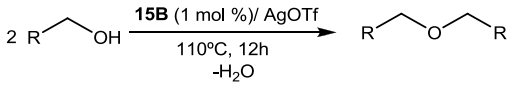

Entry	Alcohol	t(h)	Yield(%)[b]
1	*n*-butanol	12	95
2	*n*-hexanol	12	71
3	*n*-dodecanol	12	87

[a]Reaction conditions: 0.4 mmol of alcohol, 1 mol% **15B** and 0.012 mmol of AgOTf. [b]Yields determined by ^1H NMR spectroscopy.

When the results shown in Table 3.10 and Table 3.11 are compared, it seems clear that the reaction outcome (dehydrogenation of the alcohols or homo-coupling products) depends on whether a base or AgOTf are added to the reaction medium. Although we did not carry out detailed mechanistic studies, we believe that Scheme

3.20 shows two plausible mechanisms that may justify this difference. These mechanisms are supported by two previous findings described in the literature: the existence of stable species of Cp*Ir(V) formed by oxidative addition to Ir(III),[86] and the well-known formation of Ir(III) alkoxides by oxidative addition of alcohols to Ir(I) complexes.[87]

Activation with base: the first step involves the oxidative addition of an alcohol to the metal fragment giving an Ir(V)-H cationic species. In the presence of a base, this hydride is expected to be "deprotonated" to generate an Ir(III) alkoxide. This species initiates the catalytic cycle. *β*-Elimination followed by oxidative addition of another alcohol molecule generates an Ir(V) dihydride species and the corresponding carbonyl compound (ketone or aldehyde). The Ir(V) dihydride reductively eliminates hydrogen and reinitiates the cycle.

Activation with AgOTf: In this case the active species is the compound in which chloride ligands are replaced by triflates after the addition of AgOTf. First, there is an oxidative addition of an alcohol to the metal fragment to give a Ir(V)-H cationic species. This Ir(V)-H intermediate acts as Brønsted acid and activates the second molecule of alcohol by an electrophilic attack of the oxygen atom with the subsequent coupling of the alkyl group to the coordinated alkoxide fragment and loss of H_2O.

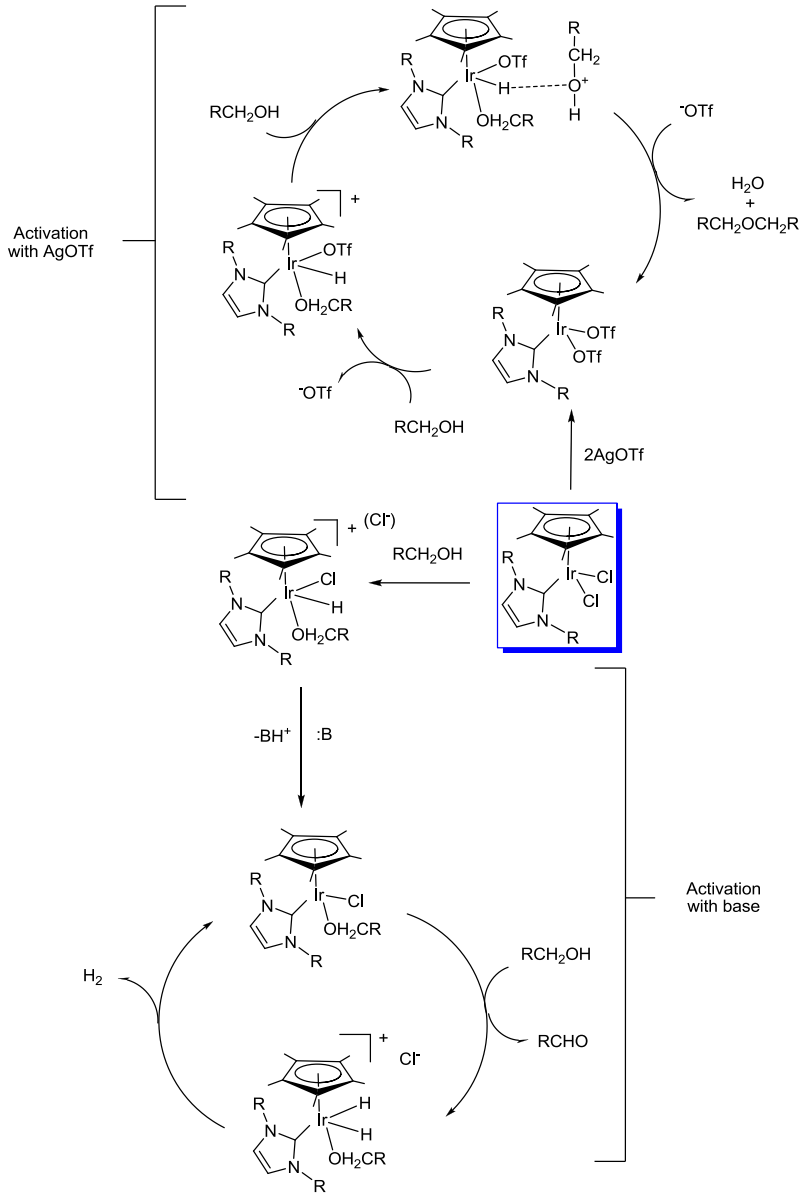
Activation with AgOTf
RCH2OH
-OTf
H2O + RCH2OCH2R
2AgOTf
RCH2OH
-OTf
(Cl-)
RCH2OH
-BH+
:B
Activation with base
H2
RCH2OH
RCHO
Cl-

Scheme 3.20

3.2.2.3 Cross-coupling of alcohols and amines

Based on the above described results for the catalytic behaviour of **15B**, and also based on our experience on hydrogen transfer processes, we thought that 'IrCp*(NHC)' complexes may also be good candidates for reactions implying the cross-coupling of alcohols and amines, in all three possible combinations. In order to check this possibility we tested the activity of **15B**, **16D** and **17F** (Scheme 3.21) in a set of coupling reactions, and also $[IrCp^*Cl_2]_2$ for comparative purposes.

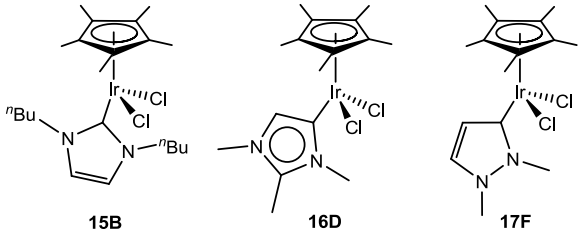

Scheme 3.21 'IrCp*(NHC)' complexes

In this regard, for a first catalyst screening we performed three experiments implying the cross-coupling of: a) benzylalcohol with *n*-butanol, b) aniline with *n*-hexylamine and c) benzylalcohol with *tert*-butylamine.

The reactions were carried out at 110-150ºC, with a catalyst loading of 1 mol %. Addition of AgOTf was needed in order to activate the catalysts. In order to check if the pre-formed 'IrCp*(NHC)$(OTf)_2$' species were more active than the *in situ* prepared ones, we also isolated the triflate compounds, but their use under the same catalytic conditions did not show any significant differences with the activities shown by the *in situ* prepared ones. Table 3.12 shows the results obtained.

All four catalysts showed good activities in all three model reactions, although catalyst **15B** achieved the best catalytic performances (entries 1, 5 and 9). The fact that **15B** behaves as a very active catalyst in such a wide set of catalytic reactions is of great interest, especially if we take into account all the synthetic applications that can be obtained by combination of these three model reactions. It

should also be mentioned, that the catalytic activity displayed by $[IrCp^*Cl_2]_2$ in the presence of AgOTf in these reactions, not being as good as that shown by **15B**, is remarkable, and encourages the use of this simple combination of reagents in other catalytic reactions for which $[IrCp^*Cl_2]_2$ has proven to be active.

Table 3.12 Comparison of the different catalysts towards cross-coupling of alcohols and amines.[a]

Entry	Reaction	Cat.	t(h)	Yield(%)[b]
1	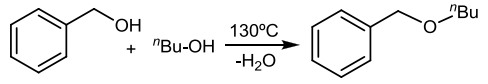	**15B**	2	>95
2		**16D**	3	91
3		**17F**	2	>95
4		$[Cp^*IrCl_2]_2$	3	90
5	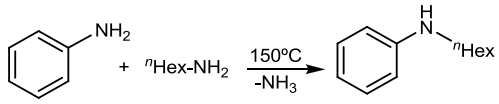	**15B**	24	>95
6		**16D**	24	75
7		**17F**	24	70
8		$[Cp^*IrCl_2]_2$	24	70
9	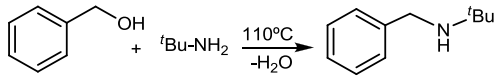	**15B**	7	>95
10		**16D**	7	75
11		**17F**	7	83
12		$[Cp^*IrCl_2]_2$	7	80

[a]Reaction conditions: **entries 1-4** 0.4 mmol of benzylalcohol, 2 mmol of *n*-butanol, 1 mol% catalyst and 0.012 mmol of AgOTf. **Entries 5-8** 0.2 mmol of aniline, 0.4 mmol of *n*-hexylamine, 5 mol% catalyst and 0.03 mmol AgOTf in toluene-d_8. **Entries 9-12** 0.2 mmol of amine, 0.24 mmol of alcohol, 5 mol% catalyst and 0.03 mmol AgOTf. [b]Yields determined by ^{1}H NMR spectroscopy.

In order to study the scope of catalyst **15B**, we decided to perform a series of reactions using a wider set of substrates for each individual cross-coupling reaction.

a) Etherification of benzylalcohol with primary and secondary alcohols

Ethers are fundamental compounds in organic chemistry and are widely used as either fragrance precursors[88] or oxygenates in reformulated gasoline.[89] The traditional method for the preparation of unsymmetrical ethers involves the reaction of an halide with an alkoxide,[90] or an halide with an alcohol and basic inorganic reagents such as

KOH, NaH, etc.[91] The development of new catalytic methods for the synthesis of unsymmetrical ethers from halide-free starting materials is highly desired.

The coupling of benzylalcohol with primary and secondary alcohols can give different products, as shown in Scheme 3.22. The most interesting product is the unsymmetrical ether (**a**), but it is also possible to obtain the homo-coupling products (**b** and **c**). In the experiments that we performed, the reactions were carried out with benzylalcohol and an excess of the primary or secondary alcohol using 1 mol % of catalyst (**15B**) in the presence of AgOTf and in the absence of solvent at different temperatures.

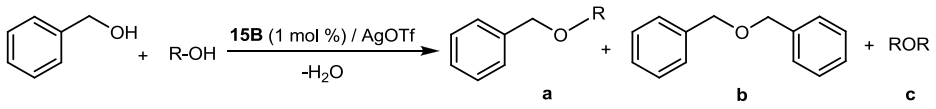

Scheme 3.22 Etherification of benzylalcohol with primary and secondary alcohols

As can be seen from the results shown in Table 3.13, the reaction is quantitative or almost quantitative for all the experiments performed, showing a high selectivity to the unsymmetrical ethers. Only for the homo-coupling reaction of benzylalcohol we obtained a very low yield in the formation of benzylether (entry 6). It is also important to mention the high performances obtained when allylalcohol was used (85 % yield). Allylethers are important starting materials for a wide variety of organic reactions, and our result is clearly improving recent reports for the same process.[92]

The results compare well and even improve previously reported results where the same or similar substrates were used.[92, 93, 94] In particular, we observed that **15B** provided higher yields in the formation of the unsymmetrical ethers than the highly active catalyst $ReBr(CO)_5$,[94] a result that is even more interesting if we consider that **15B** needed lower temperatures and shorter reaction times.

Table 3.13 Etherification of benzylalcohol with primary and secondary alcohols[a]

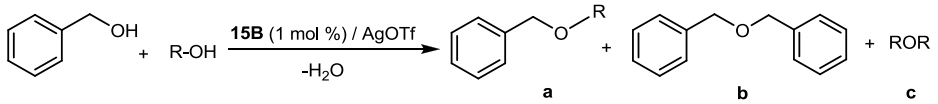

Entry	Alcohol	T (ºC)	t (h)	Conv. (%)	a(%)[b]	b(%)[b]	c(%)[c]
1	methanol	110	12	94	88	6	0
2	ethanol	110	12	>95	>95	0	6
3	*n*-butanol	130	2	>95	>95(90)	0	8
4	*n*-hexanol	130	6	>95	94	5	10
5	*n*-dodecanol	130	3	>95	95(93)	2	14
6	benzylalcohol	130	12	>95	10	-	-
7	allylalcohol	110	12	93	85	8	15
8	*i*-propylalcohol	110	12	>95	80	16	10
9	cyclohexanol	110	10	81	70	11	-

[a]Reaction conditions: 0.4 mmol of benzylalcohol, 2 mmol of primary or secondary alcohol, 1 mol% of catalyst and 0.012 mmol of AgOTf. Conversion and yields were determined by ^{1}H NMR spectroscopy. [b]Yield based on the amount of benzylalcohol. [c]Yield based on the amount of primary or secondary alcohol. Isolated yields in parenthesis.

The evolution of the reactions was monitored by ^{1}H NMR. The progress of the reactions was evaluated by comparing the signals corresponding to benzylalcohol with the signals corresponding to the ether formed.

Brønsted acids are known to catalyze the formation of ethers through the protonation of the hydroxy group that is converted into a better leaving group. For example, many studies in the homogeneous phases have been carried out with sulfuric acid,[95] although this procedure is known to give low yields when secondary and tertiary alcohols are used. In this case, the leaving groups are ROH_2^+ or $ROSO_2H^+$.[96] In order to discard catalysis simply by AgOTf or even HOTf, we carried out the reaction of benzylalcohol and *n*-butanol in the presence of each of these reactants without adding compound **15B**. These experiments showed that the addition of AgOTf did not provide any conversion to the desired ether, while addition of HOTf provided negligible conversions (22 % after 4h) to the desired unsymmetrical ether. These results confirm that the data shown in Table 3.13 for the cross-coupling of alcohols to afford the unsymmetrical ethers, are essentially due to the Ir(III)-catalyzed

process. Also, the activation of **15B** with $AgPF_6$ (instead of AgOTf), afforded much lower activities, probably because the generation of a dicationic species provides a compound with lower electron density than the neutral bistriflate adduct generated by addition of AgOTf, as previously suggested by our research group.[83]

b) N-Alkylation of anilines with aliphatic amines

The transition-metal-catalyzed alkylation of amines with amines has been described as a convenient method for the preparation of N-alkylated anilines.[12, 97] Beller and co-workers have demonstrated that Shvo's catalyst can be used to obtain selective amine coupling when one of the amines is unable to undergo oxidation. These authors proposed that this reaction proceeds through a borrowing-hydrogen mechanism in which the alkyl-amine is the hydrogen-transfer agent (Scheme 3.23). The first step of the mechanism involves the oxidation of the amine to give an imine (**I**) and a metal dihydride [M]-$(H)_2$. The imine reacts with another equivalent of the substrate amine, giving the N-alkylated imine (**II**) and elimination of ammonia. The dihydride [M]-$(H)_2$ reduces C=N double bond to give the secondary amine (**III**), recovering the catalyst.

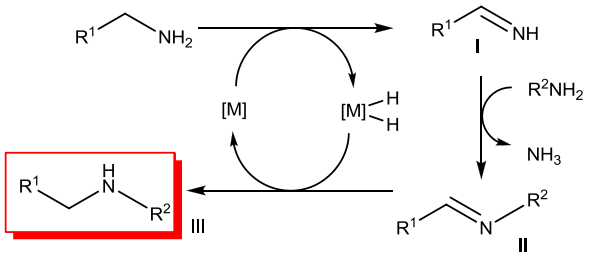

Scheme 3.23 Mechanism for the N-alkylation of anilines with amines

After proving that **15B** is a good catalyst for the N-alkylation of aniline with *n*-hexylamine (Table 3.12, entry 5), we decided to study the generality of this reaction using a wider set of substituted anilines and different alkyl amines. The reactions were carried out with an excess of aromatic amine with respect to the aliphatic one, using 5 mol % of **15B** in the presence of AgOTf in deuterated toluene, at 150ºC.

Table 3.14 N-Alkylation of anilines with aliphatic amines[a]

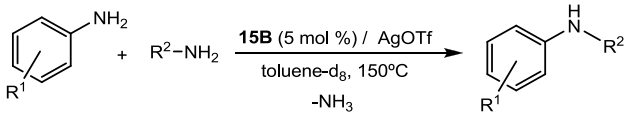

Entry	Aryl amine	Alkylamine	Conv(%)[b]	Yield(%)[b]
1	aniline	*n*-hexylamine	>95	>95(85)
2		benzylamine	>95	94
3		cyclohexylamine	>95	>95
4		*n*-dodecylamine	>95	>95
5	*o*-toluidine	*n*-hexylamine	>95	80
6		benzylamine	90	80
7		cyclohexylamine	>95	>95
8		*n*-dodecylamine	>95	70
9	*p*-toluidine	*n*-hexylamine	90	70
10	*p*-fluoroaniline		>95	>95
11	*p*-chloroaniline		>95	>95
12	*p*-methoxyaniline		50	50
13	2,4,6-methylaniline		90	90

[a]Reaction conditions: 0.2 mmol of alkyl amine, 0.4 mmol of aryl amine, 5 mol% of catalyst and 0.03 mmol of AgOTf, toluene-d_8, 24 h, 150ºC. [b]Conversions and yields were determined by ^{1}H NMR spectroscopy using 1,3,5-trimethoxybenzene (0.02 mmol) as internal standard. Isolated yields in parenthesis.

As summarized in Table 3.14, **15B** provided good to excellent conversions in the N-alkylation of a wide set of substituted anilines with several alkyl amines.

The evolution of the reactions described was followed by ^{1}H NMR. The progress of the reactions were evaluated adding 1,3,5-trimethoxybenzene (9H, s, 3.78 ppm and 3H, s, 6.11 ppm) as internal standard. As the reaction takes place, the signals corresponding to the initial substrates decreased and the new signals due to the N-alkylated amine obtained appeared. As an example, Scheme 3.24 shows the signals selected as reference to determine the progress of the reaction between aniline and *n*-hexylamine. As the reaction proceeds, the signals corresponding to the aromatic protons of the phenyl ring close to the -NH_2 group (2H, s, 6.70 ppm) and to the

protons attributed to the -CH_2NH$_2$ group of *n*-hexylamine (2H, t, 2.75 ppm) disappear while the signals corresponding to the product appear. The reference signals for the N-alkylated amine product were those corresponding to the aromatic protons of the phenyl ring close to the -NH- group (2H, s, 6.60 ppm) and to the protons due to the -CH_2NH- group (2H, t, 3.12 ppm).

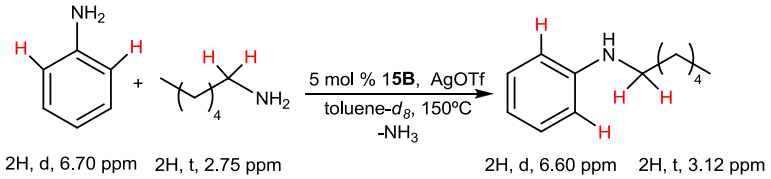

Scheme 3.24 Signals selected as reference to determine the progress of the reaction between aniline and *n*-hexylamine

For comparative reasons, we also performed a series of experiments using Shvo's catalyst under our reaction conditions. As reflected in Table 3.15, the conversions and yields achieved by **15B** and Shvo's catalyst were very similar. When the amount of catalyst added decreased, the yields were lower.

Table 3.15 N-Alkylation of anilines with *n*-hexylamine[a]

Entry	Aryl amine	Cat.	Conv.(%)[b]	Yield(%)[b]
1	aniline	**5B**	80	30
2		Shvo's	80	20
3	*o*-toluidine	**5B**	85	45
4		Shvo's	85	40
5	*p*-fluoroaniline	**5B**	>95	40
6		Shvo's	>95	50
7	*p*-trifluorometilaniline	**5B**	>95	35
8		Shvo's	>95	30

[a]Reaction conditions: 0.2 mmol of alkyl amine, 0.4 mmol aryl amine, 2 mol% of catalyst and 0.03 mmol of AgOTf, toluene-d_8, 24 h, 150ºC. [b]Conversions and yields were calculated by ^{1}H NMR spectroscopy (1,3,5-trimethoxybenzene as internal standard).

c) N-Alkylation of primary amines with primary and secondary alcohols

Finally, we studied the N-alkylation of primary amines with primary and secondary alcohols. This reaction is known to be catalyzed by Ir[16, 17, 98] and Ru[10, 99] compounds. Recently, our research group described the extraordinary high activity of the iridium complexes shown in section 3.2.1.1 (**3.1** and **3.2**, see page 67) for the selective synthesis of tertiary amines by multialkylation of ammonium salts with primary alcohols, in the absence of solvent.[42] A computational study on the reaction mechanism for this process has been reported,[100] showing that a three-step mechanism operates (Scheme 3.25), implying: metal-catalyzed-oxidation of the alcohol to the aldehyde (**I**), nucleophilic addition of the amine to the aldehyde to give an imine (**II**) and a molecule of water, and finally, metal-catalyzed reduction of the imine to the final secondary amine (**III**). In this case, the elimination of water prevails over the formation of a hemiaminal, which upon dehydrogenation would generate an amide as shown in Scheme 3.12 (see page 73).

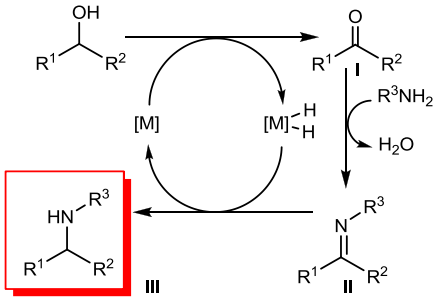

Scheme 3.25 Plausible mechanism for the N-alkylation of amines with alcohols

The N-alkylation of primary amines with primary and secondary alcohols can give two different products, secondary amines (**a**) or tertiary amines (**b**). In our experiments, the reactions were carried out with an excess of alcohol using 5 mol % of **15B** in the presence of AgOTf in neat at 110ºC (Scheme 3.26).

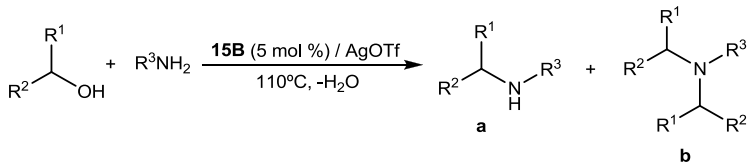

Scheme 3.26 N-Alkylation of primary amines with alcohols

As observed from the data shown in Table 3.16, all combinations of amines and alcohols provided high conversions to the corresponding N-alkylated amines. The selectivity towards the secondary (**a**) or the terciary (**b**) amine depended on the substrate used. Noteworthy, the complete conversion to the tertiary amine was observed using benzylalcohol and benzylamine (entry 2). Also, when benzylamine reacted with *n*-butanol, the conversion to the tertiary amine was moderate (entries 3 and 4).

Table 3.16 N-Alkylation of primary amines with primary and secondary alcohols[a]

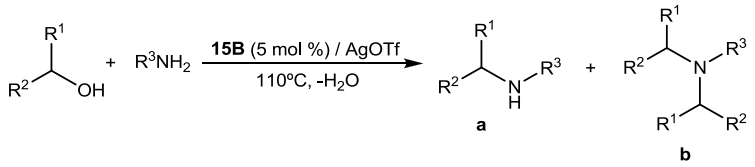

Entry	Alcohol	Amine	t(h)	Conv.(%)[b]	a (%)[b]	b (%)[b]
1	benzylalcohol	aniline	7	>95	>95	-
2		benzylamine	7	>95	-	>95(81)
3	*n*-butanol	benzylamine	7	>95	50	50
4			24[c]	>95	35	65
5	1-phenyl ethanol	*n*-hexylamine	24	>95	51	19
6			24[c]	>95	70	30
7		benzylamine	24	>95	>95	-
8			24[c]	>95	>95	-
9		cyclohexylamine	24	>95	52	13
10			24[c]	>95	45	10

[a]Reaction conditions: 0.2 mmol of amine, 1.0 mmol of alcohol, 5 mol% of **15B**, 0.03 mmol of AgOTf, 110 ºC. [b]Conversions and yields were determined by ^{1}H NMR spectroscopy using 1,3,5-trimethoxybenzene (0.02 mmol) as internal standard. [c]amine:alcohol= 1:10. Isolated yield in parenthesis.

The evolution of the reactions described was followed by ^{1}H NMR. The progress of the reactions was evaluated using 1,3,5-trimethoxybenzene as internal standard. As the reaction takes place, the signals corresponding to the initial substrates decreased and the new signals due to the N-alkylated amine obtained appeared.

These results contrast with those found in the literature, in the sense that the 'IrCp*' complexes used by Fujita and co-workers showed a complete selectivity to the secondary amines for exactly the same combination of alcohols and amines.[16]

For comparative purposes, we also tested other Ir(III) catalysts described in this work (**16D** and **17F**) and Shvo's catalyst under our reaction conditions. The catalytic performances of these complexes are refleted in Table 3.17. Complexes **15B** and **17F**, as well as Shvo's catalyst, performed very well in the N-alkylation of primary amines with benzylalcohol and 1-phenylethanol. If we pay attention to the selectivity of the reaction, we can see that using Shvo's catalyst the product of the reaction of benzylamine and benzylalcohol was the secondary amine (entry 4), while for the IrCp*(NHC) catalysts the tertiary amine (entries 1-3) was obtained.

Table 3.17 Catalyst screening in the N-alkylation of primary amines with primary and secondary alcohols

Entry	Alcohol	Amine	Cat.	t(h)	Conv. (%)[b]	a (%)[b]	b (%)[b]
1	benzylalcohol	benzylamine	**15B**	7	>95	0	>95
2			**16D**	7	60	0	20
3			**17F**	7	>95	0	>95
4			Shvo's	7	>95	>90	0
5	1-phenylethanol	*n*-hexylamine	**15B**	24	>95	51	19
6			**17F**	24	>95	50	31
7			Shvo's	24	80	30	0
8		benzylamine	**15B**	24	>95	>95	0
9			**17F**	24	85	75	0

[a]Reaction conditions: 0.2 mmol of amine, 1.0 mmol of alcohol, 5 mol % of catalyst, 0.03 mmol of AgOTf, 110ºC. [b]Conversions and yields were determined by ^{1}H NMR spectroscopy using 1,3,5-trimethoxybenzene as internal standard.

Catalyst **15B** also catalyzed the N-alkylation of secondary amines with alcohols giving the corresponding tertiary amines. For instance, Scheme 3.27 shows the reaction of N-methylaniline with benzylalcohol to give benzylmethylaniline, in which a yield of up to 95% was achieved.

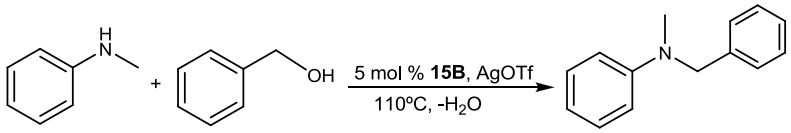

Scheme 3.27 N-alkylation of secondary amines with alcohols

As seen along this section, the catalyst **15B** provided excellent results in all three possible cross-coupling combinations. All the reactions constitute valuable processes for the preparation of biologically active species and industrial chemicals. The catalyst proved to be highly active in all the reactions tested, in most cases improving the catalytic performances of the most active catalysts recently described for the same processes. Only Shvo's catalyst shows a similar activity for the case of the N-alkylation of anilines with aliphatic amines. The catalytic reactions that we studied were carried out in the absence of base, phosphine, or any other additive (for the use of the triflate adducts there is no need to add any extra amount of AgOTf), which in fact not only simplifies the reaction workup processes (the products are more easily separated from the reaction mixtures), but also provides singular more environmentally benign process.

3.2.2.4 Functionalization of arenes

The functionalization of arenes is an important process for the preparation of a variety of industrial relevant substrates. The typical procedures for these reactions, known as Friedel-Crafts reactions, imply the use of alkyl halides and Lewis acid catalysts. In the recent years, alcohols,[101] ethers,[102] styrenes[103] and acetates[104] have been used in order to soften the reaction conditions and eliminate harmful by-products.

Given the capability of 'IrCp*(NHC)' complexes to promote C-H activation processes, we decided to explore their activity towards the benzylation of arenes using non-conventional benzylating agents such as alcohols, ethers and styrenes, thus demonstrating their wide catalytic versatility.

As for the cross-coupling reactions (Section 3.2.2.3), the addition of an excess of AgOTf was necessary in order to generate the catalytic active species. In first place, we studied the catalytic activity of **15B**, **16D**, **17F** and $[IrCp^*Cl_2]_2$ in the benzylation of toluene using benzylalcohol. The reaction was carried out in presence of 0.1 mol % of catalyst at 70 or 100ºC.

Table 3.18 Catalyst screening in the benzylation of toluene[a]

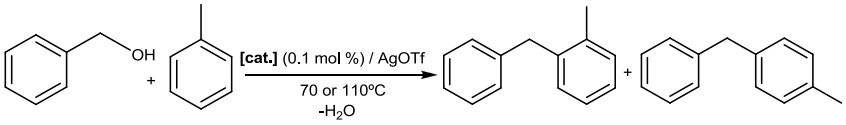

Entry	Cat.	T(ºC)	t(h)	Yield.(%)[b]
1	$[IrCp^*Cl_2]_2$	110	7	53
2	**15B**	110	3	>95
3	**15B**	70	10	>95
4	**16D**	110	7	>95
5	**17F**	110	3	>95
6	**17F**	70	10	75

[a]Reaction conditions: 3 mmol of benzylalcohol, 15 mmol of toluene, 0.1 mol% of catalyst and 0.3 mol% of AgOTf. [b]Yields were determined by ^{1}H NMR spectroscopy.

Table 3.18 shows the yields achieved for each catalyst. We observed that all complexes containing NHC ligands showed higher activity than that shown by the $[IrCp^*Cl_2]_2$/AgOTf system. Although **15B** and **17F** showed good catalytic activity, **15B** performed better at lower temperature (70ºC) (entry 3). The direct use of $[IrCp^*(OTf)_2(NHC)]$ or its *in situ* preparation from **15B** and the addition of an excess of AgOTf,[83] did not lead to any significant differences in the catalytic activities shown.

With these results in mind, we decided to explore the capability of the best catalyst (**15B**) in the benzylation of arenes using different benzylating agents such as other alcohols, ethers or styrenes derivates.

a) Benzylation of arenes with alcohols and ethers

The reaction was carried out with three different benzylating agents and several arenes in the presence of 0.1 or 1 mol % of catalyst at 110ºC.

Table 3.19 Benzylation of arenes[a]

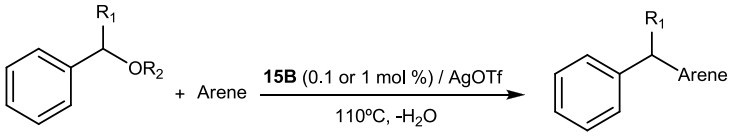

Entry	Benzylating agent	Arene	Cat. loading (%)	t(h)	Yield(%)[b]	Ratio *o*:*p*[b]
1	benzylalcohol	toluene	0.1	3	>95(89)	35:65
2		anisole	0.1	3	>95	35:65
3		benzene	0.1	6	75	-
4		*o*-xylene	0.1	3	>95	35:65
5		*p*-xylene	0.1	3	>95(89)	-
6	1-phenylethanol	toluene	0.1	4	32	10:90
7		anisole	0.1	3	>95	10:90
8		*p*-xylene	0.1	4	40	10:90
9		phenol	0.1	4	>95	40:60
10	dibenzylether	toluene	1	6	>95(90)	35:65
11		anisole	1	5	>95	35:65

[a]Reaction conditions: 1 mmol of benzylating agent, 5 or 10 mmol of arene and 1 or 0.1 mol% of catalyst and 0.3 mol% of AgOTf. [b]Yields and ratios were determined by ^{1}H NMR spectroscopy. Isolated yields in parenthesis.

Table 3.19 shows the catalytic results when benzylalcohol, 1-phenylethanol and dibenzylether were used. As can be seen from the results shown, a catalyst loading as low as 0.1 mol %, affords good to excellent conversions at short reaction times (3-4 h) when both alcohols were used (entries 1-9). The benzylation of benzene required a longer reaction time, and a maximum yield of 75% was achieved. Poor selectivities in

the production of the *ortho*/*para* isomers were obtained when benzylalcohol was used (entries 1, 2 and 4), although the selectivity improved when the higher steric demanding 1-phenylethanol was utilised (entries 6-8). The reactions carried out using dibenzylether as benzylating agent required a higher catalyst loading of 1 mol % and longer reaction times, although it also afforded full conversions to the final products (entries 10 and 11).

The progress of the reaction was determined by ^{1}H NMR spectroscopy. As the reaction takes place, the signals corresponding to the benzylating agent disappeared while the signals due to the new compounds appeared. For example, in the benzylation of phenol with 1-phenylethanol, the signals selected as reference for the starting material were the proton of the -CH group of 1-phenylethanol (1H, q, 4.89 ppm) and the proton of the -CH_3 group of the same alcohol (3H, d, 1.51 ppm) (Scheme 3.28). As the reaction goes on, we can observe the appearance of two quadruplets at 4.46 and 4.14 ppm corresponding to the proton of the -CH- group of the *ortho*- and *para*- products, and two doublets at 1.67 and 1.64 ppm corresponding to the protons of the -CH_3 groups of the same products.

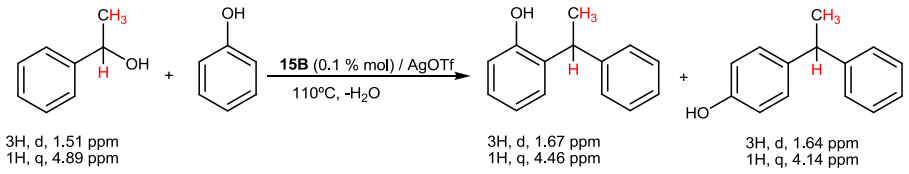

Scheme 3.28 Signals selected as reference to evaluate the progress of the reaction of 1-phenylethanol with phenol

These data compare well, and even improve, the results obtained for other recently used transition metal catalysts for the benzylation of arenes with benzyl alcohols, where higher catalyst loadings and longer reaction times were needed.[102]

b) Benzylation of arenes with styrenes

Direct addition of styrenes to arenes is an interesting alternative for the preparation of 1,1-diarylarenes.[103, 105-106] Catalyst **15B** was tested in the benzylation of arenes using a

series of styrenes. The reaction was carried out with the styrene derivate and an excess of arene, employing 0.1 or 1 mol % of catalyst at 110ºC.

Table 3.20 Reaction of styrene derivatives with arenes[a]

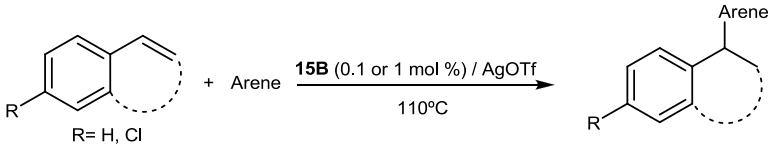

Entry	Styrene	Arene	Cat. loading (%)	t(h)	Yield(%)[b]	Ratio *o*:*p*[b]
1	styrene	toluene	1	6	30	10:90
2		anisole	0.1	4	>95(87)	10:90
3		phenol	1	4	>95	40:60
4	4-chlorostyrene		1	4	>95	15:85
5	1,2-dihydronaphthalene	anisole	0.1	4	>95	10:90
6	indene		0.1	4	>95	25:75

[a]Reaction conditions: 1 mmol of styrene derivative, 5 mmol of arene and 1 or 0.1 mol% of catalyst.
[b]Yields determined by ^{1}H NMR spectroscopy. Isolated yield in parenthesis.

As shown by the data presented in Table 3.20, compound **15B** displayed an excellent activity in this type of reaction. Besides the case of the benzylation of toluene (entry 1), the catalyst showed high activity for all other combinations of arenes and styrenes. Remarkably, in the benzylation of anisole, catalyst loadings as low as 0.1 mol % afforded full conversions in only 4 hours under the reaction conditions used. In most cases the reaction proceeds with a high selectivity to the *para*-isomers.

We also performed an experiment implying the coupling of styrene and anisole-d_8 in which we clearly observed that the deuterium from anisole selectively moved to the methyl group of the ethyl bridge in the final product (Scheme 3.29). The reaction can be regarded as an insertion of the molecule of styrene into one of the C-D bonds in a Markovnikov fashion. It has been proposed that the mechanism for this reaction operates through a metal-mediated electrophilic aromatic substitution,[105] although a mechanism implying the oxidative addition of a C-D bond of anisole to the Ir center and further insertion of the olefin in the Ir-D bond cannot be discarded. This

result is also interesting because we did not detect any further scrambling of deuterium about the molecule, as a consequence of any other C-H associated processes, considering that **15B** also proved to be a highly efficient catalyst in H/D exchange reactions.[84]

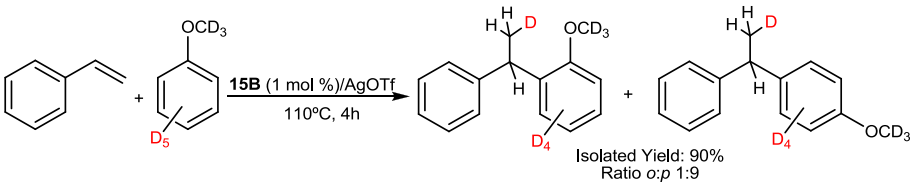

Scheme 3.29 Benzylation of anisol-d_8 with styrene

Figure 3.5 shows the deuterium NMR spectrum of the isolated product of the benzylation in the *para* position. The signal corresponding to the deuterium of the methyl group appears at 1.62 ppm.

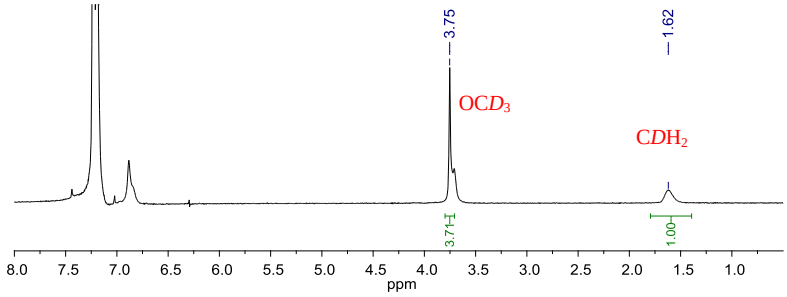

Figure 3.5 Deuterium NMR of the isolated product of the benzylation in the *para* position

c) Benzylation of aniline derivates with styrene

Compound **15B** also catalyzed the benzylation of anilines with styrenes. The reaction was carried out at 150ºC using 1 mol % of catalyst with respect to the benzylating agent and, as in the previous section, an excess of arene (aniline). The benzylation of anilines can give different products, the *-ortho* (***o***) and *-para* (***p***) products and the N-alkylated one (**N**), as shown in Scheme 3.30.

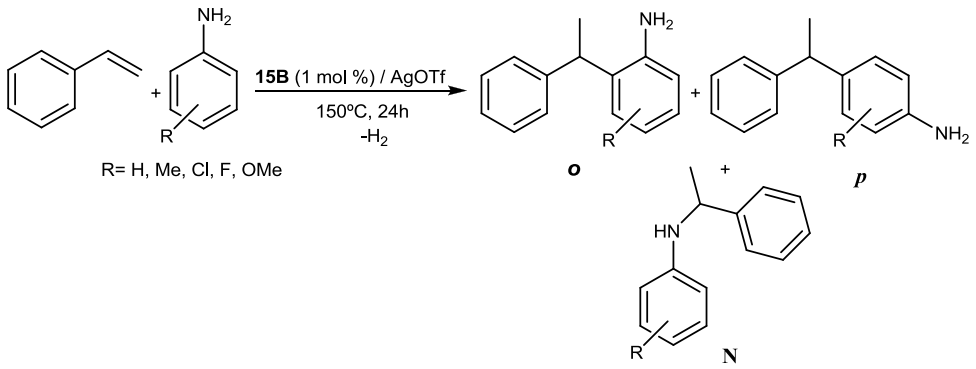

Scheme 3.30 Benzylation of aniline derivates with styrene

Table 3.21 summarizes the results obtained using catalyst **15B**. Remarkably, high conversion and selectivity were achieved when *p*-chloroaniline was used as substrate (entry 5). In all the experiments, we observed a variable percentage of the N-alkylation products. The results obtained employing **15B** are comparable with those previously reported implying the use of Brønsted acids[107] or metal complexes[108] as catalysts.

Table 3.21 Reaction of styrene with aniline derivatives[a]

Entry	Aniline	Yield(%)[b]	*o*:N[c]:*p*
1	aniline	50	72:26:2
2	*o*-methylaniline	72	70:14:16
3	*p*-methylaniline	14	90:10:-
4	*p*-fluoroaniline	75	50:50:-
5	*p*-chloroaniline	>95	90:10:-
6	*p*-methoxyaniline	50	83:17:-

[a]Reaction conditions: 1 mmol of styrene, 5 mmol of aniline derivative and 1 mol % of catalyst. [b]Yields determined by ^{1}H NMR spectroscopy. [c]N-alkylated products.

Although a wide variety of Lewis acids and transition-metal complexes have been used to catalyze the Friedel-Crafts benzylation, there are always limitations of the structure of the benzylation reagents. Again, **15B** was an efficient catalyst for a wide

set of benzylation reactions, for which different benzylating agents such as alcohols, ethers and styrenes have been used, confirming the wide applicability of this catalyst.

3.2.2.5 Tandem Catalysis: Transfer hydrogenation and benzylation of arenes

The fact that **15B** is very active in many other metal-mediated catalyzed reactions, such as transfer hydrogenation or deuteration of organic molecules,[84] prompted us to carry out a tandem process for which a standard Friedel-Crafts catalyst would be ineffective. In this sense, we carried out the reaction of benzaldehyde or acetophenone with anisole in the presence of **15B** and *i*PrOH, as shown in Scheme 3.31. Remarkably, this catalytic tandem process gathers two different reactions for which **15B** has shown excellent activities, namely, the reduction of aldehydes and ketones with *i*PrOH *via* hydrogen transfer,[83] and the benzylation of an arene with the resulting alcohol. It is important to point out that only 1.5 equivalents of *i*PrOH were needed in order to facilitate the reduction of the carbonlyl group of the aldehyde or ketone. The reaction provided full conversions to the final benzylated products.

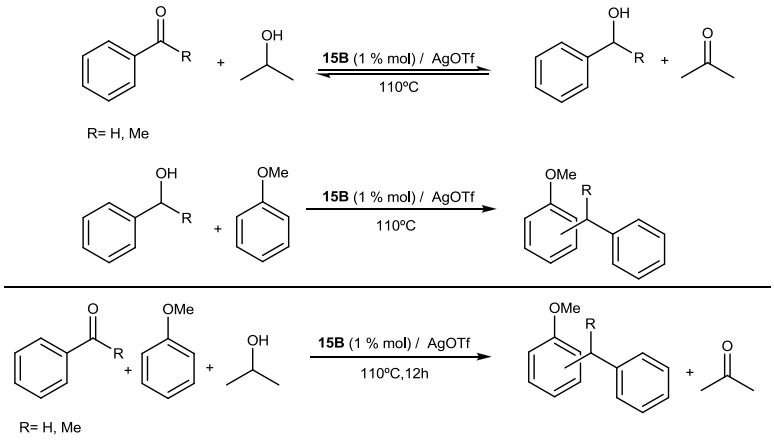

Scheme 3.31 Tandem reaction: benzylation of anisole with benzaldehyde or acetophenone

Table 3.22 Tandem catalysis. Reduction and benzylation using **15B**[a]

Entry	Benzylating agent	Yield(%)[b]	Ratio *o*:*p*[b]
1	benzaldehyde	>95(88)	35:65
2	acetophenone	>95	10:90

[a]Reaction conditions: 1 mmol of benzylating agent, 10 mmol of anisole, 1.5 mmol of *i*PrOH, 1 mol% of catalyst and 3 mol% of AgOTf. [b]Yields and ratios were determined by ^{1}H NMR spectroscopy. Isolated yield in parenthesis.

The irreversibility of the second step of the tandem processes facilitates the *i*PrOH consumption in the first step, as a consequence of the LeChatelier principle. This reaction is unprecedented in the literature, and extends the number of potential benzylating agents to ketones and aldehydes, thereby increasing the number of agents capable of producing substitutions of arenes.

The progress of the reaction was determined by ^{1}H NMR spectroscopy. The signals corresponding to the protons of *i*-propanol decreased while the aldehyde or ketones are reduced to their corresponding carbonyl products. The signals due to the protons of the alcohol formed decreased and the signals corresponding to the benzylated product (*ortho* and *para*) appeared.

For example, in the benzylation of anisole with benzaldehyde the signal corresponding to the proton of the -CHO group (1H, s, 9.99 ppm) disappeared, while we can observe the appearance of two singlets at 4.58 and 4.52 ppm belonging to the -CH_2 groups of *ortho*- and *para*- products (2H, s, 4.58 ppm and 2H, s, 4.52 ppm). While the signals due to the protons of *i*PrOH (1H, sept, 4 ppm and 6H, d, 1.17 ppm) disappeared,the signals corresponding to the protons of the ketone (2.16 ppm) appeared.

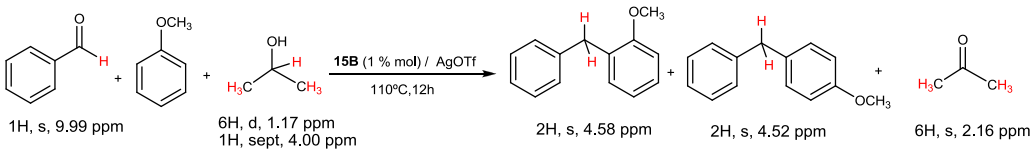

Scheme 3.32 Signals selected as references for the Tandem reaction

3.3 Conclusions

The complexes 'Ru(η^6-arene)(NHC)' and 'IrCp*(NHC)' described in Chapter 2 have been tested in several catalytic *C-H bond activation processes*, especially regarding reactions through a *borrowing-hydrogen mechanism* and functionalization of arenes.

- Both types of complexes have demonstrated high activity in several *borrowing-hydrogen processes*, paying attention to those reactions involving all possible combinations between alcohols and amines. The reactions were carried out under the 'greenest' possible conditions, thus using non-toxic solvents under the highest atom-economic conditions and minimum waste of energy.
- Complexes **3B** and **15B** have shown high activity in reactions of functionalization of arenes, specifically in chelation-assisted direct arylation and deuteration of pyridines and benzylation of arenes using "non-classical" benzylating agents. It is important to mention that both complexes contain 1,3-di-*n*butylimidazol-2-ylidene as ligand.
- The fact that **15B** is also an excellent catalyst in hydrogen transfer processes allowed us to carry out an unprecedented tandem reaction, implying the reduction of aldehydes or ketones to alcohols, which are further used as benzylating agents of arenes.

3.4 References

(1) Poyatos, M.; Mata, J. A.; Peris, E. *Chem. Rev.* **2009**, *109*, 3677; Mata, J. A.; Poyatos, M.; Peris, E. *Coord. Chem. Rev.* **2007**, *251*, 841; Corberan, R.; Mas-Marza, E.; Peris, E. *Eur. J. Inorg. Chem.* **2009**, 1700; Normand, A. T.; Cavell, K. J. *Eur. J. Inorg. Chem.* **2008**, 2781; Pugh, D.; Danopoulos, A. A. *Coord. Chem. Rev.* **2007**, *251*, 610; Diez-Gonzalez, S.; Marion, N.; Nolan, S. P. *Chem. Rev.* **2009**, *109*, 3612; Mata, J. A.; Poyatos, M. *Curr. Org. Chem.* **2011**, *15*, 3309; Herrmann, W. A. *Angew. Chem. Int. Ed.* **2002**, *41*, 1291.

(2) Bourissou, D.; Guerret, O.; Gabbai, F. P.; Bertrand, G. *Chem. Rev.* **2000**, *100*, 39.

(3) Dragutan, V.; Dragutan, I.; Delaude, L.; Demonceau, A. *Coord. Chem. Rev.* **2007**, *251*, 765.

(4) Hamid, M.; Slatford, P. A.; Williams, J. M. J. *Adv. Synth. Catal.* **2007**, *349*, 1555.

(5) Guillena, G.; Ramon, D. J.; Yus, M. *Angew. Chem. Int. Ed.* **2007**, *46*, 2358.

(6) Guillena, G.; Ramon, D. J.; Yus, M. *Chem. Rev.* **2010**, *110*, 1611.

(7) Dobereiner, G. E.; Crabtree, R. H. *Chem. Rev.* **2010**, *110*, 681.

(8) Watson, A. J. A.; Williams, J. M. J. *Science* **2010**, *329*, 635; Nixon, T. D.; Whittlesey, M. K.; Williams, J. M. J. *Dalton Trans.* **2009**, 753.

(9) Blum, Y.; Czarkie, D.; Rahamim, Y.; Shvo, Y. *Organometallics* **1985**, *4*, 1459.

(10) Hamid, M.; Williams, J. M. J. *Chem. Commun.* **2007**, 725.

(11) Shvo, Y.; Czarkie, D.; Rahamim, Y.; Chodosh, D. F. *J. Am. Chem. Soc.* **1986**, *108*, 7400.

(12) Hollmann, D.; Bahn, S.; Tillack, A.; Beller, M. *Angew. Chem. Int. Ed.* **2007**, *46*, 8291.

(13) Gnanamgari, D.; Sauer, E. L. O.; Schley, N. D.; Butler, C.; Incarvito, C. D.; Crabtree, R. H. *Organometallics* **2009**, *28*, 321.

(14) Hollmann, D.; Bahn, S.; Tillack, A.; Beller, M. *Chem. Commun.* **2008**, 3199.

(15) Kawahara, R.; Fujita, K.; Yamaguchi, R. *Adv. Synth. Catal.* **2011**, *353*, 1161.

(16) Fujita, K.; Li, Z. Z.; Ozeki, N.; Yamaguchi, R. *Tetrahedron Lett.* **2003**, *44*, 2687.

(17) Fujita, K. I.; Enoki, Y.; Yamaguchi, R. *Tetrahedron* **2008**, *64*, 1943; Fujita, K. I.; Fujii, T.; Yamaguchi, R. *Org. Lett.* **2004**, *6*, 3525.

(18) Conley, B. L.; Pennington-Boggio, M. K.; Boz, E.; Williams, T. J. *Chem. Rev.* **2010**, *110*, 2294.

(19) Dietrich, F., Stang, P. J., *Metal-Catalyzed Cross-Coupling Reactions*. ed.; Weinheim, Germany, 1998.

(20) Alberico, D.; Scott, M. E.; Lautens, M. *Chem. Rev.* **2007**, *107*, 174; Seregin, I. V.; Gevorgyan, V. *Chem. Soc. Rev.* **2007**, *36*, 1173; Giri, R.; Shi, B. F.; Engle, K. M.; Maugel, N.; Yu, J. Q. *Chem. Soc. Rev.* **2009**, *38*, 3242; Lyons, T. W.; Sanford, M. S. *Chem. Rev.* **2010**, *110*, 1147.

(21) Ackermann, L.; Novak, P. *Org. Lett.* **2009**, *11*, 4966.

(22) Bringmann, G.; Walter, R.; Weirich, R. *Angew. Chem. Int. Ed.*. **1990**, *29*, 977; Stanforth, S. P. *Tetrahedron* **1998**, *54*, 263; Silvestri, R.; Artico, M.; De Martino, G.; Ragno, R.; Massa, S.; Loddo, R.; Murgioni, C.; Loi, A. G.; La Colla, P.; Pani, A. *J. Med. Chem.* **2002**, *45*, 1567; Clarke, R.; Leonessa, F.; Welch, J. N.; Skaar, T. C. *Pharm. Rev.* **2001**, *53*, 25; Elz, S.; Kramer, K.; Leschke, C.; Schunack, W. *Eur. J. Med. Chem.* **2000**, *35*, 41; Rische, T.; Eilbracht, P. *Tetrahedron* **1999**, *55*, 1915.

(23) Daugulis, O.; Zaitsev, V. G. *Angew. Chem. Int. Ed.* **2005**, *44*, 4046; Ackermann, L.; Althammer, A.; Fenner, S. *Angew. Chem. Int. Ed.* **2009**, *48*, 201.

(24) Ackermann, L.; Born, R.; Alvarez-Bercedo, P. *Angew. Chem. Int. Ed.* **2007**, *46*, 6364.

(25) Kim, M.; Kwak, J.; Chang, S. *Angew. Chem. Int. Ed.* **2009**, *48*, 8935.

(26) Zhao, X. D.; Yu, Z. K. *J. Am. Chem. Soc.* **2008**, *130*, 8136.

(27) Do, H. O.; Khan, R. M. K.; Daugulis, O. *J. Am. Chem. Soc.* **2008**, *130*, 15185.

(28) Olah, G. A., *Friedel–Crafts and related reactions*. ed.; New York, 1965; Olah, G. A., *Friedel-Crafts and Related reactions, Vol. II, Part I*. ed.; New York, 1965.

(29) Rueping, M.; Nachtsheim, B. J. *Beils. J. Org. Chem.* **2010**, *6*.

(30) Kakiuchi, F.; Murai, S. *Acc. Chem. Res.* **2002**, *35*, 826.

(31) Panda, B. K.; Sengupta, S.; Chakravorty, A. *Eur. J. Inorg. Chem.* **2004**, 178; Jo, E. A.; Jun, C. H. *Eur. J. Org. Chem.* **2006**, 2504; Inoue, S.; Fukumoto, Y.; Chatani, N. *J. Org. Chem.* **2007**, *72*, 6588; Benhamou, L.; Wolf, J.; Cesar, V.; Labande, A.; Poli, R.; Lugan, N.; Lavigne, G. *Organometallics* **2009**, *28*, 6981; Jia, X. F.; Yang, D. P.; Wang, W. H.; Luo, F.; Cheng, J. *J. Org. Chem.* **2009**, *74*, 9470; Jia, X. F.; Yang, D. P.; Zhang, S. H.; Cheng, J. *Org. Lett.* **2009**, *11*, 4716; Chatani, N.; Inoue, S.; Yokota, K.; Tatamidani, H.;

Fukumoto, Y. *Pure Appl. Chem.* **2010**, *82*, 1443; Mizuno, H.; Tajaya, J.; Iwasawa, N. *J. Am. Chem. Soc.* **2011**, *133*.

(32) Grubbs, R. H. *Angew. Chem. Int. Ed.* **2006**, *45*, 3760; Trnka, T. M.; Grubbs, R. H. *Acc. Chem. Res.* **2001**, *34*, 18; Grubbs, R. H. *Tetrahedron* **2004**, *60*, 7117; Trnka, T. M.; Morgan, J. P.; Sanford, M. S.; Wilhelm, T. E.; Scholl, M.; Choi, T. L.; Ding, S.; Day, M. W.; Grubbs, R. H. *J. Am. Chem. Soc.* **2003**, *125*, 2546; Vougioukalakis, G. C.; Grubbs, R. H. *Chem. Rev.* **2010**, *110*, 1746; Furstner, A.; Ackermann, L.; Gabor, B.; Goddard, R.; Lehmann, C. W.; Mynott, R.; Stelzer, F.; Thiel, O. R. *Chem.-Eur. J.* **2001**, *7*, 3236; Furstner, A. *Angew. Chem. Int. Ed.* **2000**, *39*, 3013.

(33) Bugarcic, T.; Habtemariam, A.; Stepankova, J.; Heringova, P.; Kasparkova, J.; Deeth, R. J.; Johnstone, R. D. L.; Prescimone, A.; Parkin, A.; Parsons, S.; Brabec, V.; Sadler, P. J. *Inorg. Chem.* **2008**, *47*, 11470; Bugarcic, T.; Novakova, O.; Halamikova, A.; Zerzankova, L.; Vrana, O.; Kasparkova, J.; Habtemariam, A.; Parsons, S.; Sadler, P. J.; Brabec, V. *J. Med. Chem.* **2008**, *51*, 5310; Dougan, S. J.; Melchart, M.; Habtemariam, A.; Parsons, S.; Sadler, P. J. *Inorg. Chem.* **2007**, *46*, 1508; Aird, R. E.; Cummings, J.; Ritchie, A. A.; Muir, M.; Morris, R. E.; Chen, H.; Sadler, P. J.; Jodrell, D. I. *Brit. J. Canc.* **2002**, *86*, 1652; Morris, R. E.; Aird, R. E.; Murdoch, P. D.; Chen, H. M.; Cummings, J.; Hughes, N. D.; Parsons, S.; Parkin, A.; Boyd, G.; Jodrell, D. I.; Sadler, P. J. *J. Med. Chem.* **2001**, *44*, 3616.

(34) Dharmasena, U. L.; Foucault, H. M.; dos Santos, E. N.; Fogg, D. E.; Nolan, S. P. *Organometallics* **2005**, *24*, 1056; Poyatos, M.; Maisse-Francois, A.; Bellemin-Laponnaz, S.; Peris, E.; Gade, L. H. *J. Organomet. Chem.* **2006**, *691*, 2713.

(35) Viciano, M.; Sanau, M.; Peris, E. *Organometallics* **2007**, *26*, 6050.

(36) Donohoe, T. J.; O'Riordan, T. J. C.; Rosa, C. P. *Angew. Chem. Int. Ed.* **2009**, *48*, 1014.

(37) Poyatos, M.; Mata, J. A.; Falomir, E.; Crabtree, R. H.; Peris, E. *Organometallics* **2003**, *22*, 1110; Danopoulos, A. A.; Winston, S.; Motherwell, W. B. *Chem. Commun.* **2002**, 1376.

(38) Cho, C. S.; Kim, B. T.; Kim, H. S.; Kim, T. J.; Shim, S. C. *Organometallics* **2003**, *22*, 3608; Martinez, R.; Ramon, D. J.; Yus, M. *Tetrahedron* **2006**, *62*, 8988.

(39) Martinez, R.; Ramon, D. J.; Yus, M. *Tetrahedron* **2006**, *62*, 8982.

(40) Fujita, K.; Asai, C.; Yamaguchi, T.; Hanasaka, F.; Yamaguchi, R. *Org. Lett.* **2005**, *7*, 4017.

(41) da Costa, A. P.; Viciano, M.; Sanau, M.; Merino, S.; Tejeda, J.; Peris, E.; Royo, B. *Organometallics* **2008**, *27*, 1305.

(42) Segarra, C.; Mas-Marza, E.; Mata, J. A.; Peris, E. *Adv. Synth. Catal.* **2011**, *353*, 2078.

(43) Gusev, D. G. *Organometallics* **2009**, *28*, 6458.

(44) Prades, A.; Viciano, M.; Sanau, M.; Peris, E. *Organometallics* **2008**, *27*, 4254.

(45) Almeida, M. L. S.; Beller, M.; Wang, G. Z.; Backvall, J. E. *Chem.-Eur. J.* **1996**, *2*, 1533.

(46) Hanasaka, F.; Fujita, K.; Yamaguchi, R. *Organometallics* **2005**, *24*, 3422.

(47) Fujita, K.; Tanino, N.; Yamaguchi, R. *Org. Lett.* **2007**, *9*, 109.

(48) Poyatos, M.; Mas-Marza, E.; Sanau, M.; Peris, E. *Inorg. Chem.* **2004**, *43*, 1793; Cariou, R.; Fischmeister, C.; Toupet, L.; Dixneuf, P. H. *Organometallics* **2006**, *25*, 2126.

(49) Choi, J. H.; Kim, N.; Shin, Y. J.; Park, J. H.; Park, J. *Tetrahedron Lett.* **2004**, *45*, 4607; Sieffert, N.; Buhl, M. *J. Am. Chem. Soc.* **2010**, *132*, 8056; Friedrich, A.; Schneider, S. *Chemcatchem* **2009**, *1*, 72.

(50) Junge, H.; Loges, B.; Beller, M. *Chem. Commun.* **2007**, 522.

(51) Adair, G. R. A.; Williams, J. M. J. *Tetrahedron Lett.* **2005**, *46*, 8233; Kim, W.-H.; Park, I. S.; Park, J. *Org. Lett.* **2006**, *8*, 2543.

(52) Adams, J. P. *J. Chem. Soc.-Perkin Trans. 1* **2000**, 125.

(53) Gnanaprakasam, B.; Zhang, J.; Milstein, D. *Angew. Chem. Int. Ed.* **2010**, *49*, 1468; Chu, G. B.; Li, C. B. *Org. Bio. Chem.* **2010**, *8*, 4716; Landge, S. M.; Atanassova, V.; Thimmaiah, M.; Torok, B. *Tetrahedron Lett.* **2007**, *48*, 5161.

(54) Cupido, T.; Tulla-Puche, J.; Spengler, J.; Albericio, F. *Curr. Op. Drug Discov. Devel.* **2007**, *10*, 768.

(55) Gunanathan, C.; Ben-David, Y.; Milstein, D. *Science* **2007**, *317*, 790.

(56) Nordstrom, L. U.; Vogt, H.; Madsen, R. *J. Am. Chem. Soc.* **2008**, *130*, 17672; Ghosh, S. C.; Muthaiah, S.; Zhang, Y.; Xu, X. Y.; Hong, S. H. *Adv. Synth. Catal.* **2009**, *351*, 2643; Ghosh, S. C.; Hong, S. H. *Eur. J. Org. Chem.* **2010**, 4266; Dam, J. H.; Osztrovszky, G.; Nordstrom, L. U.; Madsen, R. *Chem.-Eur. J.* **2010**, *16*, 6820.

(57) Zhang, Y.; Chen, C.; Ghosh, S. C.; Li, Y. X.; Hong, S. H. *Organometallics* **2010**, *29*, 1374.

(58) Muthaiah, S.; Ghosh, S. C.; Jee, J. E.; Chen, C.; Zhang, J.; Hong, S. H. *J. Org. Chem.* **2010**, *75*, 3002.

(59) Trost, B. M.; Toste, F. D.; Pinkerton, A. B. *Chem. Rev.* **2001**, *101*, 2067; Wakatsuki, Y. *J. Organomet. Chem.* **2004**, *689*, 4092; Bruneau, C.; Dixneuf, P. H. *Acc. Chem. Res.* **1999**, *32*, 311.

(60) Pavlik, S.; Gemel, C.; Slugovc, C.; Mereiter, K.; Schmid, R.; Kirchner, K. *J. Organomet. Chem.* **2001**, *617*, 301; Katayama, H.; Nakayama, M.; Nakano, T.; Wada, C.; Akamatsu, K.; Ozawa, F. *Macromolecules* **2004**, *37*, 13; Chen, X. G.; Xue, P.; Sung, H. H. Y.; Williams, I. D.; Peruzzini, M.; Bianchini, C.; Jia, G. C. *Organometallics* **2005**, *24*, 4330.

(61) Bassetti, M.; Pasquini, C.; Raneri, A.; Rosato, D. *J. Org. Chem.* **2007**, *72*, 4558.

(62) Bassetti, M.; Marini, S.; Diaz, J.; Gamasa, M. P.; Gimeno, J.; Rodriguez-Alvarez, Y.; Garcia-Granda, S. *Organometallics* **2002**, *21*, 4815.

(63) Daniels, M.; Kirss, R. U. *J. Organomet. Chem.* **2007**, *692*, 1716.

(64) Oi, S.; Fukita, S.; Hirata, N.; Watanuki, N.; Miyano, S.; Inoue, Y. *Org. Lett.* **2001**, *3*, 2579.

(65) Ozdemir, I.; Demir, S.; Cetinkaya, B.; Gourlaouen, C.; Maseras, F.; Bruneau, C.; Dixneuf, P. H. *J. Am. Chem. Soc.* **2008**, *130*, 1156.

(66) Ozdemir, I.; Demir, S.; Gurbuz, N.; Cetinkaya, B.; Toupet, L.; Bruneau, C.; Dixneuf, P. H. *Eur. J. Inorg. Chem.* **2009**, 1942.

(67) Ackermann, L.; Vicente, R.; Potukuchi, H. K.; Pirovano, V. *Org. Lett.* **2010**, *12*, 5032.

(68) Pozgan, F.; Dixneuf, P. H. *Adv. Synth. Catal.* **2009**, *351*, 1737.

(69) Oi, S.; Tanaka, Y.; Inoue, Y. *Organometallics* **2006**, *25*, 4773; Oi, S.; Sato, H.; Sugawara, S.; Inoue, Y. *Org. Lett.* **2008**, *10*, 1823; Oi, S.; Sasamoto, H.; Funayama, R.; Inoue, Y. *Chem. Lett.* **2008**, *37*, 994; Oi, S.; Ogino, Y.; Fukita, S.; Inoue, Y. *Org. Lett.* **2002**, *4*, 1783; Oi, S.; Funayama, R.; Hattori, T.; Inoue, Y. *Tetrahedron* **2008**, *64*, 6051.

(70) Oi, S.; Sakai, K.; Inoue, Y. *Org. Lett.* **2005**, *7*, 4009.

(71) Demerseman, B.; Mbaye, M. D.; Semeril, D.; Toupet, L.; Bruneau, C.; Dixneuf, P. H. *Eur. J. Inorg. Chem.* **2006**, 1174.

(72) Demir, S.; Ozdemir, I.; Cetinkaya, B. *J. Organomet. Chem.* **2009**, *694*, 4025.

(73) Luo, Y. C.; Zhang, H. H.; Wang, Y.; Xu, P. F. *Acc. Chem. Res.* **2010**, *43*, 1317.

(74) Arockiam, P.; Poirier, V.; Fischmeister, C.; Bruneau, C.; Dixneuf, P. H. *Green Chem.* **2009**, *11*, 1871.

(75) Azua, A.; Sanz, S.; Peris, E. *Chem.-Eur. J.* **2011**, *17*, 3963.

(76) Thomas, A. F., *Deuterium Labeling in Organic Chemistry*. ed.; Meridith Corporation: New York, 1971; Lowry, T. H.; Richardson, K. S., *Mechanism and Theory in Organic Chemistry*. ed.; Harper and Row: New York, 1987; Pleiss, U.; Voges, R., *Synthesis and Applications of Isotopically Labeled Compounds*. ed.; John Wiley: New York, 2001; Vol. 7; Junk, T.; Catallo, W. J. *Chem. Soc. Rev.* **1997**, *26*, 401.

(77) Garcia-Cuadrado, D.; Braga, A. A. C.; Maseras, F.; Echavarren, A. M. *J. Am. Chem. Soc.* **2006**, *128*, 1066.

(78) Arockiam, P. B.; Fischmeister, C.; Bruneau, C.; Dixneuf, P. H. *Angew. Chem. Int. Ed.* **2010**, *49*, 6629.

(79) Simmons, E. M. H., J. F. *Angew. Chem. Int. Ed.* **2012**, *51*.

(80) Tanabe, Y.; Hanasaka, F.; Fujita, K.; Yamaguchi, R. *Organometallics* **2007**, *26*, 4618; Hanasaka, F.; Tanabe, Y.; Fujita, K.; Yamaguchi, R. *Organometallics* **2006**, *25*, 826.

(81) Hanasaka, F.; Fujita, K. I.; Yamaguchi, R. *Organometallics* **2004**, *23*, 1490; Hanasaka, F.; Fujita, K.; Yamaguchi, R. *Organometallics* **2006**, *25*, 4643.

(82) Corberan, R.; Sanau, M.; Peris, E. *Organometallics* **2006**, *25*, 4002.

(83) Corberan, R.; Peris, E. *Organometallics* **2008**, *27*, 1954.

(84) Corberan, R.; Sanau, M.; Peris, E. *J. Am. Chem. Soc.* **2006**, *128*, 3974.

(85) Viciano, M.; Feliz, M.; Corberan, R.; Mata, J. A.; Clot, E.; Peris, E. *Organometallics* **2007**, *26*, 5304.

(86) Klei, S. R.; Tilley, T. D.; Bergman, R. G. *J. Am. Chem. Soc.* **2000**, *122*, 1816.

(87) Blum, O.; Milstein, D. *J. Am. Chem. Soc.* **2002**, *124*, 11456; Blum, O.; Milstein, D. *J. Organomet. Chem.* **2000**, *593*, 479.

(88) Miles, W. H.; Connell, K. B. *J. Chem. Educ.* **2006**, *83*, 285.

(89) Pagliaro, M.; Ciriminna, R.; Kimura, H.; Rossi, M.; Della Pina, C. *Angew. Chem. Int. Ed.* **2007**, *46*, 4434.

(90) Ochiai, M.; Ito, T.; Takahashi, H.; Nakanishi, A.; Toyonari, M.; Sueda, T.; Goto, S.; Shiro, M. *J. Am. Chem. Soc.* **1996**, *118*, 7716; Gray, W. K.; Smail, F. R.; Hitzler, M. G.; Ross, S. K.; Poliakoff, M. *J. Am. Chem. Soc.* **1999**, *121*, 10711.

(91) Chen, Y. Y.; Baker, G. L. *J. Org. Chem.* **1999**, *64*, 6870; Grobelny, Z.; Stolarzewicz, A.; Maercker, A. *J. Organomet. Chem.* **2000**, *604*, 283.

(92) Saburi, H.; Tanaka, S.; Kitamura, M. *Angew. Chem. Int. Ed.* **2005**, *44*, 1730; Yadav, J. S.; Bhunia, D. C.; Krishna, K. V.; Srihari, P. *Tetrahedron Lett.* **2007**, *48*, 8306.

(93) Corma, A.; Renz, M. *Angew. Chem. Int. Ed.* **2007**, *46*, 298; Cuenca, A. B.; Mancha, G.; Asensio, G.; Medio-Simon, M. *Chem.-Eur. J.* **2008**, *14*, 1518.

(94) Liu, Y.; Hua, R. M.; Sun, H. B.; Qiu, X. Q. *Organometallics* **2005**, *24*, 2819.

(95) Feuer, H.; Hooz, J., *The Chemistry of Ether Linkage*. ed.; Interscience: London, 1967; p 457.

(96) March, J., *Advanced Organic Chemistry, Reactions, Mechanisms and Structure*. 4th ed.; Wiley: New York, 1992; p 389.

(97) Hollmann, D.; Bähn, S.; Tillack, A.; Beller, M. *Chem. Commun.* **2008**, 3199.

(98) Fujita, K.; Yamamoto, K.; Yamaguchi, R. *Org. Lett.* **2002**, *4*, 2691; Blank, B.; Madalska, M.; Kempe, R. *Adv. Synt. Catal.* **2008**, *350*, 749.

(99) Tillack, A.; Hollmann, D.; Michalik, D.; Beller, M. *Tetrahedron Lett.* **2006**, *47*, 8881; Hollmann, D.; Tillack, A.; Michalik, D.; Jackstell, R.; Beller, M. *Chem.-an Asian J.* **2007**, *2*, 403.

(100) Balcells, D.; Nova, A.; Clot, E.; Gnanamgari, D.; Crabtree, R. H.; Eisenstein, O. *Organometallics* **2008**, *27*, 2529.

(101) Sun, H. B.; Li, B.; Chen, S.; Li, J.; Hua, R. *Tetrahedron* **2007**, *63*, 10185; Podder, S.; Choudhury, J.; Roy, S. *J. Org. Chem.* **2007**, *72*, 3129.

(102) Podder, S.; Roy, S. *Tetrahedron* **2007**, *63*, 9146.

(103) Rueping, M.; Nachtsheim, B. J.; Scheidt, T. *Org. Lett.* **2006**, *8*, 3717.

(104) Mertins, K.; Lovel, I.; Kischel, J.; Zapf, A.; Beller, M. *Adv. Synth. Catal.* **2006**, *348*, 691; Mertins, K.; Iovel, I.; Kischel, J.; Zapf, A.; Beller, M. *Angew. Chem. Int. Ed.* **2005**, *44*, 238; Iovel, I.; Mertins, K.; Kischel, J.; Zapf, A.; Beller, M. *Angew. Chem. Int. Ed.* **2005**, *44*, 3913.

(105) Kischel, J.; Jovel, I.; Mertins, K.; Zapf, A.; Beller, M. *Org. Lett.* **2006**, *8*, 19.

(106) Martinez, R.; Genet, J. P.; Darses, S. *Chem. Commun.* **2008**, 3855.

(107) Babu, N. S.; Reddy, K. M.; Prasad, P. S. S.; Suryanarayana, I.; Lingaiah, N. *Tetrahedron Lett.* **2007**, *48*, 7642; Cherian, A. E.; Domski, G. J.; Rose, J. M.; Lobkovsky, E. B.; Coates, G. W. *Org. Lett.* **2005**, *7*, 5135.

(108) Michaux, J.; Terrasson, V.; Marque, S.; Wehbe, J.; Prim, D.; Campagne, J. M. *Eur. J. Org. Chemistry* **2007**, 2601; Kaspar, L. T.; Fingerhut, B.; Ackermann, L. *Angew. Chem. Int. Ed.* **2005**, *44*, 5972; Uchimaru, Y. *Chem. Commun.* **1999**, 1133; Beller, M.; Thiel, O. R.; Trauthwein, H. *Synlett* **1999**, 243.

Chapter 4

N-heterocyclic-carbene-based ditopic ligands for the design of dimetallic complexes

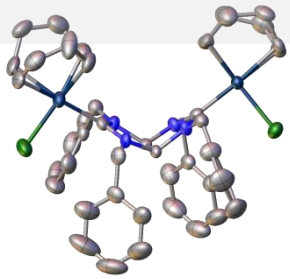

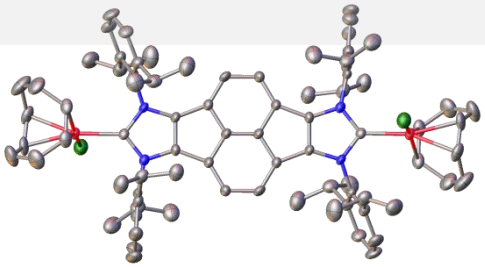

4.1 Introduction

Chapters 2 and 3 of this Thesis were focused on the preparation and coordination of a series of simple mono-NHC-based ligands. Di-, tri-, and other multitopic NHC-based ligands have also been widely studied.[1] In particular, ditopic NHC-based ligands are often poised (and designed) to preferentially bind to one metal center in a chelating form[2] (**4.1**, Figure 4.1). Notable exceptions include those systems in which a bis-carbene ligand is bridging two metal fragments, thus forming a bimetallic structure (**4.2**, Figure 4.1),[3] although the factors governing the preferences of the ligand to bind in a bridging or chelating form are not always easy to rationalize.

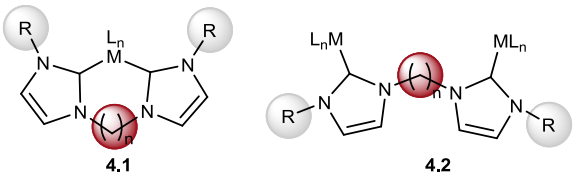

Figure 4.1 Chelating (**4.1**) *vs* bridging (**4.2**) coordination of a bis-NHC ligand

Whether the bis-NHC ligand coordinates in a chelating or a bridging coordination mode, several parameters can affect the orientation of the azole rings.[4-5] Crabtree and co-workers carried out a detailed study covering aspects such as the steric size of the N-substituents (R), the length of the alkylidene linker between the two azole rings and the nature of the counterion of the ligand precursor.[4] If small N-substituents (R) are used, long linkers favor chelation due to their ability to avoid the steric clash between R and the other ligands (L). However, when bulkier R groups are used (i. e., *t*Bu), long linkers are expected to bring the two bulky substituents too close to each other, so the chelation coordination is avoided, while short linkers and bulky R groups can then form chelates. The nature of the anion also affects the formation of either the chelated or the bridged species. The absence of halides in the reaction medium (either by abstraction of the halides in the metal precursor or by directly using a metal precursor without halide ligands) favors the formation of cationic chelate complexes instead of the 2:1 metal/ligand ones.

In the search of new poly-NHC ligands with new topologies, Bielawski and co-workers described a series of benzobis(imidazolylidene) ligands that show facially opposed coordination abilities to two metallic fragments. This type of ligands is commonly known as *Janus*-Head-type ligands.[6] The denomination *Janus*-Head is attributed to its analogy to the representation of the Roman God *Janus*, who had two faces looking at opposite directions (Figure 4.2).

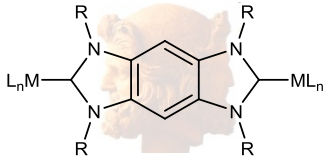

Figure 4.2 Schematic analogy between an NHC-based ligand with facially opposed coordination ability and the Roman God *Janus*

Albrecht and co-workers reported the electrochemical and spectroelectrochemical analyses of the di-iron and di-ruthenium complexes containing this ditopic bridging ligand. Contrary to their expectations, the electrochemical analyses and comparative studies using analogous monometallic carbene complexes indicate that intermetallic coupling is only weak, particularly in the di-ruthenium complexes.[7] Bielawski and co-workers showed that there is a modest intermetallic interaction in di-iridium(I) complexes.[8] Despite these results, it was suggested that the use of ditopic carbene ligands combined with a careful choice of the metal centers and the ancillary ligands, should provide access to novel and useful materials for application in molecular electronics.[8]

In the same context, our group of research has proposed a triazol-di-ylidene ligand as the simplest class of *Janus*-Head-type NHC ligand, capable to coordinate to two metal fragments in a facially opposed manner. This ligand can be easily prepared starting from 1,2,4-trialkylated triazolium salts, as described by Curphey in 1972.[9] The possibility of obtaining dicationic triazolium biscarbene precursors to potencially bind two metal centers was already suggested by Bertrand and co-workers, who described a polymeric silver biscarbene compound.[10]

In particular, our group of research demonstrated the extraordinary potential of the 1,2,4-trimethyltriazol-3,5-diylidene ligand (*ditz*, Figure 4.3). Homo-dimetallic[11-13] and hetero-dimetallic[11, 13-15] complexes with *ditz* as a linker were obtained allowing the study of their catalytic activity in tandem processes.

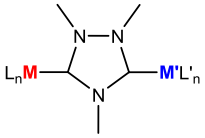

Figure 4.3 Dimetallic complex containing *ditz* ligand

For instance, the hetero-dimetallic complex **4.3** shown in Scheme 4.1, in which *ditz* connects an Ir(III) and a Pd(II) centers, was an excellent catalyst in different tandem processes in which each metal mediated mechanistically distinct reactions: (a) dehalogenation and hydrogen transfer of haloacetophenones; (b) Suzuki C-C coupling and hydrogen transfer of *p*-bromoacetophenone; (c) Suzuki C-C coupling and α-alkylation of *p*-bromoacetophenone (Scheme 4.1).[14] As a consequence of this research, the catalytic behavior of the hetero-dimetallic species suggested that the two metals are mutually collaborating in the activation of each individual catalytic reaction comprised in the tandem sequence. However, this *catalytic cooperativity* needs further study from electrochemical and computational approaches.

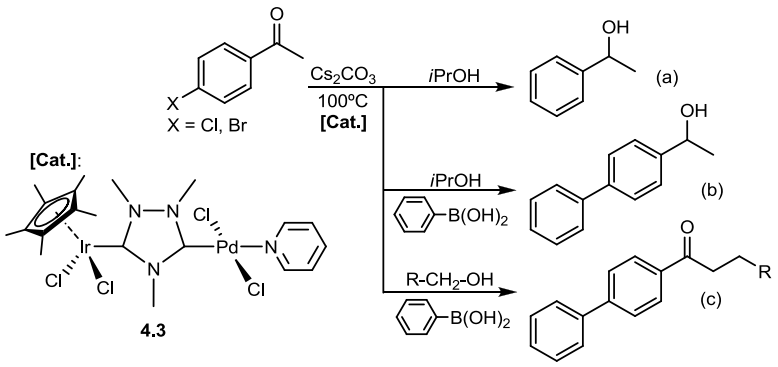

Scheme 4.1

Despite the excellent results provided by *ditz*-based complexes in tandem processes, we found some problems when using 1,2,4-triazol-3,5-diylidene ligands. Firstly, the modification of the *ditz* ligand precursor is not straightforward, therefore the stereoelectronic properties of the ligand cannot be easily modified. In addition, *ditz*-based hetero-dimetallic complexes can suffer transmetallation reactions under the harsh reaction conditions normally required in catalysis. Aiming to overcome these two drawbacks, we decided to prepare two different types of NHC-based ditopic ligands, which will be described in the following sections of this chapter. The first of these new ligands was prepared by double C-H activation of a $C(sp^3)$-H_2 group of neutral N-heterocycles, an alternative to the use of the traditional azolium precursors. The second family of ligands was prepared from imino-type ligands, earlier described in the literature.

4.1.1 Synthesis of metal complexes by double C-H bond activation

In a certain number of cases, carbenes may be generated by double C-H bond activation of $C(sp^3)$-H_2 groups.[16] Most of the known examples are referred to cyclic ethers, such as those described by Carmona and co-workers, who discovered a novel route to traditional Fischer carbenes by double αC-H bond activation.[17] They observed the formation of the carbene when a bis(ethane)iridium(I) complex, bearing a tris-pyrazolylborate ligand, was refluxed in tetrahydrofuran. As depicted in Scheme 4.2, two competitive pathways *via* an isolable intermediate originate the formation of a carbene complex (**4.4**) and a *n*-butylhydride iridium(III) complex (**4.5**).

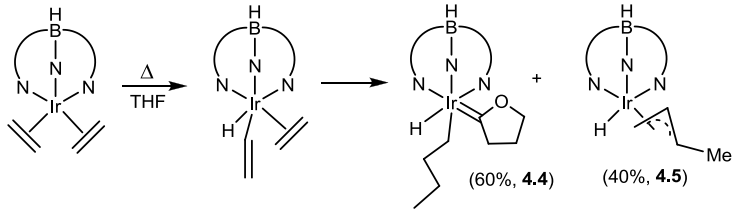

Scheme 4.2 Double αC-H bond activation to form a carbene complex (**4.4**) and a hydride-alkyl species (**4.5**)

Also, Crabtree and co-workers observed a rare double C–H activation that provided a mild and fast synthetic method to generate chelating Fischer carbene complexes.[18] In 2011, Caulton and co-workers described the only example in which a double C(sp^3)-H_2 dehydrogenation of a saturated heterocycle (imidazolidine), afforded a Ru-NHC (complex **4.6**, Scheme 4.3).[19] The NHC complex was obtained without co-products, by adding an equivalent of *tert*-butylethylene as hydrogen acceptor to the reaction mixture. *Neo*-hexane, which results from the hydrogenation of this sacrificial olefin, was readily removed under vacuum.

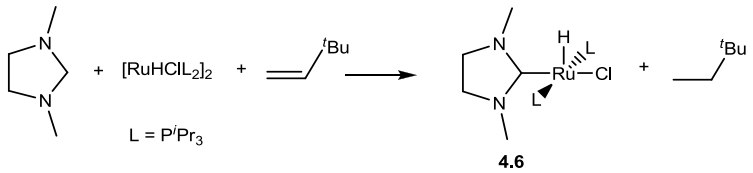

Scheme 4.3 Synthesis of a Ru-NHC complex by double C(sp^3)-H_2 dehydrogenation of an imidazolidine

4.2 Results and Discussion

4.2.1 Synthesis of new complexes bearing imidazolinylidene ligands by double C-H bond activation of $C(sp^3)H_2$ groups

In order to check the general applicability of the alternative synthetic route to NHC-based complexes described by Caulton,[19] we investigated the possibility that simple neutral N-heterocycles might react with iridium or rhodium complexes if a suitable hydrogen-acceptor is added to the reaction medium to facilitate the formation of the N-heterocyclic carbene.

The neutral N-heterocycle 1,3-dibenzyl-1,3-diazolidine (**H**H2, Scheme 4.5) was chosen for our purposes. According to the literature, **H**H2 was prepared in three steps (Scheme 4.4).[20] First, the reaction of diethyloxalate and two equivalents of benzylamine allowed the formation of N,N'-dibenzyloxamide (a). Then, N,N'-dibenzyloxamide (a) was reduced with an excess of lithium aluminium hydride giving N,N'-dibenzyl-ethylenediamine (b). The last step involves the cyclization of N,N'-dibenzyl-ethylenediamine (b) to yield the desired N-heterocycle **H**H2.

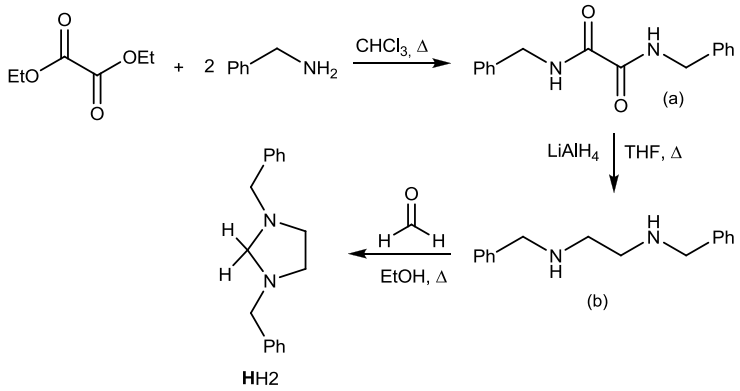

Scheme 4.4 Synthesis of diazolidine **H**H2

The reaction of **H**H2 with $[MCl(COD)]_2$ (M = Rh and Ir, COD = 1,5-cyclooctadiene) in refluxing acetonitrile afforded the monometallic complexes shown in Scheme 4.5. Complexes **18H** and **19H** were purified by column chromatography and were

precipitated from a mixture of dichloromethane/diethyl ether to give yellow solids. In the absence of a sacrificial hydrogen acceptor, the yields obtained were moderate (38 % for **18H** and 45 % for **19H**). The Gas-Chromatography (GC) analysis of the reaction products revealed that cyclooctene (COE) was formed, and that the amount of the monoolefin was closely related to the yields observed for **18H** and **19H**. These experiments were carried out adding an internal standard (anisole) to the reaction mixture. This result clearly suggests that 1,5-cyclooctadiene (COD) is acting as an internal hydrogen acceptor, and is released from the metal as cyclooctene. It is important to point out, that cyclooctane (COA) was not detected from the reaction products, thus suggesting that COD is only capable of accepting one molecule of H_2. For obvious stoichiometric reasons, the reaction yield is restricted to a maximum of 50%, unless an external amount of hydrogen acceptor is added to the reaction medium.

We performed several experiments adding different classical hydrogen acceptors such as *tert*-butylethylene (TBE), acetone or cyclohexanone. However, neither the reaction yields were improved nor the hydrogenated partners of the hydrogen acceptors used were observed. Noteworthy, when we added an extra amount of COD (5 equivalents), we observed that the reaction products were obtained in yields higher than 50% (60 for **18H** and 65% for **19H**), thus implying that the chelating nature of the hydrogen acceptor is needed in order to facilitate the process. Again, the formation of COE perfectly matched with the complex yields.

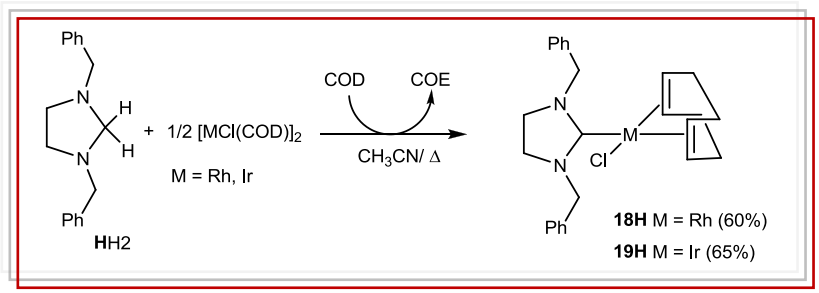

Scheme 4.5 Synthesis of **18H** and **19H** by double $C(sp^3)H_2$ bond activation

In order to confirm that chelating olefins are needed to promote the process, we carried out a reaction using $[RhCl(NBD)]_2$ (NBD = 2,5-norbornadiene), and also adding 5 equivalents of NBD to the reaction mixture. Under the same reaction conditions as those described above, we obtained the NBD-based complex **20H** (Scheme 4.6). The complex was purified by column chromatography and was precipitated from a mixture of dichloromethane/diethyl ether to give a yellow solid in high yield (67%). The GC analysis of the reaction mixture revealed the formation of norbornene (NBE), and its amount was coincident with the yield observed for **20H**.

On the other hand, when the reaction was performed with $[MCl(COE)_2]_2$ (M = Rh, Ir), in the presence of an excess of cyclooctene, the metallation of the diamino-heterocycle did not take place.

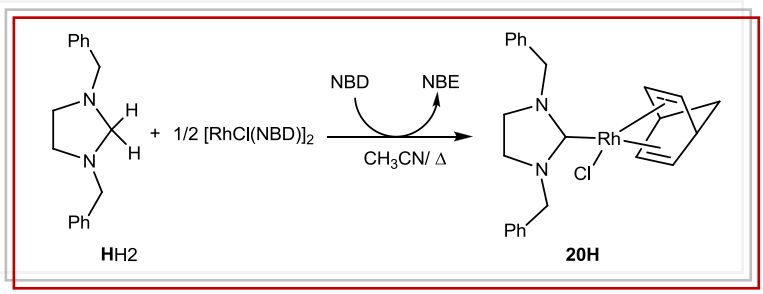

Scheme 4.6 Synthesis of **20H** by double $C(sp^3)H_2$ bond activation

All new mono-imidazolinylidene-complexes were characterized by NMR and mass spectrometry and elemental analysis. Due to the similarity of these compounds, only the spectroscopic characterization of **18H** is discussed in detail.

*^{1}H NMR spectrum of complex **18H***

Figure 4.4 shows the ^{1}H NMR spectrum of **18H**. The signals due to the protons of the CH_2 of the benzyl group appear as an AB system at 5.47 and 5.37 ppm (a). The resonances due to the protons of the CH_2 of the benzyl group appear as an AB system in most of the examples described throughout this chapter. The signal corresponding to the protons of the CH_2 of the imidazol ring appears also as an AB system at 3.32

and 3.28 ppm (b). The rest of the signals corresponding to the phenyl and COD protons are conveniently displayed on the NMR spectrum shown in Figure 4.4.

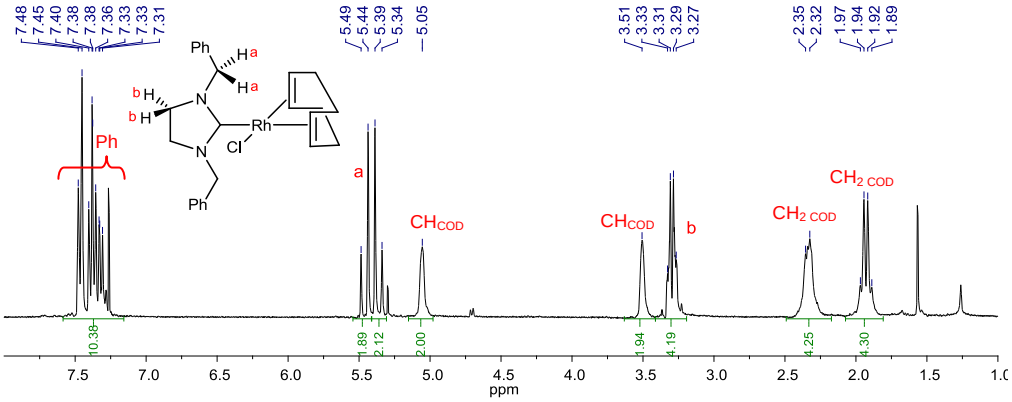

Figure 4.4 ^{1}H NMR spectrum of complex **18H** in $CDCl_3$

*$^{13}C\ \{^{1}H\}$ NMR spectrum of complex **18H***

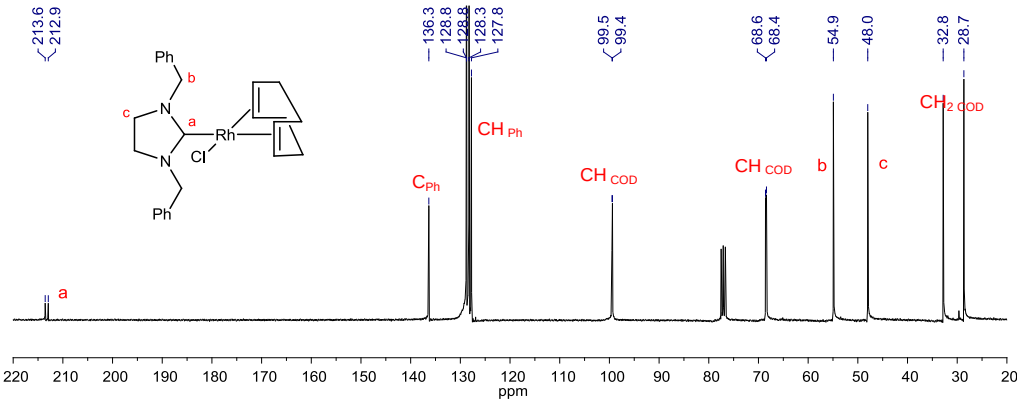

Figure 4.5 ^{13}C $\{^{1}$H$\}$ NMR spectrum of complex **18H** in $CDCl_3$

Figure 4.5 shows the ^{13}C NMR spectrum of **18H**. The most characteristic signal is the doublet attributed to the metallated carbon as a result of the Rh-C coupling ($^{1}J_{Rh\text{-}C}$ = 52.5 Hz) at 213.3 ppm (a). This chemical shift is similar to those shown for other Rh(I)-(imidazolinylidene) complexes reported in the literature.[21] The signal due to the carbons of the CH_2 of benzyl group is displayed at 54.9 ppm (b). The signal attributed to the carbon of CH_2 of the imidazolinylidene ligand appears at 48.8 ppm (c). All the

rest of the signals including those due to the phenyl and COD carbons, are conveniently displayed on the spectrum shown, and are consistent with the structure assigned to the complex.

We envisaged that the unprecedented reaction shown in Scheme 4.5 and Scheme 4.6 should have some important implications in the formation of new NHC complexes with sophisticated architectures not accessible from the classical azolium carbene precursors. In this regard, we thought that the tetraazabicyclooctane **I**H4 (Scheme 4.8) might be an excellent ligand precursor to further study this route. The synthesis of **I**H4 was carried out following the procedure described in the literature (Scheme 4.7).[22] Formaldehyde and glyoxal were added to a solution of benzylamine and formic acid. The mixture was then stirred at room temperature for five days and the desired product was collected by filtration.

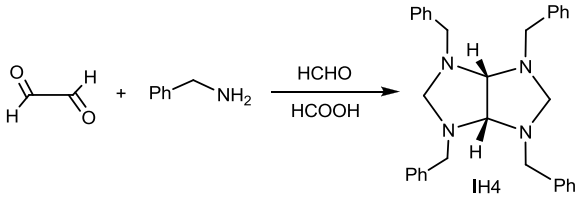

Scheme 4.7 Synthesis of **I**H4

The reaction of **I**H4 with $[MCl(COD)]_2$ (M = Rh and Ir) in refluxing acetonitrile, afforded the corresponding monometallated-NHC species **21I** and **22I**, as depicted in Scheme 4.8. The complexes were purified by column chromatography. Both complexes were precipitated from a mixture of dichloromethane/hexane to give yellow solids. Under these reaction conditions the yields were very low (<30%), but again the addition of an excess of COD allowed their isolation in much higher yields (55 % for **21I** and 65% for **22I**), with the concomitant production of the same amount of COE, which was detected by GC. When the reaction was carried out using $[RhCl(NBD)]_2$ in refluxing acetonitrile, in the presence of NBD, the monometallic compound **23I** was obtained (Scheme 4.8) in 71% yield, with the concomitant production of the same amount of NBE, which was detected by GC. These results are

in agreement with the previously described observations for the preparation of complexes **18H**, **19H** and **20H**, in which the hydrogen acceptor character of the diolefine was clearly established.

Interestingly, the restricted rotation about the M-C bond of the carbene ligand in **21I** and **22I**, allowed to obtain only the less sterically crowded rotamers (see Figure 4.9, on page 137), while the more sterically hindered ones could only be detected as traces in the ^{1}H NMR spectra of the reaction mixtures. The formation of the two possible rotamers will be discussed in more detail later, together with the situation generated by the substitution of the bulky COD ligand by the smaller COs (Section 4.2.1.1). For the Rh-NBD-based complex, **23I**, two rotamers were detected in the ^{1}H NMR spectrum, in a 67:33 ratio (**23I'**:**23I''**).

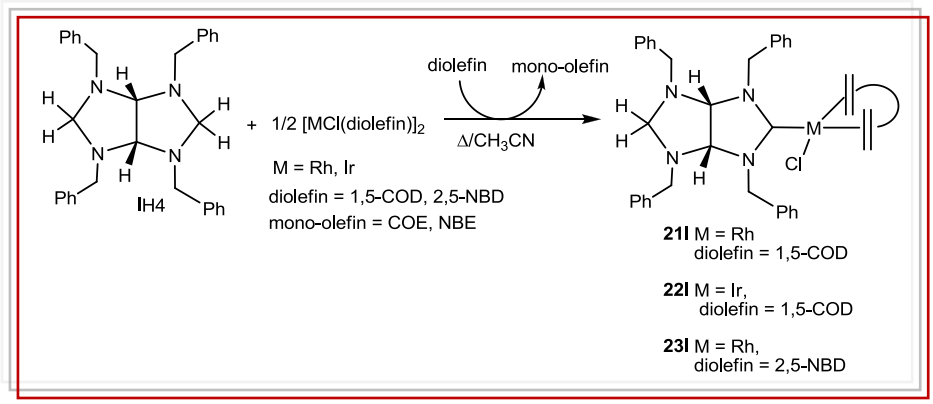

Scheme 4.8 Synthesis of **21I**, **22I** and **23I** by double C(sp^{3})H$_{2}$ bond activation

The new compounds were characterized by NMR and mass spectrometry and elemental analysis. The ^{1}H NMR spectra reveal that the ligand is coordinated to only one metal fragment, thus losing the twofold symmetry of **I**H4, as shown by the two doublets due to the inequivalent NC*H*$_{2}$N protons of the uncoordinated ring. Due to the similarity of these two compounds, only the spectroscopic characterization of **22I** is described in detail.

*^{1}H NMR spectrum of complex **22I***

Figure 4.6 shows the ^{1}H NMR spectrum of **22I**. The signals corresponding to the protons of the CH_2 of the benzyl group close to the metal fragment, appear as two doublets at 6.27 ppm (a) and 4.41 ppm (c). The signal due to the protons of the CH groups of the bicyclic ligand appears as a singlet at 4.61 ppm (b). The signals corresponding to the protons of the CH_2 of the benzyl group remote to the metal fragment are shown as an AB system at 3.83 and 3.65 ppm (d). The signals assigned to the protons of the N(CH_2)N of the uncoordinated side of the ligand also appear as an AB system at 3.51 and 3.44 ppm (e). All the rest of the signals, including those due to the phenyl and COD protons, are conveniently displayed on the spectrum shown and are consistent with the structure assigned to the complex.

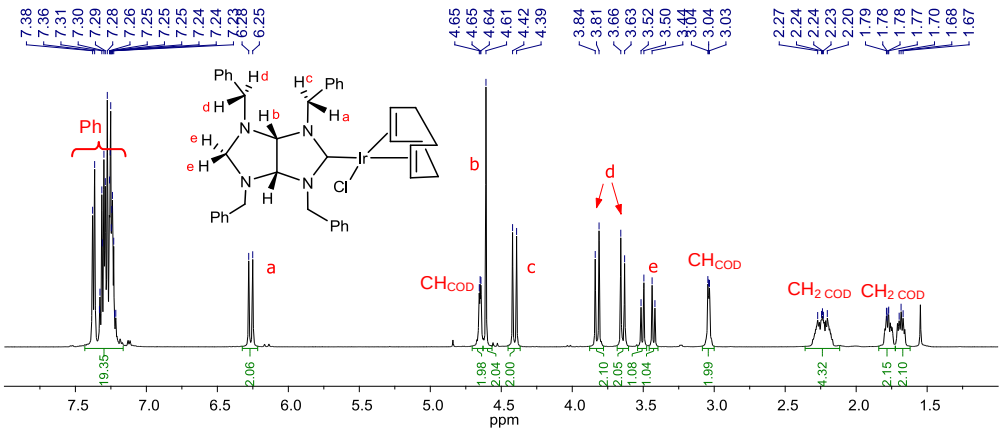

Figure 4.6 ^{1}H NMR spectrum of complex **22I** in $CDCl_3$

*^{13}C {^{1}H} NMR spectrum of complex **22I***

Figure 4.7 shows the ^{13}C NMR spectrum of **22I**. The most characteristic signal is the one attributed to the Ir(I)-$C_{carbene}$ at 207.4 ppm (a), in the region where metallated carbene-carbons of other Ir(I)-(imidazolinylidene) complexes appear.[23] The signal due to the carbon of the CH groups at the connection between the two rings of the bicyclic ligand appears at 81.4 ppm (b). The signal assigned to the carbon atom of the N(CH_2)N of the uncoordinated side of the ligand is shown at 69.3 ppm (c). The signal

due to the carbons of the CH_2 of the benzyl group remote to the metal fragment is displayed at 57.5 ppm (d). The signal attributed to the other two carbons of the CH_2 of the benzyl group close to the metal fragment is displayed at 52.1 ppm (e). The rest of the signals corresponding to the COD and phenyl carbons, are conveniently displayed on the spectrum shown and are consistent with the structure assigned to the complex.

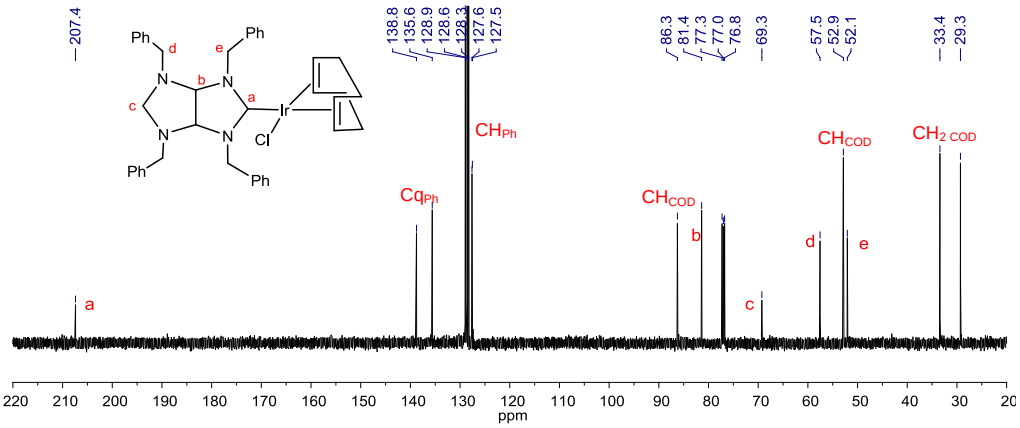

Figure 4.7 ^{13}C {^{1}H} NMR spectrum of complex **22I** in $CDCl_3$

^{13}C HSQC NMR experiments were carried out in order to fully assign the signals in the ^{13}C NMR spectrum of **22I**. The ^{13}C HSQC NMR spectrum of **22I** has been included in the Experimental Section.

*^{1}H NMR spectrum of complex **23I***

As previously mentioned, the synthesis of **23I** affords two different rotamers that we were unable to separate. In this regard, the most stable situation (therefore generating the major rotamer) arises from the orientation of the two benzyl groups close to the chloride ligand (Scheme 4.9). Figure 4.8 shows the ^{1}H NMR spectrum of **23I**. The signals attributed to the protons of the complex are displayed at similar chemical shifts as those of **22I**, but two rotamers are observed, **23I'** and **23I''** (Scheme 4.9). The signals corresponding to the protons of the CH_2 of the benzyl group close to the metal fragment appeared as two doublets at 6.34 (a) and 4.47 ppm (c) (**23I'**) and at

6.37 (a) and 4.61 ppm (c) (**23I''**). The signal due to the protons of the CH groups at the linker between the two rings of the ligand appears as a singlet at 4.54 ppm (b) for **23I'** and at 4.71 (b) for **23I''**.

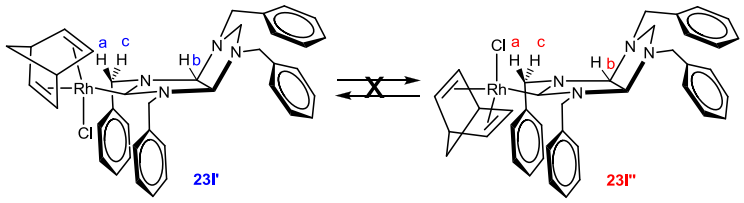

Scheme 4.9 Rotamers **23I'** and **23I''** observed by NMR spectroscopy

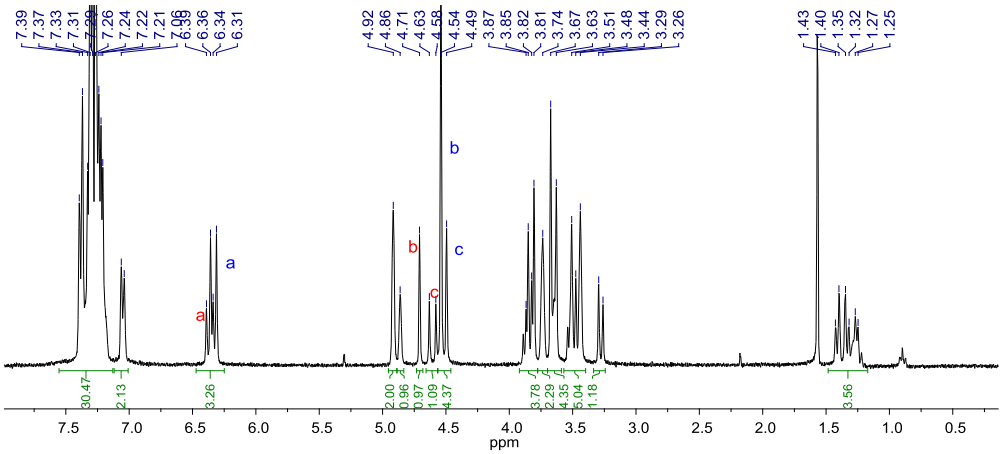

Figure 4.8 ^{1}H NMR spectrum of complex **23I** in $CDCl_3$

The $^{13}C\{^{1}H\}$ NMR spectrum of **23I** shows the signals attributed to the carbons of the complex at similar chemical shifts as those of **22I**, although the two rotamers are observed as well (see Experimental Section).

*Molecular structure of **22I***

Crystals of **22I** suitable for X-ray diffraction analysis were obtained by slow diffusion of pentane into a dichloromethane solution of the compound. The molecular structure of **22I**, shown in Figure 4.9, confirms the mono-coordination of the bicyclic-N-heterocyclic carbene to the Ir(I) centre. One chloride and one 1,5-cyclooctadiene ligands complete the coordination sphere about the metal centre.

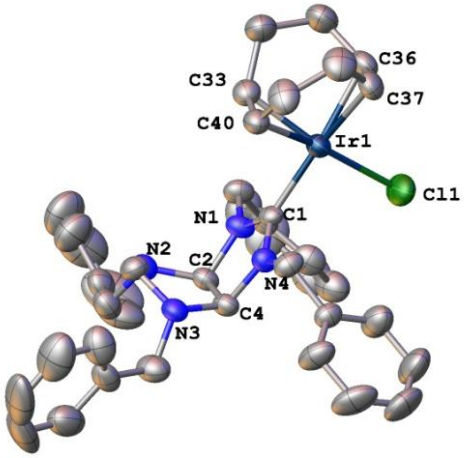

Figure 4.9 Molecular diagram of complex **22I**. Ellipsoids are at 30% probability. Hydrogen atoms have been omitted for clarity

Table 4.1 Selected bond lengths (Å) and angles (º) of complex **22I**

Bonds		**Angles**	
Ir(1)-C(1)	2.021(5)	C(1)-Ir(1)-Cl(1)	90.31(16)
Ir(1)-Cl(1)	2.3541(17)		
Ir(1)-C(40)	2.093(6)		
Ir(1)-C(33)	2.093(6)		
Ir(1)-C(36)	2.192(6)		
Ir(1)-C(37)	2.195(6)		

Table 4.1 shows the most representative bond lengths (Å) and angles (º) of complex **22I**. The Ir-$C_{carbene}$ distance is 2.021 Å, in the range of other 'Ir(COD)(NHC)' complexes.[24-25] Because the bicyclic ligand is folded along the connecting C(2)-C(4) bond, the four N-benzyl groups are occupying the less sterically strained orientation, out of the folded structure. The two N-benzyl groups at the metallated ring are closer to the chloride ligand, avoiding the bulkier COD ligand.

*Molecular structure of **23I'***

Crystals of **23I'** suitable for X-ray diffraction analysis were obtained by slow diffusion of hexane into a dichloromethane solution of the compound. The rotamer

that crystallized was the one that presents the most stable situation, namely, the one that orientates the two benzyl groups close to the chloride ligand (**23I'**).

The molecular structure of **23I'**, shown in Figure 4.10, confirms the mono-coordination of the bicyclic-N-heterocyclic carbene to the Rh(I) centre. One chloride and one 2,5-norbonadiene ligand complete the coordination sphere about the rhodium atom.

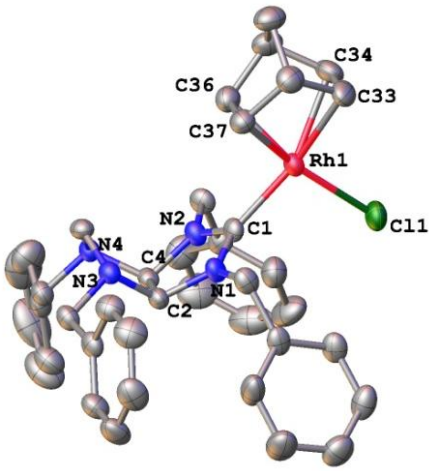

Figure 4.10 Molecular diagram of complex **23I'**. Ellipsoids are at 30% probability. Hydrogen atoms have been omitted for clarity

Table 4.2 Selected bond lengths (Å) and angles (º) of complex **23I'**

Bonds		Angles	
Rh(1)-C(1)	2.004(3)	C(1)-Rh(1)-Cl(1)	96.43(9)
Rh(1)-Cl(1)	2.3754(9)		
Rh(1)-C(33)	2.234(4)		
Ir(1)-C(34)	2.222(4)		
Ir(1)-C(35)	2.087(3)		
Ir(1)-C(36)	2.104(3)		

Table 4.2 shows the most representative bond lengths (Å) and angles (º) of complex **23I'**. The Rh-$C_{carbene}$ distance is 2.004 Å, in the range of other 'Rh(NBD)(NHC)' complexes.[26] The N-benzyl groups are occupying the less sterically strained orientation, as we observed for **22I**.

Synthesis of dimetallic compounds

When the reaction of **IH4** with $[IrCl(COD)]_2$ was carried out in refluxing toluene in the presence of 10 equivalents of COD, for 48 hours, the bimetallic compound **24I** with a bis-NHC bridging ligand was obtained. Compound **24I** can also be obtained starting from **22I**, as shown in Scheme 4.10. The complex was purified by column chromatography. **24I** was precipitated as a yellow solid from a mixture of dichloromethane/hexane in 61% yield. As will be discussed later (section 4.2.1.1), as a consequence of the formation of the dimetallic compound three different rotamers may arise, although in the case of the formation of **24I** only the more sterically favored one was obtained.

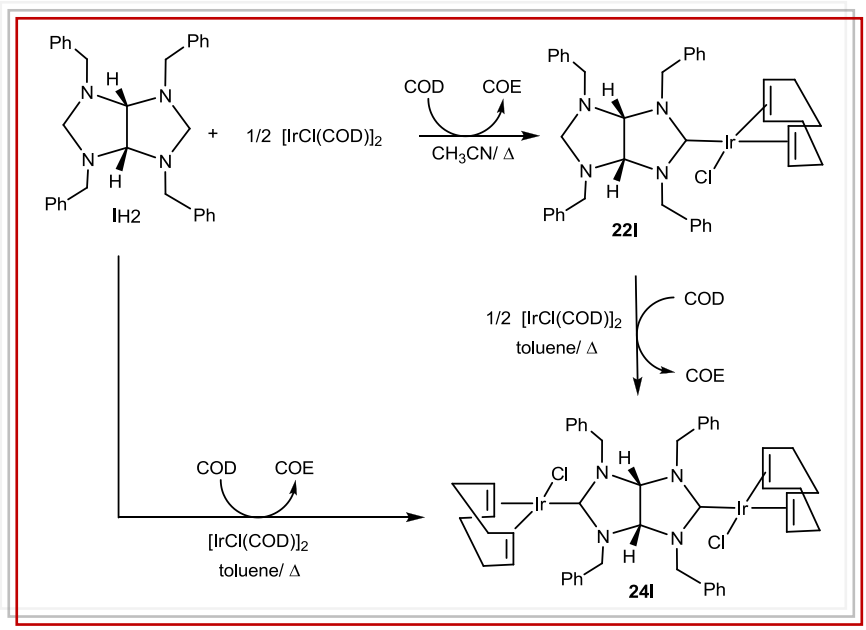

Scheme 4.10 Synthesis of **24I** by double $C(sp^3)H_2$ bond activation

Compound **24I** was characterized by NMR and mass spectrometry and elemental analysis.

*^{1}H NMR spectrum of complex **24I***

Figure 4.11 shows the ^{1}H NMR spectrum of **24I**. The signals due to the two NCH_2N protons disappeared compared to the spectrum of the starting bisimidazolinylidine,

indicating that the double metallation had occurred. The number of signals that appear in the spectrum is consistent with the binary symmetry of the molecule. The signals due to the protons of the CH_2 of the benzyl group appeared as two doublets at 6.04 (a) and 4.67 ppm (c). The signal assigned to the protons of the CH groups at the linker between the two rings of the biscarbene ligand is displayed as a singlet at 4.98 ppm (b). The rest of the signals are conveniently assigned in Figure 4.11.

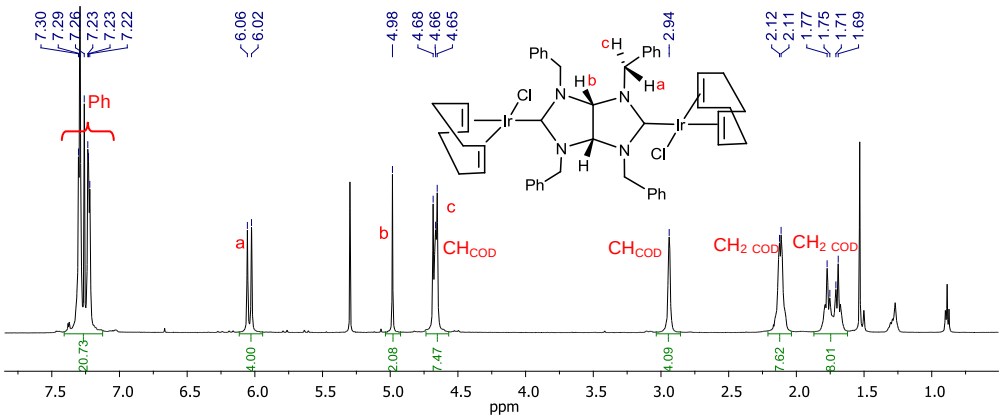

Figure 4.11 ^{1}H NMR spectrum of complex **24I** in $CDCl_3$

*^{13}C {^{1}H} NMR spectrum of complex **24I***

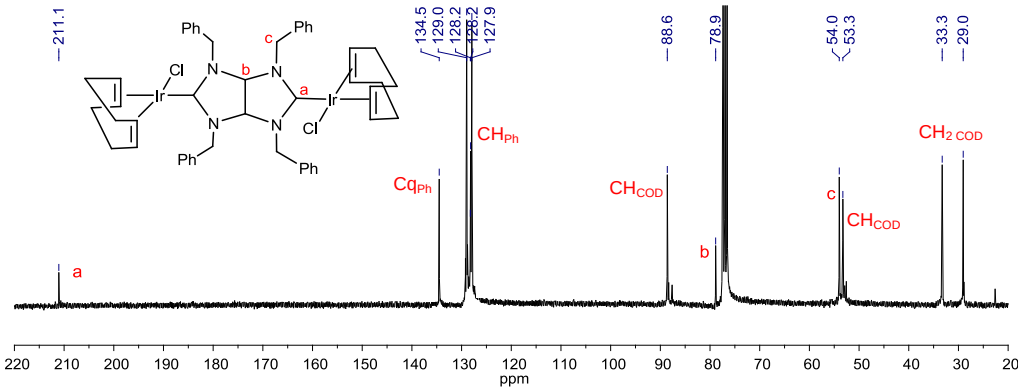

Figure 4.12 ^{13}C {^{1}H} NMR spectrum of complex **24I** in $CDCl_3$

Figure 4.12 shows the ^{13}C {^{1}H} NMR spectrum of **24I**. The most characteristic signal is that attributed to the metallated carbon, at 211.1 ppm (a). The signal attributed to the carbons of the CH groups appears at 79.0 ppm (b). The signal due to the protons

of the CH_2 of the benzyl group is shown at 54.0 ppm (c). The rest of the signals corresponding to the COD and phenyl carbons, are conveniently assigned on the spectrum.

*Molecular structure of **24I***

Crystals of **24I** suitable for X-ray diffraction analysis were obtained by slow diffusion of hexane in a concentrated solution of the compound in dichloromethane. The molecular structure of **24I**, shown in Figure 4.13, confirms the bimetallic nature of the compound. The molecule has a pseudo-C_{2v} symmetry. The bicyclic bis-NHC is bridging two iridium fragments, which complete their coordination sphere with a chloride and a COD ligand.

Table 4.3 shows the most representative bond lengths (Å) and angles (º). The Ir-$C_{carbene}$ distances are approximately 2.02 Å, similar to those of the bimetallic triazolylidene Ir(I) complex described in our group.[11] Due to the angular nature of the bicyclic ligand, the through-space distance between the two metals is 7.166 Å, while the through-bond distance is 8.5 Å. As observed for the monometallic complex **22I**, the N-benzyl groups are pointing towards the chloride ligands, adopting the configuration of minimum steric clash. The bis-heterocyclic ligand displays an average angle of 96.5º with respect to the metal coordination planes.

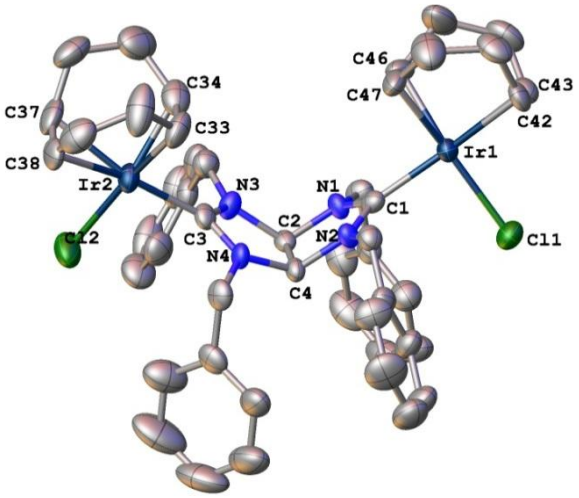

Figure 4.13 Molecular diagram of complex **24I**. Ellipsoids are at 30% probability. Hydrogen atoms and solvent (hexane) have been omitted for clarity

Table 4.3 Selected bond lengths (Å) and angles (º) of complex **24I**

Bonds		**Angles**	
Ir(1)-C(1)	2.017(7)	C(1)-Ir(1)-Cl(1)	90.86(18)
Ir(1)-Cl(1)	2.3509(19)	C(3)-Ir(2)-Cl(2)	92.47(19)
Ir(1)-C(46)	2.107(7)		
Ir(1)-C(47)	2.114(8)		
Ir(1)-C(42)	2.202(7)		
Ir(1)-C(43)	2.211(7)		
Ir(2)-C(3)	2.018(7)		
Ir(2)-Cl(2)	2.345(2)		
Ir(2)-C(34)	2.078(9)		
Ir(2)-C(33)	2.087(9)		
Ir(2)-C(38)	2.202(7)		
Ir(2)-C(37)	2.204(7)		

4.2.1.1 Carbonyl derivatives of 21I, 22I and 24I

The study of the carbonyl stretching frequencies by Infrared Spectroscopy provides valuable information about the electron-donating ability of the co-ligands coordinated to the metal center. In order to study whether the double coordination of the bis-

carbene ligand affects to the electron-donating ability of the ligand, the mono-metallic complexes **21I** and **22I** and the dimetallic complex **24I** were transformed into their corresponding carbonyl derivatives. The exchange of the COD ligand by CO was carried out by bubbling carbon monoxide into a solution of the COD-substituted complexes in dichloromethane at 0ºC (Scheme 4.11 and Scheme 4.12).

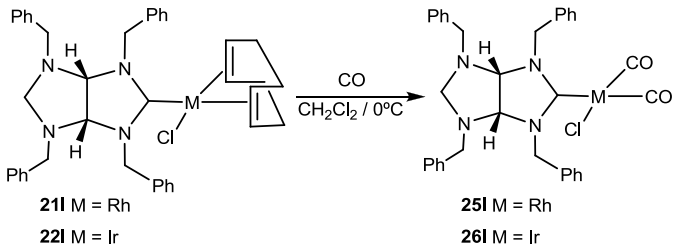

Scheme 4.11 Synthesis of **25I** and **26I**

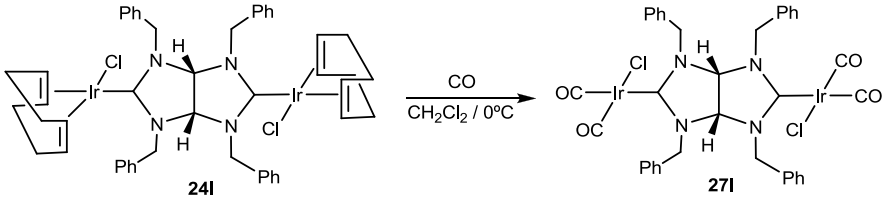

Scheme 4.12 Synthesis of **27I**

Each carbonylation yielded different rotamers that we could not separate, and that we attributed to the restricted rotation of the carbene about the M-$C_{carbene}$ bond. Variable temperature NMR experiments, together with spin-polarization-transfer-NMR (SPT) experiments allowed us to confirm that these rotamers do not interconvert. Interestingly, this situation does not apply for the COD-substituted complexes **21I**, **22I** and **24I**, for which the isomers with the benzyl groups close to the chloride ligand are strongly preferred (see molecular diagrams in Figure 4.9 and Figure 4.13) over the related orientation close to the bulkier COD ligand. This situation arises from the restricted rotation of the benzyl groups about the N-C bonds due to the special topology of the ligand. The four benzyl groups are forced to point out of the inner cavity formed by the two folded planes. For the monoazole-derived complexes **18H-20H**, the situation is completely different because the benzyl groups are free to rotate

about the N-C bond, so the two possible orientations of the benzyl groups can be achieved by the free N-C rotation while the M-C rotation is still restricted.

*A) Monometallic dicarbonyl complexes **25I** and **26I**: structural features*

As previously mentioned, in the preparation of the COD-substituted complex **21I**, the formation of two rotamers (**21I'** and **21I''**, Figure 4.14) also occurred, although the one with the chloride ligand oriented close to the benzyl groups (**21I'**), was strongly favored. Trace amounts of the more sterically constrained rotamer in which the bulky COD ligand is orientated close to the benzyl groups, were also detected (**21I''**, Figure 4.14).

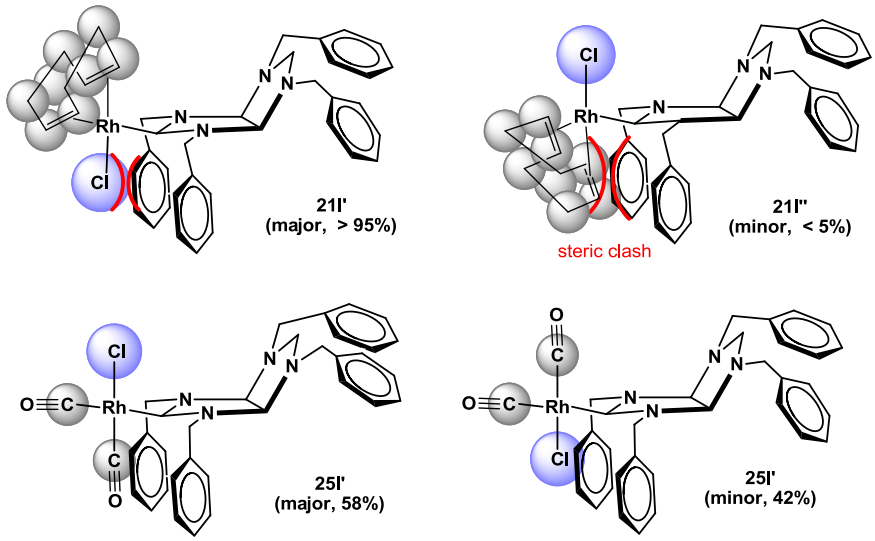

Figure 4.14 Two possible rotamers for the COD- and CO-based Rh complexes with ligand **I**

The substitution COD by the smaller CO in **21I** renders to a different situation in which none of the two rotamers formed is strongly favoured over the other, therefore yielding a mixture of two isomers in a 58:42 molar ratio (**25I**' and **25I''**, respectively in Figure 4.14). We assigned the structure of the major rotamer to that in which the chloride ligand and the benzyl groups avoid the steric interaction (**25I'**) yielding a more sterically relieved configuration.

The same effect is observed for the related Ir-based complexes. The displacement of the COD ligand in **22I** yielded a mixture of two isomers in a 61:39 molar ratio (**26I'** and **26I''**).

The ^{1}H and ^{13}C NMR spectra of the mixture of rotamers for **25I** and **26I** are given and explained in detail bellow.

*^{1}H NMR spectrum of complex **25I***

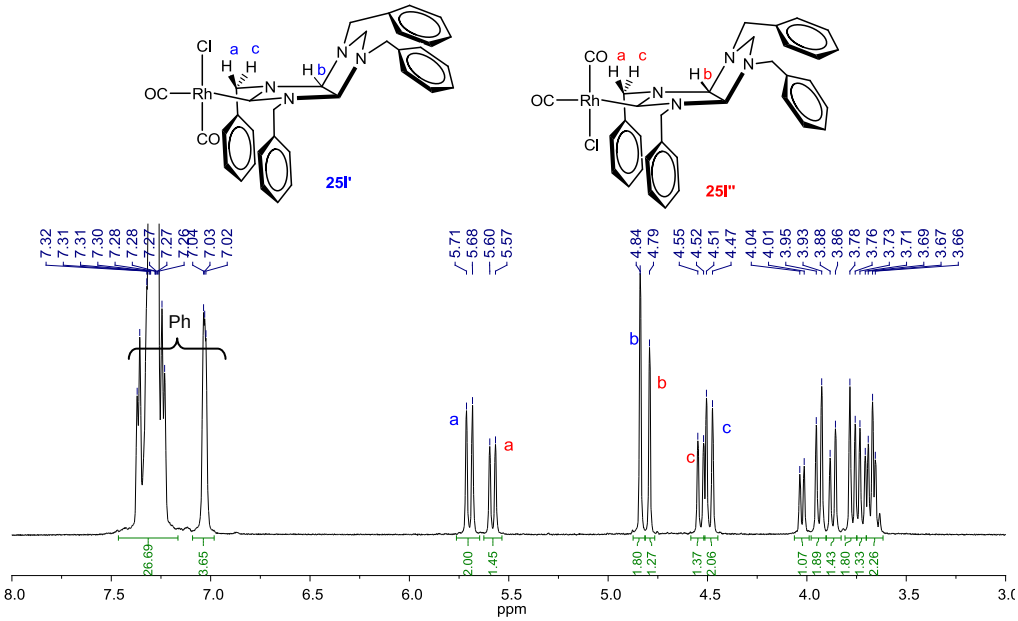

Figure 4.15 ^{1}H NMR spectrum of complex **25I** in $CDCl_3$

Figure 4.15 shows the ^{1}H NMR spectrum of **25I**. The signals corresponding to the protons of the CH_2 of the benzyl group close to the metal fragment appear as two distanced doublets at 5.70 (a) and 4.49 ppm (c) for **25I'** and at 5.59 (a) and 4.54 ppm (c) for **25I''**. The signal attributed to the protons of the CH groups of the ligand appears as a singlet at 4.84 ppm (b) for **25I'** and 4.79 ppm (b) for **25I''**.

*^{1}H NMR spectrum of complex **26I***

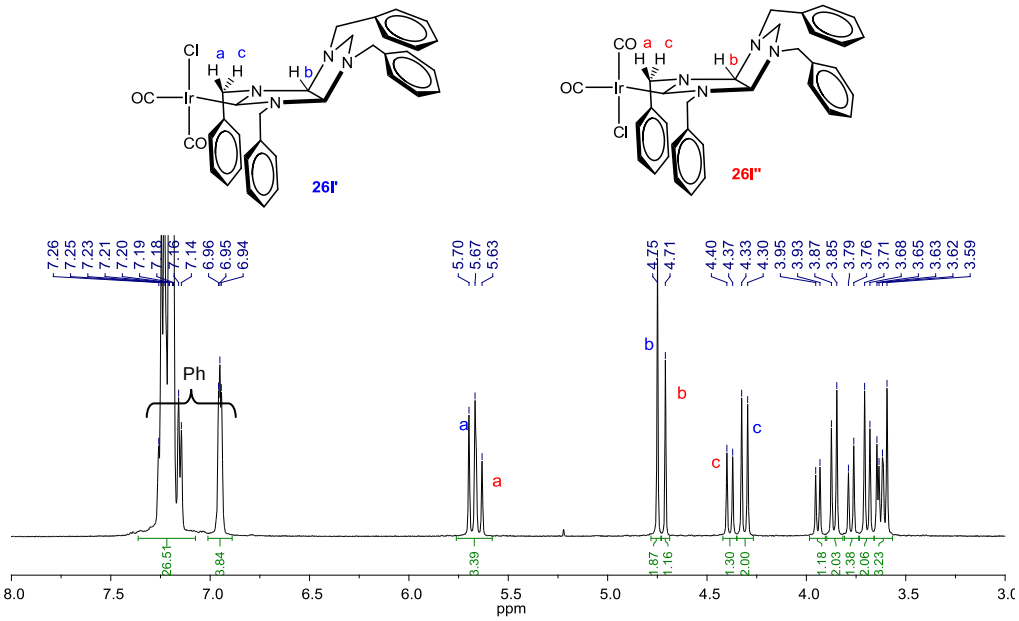

Figure 4.16 ^{1}H NMR spectrum of complex **26I** in $CDCl_3$

Figure 4.16 shows the ^{1}H NMR spectrum of **26I**. The signals corresponding to the protons of the CH_2 of the benzyl group close to the metal fragment appeared as two doublets at 5.69 (a) and 4.32 ppm (c) for **26I'** and at 5.61 (a) and 4.39 ppm (c) for **26I''**. The signal due to the protons of the CH of the bridge of the ligand appears as a singlet at 4.75 ppm (b) for **26I'** and at 4.71 (b) for **26I''**.

*^{13}C {^{1}H} NMR spectrum of complex **26I***

The ^{13}C {^{1}H} NMR spectra of the complexes revealed also the presence of two rotamers. Figure 4.17 shows the ^{13}C {^{1}H} NMR spectrum of **26I**. The most characteristic signal is the one attributed to the metallated carbon, at 199.5 ppm (a) for **26I'** and 198.4 ppm (a) for **26I''**. The appearance of the signals corresponding to the carbons of the carbonyl ligand at 181.5 and 168.6 ppm for **26I'** and at 181.3 and 168.0 ppm for **26I''**, revealed that the reaction had taken place. The rest of the signals

corresponding to the phenyl and the ligand carbons, are conveniently displayed on the spectrum shown.

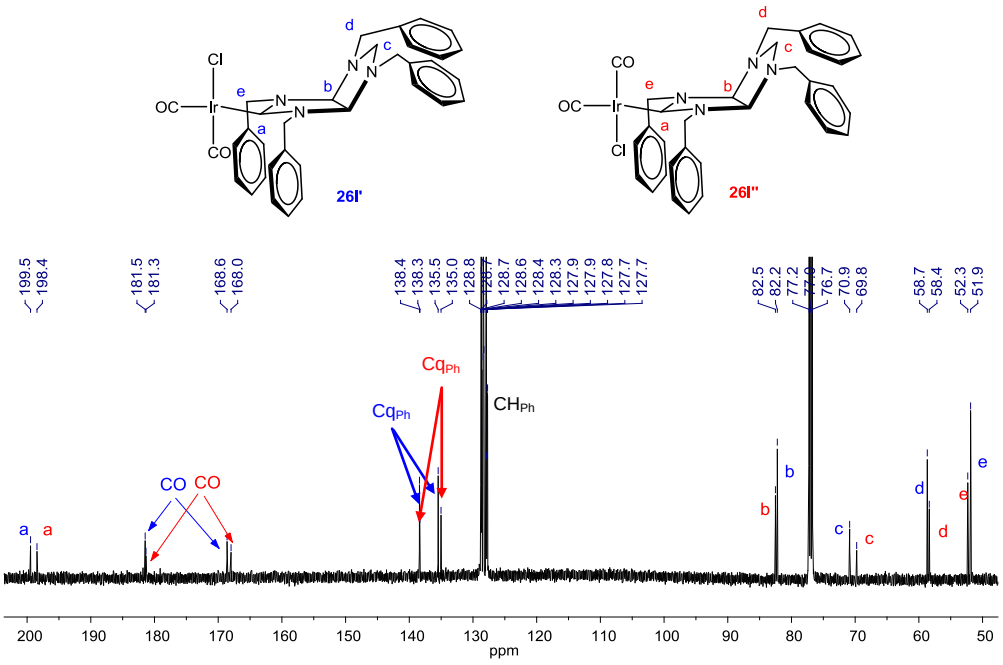

Figure 4.17 $^{13}C\{^{1}H\}$ NMR spectrum of complex **26I** in $CDCl_3$

*B) Dimetallic dicarbonyl complex **27I***

As a consequence of the formation of the dimetallic structures, three different rotamers may arise depending of the orientation of the chloride with respect to the N-benzyl groups of the bis-NHC ligand. As stated earlier, only one of these three possible rotamers is obtained for the COD-substituted complex **24I**, and may be attributed to the more released situation in which the two chloride ligands are oriented close to the benzyl groups (**24I'**, in Figure 4.18).

When the bulky COD ligand in **24I** was exchanged by CO, the three possible rotamers were clearly detected by NMR spectroscopy. These three rotamers (**27I'**, **27I''**, **27I'''**, Figure 4.18) were obtained in a 50:42:8 molar ratio, respectively.

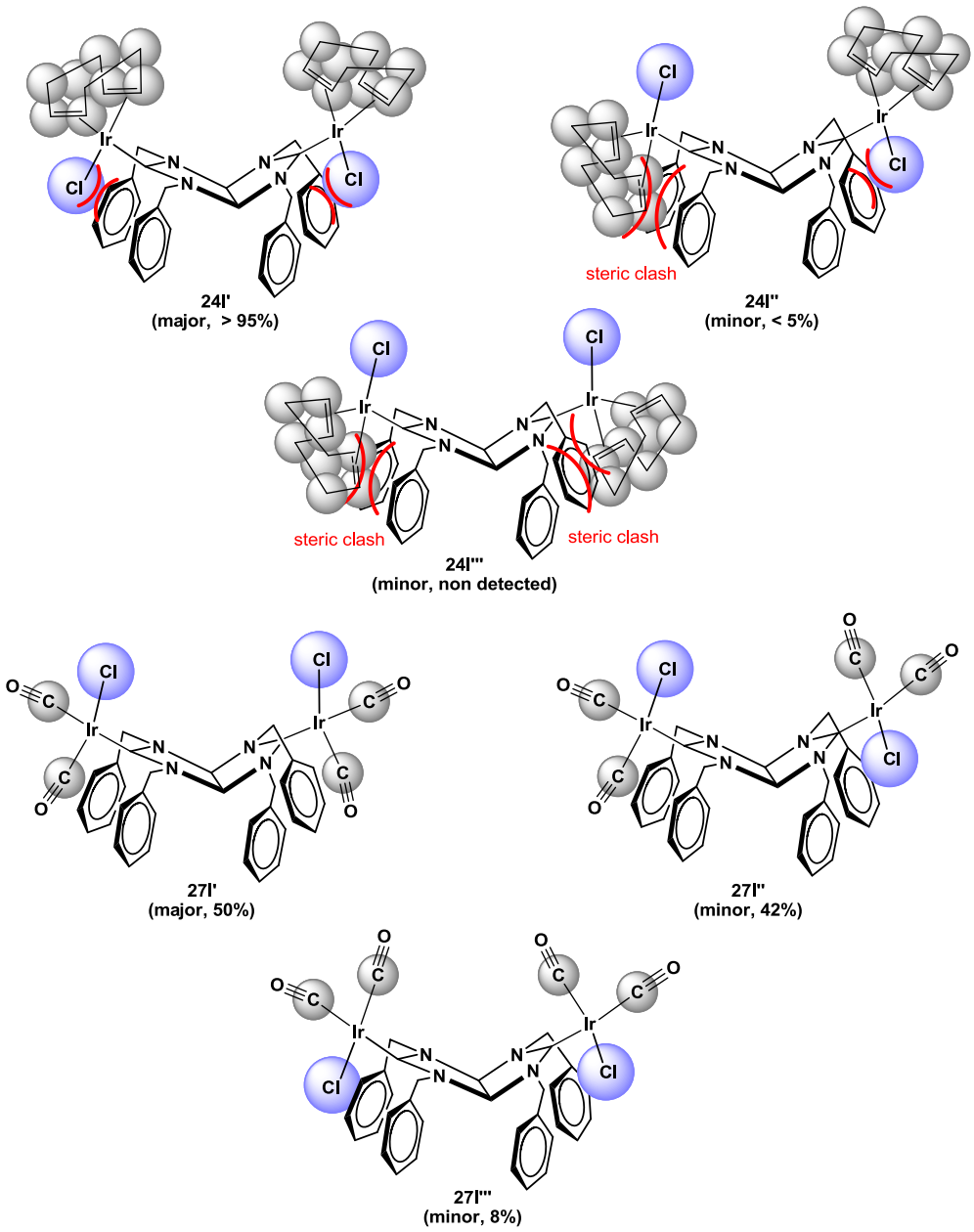

Figure 4.18 The three possible rotamers for the dimetallic COD- and CO-based complexes with ligand **I**

*^{1}H NMR spectrum of complex **27I***

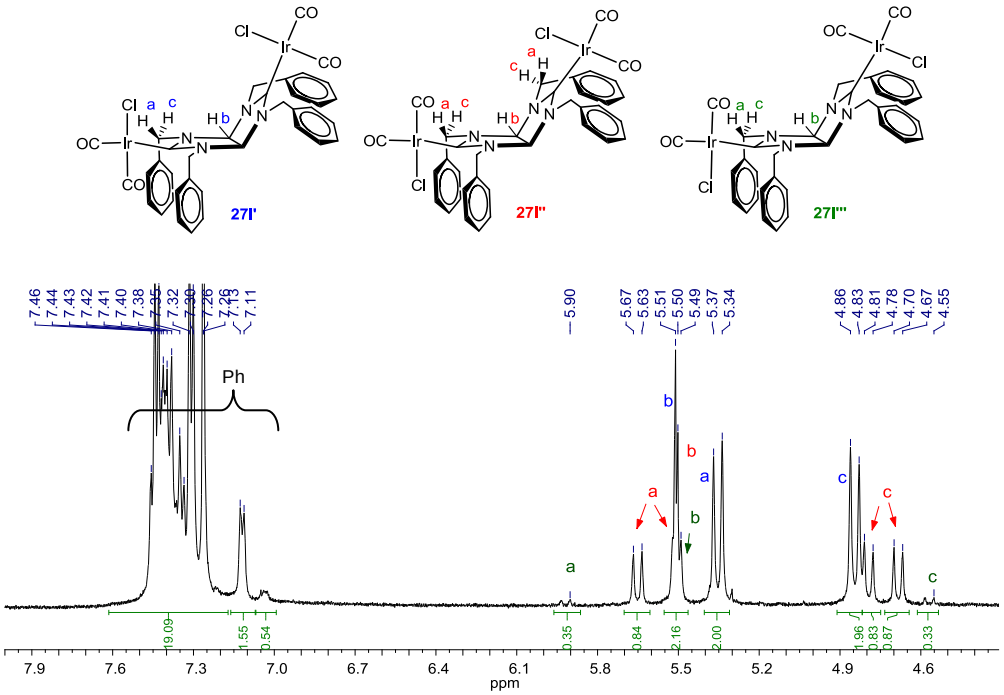

Figure 4.19 ^{1}H NMR spectrum of complex **27I** in $CDCl_3$

Figure 4.19 shows the ^{1}H NMR spectrum of **27I**. The signals corresponding to the protons of the CH_2 of the benzyl group appear as two doublets at 5.36 (a) and 4.85 ppm (c) for **27I'**, four different doublets are showed at 5.65 and 5.50 (a) and at 4.80 and 4.69 ppm (c) for **27I''**. Finally, two doublets are displayed at 5.90 (a) and 4.55 ppm (c) for **27I'''**. The signal due to the protons of the CH groups of the ligand appears at a very similar chemical shift for the three rotamers (5.50 ppm, b).

The existence of the different isomers does not change the local symmetry about the metals nor the electron-donating power of the ligands, and this explains why the IR spectra of **25-27I** display only two CO stretching bands, as expected for the *cis* disposition of the carbonyl ligands.

Table 4.4 Carbonyl streching frequencies

Complex	ν(CO)(cm^{-1})
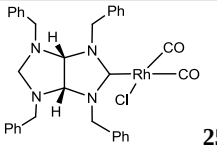 **25I**	2077 , 1995
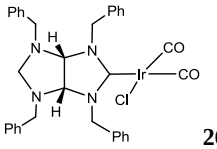 **26I**	2063, 1978
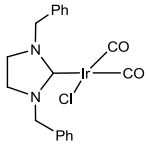	2064, 1974[23]
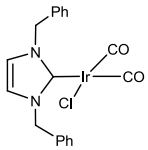	2064, 1979[23]
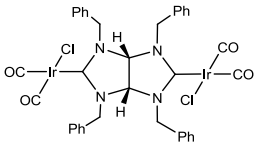 **27I**	2071, 1986
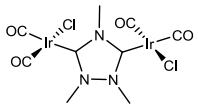	2072, 1987[11]

Table 4.4 shows the carbonyl stretching frequencies [ν(CO)] of complexes **25-27I** and also the frequency of some examples of saturated and insaturated NHC ligands coordinated to Ir(I). The ν(CO)s of the bimetallic complex **27I** were compared to those of a *ditz*-based Ir(I) dimetallic complex. For the monometallic compounds, these bands appear at 2077 and 1995 cm^{-1} for **25I**, and 2063 and 1978 cm^{-1} for **26I**, which correlate well with the previously described saturated and insaturated mono-NHC analogue complexes of Rh[27] and Ir.[23] The bimetallic compound **27I** displays its CO stretching bands at 2071 and 1986 cm^{-1}, thus indicating that the double coordination of the bis-carbene ligand slightly lowers the electron-donating capacity

of the carbene with respect to its monocoordinated form. The ν(CO)s for complex **27I** are very similar to those of the *ditz*-based Ir(I) dimetallic complex described by our group.[11]

4.2.1.2 Reactivity of mono-metallated complex 22I

Most of the NHC-based iridium complexes reported in the literature are Ir(I) species with 1,5-cyclooctadiene (COD) or CO ligands,[23, 28] or derivatives of the [Cp*Ir(III)] fragment.[29] As an alternative to overcome this structural monotony and increase the arsenal of possible catalyst design, a versatile entry into the chemistry of iridium NHC complexes, *via* the labile cationic complex $[Ir(COMe_2)(COD)(NHC)]PF_6$ was reported.[30] The experiments described in this section were performed during a short stay at the *Instituto de Ciencia de Materiales de Aragón, Universidad de Zaragoza-CSIC* under the supervision of Dr. Eduardo Sola.

A solution of **22I** in acetone was treated with 1 equivalent of $AgPF_6$ in order to remove the chloride ligand. The mixture was stirred in the dark at room temperature. The resulting suspension was filtered and the solvent was removed under vacuum. Addition of diethyl ether allowed the formation of a yellow solid, which was separated by decantation, washed with diethyl ether, and dried in vacuum. The acetone adduct **28I** was obtained in a 62% yield. The acetone ligand can be replaced by other coordinating solvents such as acetonitrile by stirring **28I** at room temperature in acetonitrile (Scheme 4.13).

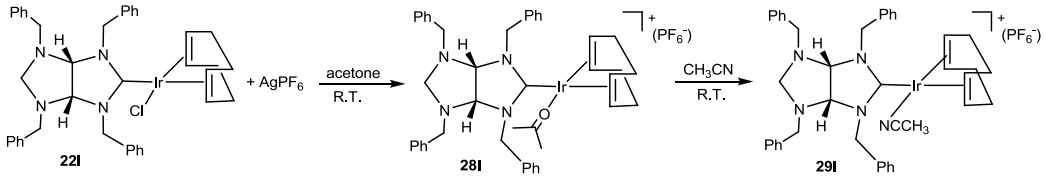

Scheme 4.13 Synthesis of complexes **28I** and **29I**

As an example, the ^1H NMR spectrum of the acetonitrile adduct will be described below.

*^{1}H NMR spectrum of complex **29I***

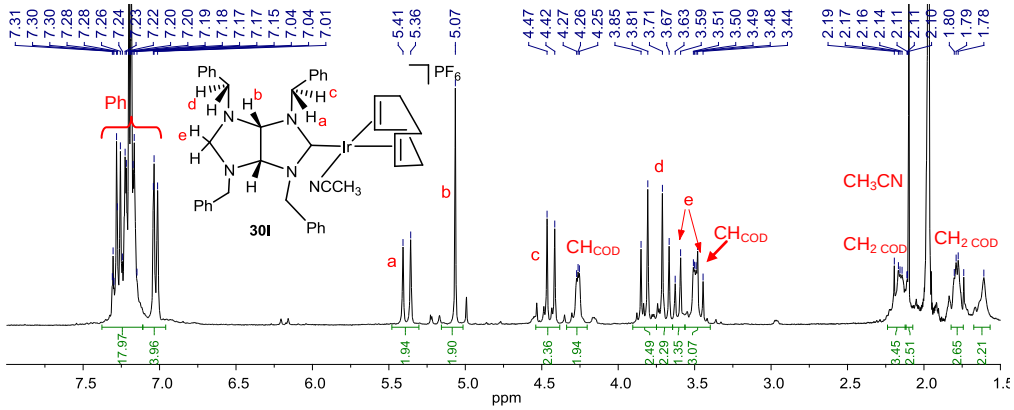

Figure 4.20 ^{1}H NMR spectrum of complex **29I** in $CDCl_3$

Figure 4.20 shows the ^{1}H NMR spectrum of **29I**. The signals are conveniently displayed on the spectrum shown and are consistent with the structure assigned to the complex. The signal attributed to the proton of the methyl group of the acetonitrile ligand is shown as a singlet at 2.11 ppm.

The hydrogenation of the COD ligand in complex **28I** in the presence of drops of acetonitrile, led to the dihydride Ir(III)-NHC complex **30I** (Scheme 4.14). The reaction was carried out in a reactor system with a P_{H2} of 10bar in $CDCl_3$ during 20 minutes.

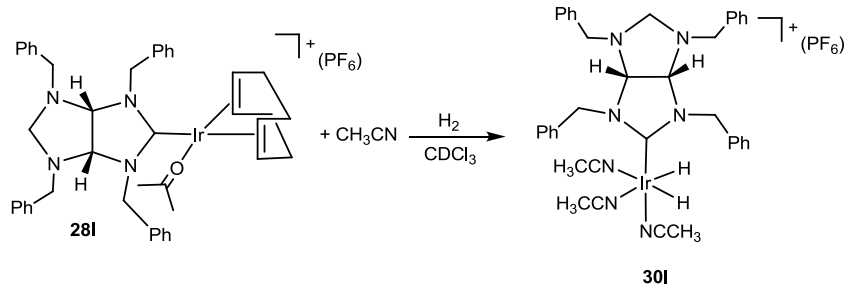

Scheme 4.14 Synthesis of complex **30I**

The characterization of the complex was carried out without further purification, directly from the reactor. When the H_2 atmosphere created in the reactor was

eliminated, we observed that **30I** was transformed into other products that could not be identified.

*^{1}H NMR spectrum of complex **30I***

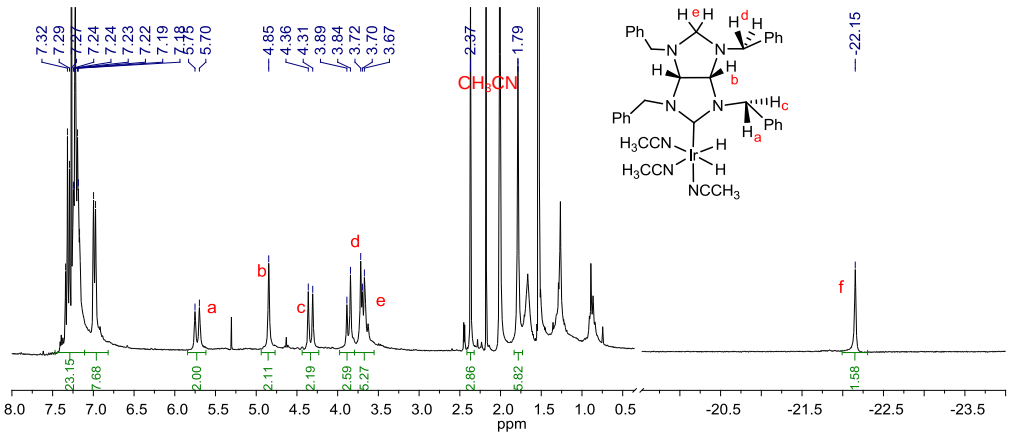

Figure 4.21 ^{1}H NMR spectrum of complex **30I** in $CDCl_3$

Figure 4.21 shows the ^{1}H NMR spectrum of **30I**. The disappearance of the signals attributed to the protons of the COD ligand evidences that the complex has been hydrogenated. The signals corresponding to the protons of the CH_2 of the benzyl groups (a, c and d), the CH of the bridge (b) and the CH_2 of the uncoordinated side of the ligand (e) appear at similar chemical shifts as those of previously described complexes. The signals due to the protons of the methyl group of the acetonitrile ligand appear as a two singlets at 2.3 and 1.79 ppm. The rest of the signals that appear in the aliphatic region of the spectrum are attributed to the released acetone, acetonitrile in excess and COA formed. Finally, the most significant signal corresponding to the dihydride is displayed as a singlet at -22.15 ppm. These spectroscopic data are in agreement with those reported in the literature for other Ir(III) dihydride complexes.[30-31]

*Molecular structure of **30I***

Crystals of **30I** suitable for X-ray diffraction analysis were obtained in acetone at -15ºC. The molecular structure of **30I**, shown in Figure 4.22, confirms the formation of the dihydride complex. The nearly perfect octahedral structure of **30I** features two very long Ir-N distances *trans* to the hydride ligand that should correspond to readily dissociable acetonitrile ligands (2.123 and 2.135 Å), in the range of other Ir(III) complexes with acetonitrile ligands described in the literature.[30] The most important structural parameters of the molecular of **30I** are collected in Table 4.5.

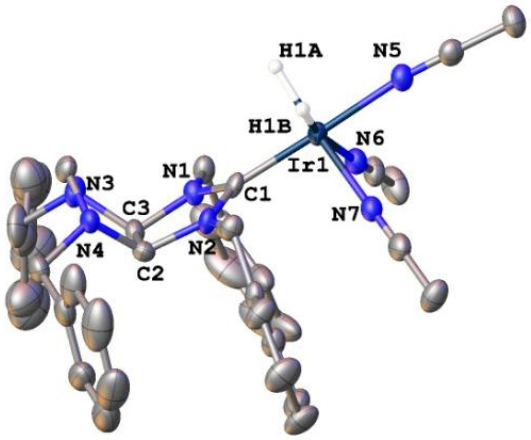

Figure 4.22 Molecular diagram of complex **30I**. Ellipsoids are at 30% probability. Hydrogen atoms, solvents (acetone and diethyl ether) and counteranion (PF_6^-) have been omitted for clarity

Table 4.5 Selected bond lengths (Å) and angles (º) of complex **30I**

Bonds		Angles	
Ir(1)-C(1)	1.982(6)	C(1)-Ir(1)-N(5)	176.0(2)
Ir(1)-N(5)	2.068(5)	C(1)-Ir(1)-N(7)	94.5(2)
Ir(1)-N(7)	2.123(5)	C(1)-Ir(1)-N(6)	97.3(2)
Ir(1)-N(6)	2.135(6)	N(5)-Ir(1)-N(6)	86.6(2)
Ir(1)-H(1A)	1.6044	N(7)-Ir(1)-N(6)	92.6(2)
Ir(1)-H(1B)	1.6128		

4.2.1.3 Reaction of imidazolidines with metal halides

Our research group, along with Prof. Dmitri Gusev, wanted to learn more about the NHC formation by double $C(sp^3)H_2$ bond activation starting from neutral N-hererocycles. We decided to study the reaction of a series of imidazolidines with chloride complexes of Ir, Rh and Ru. For our experiments, we selected $[MCp^*Cl_2]_2$ (M = Rh, Ir) and $[RuCl_2(p\text{-cymene})]_2$ since this species typically undergo symmetrical cleavage to give $16e^-$ complexes capable to coordinate to an amine. We avoided dimetallic species with potential hydrogen acceptors, such as $[MCl(diolefin)]_2$ (M = Rh, Ir; diolefin = COD, NBD) since these complexes readily undergo metallation upon reaction with imidazolidines (as stated in section 4.2.1).[32]

In this regard, the reaction of imidazolidine **H**H2 with $[IrCp^*Cl_2]_2$ at room temperature, instantaneously and quantitatively formed the corresponding imidazolinium salt ([**H**H]Cl), together with the corresponding metal-hydride product $[IrCp^*(\mu\text{-H})Cl]_2$ (Scheme 4.15). Similar behavior was observed when using $[RhCp^*Cl_2]_2$ and $[RuCl_2(p\text{-cymene})]_2$, although in these cases the mono-hydrido species $[Rh_2Cp^*_2(\mu\text{-Cl})(\mu\text{-H})Cl_2]$ and $[Ru_2(\mu\text{-Cl})(\mu\text{-H})Cl_2(p\text{-cymene})_2]$, respectively, were formed along with the imidazolinium salt [**H**H]Cl. In this series of reactions, the cyclic amine is formally acting as a hydride source and the metal complex, which undergoes Cl^-/H^- metathesis, is the hydride acceptor.

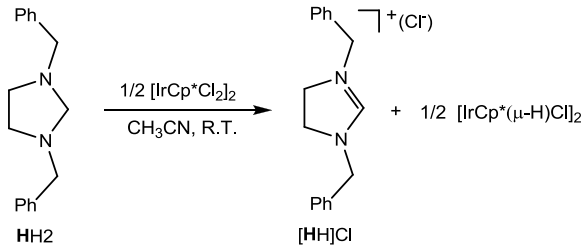

Scheme 4.15 Reaction of **H**H2 with $[IrCp^*Cl_2]_2$

In order to shed some light on the mechanism of the reactions leading to metal hydrides starting from the metal halide dimers and cyclic aminals, Prof. Gusev

performed a computational study to elucidate the structures and energies of possible metal intermediates in these reactions.

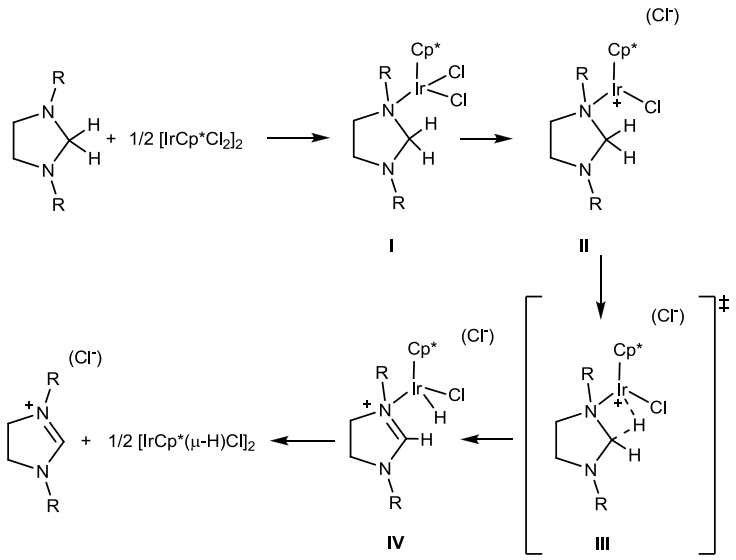

Scheme 4.16 Reaction intermediates according to the DFT calculations for the reduction of $[IrCp^*Cl_2]_2$ with imidazolidines

According to the computational study, the reaction proceeds *via* N-coordination of the substrate to the metal fragment to give a $18e^-$ intermediate, **I**. Chloride elimination and formation of the $16e^-$ cation intermediate (**II**) can undergo β-hydride elimination *via* a transition state **III** to give the unstable intermediate **IV**. The β-hydride elimination allows the formation of the azolium cation and the dimerization of the metal fragment to $[IrCp^*(\mu\text{-}H)Cl]_2$ (Scheme 4.16).

This mechanism should also account for the formation of complexes containing imidazolin-2-ylidenes by double C-H bond activation of imidazolidines, as described in Section 4.2.1. At this point, we have to mention that in the article that we published regarding this new type of coordination, we proposed a completely different mechanism based on the related existing literature.[33] As shown in Scheme 4.17, we believed that the formation of **18H** and **19H** from the reaction of **H**H2 and $[MCl(COD)]_2$ (M = Rh and Ir) implies, first, the oxidative addition of a $C(sp^3)$-H

bond to the metal. The oxidative addition should afford the formation of the M(III) hydride **I**, which may evolve to intermediate **II** through olefin insertion into the M-H bond and α-elimination of the N-heterocycle. The final step would imply the release of the mono-olefin by reductive elimination and coordination of COD to facilitate the formation of the final products.

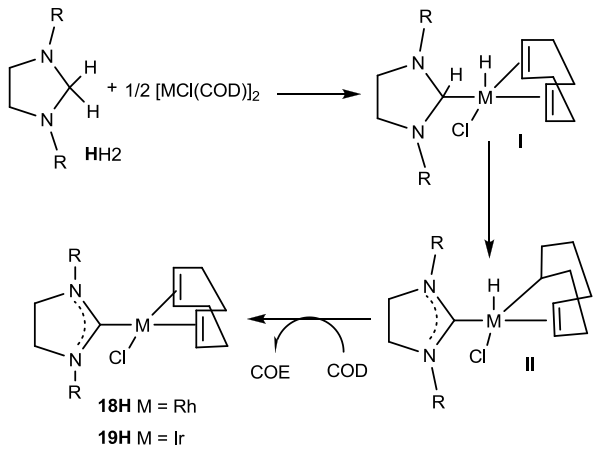

Scheme 4.17

Taking into account the mechanism for the formation of metal hydrides from imidazolidines shown in Scheme 4.16, we now believe that a more plausible mechanism for the formation of complexes containing imidazolin-2-ylidenes, should be close to the one shown in Scheme 4.18. The first step of reaction may imply the N-coordination of the imidazolidine to the metal fragment giving a $16e^-$ intermediate, **I**. *β*-Hydride elimination *via* the transition state **II** should give the unstable intermediate **III**, which undergoes oxidative addition of the azolium cation to give a Rh(III)-dihydride carbene (**IV**). Olefin insertion into the M-H bond would give intermediate **V**. The final step involves the release of the monoolefin by reductive elimination, and the coordination of a new molecule of COD to form the final product **18H**.

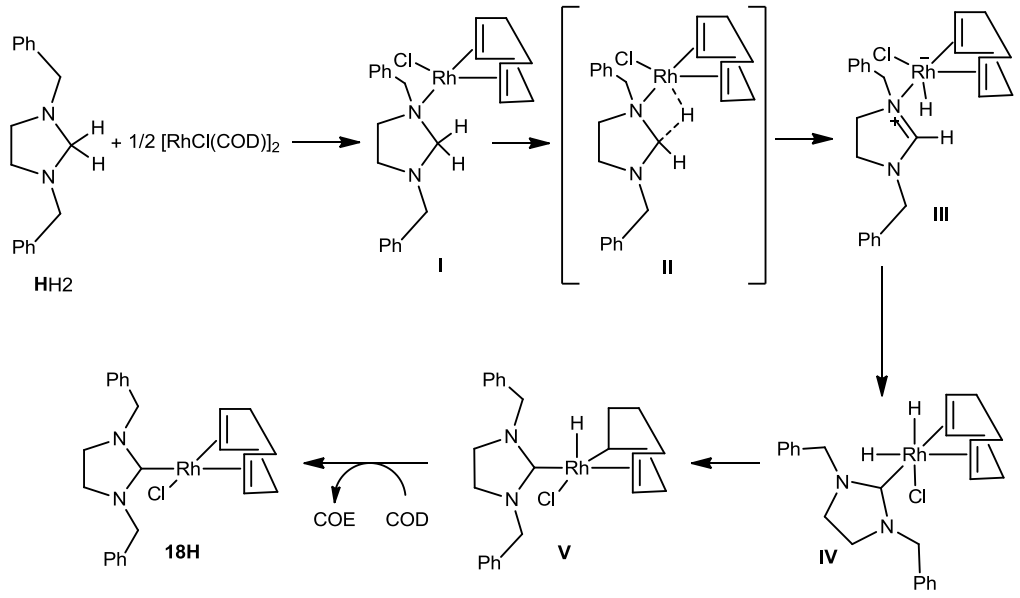

Scheme 4.18 Plausible mechanism for the formation of complexes containing imidazolin-2-ylidenes

In order to provide experimental evidences to support the results extracted from the DFT calculations, we monitored the reaction depicted in Scheme 4.19 by means of NMR and Mass Spectroscopy. The analysis of this model reaction by ^{1}H NMR did not provide any useful information about the intermediates of the process, probably because these are present in very low concentrations in the reaction media.

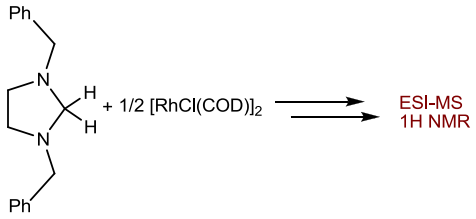

Scheme 4.19 Reaction monitored by ^{1}H NMR and ESI-MS

Mass Spectrometry techniques have appeared as a breakthrough for the rapid and sensitive characterization of organometallic compounds, since they allow pre-existing

molecules in solution to be transferred to the gas phase with minimal fragmentation. In particular, electrospray ionization mass spectrometry (ESI-MS) and its tandem version (MS/MS) are the techniques of choice for solution mechanistic studies in chemistry and biochemistry and for high-throughput screening of homogeneous catalysis reactions. Whereas ESI-MS can provide information about the molecular formulas of the species present in the reaction mixture, tandem MS/MS can help to confirm their molecular organization. This technique has allowed our group of research to study the mechanism of the hydrosilylation of terminal alkynes.[34]

The two reagents were placed together in a small vial and dissolved in acetonitrile. After 30 minutes, the sample was analyzed by ESI-MS and the fragmentation of some of the species detected was further studied by MS/MS. After 30 minutes of reaction, the ESI-MS showed the presence of two most significative peaks at *m/z* 499.2 and 463.2. In principle, the peak at m/z 499.2, could correspond to the protonated form of intermediate **I**, as shown in Scheme 4.18. This assumption is supported by the fact that the fragmentation of such a peak using MS-MS (Figure 4.23) revealed that this species losses HCl and a Rh(COD) fragment, giving species with *m/z* 463.2 and 253.2, respectively.

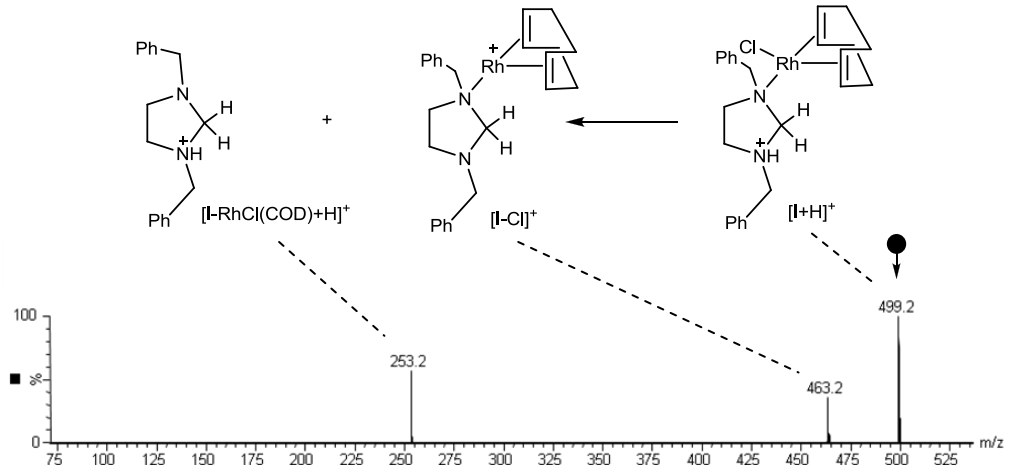

Figure 4.23 ESI-(+)-MS/MS tandem spectra of intermediate [**I**+H]$^+$ at 10eV

The peak at *m/z* 463.2 could be attributed to two different species shown in Scheme 4.18, [**III**-Cl]$^+$ and [**IV**-Cl]$^+$. The ESI-MS/MS tandem spectrum of this species is shown in Figure 4.24. According to the MS/MS spectra, the fragmentation of this peak leads to a species whose *m/z* has decreased in two units (461.2), which reveals the loss of molecular hydrogen. The loss of a COD ligand and a rhodium atom is also observed, giving species with *m/z* 353.1 and 251.2, respectively.

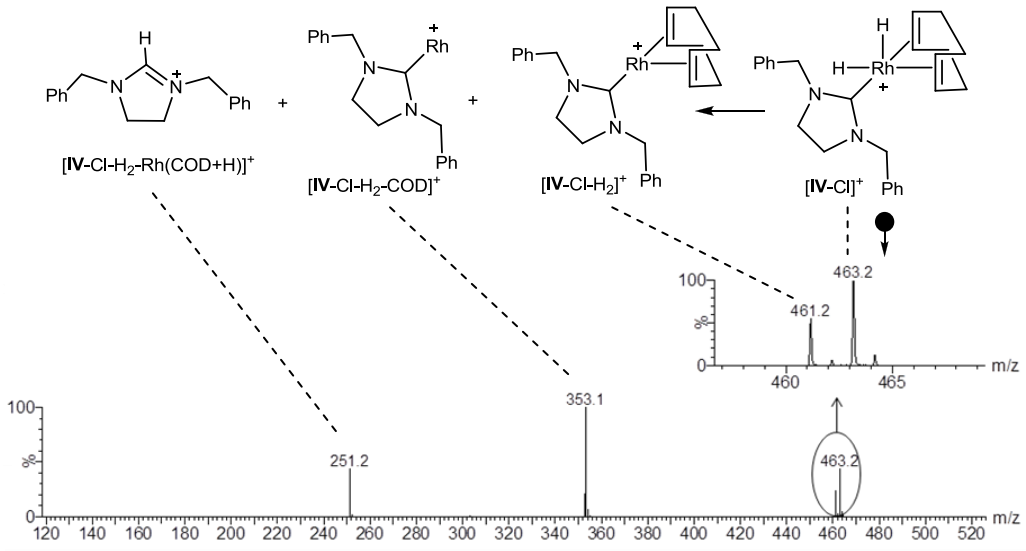

Figure 4.24 ESI-(+)-MS/MS tandem spectra of intermediate [**IV**-Cl]$^+$ at 25eV

Although we are aware that these experiments do not fully confirm our proposed mechanism (Scheme 4.18), we believe that the theoretical calculations and the experimental results afford a strong support to it.

Summarizing, the methodology used in this section provides an interesting alternative to the use of the traditional azolium salts. First, saturated N-heterocyclic carbenes of rhodium and iridium were easily prepared by simple reaction of cyclic neutral N-heterocycles and the widely used [MCl(diolefine)]$_2$ metal sources. The reactions can be triggered by the addition of an external amount of diolefine, which

acts as hydrogen acceptor, and offers several advantages over the use of the regular preligand activating agents when azolium salts are used.

This method to generate NHC-complexes by double $C(sp^3)H_2$ bond activation allowed the easy preparation of new metal compounds with sophisticated architectures, as the ones that we have shown for complexes **21I-31I**.

[MCl(COD)(NHC)] complexes (**21I** and **22I)** and $[Ir_2Cl_2(COD)_2(NHC)]$ complex (**24I**) were transformed into their corresponding carbonylated derivatives, $[MCl(CO)_2(NHC)]$ (**25I** and **26I)** and $[Ir_2Cl_2(CO)_4(NHC)]$ (**27I**). The formation of different rotamers for these species was observed. The reactivity of **22I** was also demonstrated obtaining a dihydride complex of Ir(III).

DFT calculations and Mass Spectroscopy experiments have been carried out to elucidate a possible mechanism for the generation NHC-complexes by double $C(sp^3)H_2$ bond activation.

4.2.2 Synthesis and coordination of a new bis-NHC ligand containing a pyracene scaffold

Molecules with tunable electronic interactions between redox-active centers are of interest because they offer the possibility of extended delocalization of electron density. Apart from being intrinsically interesting, the mediation of electronic coupling in redox-active bridging ligands is pertinent to the design of molecular electronic devices and the understanding of biochemical processes.[35] Despite the great versatility and accessibility of N-heterocyclic carbenes (NHCs), very few ligands containing two NHC moieties linked by a rigid π-conjugated system have been used in the preparation of dimetallic complexes. In these complexes the metal-metal interactions can potentially modify the existing characteristic of the individual metal atoms.[36]

Cowley and co-workers described the synthesis of a tetrakis(imino)pyracene (TIP) ligand, a class of bis(imino)acenaphthene (BIAN) type ligand.[37] They reported interesting redox behaviour of this new type of bridging ligand by treatment with PI_3, TeI_4 or BI_3. In order to extend the synthesis of new class of ligands, which can act as a bridge between two metal fragments, we thought that TIP ligand can be a good precursor for a new *Janus*-Head dicarbene ligand. The new bisimidazolium salt described in this section was prepared during a stay at the *Max Planck Institute für Kohlenforschung (Mülheim an der Ruhr-Germany)* under the co-supervision of Dr. Manuel Alcarazo.

The tetrakis(imino)pyracene (TIP) ligand was prepared according to literature procedures (Scheme 4.20).[37-38] First, oxalyl bromide and fresh aluminum bromide were added to a solution of acenaphthene in carbon disulfide giving 1,2-diketopyracene as a yellow crystalline solid (a). Then, a solution of diketopyracene (a) and 2 equivalents of benzeneseleninic anhydride in chlorobenzene was heated to give 1,2,5,6-tetraketopyracene (b). Finally, 1,2,5,6-tetraketopyracene was dissolved in a mixture 1:1 CH_3CN:CH_3COOH and 5 equivalents of diisopropylaniline were added. The mixture was heated at 80ºC overnight to obtain TIP in a 8 % overall yield, in agreement with the literature data.

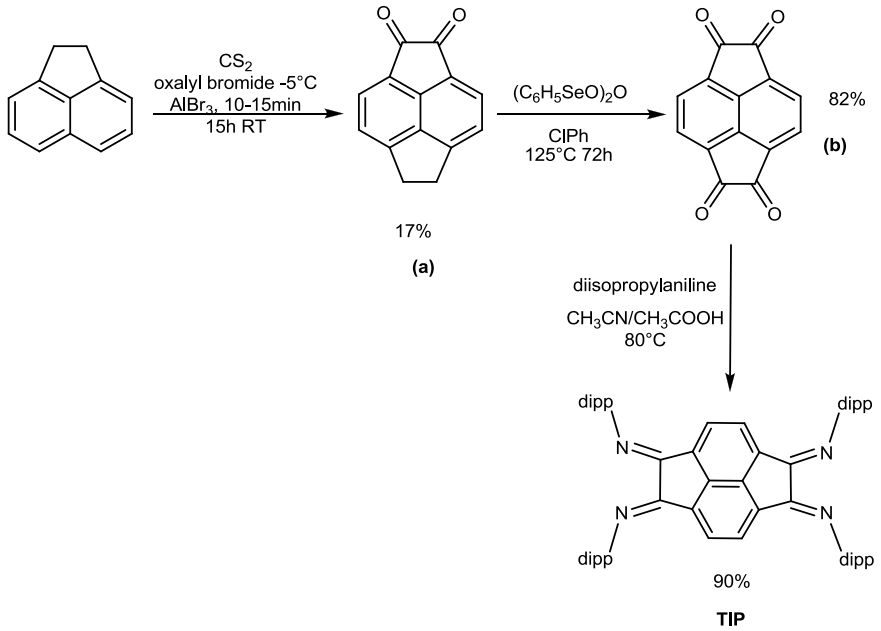

Scheme 4.20 Synthesis of **TIP** ligand

TIP reacted with chloro(methoxy)methane to afford the violet bisimidazolium salt [H**J**H](Cl)$_2$ in 65% yield. The reaction was carried out in the absence of solvent at 100°C, as shown in Scheme 4.21.

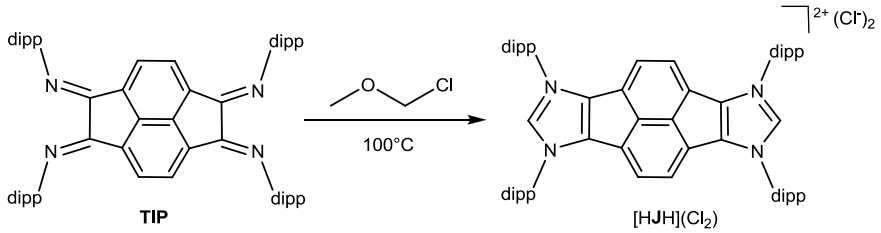

Scheme 4.21 Synthesis of bisimidazolium salt [H**J**H](Cl)$_2$

[H**J**H](Cl)$_2$ was characterized by NMR and mass spectrometry and elemental analysis. The presence of a signal at 9.27 ppm in the ^{1}H NMR spectrum, corresponding to the two acidic protons, revealed that the cyclization had occurred.

The reaction of the bisimidazolium salt [H**J**H](Cl)$_2$ with [MCl(COD)]$_2$ (M = Rh, Ir) gave the homodimetallic complexes **31J** and **32J** (Scheme 4.22). The reactions

were carried out in the presence of *t*BuOK in toluene at room temperature. **31J** and **32J** were purified by column chromatography and were precipitated from a mixture of dichloromethane/hexane to give green solids in 61% and 58% yield, respectively.

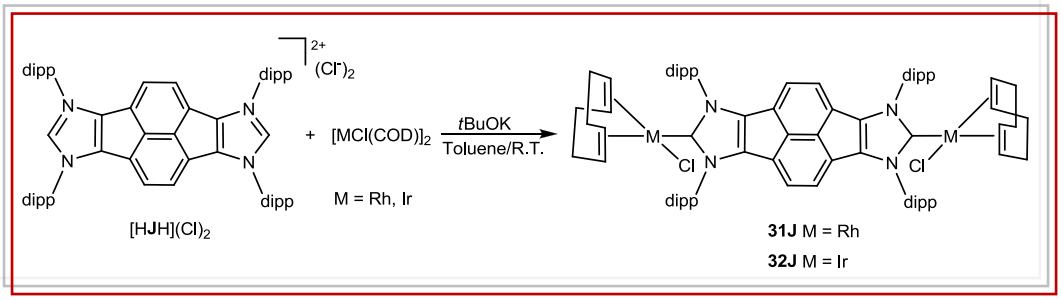

Scheme 4.22 Synthesis of complexes **31J** and **32J**

Complexes **31J** and **32J** were characterized by NMR and mass spectrometry and elemental analysis. The ^{1}H NMR spectroscopic data revealed that metallation of the biscarbene ligand had occurred, as evidenced by the disappearance of the signals for the acidic protons. Due to the similarity of these two compounds, only the spectroscopic characterization of **31J** is discussed in detail.

*^{1}H NMR spectrum of complex **31J***

Figure 4.25 shows the ^{1}H NMR spectrum of **31J**. The signals attributed to the aromatic protons of the four 1,5-diisopropilbenzene groups appear at 7.43 ppm as a triplet (a) and at 7.29 ppm as a doublet (b). The signal corresponding to the protons of the CH group of the pyracene is shown as a singlet at 5.32 ppm (c). The signal attributed to the protons of the CH of the isopropyl groups appears as a broad singlet at 2.30 ppm (d). The signals due to the protons of the methyls of the isopropyl groups are shown as two doublets at 1.35 and 1.05 ppm (e). The signals attributed to the protons of the COD ligand are displayed at similar chemical shifts as those in **24I**.

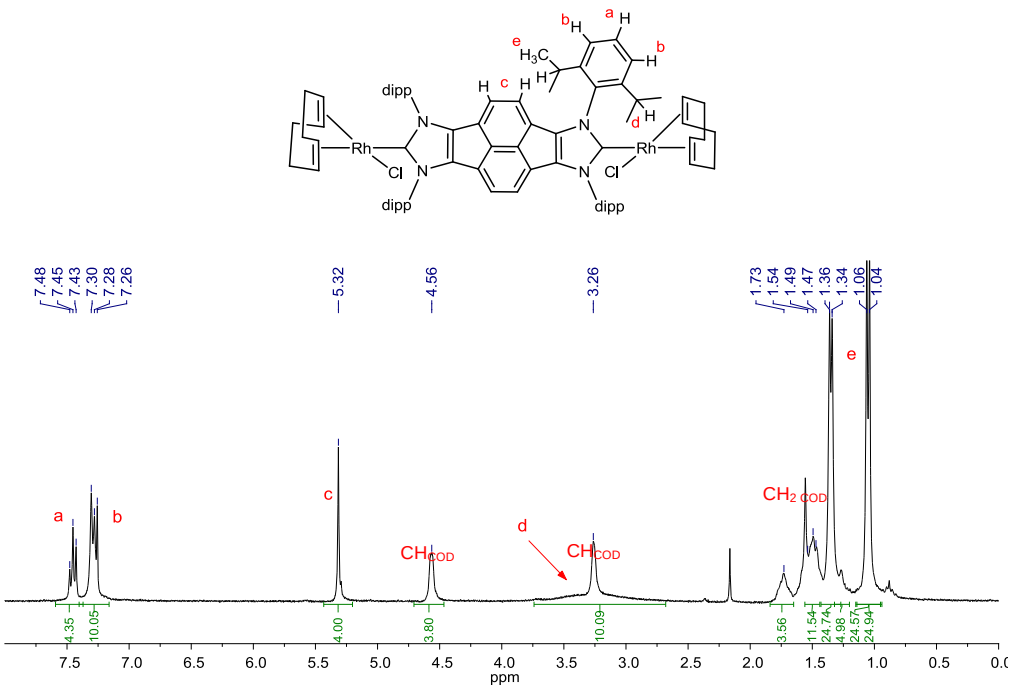

Figure 4.25 ^{1}H NMR spectrum of complex **31J** in $CDCl_3$

*$^{13}C\{^{1}H\}$ NMR spectrum of complex **31J***

Figure 4.26 shows the $^{13}C\{^{1}H\}$ NMR spectrum of **31J**. The most characteristic signal is the doublet attributed to the metallated carbon as a result of Rh-$C_{carbene}$ coupling ($^{1}J_{Rh\text{-}C}$ = 52.5 Hz) at 195.9 ppm (a). The rest of the signals corresponding to the pyracene, diisopropylarene and COD carbons, are conveniently displayed on the spectrum.

^{13}C HSQC and ^{13}C HMBC NMR experiments were carried out in order to fully assign the signals in the ^{13}C NMR spectrum of **31J**. Both spectra have been included in the Experimental Section.

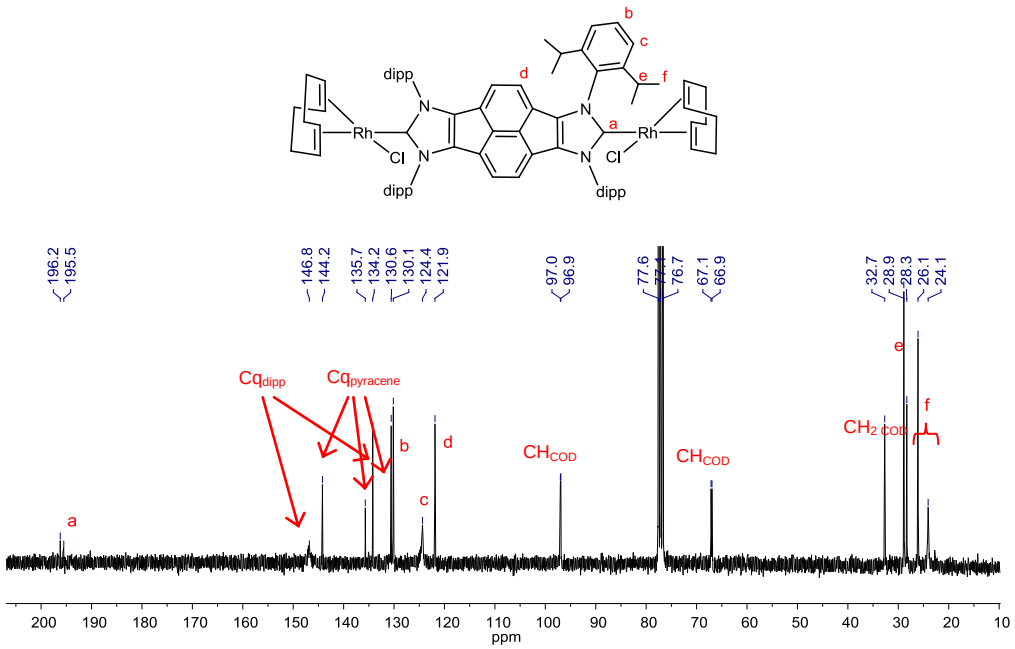

Figure 4.26 ^{13}C **{**^{1}H} NMR spectrum of complex **31J** in $CDCl_3$

*Molecular structure of **31J***

Crystals of **31J** suitable for X-ray diffraction analysis were obtained by slow evaporation from a concentrated solution of the compound in chloroform. Figure 4.27 shows two perspectives of the molecular diagram of **31J**, which confirms the bimetallic nature of the compound with two Rh centers in a pseudo-square-planar configuration. Table 4.6 shows the most representative bond lengths (Å) and angles (º) of complex **31J**. The bis-NHC is bridging the two metals, which complete their coordination spheres with a chloride and a 1,5-cyclooctadiene ligands.

Table 4.6 Selected bond lengths (Å) and angles (º) of complex **31J**

Bonds		**Angles**	
Rh(1)-C(3)	2.058(4)	C(3)-Rh(1)-Cl(2)	89.07(12)
Rh(1)-Cl(2)	2.3899(13)		
Rh(1)-C(37)	2.097(5)		
Rh(1)-C(38)	2.099(5)		
Rh(1)-C(41)	2.191(5)		
Rh(1)-C(42)	2.200(5)		

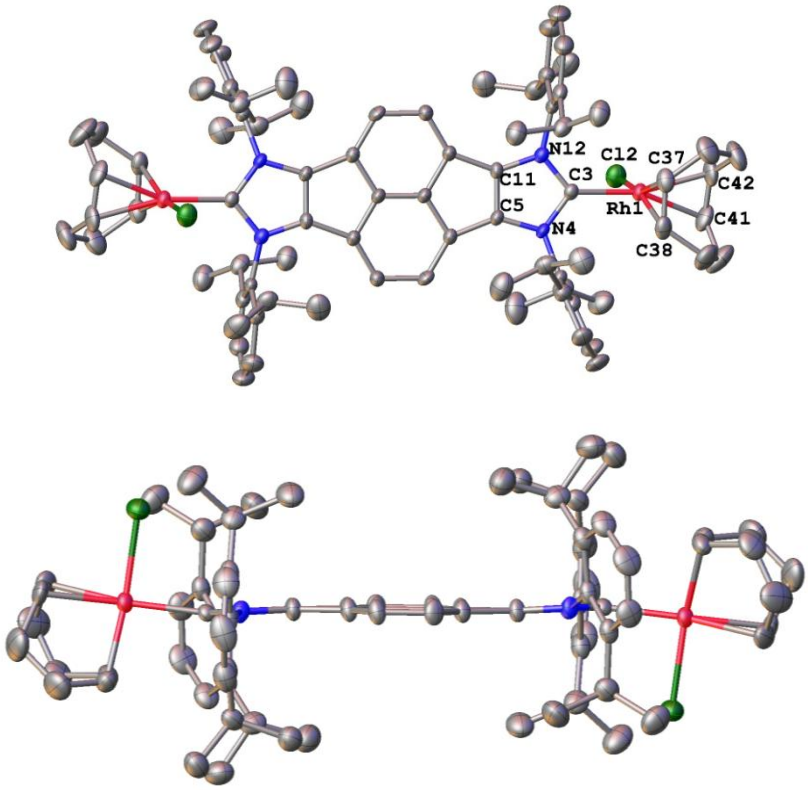

Figure 4.27 Perspectives of the molecular diagram of **31J** (ellipsoids at 30% probability). Hydrogen atoms and solvent (chloroform) have been omitted for clarity

The two Rh atoms are in the plane of the azole ring, with the chloride ligands arranged perpendicular to this plane in a relative *anti* disposition. As expected, the Rh-C_{COD} distances in **31J** which are *trans* to the carbene carbon atom are longer than the Rh-C_{COD} bond lengths *trans* to the other olefin, because of the *trans* influence of the NHC ligand. The Rh-$C_{carbene}$ bond length is 2.058 Å, and the through-space distance between the two metals is 14.02 Å.

4.2.2.1 Carbonyl derivate of complex 32J

Compound **32J** can be transformed into its corresponding carbonylated derivative (**33J**) by reaction of the former with CO in dichloromethane at 0ºC, in 80% yield (Scheme 4.23).

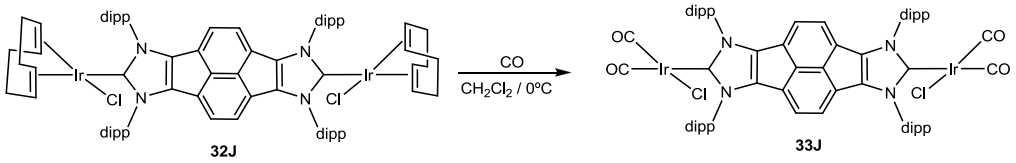

Scheme 4.23 Sythesis of complex **33J**

The IR spectrum of **33J** displays two CO stretching bands at 1968 and 2054 cm^{-1}, as expected for the *cis* disposition of the carbonyl ligands. The values for **33J** correlate well with those previously reported for the mono-NHC analogue IPr(BIAN)[Ir$(CO)_2$Cl] (Figure 4.28), where IPr(BIAN) is a bis(imino)acenaphthene-supported N-heterocyclic carbene.[39]

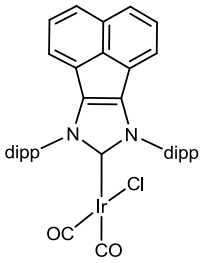

Figure 4.28 IPr(BIAN)[Ir$(CO)_2$Cl] complex

The dimetallic complex **33J** was characterized by NMR and mass spectrometry and elemental analysis. The most characteristic of the ^{1}H NMR spectrum is the disappearance of the signals attributed to the protons of the COD ligand, proving that the complex has been carbonylated. The most characteristical signals of the ^{13}C {^{1}H} NMR spectrum are those corresponding to the carbonyl ligands, displayed at 183.3 and 168.4 ppm. Also, the signals corresponding to the carbons of the COD ligands have disappeared (see Experimental Section).

4.2.3 Cyclic Voltammetry studies

Cyclic Voltammetry studies have recently been proposed as a valuable tool for the study the electronic properties of NHC ligands in rhodium and iridium complexes.[25,40] In our case, we were interested in studying the metal-metal electronic communication across the ditopic bis(NHC) ligand. The mesuraments were carried out in an Echochemie pgstat 20 electrochemical analyzer at room temperature with a conventional three-electrode configuration consisting of platinum working and auxiliary electrodes and an Ag/AgCl reference electrode containing aqueous 3M KCl. Dichloromethane was used as solvent in all the experiments and $[NBu_4]PF_6$ was used as supporting electrolyte.

We measured the redox potentials of **21I**, **22I** and **24I** referred to the $E(M^I/M^{II})$ process. **21I** exhibits a quasi-reversible oxidation at $E_{1/2}$ = 0.91 V arising from the $Rh^{I/II}$ redox couple (Figure 4.29). For **22I**, an irreversible anodic peak reveals about E_{pa} = 0.93 V corresponding to the $Ir^{I/II}$ oxidation (Figure 4.30). The redox potentials are in the range of other Rh and Ir complexes with saturated NHC ligands.[25, 40]

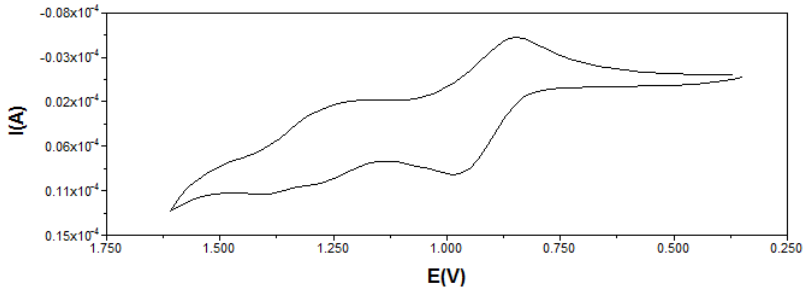

Figure 4.29 Cyclic voltammetry diagram of complex **21I**

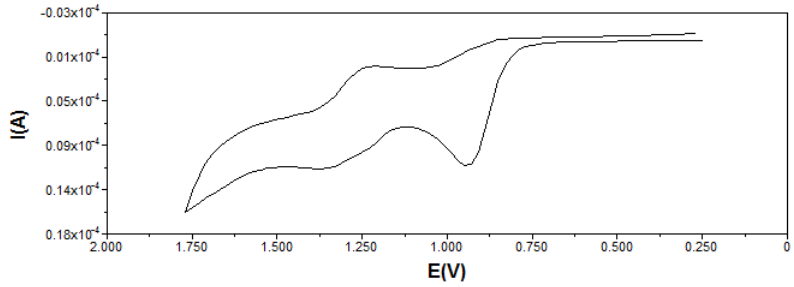

Figure 4.30 Cyclic voltammetry diagram of complex **22I**

The redox potential of the bimetallic complex **24I** is 0.950V (Figure 4.31), referred to a two-electron oxidation process. This value confirms that the bis-carbene ligand has a lower electron donating character than its monodentate counterpart in **22I**, in agreement with what we observed by IR spectroscopy. The fact that **24I** shows a unique reversible sharp oxidation (ΔE = 60 mV), is consistent with the presence of two fully independent redox-active sites. Although we have proved that there is not any measurable electronic communication between the metals in **24I**, they are mutually affected by the coordination of the bis-NHC as observed by the lowering of the electron donating character of the carbene ligand.

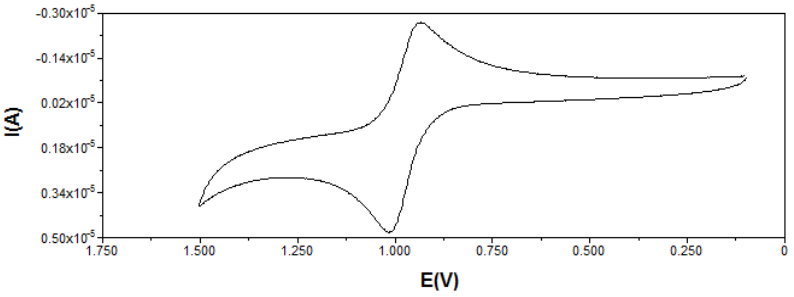

Figure 4.31 Cyclic voltammetry diagram of complex **24I**

We also studied the carbonylated complexes **25I**, **26I** and **27I** as such complexes were available from the IR studies. However, the electrochemistry of these complexes was irreversible. This is probably, as described by Plenio and co-workers, due to the loss of CO ligands following the oxidation of the M^I center.

The dinuclear metal systems **31J** and **32J** displayed a considerably reversible oxidation sharper at $E_{1/2}$ = 0.92V for **31J** (red) and at $E_{1/2}$ = 0.86V for **32J** (blue) arising from the $Rh^{I/II}$ and $Ir^{I/II}$ redox couples, respectively (Figure 4.32). The only single metal-based redox event indicated, such as with **24I**, that the two metal centers in these complexes were electronically decoupled.

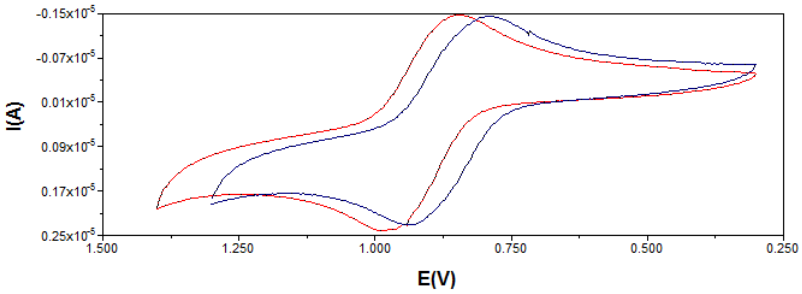

Figure 4.32 Cyclic voltammetry diagram of complexes **31J** (red) and **32J** (blue)

A very weak interaction was also reported for the benzobis(imidazolylidene) ligand.[7-8] In principle, this result may be interpreted by the pressumably weak π-interaction between the metal and the bis-NHC ligand, which leaves the two metal centers disconnected with the π-conjugated system of the bridging ligand. However, this lack of electronic coupling does not discard that the electronic properties of the ligand are affected by the nature of the two metal centers bound at its two edges by an extended polarization effect.

4.3 Conclusions

Two different classes of bis-NHC ligands coordinated to Ir(I) and Rh(I) metal centers have been described in this chapter.

- The methodology used in the first section (4.2.1) provides an alternative to the use of the traditional azolium salts. The double $C(sp^3)$-H_2 dehydrogenation of a saturated heterocycle is a novel and interesting way to obtain complexes containing different architectures.
- The second family of complexes was obtained from a bisimidazolium salt [H**J**H]$(Cl)_2$. The bis-NHC contains in its structure four aromatic rings. Studies of the preligand (TIP) indicates a redox behaviour but cyclic voltammetry studies of Rh(I) and Ir(I) complexes did not reveal an electronical coupled.

The possibility to prepare dimetallic complexes suggests that we may soon find the way to prepare hetero-dimetallic species, potentially useful for the design of new tandem catalytic processes. Studies in order to extend the use of our new bis-carbene ligands to other metal species and explore their catalytic properties are underway.

4.4 References

(1) Poyatos, M.; Mata, J. A.; Peris, E. *Chem. Rev.* **2009**, *109*, 3677; Corberan, R.; Mas-Marza, E.; Peris, E. *Eur. J. Inorg. Chem.* **2009**, 1700.

(2) Mata, J. A.; Poyatos, M.; Peris, E. *Coord. Chem. Rev.* **2007**, *251*, 841.

(3) Herrmann, W. A.; Elison, M.; Fischer, J.; Kocher, C.; Artus, G. R. J. *Chem.-Eur. J.* **1996**, *2*, 772; Simons, R. S.; Custer, P.; Tessier, C. A.; Youngs, W. J. *Organometallics* **2003**, *22*, 1979; Chiu, P. L.; Chen, C. Y.; Zeng, J. Y.; Lu, C. Y.; Lee, H. M. *J. Organomet. Chem.* **2005**, *690*, 1682; Wang, X.; Liu, S.; Weng, L.-H.; Jin, G.-X. *Chemistry* **2007**, *13*, 188; Mercs, L.; Neels, A.; Stoeckli-Evans, H.; Albrecht, M. *Inorg. Chem.* **2011**, *50*, 8188; Su, G.; Huo, X. K.; Jin, G. X. *J. Organomet. Chem.* **2011**, *696*, 533.

(4) Leung, C. H.; Incarvito, C. D.; Crabtree, R. H. *Organometallics* **2006**, *25*, 6099.

(5) Mata, J. A.; Chianese, A. R.; Miecznikowski, J. R.; Poyatos, M.; Peris, E.; Faller, J. W.; Crabtree, R. H. *Organometallics* **2004**, *23*, 1253; Wanniarachchi, Y. A.; Khan, M. A.; Slaughter, L. M. *Organometallics* **2004**, *23*, 5881; Burling, S.; Field, L. D.; Li, H. L.; Messerle, B. A.; Turner, P. *Eur. J. Inorg. Chem.* **2003**, 3179.

(6) Boydston, A. J.; Williams, K. A.; Bielawski, C. W. *J. Am. Chem. Soc.* **2005**, *127*, 12496; Khramov, D. M.; Boydston, A. J.; Bielawski, C. W. *Angew. Chem. Int. Ed.* **2006**, *45*, 6186; Boydston, A. J.; Rice, J. D.; Sanderson, M. D.; Dykhno, O. L.; Bielawski, C. W. *Organometallics* **2006**, *25*, 6087; Boydston, A. J.; Bielawski, C. W. *Dalton Trans.* **2006**, 4073; Williams, K. A.; Boydston, A. J.; Bielawski, C. W. *Chem. Soc. Rev.* **2007**, *36*, 729.

(7) Mercs, L.; Neels, A.; Albrecht, M. *Dalton Trans.* **2008**, 5570.

(8) Tennyson, A. G.; Rosen, E. L.; Collins, M. S.; Lynch, V. M.; Bielawski, C. W. *Inorg. Chem.* **2009**, *48*, 6924.

(9) Curphey, T. J.; Prasad, K. S. *J. Org. Chem.* **1972**, *37*, 2259.

(10) Guerret, O.; Sole, S.; Gornitzka, H.; Teichert, M.; Trinquier, G.; Bertrand, G. *J. Am. Chem. Soc.* **1997**, *119*, 6668.

(11) Mas-Marza, E.; Mata, J. A.; Peris, E. *Angew. Chem. Int. Ed.* **2007**, *46*, 3729.

(12) Zanardi, A.; Mata, J. A.; Peris, E. *Organometallics* **2009**, *28*, 4335.

(13) Zanardi, A.; Corberan, R.; Mata, J. A.; Peris, E. *Organometallics* **2008**, *27*, 3570.

(14) Zanardi, A.; Mata, J. A.; Peris, E. *J. Am. Chem. Soc.* **2009**, *131*, 14531.

(15) Zanardi, A.; Mata, J. A.; Peris, E. *Chem. Eur. J.* **2010**, *16*, 13109 ; Zanardi, A.; Mata, J. A.; Peris, E. *Chem.-Eur. J.* **2010**, *16*, 10502.

(16) Werner, H. *Angew. Chem. Int. Ed.* **2010**, *49*, 4714.

(17) Gutierrez-Puebla, E.; Monge, A.; Nicasio, M. C.; Perez, P. J.; Poveda, M. L.; Carmona, E. *Chem.-Eur. J.* **1998**, *4*, 2225; Slugovc, C.; Mereiter, K.; Trofimenko, S.; Carmona, E. *Angew. Chem. Int. Ed.* **2000**, *39*, 2158.

(18) Lee, D. H.; Chen, J. Y.; Faller, J. W.; Crabtree, R. H. *Chem. Commun.* **2001**, 213.

(19) Ho, V. M.; Watson, L. A.; Huffman, J. C.; Caulton, K. G. *New J. Chem.* **2003**, *27*, 1446; Coalter, J. N.; Ferrando, G.; Caulton, K. G. *New J. Chem.* **2000**, *24*, 835.

(20) Lambert, J. B.; Huseland, D. E.; Wang, G. T. *Synthesis-stuttgart* **1986**, 657.

(21) Cetinkaya, B.; Ozdemir, I.; Dixneuf, P. H. *J. Organomet. Chem.* **1997**, *534*, 153; Ozdemir, I.; Yigit, B.; Cetinkaya, B.; Ulku, D.; Tahir, M. N.; Arici, C. *J. Organomet. Chem.* **2001**, *633*, 27.

(22) Nielsen, A. T.; Nissan, R. A.; Chafin, A. P.; Gilardi, R. D.; George, C. F. *J. Org. Chem.* **1992**, *57*, 6756.

(23) Chang, Y. H.; Fu, C. F.; Liu, Y. H.; Peng, S. M.; Chen, J. T.; Liu, S. T. *Dalton Trans.* **2009**, 861.

(24) Herrmann, W. A.; Schutz, J.; Frey, G. D.; Herdtweck, E. *Organometallics* **2006**, *25*, 2437.

(25) Leuthausser, S.; Schwarz, D.; Plenio, H. *Chem.-Eur. J.* **2007**, *13*, 7195.

(26) Mata, J. A.; Peris, E.; Incarvito, C.; Crabtree, R. H. *Chem. Commun.* **2003**, 184.

(27) Denk, K.; Sirsch, P.; Herrmann, W. A. *J. Organomet. Chem.* **2002**, *649*, 219.

(28) Appelhans, L. N.; Incarvito, C. D.; Crabtree, R. H. *J. Organomet. Chem.* **2008**, *693*, 2761; Zanardi, A.; Peris, E.; Mata, J. A. *New J. Chem.* **2008**, *32*, 120; Viciano, M.; Poyatos, M.; Sanau, M.; Peris, E.; Rossin, A.; Ujaque, G.; Lledos, A. *Organometallics* **2006**, *25*, 1120; Viciano, M.; Mas-Marza, E.; Sanau, M.; Peris, E. *Organometallics* **2006**, *25*, 3063.

(29) Corberan, R.; Sanau, M.; Peris, E. *J. Am. Chem. Soc.* **2006**, *128*, 3974; Corberan, R.; Sanau, M.; Peris, E. *Organometallics* **2006**, *25*, 4002; Hanasaka, F.; Fujita, K. I.; Yamaguchi, R. *Organometallics* **2004**, *23*, 1490; Hanasaka, F.; Fujita, K.; Yamaguchi, R. *Organometallics* **2006**, *25*, 4643; Azua, A.; Sanz, S.; Peris, E. *Chem.-Eur. J.* **2011**, *17*, 3963; da Costa, A. P.; Viciano, M.; Sanau, M.; Merino, S.; Tejeda, J.; Peris, E.; Royo, B. *Organometallics* **2008**, *27*, 1305.

(30) Torres, O.; Martin, M.; Sola, E. *Organometallics* **2009**, *28*, 863.

(31) Sola, E.; Navarro, J.; Lopez, J. A.; Lahoz, F. J.; Oro, L. A.; Werner, H. *Organometallics* **1999**, *18*, 3534.

(32) Poyatos, M. P., A.; Gonell, S.; Gusev, D. G.; Peris E. *Chem. Sci.* **2012**.

(33) Prades, A.; Poyatos, M.; Mata, J. A.; Peris, E. *Angew. Chem. Int. Ed.* **2011**, *50*, 7666.

(34) Vicent, C.; Viciano, M.; Mas-Marza, E.; Sanau, M.; Peris, E. *Organometallics* **2006**, *25*, 3713.

(35) Vasudevan, K. V.; Vargas-Baca, I.; Cowley, A. H. *Angew. Chem. Int. Ed.* **2009**, *48*, 8369.

(36) Tennyson, A. G.; Ono, R. J.; Hudnall, T. W.; Khramov, D. M.; Er, J. A. V.; Kamplain, J. W.; Lynch, V. M.; Sessler, J. L.; Bielawski, C. W. *Chem.-Eur. J.* **2010**, *16*, 304; Comas-Vives, A.; Harvey, J. N. *Eur. J. Inorg. Chem.* **2011**, 5025; Alcarazo, M.; Stork, T.; Anoop, A.; Thiel, W.; Furstner, A. *Angew. Chem.-Int. Ed.* **2010**, *49*, 2542; Antonova, N. S.; Carbo, J. J.; Poblet, J. M. *Organometallics* **2009**, *28*, 4283; Jacobsen, H.; Correa, A.; Poater, A.; Costabile, C.; Cavallo, L. *Coord. Chem. Rev.* **2009**, *253*, 687; Kausamo, A.; Tuononen, H. M.; Krahulic, K. E.; Roesler, R. *Inorg. Chem.* **2008**, *47*, 1145; Hahn, F. E.; Zabula, A. V.; Pape, T.; Hepp, A.; Tonner, R.; Haunschild, R.; Frenking, G. *Chem.-Eur. J.* **2008**, *14*, 10716; Penka, E. F.; Schlapfer, C. W.; Atanasov, M.; Albrecht, M.; Daul, C. *J. Organomet. Chem.* **2007**, *692*, 5709; Fantasia, S.; Petersen, J. L.; Jacobsen, H.; Cavallo, L.; Nolan, S. P. *Organometallics* **2007**, *26*, 5880; Khramov, D. M.; Lynch, V. M.; Bielawski, C. W. *Organometallics* **2007**, *26*, 6042; Jacobsen, H.; Correa, A.; Costabile, C.; Cavallo, L. *J. Organomet. Chem.* **2006**, *691*, 4350; Sanderson, M. D.; Kamplain, J. W.; Bielawski, C. W. *J. Am. Chem. Soc.* **2006**, *128*, 16514.

(37) Vasudevan, K. V.; Findlater, M.; Cowley, A. H. *Chem. Commun.* **2008**, 1918.

(38) Trost, B. M. *J. Am. Chem. Soc.* **1969**, *91*, 918; Clayton, M. D.; Marcinow, Z.; Rabideau, P. W. *J. Org. Chem.* **1996**, *61*, 6052.

(39) Vasudevan, K. V.; Butorac, R. R.; Abernethy, C. D.; Cowley, A. H. *Dalton Trans.* **2010**, *39*, 7401.

(40) Wolf, S.; Plenio, H. *J. Organomet. Chem.* **2009**, *694*, 1487.

Chapter 5

Experimental Section

5.1 Analytical techniques

Nuclear Magnetic Resonance (NMR)

^{1}H and ^{13}C NMR spectra were recorded on the following spectrometers at 298 K:

- Varian Innova 300 MHz (^{1}H 300 MHz, ^{13}C 75 MHz)
- Varian Innova 400 MHz (^{1}H 500 MHz, ^{13}C 100 MHz)
- Varian Innova 500MHz (^{1}H 500 MHz, ^{13}C 125 MHz)

Chemical shifts are given in ppm (δ), referred to the residual peak of the deuterated solvent ($CDCl_3$, CD_2Cl_2, CD_3CN, CD_3OD, toluene-d_8 and DMSO-d_6) and reported downfield of $SiMe_4$.

Electrospray Mass Spectra (ESI-MS)

Electrospray Mass Spectra (ESI-MS) were recorded on a Micromass Quatro LC instrument; CH_3OH or CH_3CN were used as mobile phase and nitrogen was employed as the drying and nebulizing gas. High Resolution Mass Spectra (HR MS) were recorded on a Q-TOF Premier instrument.

Elemental Analysis

Elemental analyses were carried out on a EuroEA3000 Eurovector Analyser.

Gas Chromatography (GC)

GC analyses were obtained on a Shimadzu GC-2010 apparatus equipped with a FID and a Teknokroma (TRB-5MS, 30 m x 0.25 mm x 0.25 µm) column was used.

Infrared Spectroscopy (IR)

Infrared spectra (FT-IR) were performed on a Bruker EQUINOX 55 spectrometer with a spectral window of 4000-600 cm^{-1}. Liquid samples were placed between KBr windows.

Electrochemical measurements

The measurements were carried out on an Echochemie pgstat 20 electrochemical analyzer at room temperature with a conventional three-electrode configuration consisting of platinum working and auxiliary electrodes and a Ag/AgCl reference electrode containing aqueous 3M KCl. Dichloromethane was used as solvent used for all experiments. $[NBu_4]PF_6$ was used as supporting electrolyte.

5.2 Synthesis of complexes

The synthesis of ligand precursors and transmetallation reactions were carried out under air atmosphere. The rest of reactions were carried out under nitrogen or argon atmosphere using the standard Schlenk techniques. $[RuCl_2(p\text{-cymene})]_2$,[1] $[RuCl_2(CMe)_6]_2$,[2] $[RuCl_2(methylbenzoate)]_2$,[3] $[IrCp^*Cl_2]_2$,[4] $[IrCl(COD)]_2$,[5] $[RhCl(COD)]_2$,[6] $[RhCl(NBD)]_2$,[7] 1,3-dimethylimidazolium iodide [**A**H]I,[8] 1,3-dibutylimidazolium iodide [**B**H]I,[8] 1,2,3-trimethylimidazolium iodide [**D**H]I,[9] 1,2-dimethylpyrazolium iodide [**F**H]I,[10] **H**H2[11], **I**H4[12] and organometallic complexes **1A**,[13] **3B**,[14] **15B**[15] and **16D**[16] were prepared according to literature procedures.

5.2.1 Synthesis of azolium salts

Synthesis of 1,3-di-*n*-octylimidazolium iodide, [CH]I:

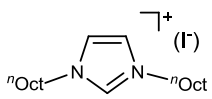

Imidazole (480 mg, 7 mmol), NaOH (420 mg, 10.5 mmol), TBAB (50 mg, 0.15 mmol) and a few drops of water were placed together in a round-bottom flask. The mixture was stirred at room temperature for 1 h, and then iodooctane (1.3 mL, 7 mmol) was added. After 48 h at room temperature, the reaction mixture was extracted with CH_2Cl_2/H_2O and the organic extracts were collected and dried over Na_2SO_4. Evaporation of the solvent under vacuum gave an oil which was further reacted with iodooctane (1.3 mL, 7 mmol). The mixture was refluxed overnight to give [**C**H]I as an orange oil. Yield: 2.6 g (90%). ^{1}H NMR (300 MHz, $CDCl_3$): δ = 10.22 (s, 1H, NCHN), 7.41 (s, 2H, CH_{imid}),

4.34 (t, $^{3}J_{H,H}$ = 7.35 Hz, 4H, $NCH_{2\ nOct}$), 1.92 (m, 4H, $CH_{2\ nOct}$), 1.31 (m, 20H, $CH_{2\ nOct}$) and 0.85 ppm (t, $^{3}J_{H,H}$ = 6.00 Hz, 6H, $CH_{3\ nOct}$). $^{13}C\{^{1}H\}$ NMR (75 MHz, $CDCl_3$): δ = 136.7 (NCHN), 122.7 (CH_{imid}), 50.4 ($NCH_{2\ nOct}$), 31.8 ($CH_{2\ nOct}$), 30.4 ($CH_{2\ nOct}$), 29.1 ($CH_{2\ nOct}$), 29.0 ($CH_{2\ nOct}$), 26.3 ($CH_{2\ nOct}$), 22.7 ($CH_{2\ nOct}$) and 14.1 ppm ($CH_{3\ nOct}$). Electrospray MS (15 V): *m/z* = 93.3 $[M - I]^{+}$. Anal. calcd. for $C_{19}N_2H_{37}I$ (mol. wt. 420.41): C, 54.28; H, 8.87; N, 6.66. Found: C, 54.56; H, 8.78; N, 6.59.

Synthesis of 1,3-trimethyl-2-phenylimidazolium iodide, [EH]I:

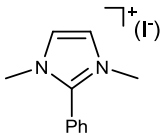

2-Phenylimidazole (1 g, 6.9 mmol), NaOH (416 mg, 10.4 mmol), TBAB (50 mg, 0.15 mmol), and a few drops of water were placed together in a round-bottomed flask. The mixture was stirred at room temperature for 1 h, and then iodomethane (650 μL, 10.40 mmol) was added. After being stirred for 48 h at room temperature, the reaction mixture was extracted with CH_2Cl_2/H_2O and the organic extracts were collected and dried over Na_2SO_4. Evaporation of the solvent under vacuum gave an oil. The oil was redissolved in CH_3CN (10 mL), and iodomethane (650 μL, 10.40 mmol) was added. The mixture was refluxed overnight. The volatile components were removed under vacuum, and the product was washed with CH_2Cl_2 to give [**E**H]I as a white solid. Yield: 1.6 g (80%). ^{1}H NMR (500 MHz, DMSO-d_6): δ = 7.87 (s, 2H, CH_{imid}), 7.77-7.69 (m, 5H, CH_{Ph}) and 3.69 ppm (s, 6H, NCH_3). $^{13}C\{^{1}H\}$ NMR (125 MHz, DMSO-d_6): δ = 144.9 (Cq), 133.0 (Cq_{Ph}), 131.3 (CH_{imid}), 130.1, 123.9, 121.9 (CH_{Ph}) and 36.5 ppm (NCH_3). Electrospray MS (15 V): *m/z* = 173.3 $[M - I]^{+}$. Anal. calcd. for $C_{11}N_2H_{13}I$ (mol wt. 300.14): C, 44.02; H, 4.37; N, 9.33. Found: C, 44.51; H, 4.68; N, 9.58.

Synthesis of 1,4-dibutyl-3-methyl-1,2,3-triazolium iodide, [GH]I:

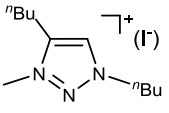

To a solution of 1,4-dibutyl-1,2,3-triazole (1 g, 5.5 mmol) in acetonitrile (7 mL) was added iodomethane (3.5 mL, 55 mmol) and the mixture was stirred under microwave irradiation for 5 h at 90ºC. The solvent was removed in vacuo. The oil residue was washed with diethyl ether several times and dried to afford the triazolium salt [**G**H]I. Yield: 1.5 g (85%). A full-

assignment of the ^{1}H and ^{13}C NMR spectra of [**G**H]I was carried out with the aid of COSY (Figure 5.1) and HSQC NMR (Figure 5.2) experiments. ^{1}H NMR (400 MHz, $CDCl_3$): δ = 9.09 (s, 1H, CH_{trz}), 4.68 (t, $^{3}J_{H,H}$ = 8.00 Hz, 2H, $NCH_{2\ nBu}$), 4.28 (s, 3H, NCH_3), 2.92 (t, $^{3}J_{H,H}$ = 8.00 Hz, 2H, C_{trz}-$CH_{2\ nBu}$), 1.98, 1.75, 1.47 (m, 6H, $CH_{2\ nBu}$) and 0.99 ppm (t, $^{3}J_{H,H}$ = 6.00 Hz, 6H, $CH_{3\ nBu}$). $^{13}C\{^{1}H\}$ NMR (100 MHz, $CDCl_3$): δ = 144.6 (C_{trz}-^{n}Bu), 129.2 (CH_{trz}), 54.0 ($NCH_{2\ nBu}$), 38.8 (CH_3), 31.3, 39.0, 23.7, 22.2, 19.4 ($CH_{2\ nBu}$), 13.6 and 13.3 ppm ($CH_{3\ nBu}$). Electrospray MS (30 V): *m/z* = 196.3 [M - I]$^{+}$. Anal. Calcd for $C_{11}H_{22}N_3I{\cdot}H_2O$ (mol wt. 341.10): C, 38.72; H, 7.09; N, 12.31. Found: C, 38.59; H, 7.17; N, 12.10.

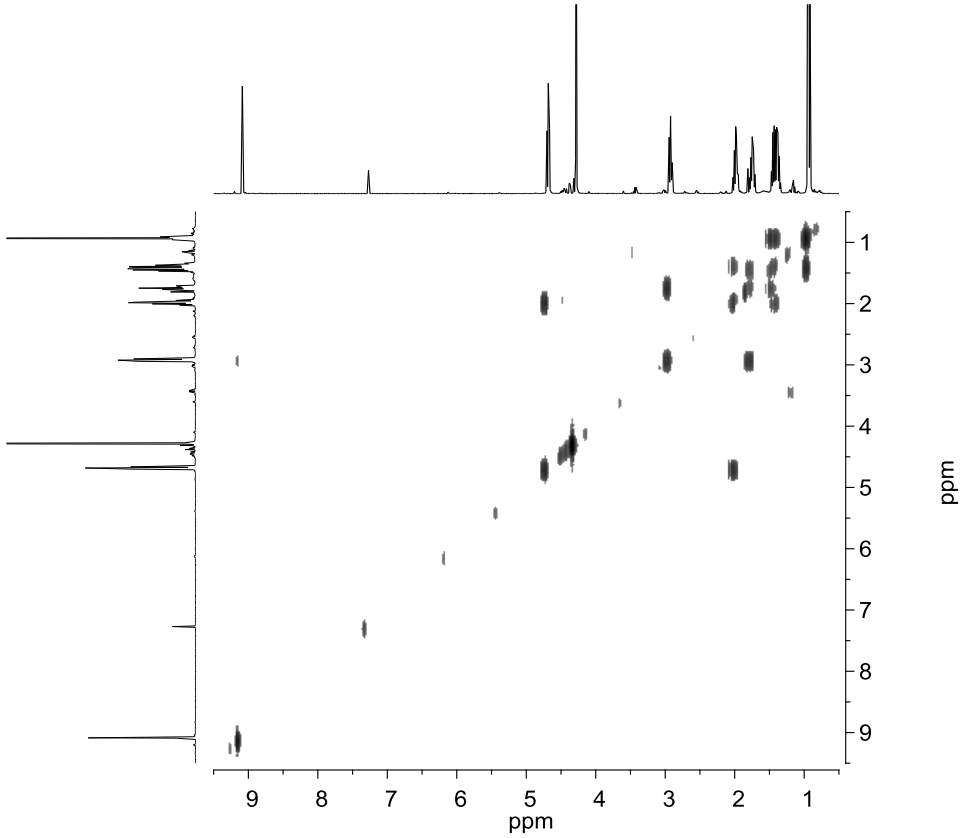

Figure 5.1 COSY NMR (^{1}H, 400 MHz) of [**G**H]I

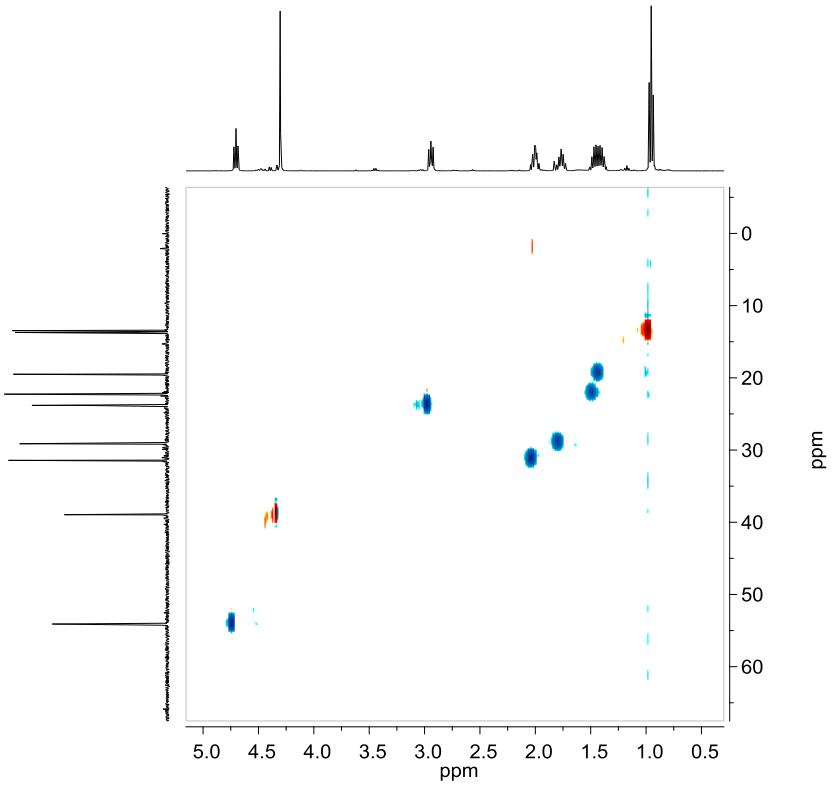

Figure 5.2 ^{13}C HSQC NMR (^{1}H, 400 MHz and ^{13}C, 100 MHz) of [**G**H]I

Bisimidazolium pyracene chloride, [HJH](Cl)$_2$:

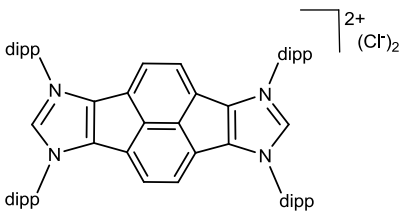

Tetrakis(imino)pyracene ligand (200 mg, 0.28 mmol) and methoxy(methyl)chloride (920 mg, 11.4 mmol) were placed together in a Schlenk tube under Ar atmosphere. The mixture was stirred at 100°C for 20 h. The mixture was cooled and the violet precipitate was filtered and washed with ether. Yield: 170 mg (62%). ^{1}H NMR (400 MHz, CD_2Cl_2): δ = 9.27 (s, 2H, CH_{imid}), 7.72 (t, $^{3}J_{H,H}$ = 8.00 Hz, 4H, CH-Ar_{dipp}), 7.54 (d, $^{3}J_{H,H}$ = 8.00 Hz, 8H, CH-Ar_{dipp}), 6.46 (s, 4H, CH-$Ar_{pyracene}$), 2.83 (sept, $^{3}J_{H,H}$ = 6.80 Hz, 8H, $CH_{isop\ dipp}$), 1.26 (d, $^{3}J_{H,H}$ = 6.80 Hz, 24H, $CH_{3\ isop\ dipp}$) and 1.24 ppm (d, $^{3}J_{H,H}$ =6.80 Hz, 24H, $CH_{3\ isop\text{-}dipp}$). ^{13}C{^{1}H} NMR (100 MHz, CD_3CN): δ = 144.9 (Cq-Ar_{dipp}), 142.6 (NCHN), 141.9, 134.2 ($Cq_{pyracene}$), 133.1 (CH-

Ar_{dipp}), 128.3 ($Cq_{pyracene}$), 127.9 (Cq-Ar_{dipp}), 125.7 (CH-Ar_{dipp}), 125.4 ($CH_{pyracene}$), 28.6 ($CH_{isop\ dipp}$), 23.5 and 22.3 ppm ($CH_{3\ isop\ dipp}$). Electrospray MS (15 V): *m*/*z* = 897.6 $[M - 2Cl]^{2+}$. Anal. Calcd for $C_{64}H_{74}N_4Cl_2$ (mol wt. 968.5): C, 79.23; H, 7.69; N, 5.77. Found: C, 78.95; H, 7.35; N, 6.00.

5.2.2 Synthesis of Ru(II) monocarbene complexes

Synthesis of 2A:

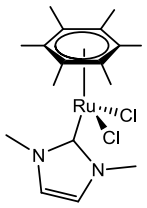

A mixture of $[RuCl_2(\eta^6\text{-}CMe)_6]_2$ (200 mg, 0.30 mmol), 1,3-dimethylimidazolium iodide (150 mg, 0.67 mmol) and Cs_2CO_3 (1.5 g, 4.70 mmol) in CH_3CN was refluxed for 6 h. The mixture was filtered, the solvent was evaporated and the crude solid was purified by column chromatography. Elution with CH_2Cl_2/acetone (9:1) afforded the separation of a yellow band that contained compound **2A**. Compound **2A** was obtained as a yellow solid by precipitation with diethyl ether. Yield: 215 mg (50%). ^{1}H NMR (300 MHz, $CDCl_3$): δ = 6.88 (s, 2H, CH_{imid}), 3.64 (s, 6H, NCH_3) and 2.10 ppm [s, 18H, $(CH_3)_6$]. $^{13}C\{^1H\}$ NMR (75 MHz, $CDCl_3$): δ = 181.9 (Ru-$C_{carbene}$), 123.4 (CH_{imid}), 92.8 [$(CCH_3)_6$], 37.2 (NCH_3) and 15.7 ppm [$(CCH_3)_6$]. Electrospray MS (15 V): *m*/*z* = 395.4 $[M - Cl]^+$. Anal. calcd. for $C_{17}H_{26}N_2Cl_2Ru$ (mol. wt. 430.38): C, 47.44; H, 6.09; N, 6.51. Found: C, 47.56; H, 6.05; N, 6.42.

General procedure for transmetallation reactions (4B-12G): A solution of the appropriate azolium salt (1 equivalent) and silver oxide (0.5 equivalents) was stirred at room temperature for 1h under exclusion of light. Then, the mixture was filtered through Celite to remove the unreacted silver oxide and insoluble residues. The appropriate Ru(II)-arene precursor (0.5 equivalents) was added to the solution. Immediately, a white precipitate was formed. The suspension was refluxed for the desired time. The reaction mixture was filtered through Celite to remove the silver salts and the solution was concentrate under reduce pressure. The crude solid was purified by column chromatography or precipitation.

Synthesis of 4B:

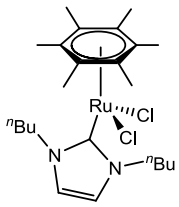

Transmetallation was carried out in dichloromethane with 1,3-dibutylimidazolium iodide (154 mg, 0.50 mmol), Ag_2O (58 mg, 0.25 mmol) and $[RuCl_2(CMe)_6]_2$ (167 mg, 0.25 mmol). The suspension was refluxed for 2h. The crude solid was purified by column chromatography. Elution with a mixture of CH_2Cl_2/acetone (4:1) afforded the separation of an orange band containing compound **4B**. Compound **4B** was obtained as an orange solid by precipitation with diethyl ether. Yield: 160 mg (62%). ^{1}H NMR (500 MHz, $CDCl_3$): δ = 7.04 (s, 2H, CH_{imid}), 4.55 (td, $^3J_{H,H}$ = 12.00 Hz, $^2J_{H,H}$ = 5.00 Hz, 2H, $NCH_{2\ n\mathrm{Bu}}$), 3.66 (td, $^3J_{H,H}$ = 12.00 Hz, $^2J_{H,H}$ = 5.00 Hz, 2H, $NCH_{2\ n\mathrm{Bu}}$), 1.99 [s, 18H, $(CH_3)_6$], 1.63 (m, 2H, $CH_{2\ n\mathrm{Bu}}$), 1.51 (m, 2H, $CH_{2\ n\mathrm{Bu}}$), 1.38 (m, 4H, $CH_{2\ n\mathrm{Bu}}$) and 0.98 ppm (t, $^3J_{H,H}$ =7.25 Hz, 6H, $CH_{3\ n\mathrm{Bu}}$). ^{13}C{^{1}H} NMR (125 MHz, $CDCl_3$): δ =176.1 (Ru-$C_{carbene}$), 121.8 (CH_{imid}), 93.6 [($CCH_3)_6$], 51.2 ($NCH_{2\ n\mathrm{Bu}}$), 34.0, 20.4 ($CH_{2\ n\mathrm{Bu}}$), 15.6 [($CCH_3)_6$] and 14.1 ppm ($CH_{3\ n\mathrm{Bu}}$). Electrospray MS (15 V): *m/z* = 479.2 $[M - Cl]^+$. Anal. calcd. for $C_{23}H_{38}N_2Cl_2Ru$ (mol. wt. 514.54): C, 53.69; H, 7.44; N, 5.44. Found: C, 53.75; H, 7.47; N, 5.41.

Synthesis of 5B:

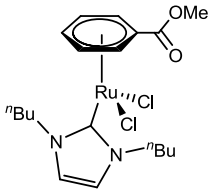

Transmetallation was carried out in dichloromethane with 1,3-dibutylimidazolium iodide (100 mg, 0.324 mmol), Ag_2O (37.5 mg, 0.162 mmol) and $[RuCl_2(methylbenzoate)]_2$ (100 mg, 0.162 mmol). The suspension was refluxed for 12h. Complex **5B** was obtained as a moderately unstable red solid by precipitation from CH_2Cl_2/diethyl ether. Yield: 99 mg (62%). ^{1}H NMR (300 MHz, $CDCl_3$): δ = 7.06 (s, 2H, CH_{imid}), 6.27 (d, $^3J_{H,H}$ = 6.00 Hz, 2H, $CH_{o\text{-benzoate}}$), 5.84 (t, $^3J_{H,H}$ = 5.50 Hz, 1H, $CH_{p\text{-benzoate}}$), 5.71 (t, $^3J_{H,H}$ = 5.80 Hz, 2H, $CH_{m\text{-benzoate}}$), 4.40 (br, 2H, N-$CH_{2\ n\mathrm{Bu}}$), 3.98 (br, 2H, $NCH_{2\ n\mathrm{Bu}}$), 3.89 (s, 3H, -$COOCH_3$), 1.89 (br, 2H, $CH_{2\ n\mathrm{Bu}}$), 1.65 (br, 2H, $CH_{2\ n\mathrm{Bu}}$), 1.41 (m, 4H, $CH_{2\ n\mathrm{Bu}}$) and 0.97 ppm (t, $^3J_{H,H}$ =7.20 Hz, 6H, $CH_{3\ n\mathrm{Bu}}$). ^{13}C{^{1}H} NMR (75 MHz, $CDCl_3$): δ = 168.4 (Ru-$C_{carbene}$), 166.4 ($COOCH_3$), 122.1 (CH_{imid}), 90.9 ($Cq_{benzoate}$),

88.3, 86.7 ($CH_{benzoate}$), 82.5 ($Cq_{benzoate}$), 53.4 ($COOCH_3$), 51.4 (NCH_2 $_{n}$Bu), 34.0, 20.3 (CH_2 $_{n}$Bu) and 14.1 ppm (CH_3 $_{n}$Bu). Electrospray MS (15 V): *m/z* = 453.5 $[M - Cl]^+$; FT-IR(KBr): ν = 1723 cm^{-1} ($\nu_{C=O}$).

Synthesis of 6C:

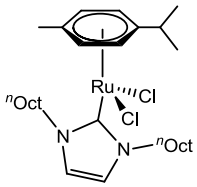

Transmetallation was carried out in dichloromethane with 1,3-di-*n*-octylimidazolium iodide (138 mg, 0.33 mmol), Ag_2O (76 mg, 0.33 mmol) and $[RuCl_2(p\text{-cymene})]_2$ (100 mg, 0.16 mmol). The suspension was refluxed for 3h. The crude solid was purified by column chromatography. Elution with a mixture of CH_2Cl_2/acetone (9:1) afforded the separation of an orange band that contained compound **6C**. Compound **6C** was obtained as an orange solid by precipitation with ether. Yield: 105 g (53%). ^{1}H NMR (300 MHz, $CDCl_3$): δ = 7.05 (s, 2H, CH_{imid}), 5.37, 5.06 (d, $^3J_{H,H}$ = 6.00 Hz, 4H, $CH_{p\text{-cym}}$), 4.56 (br, 2H, NCH_2 $_{n}$Oct), 3.97 (br, 2H, NCH_2 $_{n}$Oct), 2.91 (sept, $^3J_{H,H}$ = 6.90 Hz, 1H, $CH_{isop\ p\text{-cym}}$), 2.03 (s, 3H, CH_3 $_{p\text{-cym}}$), 1.97 (br, 2H, CH_2 $_{n}$Oct), 1.67 (br, 2H, CH_2 $_{n}$Oct), 1.30 (br, 20H, CH_2 $_{n}$Oct), 1.25 (d, $^3J_{H,H}$ = 7.20 Hz, 6H, $CH_{3isop\ p\text{-cym}}$) and 0.87 ppm (t, $^3J_{H,H}$ = 6.60 Hz, 6H, CH_3 $_{n}$Oct). $^{13}C\{^1H\}$ NMR (75 MHz, $CDCl_3$): δ =173.4 (Ru-$C_{carbene}$), 121.7 (CH_{imid}), 108.0 ($CH_{isop\ p\text{-cym}}$), 99.3 ($Cq_{p\text{-cym}}$), 85.3 ($CH_{p\text{-cym}}$), 83.0 ($CH_{p\text{-cym}}$), 51.7 (NCH_2), 32.0 (CH_2 $_{n}$Oct), 30.9 ($CH_{isop\ p\text{-cym}}$), 29.6, 29.3 (CH_2 $_{n}$Oct), 27.1 ($CH_{3isop\ p\text{-cym}}$), 22.8 (CH_2 $_{n}$Oct), 22.7 (CH_2 $_{n}$Oct), 18.8 (CH_3 $_{p\text{-cym}}$) and 14.2 ppm (CH_3 $_{n}$Oct). Electrospray MS (15 V): *m/z* = 563.3 $[M - Cl]^+$. Anal. calcd. for $C_{29}H_{50}N_2Cl_2Ru$ (mol. wt. 598.70): C, 58.18; H, 8.42; N, 4.68. Found: C, 57.96; H, 8.47; N, 4.67.

Synthesis of 7D:

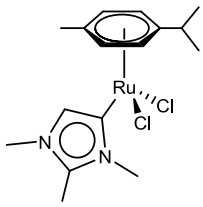

Transmetallation was carried out in dichloromethane with 1,2,3-trimethylimidazolium iodide (93 mg, 0.39 mmol), Ag_2O (136 mg, 0.59 mmol) and $[RuCl_2(p\text{-cymene})]_2$ (100 mg, 0.16 mmol). The suspension was refluxed for 3h. The crude solid purified by column chromatography using silica gel. Elution with CH_2Cl_2/MeOH (9:1) afforded the separation of an orange band that contained **7D**.

Complex **7D** was obtained as a brown solid by precipitation from CH_2Cl_2/Et_2O solution. Yield: 53 mg (40%). ^{1}H NMR (300 MHz, $CDCl_3$): δ = 6.59, (s, 1H, CH_{imid}), 5.22, 5.08 (d, $^3J_{H,H}$ = 5.70 Hz, 4H, $CH_{p\text{-cym}}$), 3.81 (s, 3H, NCH_3), 3.55 (s, 3H, NCH_3), 2.75-2.66 (m, 1H, $CH_{isop\ p\text{-cym}}$), 2.47 (s, 3H, CCH_3), 2.09 (s, 3H, $CH_{3p\text{-cym}}$) and 1.18 ppm (d, $^3J_{H,H}$ = 6.90 Hz, 6H, $CH_{3\ isop\ p\text{-cym}}$). $^{13}C\{^1H\}$ NMR (75 MHz, $CDCl_3$): δ = 152.2 (Ru-$C_{carbene}$), 141.0 (Cq_{imid}), 125.1 (CH_{imid}), 103.1, 99.1 ($Cq_{p\text{-cym}}$), 83.9, 83.8 ($CH_{p\text{-cym}}$), 37.1, 34.3 (NCH_3), 30.8 ($CH_{isop\ p\text{-cym}}$), 22.6 ($CH_{3isop\ p\text{-cym}}$), 18.6 ($CH_{3p\text{-cym}}$) and 10.7 ppm (CCH_3). Electrospray MS (25 V): *m*/*z* = 381.3 $[M - Cl]^+$. Anal. Calcd for $C_{16}H_{24}N_2Cl_2Ru$ (mol. wt. 416.04): C, 46.16; H, 5.81; N, 5.73. Found: C, 45.96; H, 5.95; N, 5.75.

Synthesis of 8E:

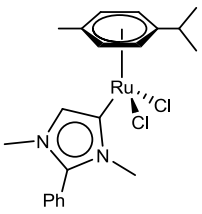

Transmetallation was carried out in dichloromethane with 1,3-dimethyl-2-phenylimidazolium iodide (176 mg, 0.59 mmol), Ag_2O (204 mg, 0.88 mmol) and $[RuCl_2(p\text{-cymene})]_2$ (150 mg, 0.25 mmol). The suspension was refluxed for 2h. The mixture was refluxed for 3 h, and the white precipitate formed (silver halide) was separated by filtration through Celite. The solvent was evaporated, and the crude solid was purified by column chromatography using silica gel. Elution with CH_2Cl_2/acetone (4:1) afforded the separation of an orange band that contained **8E**. Complex **8E** was obtained as a brown solid by precipitation from mixture of CH_2Cl_2/Et_2O. Yield: 155 mg (65%). ^{1}H NMR (300 MHz, $CDCl_3$): δ = 7.61-7.59 (m, 3H, CH_{Ph}), 7.38-7.37 (m, 2H, CH_{Ph}), 6.91 (s, 1H, CH_{imid}), 5.31, 5.17 (d, $^3J_{H,H}$ = 6.00 Hz, 4H, $CH_{p\text{-cym}}$), 3.81, 3.51 (s, 6H, NCH_3), 2.86-2.74 (m, 1H, $CH_{isop\ p\text{-cym}}$), 2.15 (s, 3H, $CH_{3\ p\text{-cym}}$) and 1.23 ppm (d, $^3J_{H,H}$ = 6.90 Hz, 6H, $CH_{3isop\ p\text{-cym}}$). $^{13}C\{^1H\}$ NMR (125 MHz, $CDCl_3$): δ = 154.3 (Ru-$C_{carbene}$), 143.6 (Cq_{imid}), 131.5 (CH_{imid}), 130.2, 129.8, 126.4 (CH_{Ph}), 124.6 (Cq_{Ph}), 102.8, 99.3 ($Cq_{p\text{-cym}}$), 84.1, 84.0 ($CH_{p\text{-cym}}$), 34.8 ($CH_{isop\ p\text{-cym}}$), 31.1, 30.9 (NCH_3), 22.6 ($CH_{3isop\ p\text{-cym}}$) and 18.6 ppm ($CH_{3\ p\text{-cym}}$). Electrospray MS (20 V): *m*/*z* = 443.1 $[M - Cl]^+$. Anal. calcd for $C_{21}H_{26}N_2Cl_2Ru$ (mol wt. 478.42): C, 52.72; H, 5.48; N, 5.86. Found: C, 52.78; H, 5.60; N, 5.71.

Synthesis of 9F:

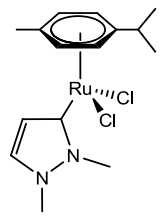

Transmetallation was carried out in dichloromethane with 1,2-dimethylpyrazolium iodide (110 mg, 0.50 mmol), Ag_2O (174 mg, 0.75 mmol) and $[RuCl_2(p\text{-cymene})]_2$. The mixture was refluxed for 3 h. The crude solid was purified by column chromatography. Elution with a mixture of CH_2Cl_2/MeOH (9:1) afforded a yellow band that contained compound **9F**. The pure compound was precipitated from a mixture of CH_2Cl_2/hexanes. Yield: 120 mg (60%). ^{1}H NMR (500 MHz, $CDCl_3$): δ = 7.34 (d, $^3J_{H,H}$ = 5.00 Hz, 1H, $CH_{pyrazole}$), 6.58 (d, $^3J_{H,H}$ = 5.00 Hz, 1H, $CH_{pyrazole}$), 5.26, 5.10 (d, $^3J_{H,H}$ = 5.99 Hz, 4H, $CH_{p\text{-cym}}$), 4.09 (s, 3H, NCH_3), 3.85 (s, 3H, NCH_3), 2.78-2.66 (m, 1H, $CH_{isop\ p\text{-cym}}$), 2.03 (s, 3H, $CH_{3\ p\text{-cym}}$) and 1.22 ppm (d, $^3J_{H,H}$ = 10 Hz, 6H, $CH_{3isop\ p\text{-cym}}$). $^{13}C\{^1H\}$ NMR (75 MHz, $CDCl_3$): δ = 180.3 (Ru-$C_{carbene}$), 133.0, 117.1 ($CH_{pyrazole}$), 104.8, 99.3 ($Cq_{p\text{-cym}}$), 84.5, 84.1 ($CH_{p\text{-cym}}$), 37.7 ($CH_{isop\ p\text{-cym}}$), 31.8 ($CH_{3isop\ p\text{-cym}}$), 22.8, 22.5 (NCH_3) and 14.3 ppm ($CH_{3\ p\text{-cym}}$). Electrospray MS (15 V): *m*/*z* = 367.0 $[M - Cl]^+$. Anal. calcd for $C_{15}H_{22}N_2Cl_2Ru$ (mol wt. 402.3): C, 44.78; H, 5.51; N, 6.96. Found: C, 44.65; H, 5.62; N, 6.88.

Synthesis of 10F:

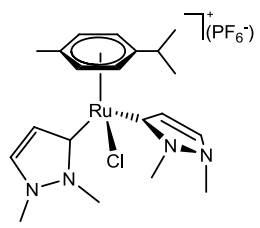

Transmetallation was carried out in dichloromethane with 1,2-dimethylpyrazolium iodide (172 mg, 0.78 mmol), Ag_2O (274 mg, 1.18 mmol) and $[RuCl_2(p\text{-cymene})]_2$ (120 mg, 0.20 mmol). The mixture was refluxed for 3 h. Elution with 20 mL of CH_2Cl_2/acetone (1:1) with 30 mg of KPF_6 afforded the separation of a yellow band that contained compound **10F** and residual KPF_6, which was filtered off. Complex **10F** was obtained as a green solid by precipitation from a CH_2Cl_2/Et_2O solution. Yield: 85 mg (35%). ^{1}H NMR (300 MHz. $CDCl_3$): δ = 7.44, 6.55 (d, $^3J_{H,H}$ = 6.00 Hz, 4H, $CH_{pyrazole}$), 5.44, 5.16 (d, $^3J_{H,H}$ = 6.00 Hz, 4H, $CH_{p\text{-cym}}$), 3.90 (s, 6H, NCH_3), 3.53 (s, 6H, NCH_3), 2.70-2.60 (m, 1H, $CH_{isop\ p\text{-cym}}$), 1.88 (s, 3H, $CH_{3\ p\text{-cym}}$) and 1.16 ppm (d, $^3J_{H,H}$ = 6.90 Hz, 6H, $CH_{3isop\ p\text{-cym}}$). $^{13}C\{^1H\}$ NMR (75

MHz, $CDCl_3$): δ = 175.1 (Ru-$C_{carbene}$), 133.6, 118.4 ($CH_{pyrazole}$), 112.2, 100.9 ($Cq_{p\text{-}cym}$), 92.0, 88.8 ($CH_{p\text{-}cym}$), 37.2, 36.8 (NCH_3), 30.6 ($CH_{isop\ p\text{-}cym}$), 22.6 ($CH_{3isop\ p\text{-}cym}$) and 18.5 ppm ($CH_{3\ p\text{-}cym}$). Electrospray MS (15 V): *m/z* = 463.1 $[M - PF_6]^+$. Anal. calcd for $C_{20}H_{30}N_4ClRuPF_6$ (mol wt. 607.97): C, 39.51; H, 4.97; N, 9.22. Found: C, 39.35; H, 5.27; N, 5.90.

Synthesis of 11G:

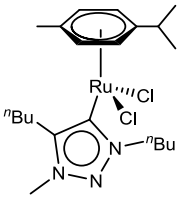

Transmetallation was carried out in dichloromethane with [**G**H]I (150 mg, 0.46 mmol), Ag_2O (107 mg, 0.46 mmol) and $[RuCl_2(p\text{-cymene})]_2$ (140 mg, 0.23 mmol). The mixture was stirred at room temperature for 3 h. The crude solid was purified by column chromatography. Elution with a CH_2Cl_2/acetone (9/1) mixture afforded the separation of an orange band that contained **11G**. Addition of cold Et_2O induced the precipitation of **11G** as an orange solid. Yield: 164 mg (71%). ^1H NMR (300 MHz, $CDCl_3$): δ = 5.35, 5.03 (d, $^3J_{H,H}$ = 6.0 Hz, 4H, $CH_{p\text{-}cym}$), 4.61 (m, 2H, $NCH_{2\ n\text{Bu}}$), 3.97 (s, 3H, NCH_3), 2.98 (m, 2H, C_{trz}-$CH_{2\ n\text{Bu}}$), 2.94 (m, 1H, $CH_{isop\ p\text{-}cym}$), 2.03 (s, 3H, $CH_{3\ p\text{-}cym}$), 1.99 (m, 2H, $CH_{2\ n\text{Bu}}$), 1.56 (m, 2H, $CH_{2\ n\text{Bu}}$), 1.48 (m, 4H, $CH_{2\ n\text{Bu}}$), 1.29 (d, $^3J_{H,H}$ = 6.0 Hz, 6H, $CH_{3\ isop\ p\text{-}cym}$) and 0.98 ppm (m, 6H, $CH_{3\ n\text{Bu}}$). $^{13}C\{^1H\}$ NMR (100 MHz, $CDCl_3$): δ = 160.9 (Ru-$C_{carbene}$), 147.2 (C_{trz}-*n*Bu), 106.9, 97.1 ($Cq_{p\text{-}cym}$), 84.9, 82.7 ($CH_{p\text{-}cym}$), 54.4 ($NCH_{2\ n\text{Bu}}$), 36.3 (NCH_3), 33.0 ($CH_{iso\ p\text{-}cym}$) 32.0, 30.7, 26.0, 23.1 ($CH_{2\ n\text{Bu}}$), 22.7 ($CH_{3\ isop\ p\text{-}cym}$), 20.2 ($CH_{2\ n\text{Bu}}$), 18.7 ($CH_{3\ p\text{-}cym}$), 13.9 and 13.8 ppm ($CH_{3\ n\text{Bu}}$). Electrospray MS (30 V): *m/z* = 466.1 $[M - Cl]^+$. Anal. Calcd for $C_{21}H_{35}N_3Cl_2Ru$ (mol wt. 501.50): C, 50.29; H, 7.03; N, 8.38. Found: C, 50.08; H, 7.13; N, 8.11.

Synthesis of 12G:

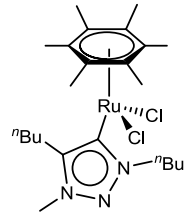

Transmetallation was carried out in dichloromethane with [**G**H]I (150 mg, 0.46 mmol), Ag_2O (107 mg, 0.46 mmol) and $[RuCl_2(CMe)_6]_2$ (140 mg, 0.23 mmol). The mixture was stirred at room temperature for 3 h. The crude solid was purified by column chromatography. Elution with a CH_2Cl_2/acetone (9/1) mixture induced the separation of **12G** as an orange band. Yield: 149 mg (62%). ^{1}H NMR (300 MHz, $CDCl_3$): δ = 4.75 (m, 1H, $NCH_{2\ n\mathrm{Bu}}$), 4.06 (m, 1H, $NCH_{2\ n\mathrm{Bu}}$), 3.96 (s, 3H, NCH_3), 2.96 (m, 1H, C_{trz}-$CH_{2\ n\mathrm{Bu}}$), 2.51 (m, 1H, C_{trz}-$CH_{2\ n\mathrm{Bu}}$), 2.05(m, 1H, $CH_{2\ n\mathrm{Bu}}$), 1,95 [s, 18H, $(CH_3)_6$], 1.87 (m, 1H, $CH_{2\ n\mathrm{Bu}}$), 1.47 (m, 4H, $CH_{2\ n\mathrm{Bu}}$) and 0.96 ppm (m, 6H, $CH_{3\ n\mathrm{Bu}}$). ^{13}C{^{1}H} NMR (100 MHz, $CDCl_3$): δ = 165.5 (Ru-$C_{carbene}$), 146.7 (C_{trz}-^{n}Bu), 92.8 [(CCH$_3$)$_6$], 54.3 ($NCH_{2\ n\mathrm{Bu}}$), 36.5 (NCH_3), 33.2, 31.5, 26.5, 23.4, 20.6 ($CH_{2\ n\mathrm{Bu}}$), 15.6 [(CCH$_3$)$_6$], 14.1 and 14.0 ppm ($CH_{3\ n\mathrm{Bu}}$). Electrospray MS (30 V): *m/z* = 494.1 $[M - Cl]^+$. Anal. calcd for $C_{23}H_{39}N_3Cl_2Ru$ (mol wt. 529.55): C, 52.17; H, 7.42; N,7.94. Found: C, 52.15; H, 7.70; N, 7.99.

Synthesis of 13G:

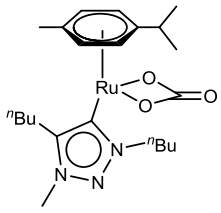

Sodium carbonate (42.6 mg, 0.4 mmol) was added to a solution of **11G** (40 mg, 0.08 mmol) in EtOH (15 mL). The suspension was stirred at room temperature for 3 h. The yellow solution was filtered through Celite, and the solvent was removed. The solid was redissolved in CH_2Cl_2 (10 mL) and filtered again. Concentration of the solution and subsequent precipitation with cold Et_2O gave **13G** as a yellow solid. Yield: 18 mg (45%). A full-assignment of the ^{13}C NMR spectra of **13G** was carried out with the aid HSQC NMR experiment (Figure 5.3). ^{1}H NMR (400 MHz, $CDCl_3$): δ = 5.42, 5.06 (d, $^3J_{H,H}$ = 8.0 Hz, 4H, $CH_{p\text{-}cym}$), 4.34 (t, $^3J_{H,H}$ = 8.0 Hz, 2H, $NCH_{2\ n\mathrm{Bu}}$), 3.96 (s, 3H, NCH_3), 2.80 (m, 1H, C_{trz}-$CH_{2\ n\mathrm{Bu}}$), 2.74 (m, 1H, $CH_{isop\ p\text{-}cym}$), 2.64 (m, 1H, C_{trz}-$CH_{2\ n\mathrm{Bu}}$), 2.07 (s, 3H, $CH_{3\ p\text{-}cym}$), 2.03 (m, 1H, $CH_{2\ n\mathrm{Bu}}$), 1.91 (m, 2H, $CH_{2\ n\mathrm{Bu}}$), 1.73 (m, 1H, $CH_{2\ n\mathrm{Bu}}$), 1.46 (m, 4H, $CH_{2\ n\mathrm{Bu}}$), 1.32 (d, $^3J_{H,H}$ = 8.0 Hz, 6H,$CH_{3\ isop\ p\text{-}cym}$) and 1.00 ppm (m, 6H, $CH_{3\ n\mathrm{Bu}}$). ^{13}C{^{1}H} NMR (100 MHz,

$CDCl_3$): δ = 166.7 (CO_3), 165.1 (Ru-$C_{carbene}$), 146.5 (C_{trz}-Bu), 105.6, 94.3 ($Cq_{p\text{-cym}}$), 82.7, 80.4 ($CH_{p\text{-cym}}$), 53.8 ($NCH_{2\ n\text{Bu}}$), 36.1 (NCH_3), 32.2 ($CH_{isop\ p\text{-cym}}$), 31.9, 31.8, 25.4, 23.1 ($CH_{2\ n\text{Bu}}$), 22.9 ($CH_{3\ isop\ p\text{-cym}}$), 20.2 ($CH_{2\ n\text{Bu}}$), 19.1 ($CH_{3\ p\text{-cym}}$), 13.8 and 13.7 ppm ($CH_{3\ n\text{Bu}}$). IR (KBr): ν=1611 cm^{-1} ($\nu_{C=O}$). Electrospray MS (30V): *m/z* = 448.2 [M - CO_3 + OH]$^+$; 492.2 [M + H]$^+$. Anal. calcd for $C_{22}H_{35}N_3O_3Ru$ (mol wt. 490.60): C, 53.86; H, 7.19; N, 8.57.Found: C, 53.61; H, 7.16; N, 8.48.

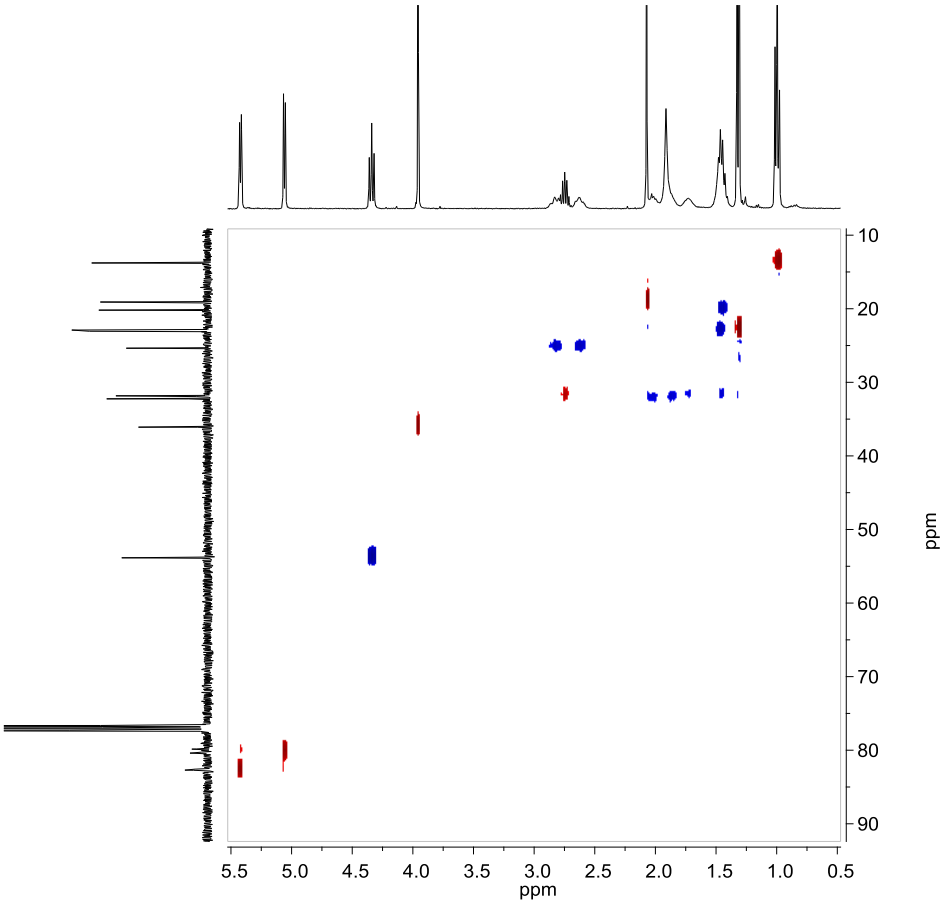

Figure 5.3 ^{13}C HSQC NMR (^1H, 400 MHz and ^{13}C, 100 MHz) of **13G**

Synthesis of 14G.

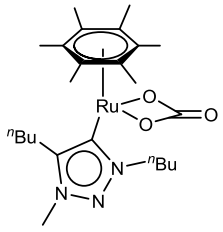

In analogous manner as that described for **13G**, complex **14G** was obtained from **12G** (53 mg, 0.1 mmol) and Na_2CO_3 (42.6 mg, 0.4 mmol) in EtOH (15 mL) as a yellow solid (39 mg, 75%). ^{1}H NMR (400 MHz, $CDCl_3$): δ = 4.25, 4.15 (m, 2H, $NCH_{2\ n\mathrm{Bu}}$), 3.95 (s, 3H, NCH_3), 2.62 (m, 2H, C_{trz}-$CH_{2\ n\mathrm{Bu}}$), 2.09 [s, 18H, $(CH_3)_6$], 1.84, 1.77 (m, 1H, $CH_{2\ n\mathrm{Bu}}$), 1.45 (m, 4H,$CH_{2\ n\mathrm{Bu}}$) and 0.97 ppm (m, 6H, $CH_{3\ n\mathrm{Bu}}$). ^{13}C{^{1}H} NMR (100 MHz, $CDCl_3$): δ = 169.0 (CO_3), 166.8 (Ru-$C_{carbene}$), 146.2 (C_{trz}-Bu), 91.6 [($C$$CH_3)_6$] , 53.8 ($NCH_{2\ n\mathrm{Bu}}$), 36.3 ($NCH_3$), 32.0, 31.2, 25.5, 23.3, 20.4 ($CH_{2\ n\mathrm{Bu}}$), 16.0 [(C$C$$H_3)_6$], 13.9 and 13.8 ppm ($CH_{3\ n\mathrm{Bu}}$). IR (KBr): ν = 1602 cm^{-1} ($\nu_{C=O}$). Electrospray MS (30 V): *m/*z = 476.2 $[M - CO_3 + OH]^+$; 520.2 $[M + H]^+$. Anal. calcd for $C_{24}H_{39}N_3O_3Ru$ (mol wt. 518.6): C, 55.38; H, 7.58; N, 8.10. Found: C, 55.12; H, 7.70; N, 7.97.

5.2.3 Synthesis of Ir(III) monocarbene complex

Synthesis of 17F:

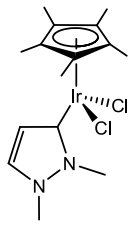

A suspension of 1,2-dimethylpyrazolium iodide (74 mg, 0.33 mmol) and silver oxide (176 mg, 0.50 mmol) in acetonitrile (20 mL) was stirred at room temperature for 2 h. The mixture was filtered through Celite and $[IrCp^*Cl_2]_2$ (120 mg, 0.15 mmol) was added. The mixture was refluxed for 3 h, the suspension was filtered through Celite and the solvent was evaporated under reduce pressure. The crude solid was purified by column chromatography. Elution with a mixture of CH_2Cl_2/acetone (1:1) afforded a yellow band that contained compound **17F**. The pure compound was precipitated from a mixture of CH_2Cl_2/Et_2O as a yellow solid. Yield: 60 mg (40%). ^{1}H NMR (300 MHz, $CDCl_3$): δ = 7.39, 6.46 (d, $^3J_{H,H}$ = 2.70 Hz, 2H, $CH_{pyrazole}$), 4.09, 3.92 (s, 6H, NCH_3) and 1.60 ppm (s, 15H, $CH_{3\ Cp^*}$); ^{13}C{^{1}H} NMR (75 MHz, $CDCl_3$): δ = 162.4 (Ir-$C_{carbene}$), 133.5, 117.2 ($CH_{pyrazole}$), 87.8 (Cq_{Cp^*}), 36.8, 36.7 (NCH_3) and 8.6 ppm ($CH_{3\ Cp^*}$). Electrospray MS (30 V): *m/z* = 459.2 $[M\text{-}Cl]^+$; Anal. calcd. (%) for

$C_{15}H_{23}N_2Cl_2Ir$ (mol wt. 494.48): C 36.43, H 4.69, N 5.67; found: C 36.43, H 4.89, N 5.66.

5.2.4 Synthesis of Ir(I), Ir(III) and Rh(I) complexes by double C-H activation

Synthesis of 18H:

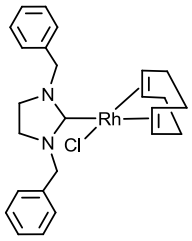

A mixture of 1,3-dibenzyl-1,3-diazolidine (**H**H2, 101 mg, 0.4 mmol), $[RhCl(COD)]_2$ (100 mg, 0.2 mmol) and 1,5-cyclooctadiene (248 µL, 2 mmol) was refluxed in dry acetonitrile overnight. After removal of the volatiles, the crude solid was dissolved in CH_2Cl_2 and purified by column chromatography using silica gel. Elution with CH_2Cl_2 afforded a yellow band that contained compound **18H**. Yield: 118 mg (60 %). ^{1}H NMR (300 MHz, $CDCl_3$): δ = 7.40-7.19 (m, 10H, CH_{Ph}), 5.38, 5.29 (AB, J_{AB} = 15 Hz, 4H, CH_2Ph), 4.98 (m, 2H, CH_{COD}), 3.43 (m, 2H, CH_{COD}), 3.23-3.19 (m, 4H, NCH_2CH_2N), 2.26 (m, 4H, $CH_{2\ COD}$) and 1.85 ppm (m, 4H, $CH_{2\ COD}$). ^{13}C {^{1}H} NMR (75 MHz, $CDCl_3$): δ = 213.2 (d, $^1J_{Rh\text{-}C}$ = 47 Hz, Rh-$C_{carbene}$), 136.3 (Cq_{Ph}), 128.8, 128.3, 127.8 (CH_{Ph}), 99.4 (d, $^1J_{Rh\text{-}C}$ = 6 Hz, CH_{COD}), 68.5 (d, $^1J_{Rh\text{-}C}$ = 14 Hz, CH_{COD}), 54.9 (CH_2Ph), 48.0 (NCH_2CH_2N), 32.8 and 28.7 ppm ($CH_{2\ COD}$). Electrospray MS (20 V): *m/z* = 461.3 $[M - Cl]^+$, 502.2 $[M - Cl + CH_3CN]^+$. Anal. calcd. for $C_{25}H_{30}N_2ClRh$ (mol wt. 496.88): C, 60.43; H, 6.09; N, 5.64. Found: C, 60.75; H, 6.25; N, 5.33.

Synthesis of 19H:

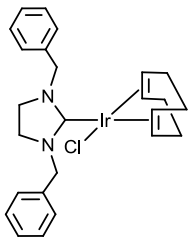

A mixture of 1,3-dibenzyl-1,3-diazolidine (**H**H2, 76 mg, 0.3 mmol), $[IrCl(COD)_2]_2$ (100 mg, 0.15 mmol) and 1,5-cyclooctadiene (186 µL, 1.5 mmol) was refluxed in dry acetonitrile overnight. After removal of the volatiles, the crude solid was dissolved in CH_2Cl_2 and purified by column chromatography using silica gel. Elution with CH_2Cl_2 afforded a yellow band that

contained compound **19H**. Yield: 114 mg (65 %). ^{1}H NMR (300 MHz, $CDCl_3$): δ = 7.46-7.30 (m, 10H, CH_{Ph}), 5.39, 5.11 (AB, J_{AB} = 15 Hz, 4H, CH_2Ph), 4.62 (m, 2H, CH_{COD}), 3.37-3.28 (m, 4H, NCH_2CH_2N), 3.15 (m, 2H, CH_{COD}), 2.18 (m, 4H, $CH_{2\ COD}$) and 1.70 ppm (m, 4H, $CH_{2\ COD}$). ^{13}C {^{1}H} NMR (75 MHz, $CDCl_3$): δ = 207.4 (Ir-$C_{carbene}$), 136.2 (Cq_{Ph}), 128.7, 128.5, 128.0 (CH_{Ph}), 85.5 (CH_{COD}), 54.7 (CH_{COD}), 52.3 (CH_2Ph), 48.1 (NCH_2CH_2N), 33.4 and 29.7 ppm ($CH_{2\ COD}$). Electrospray MS (20 V): *m/z* = 592.2 [M - Cl + CH_3CN]$^{+}$. Anal. calcd. for $C_{25}H_{30}N_2ClIr$ (mol wt. 586.19): C, 51.22; H, 5.16; N, 4.78. Found: C, 51.16; H, 5.04; N, 4.57.

Synthesis of 20H:

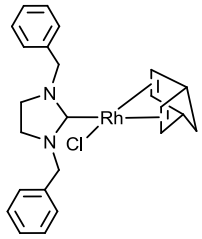

A mixture of 1,3-dibenzyl-1,3-diazolidine (**H**H2, 109 mg, 0.44 mmol), $[RhCl(NBD)]_2$ (100 mg, 0.22 mmol) and 2,5-norbornadiene (228 µL, 2.2 mmol) was refluxed in dry acetonitrile overnight. After removal of the volatiles, the crude solid was dissolved in CH_2Cl_2 and purified by column chromatography using silica gel. Elution with CH_2Cl_2 afforded a yellow band that contained compound **20H**. Yield: 142 mg (67 %). ^{1}H NMR (500 MHz, $CDCl_3$): δ = 7.44-7.30 (m, 10H, CH_{Ph}), 5.45, 5.38 (AB, J_{AB} = 15 Hz, 4H, CH_2Ph), 4.88 (m, 2H, CH_{NBD}), 3.73 (m, 2H, CH_{NBD}), 3.55 (m, 2H, CH_{NBD}), 3.31-3.25 (m, 4H, NCH_2CH_2N), 1.38 and 1.30 ppm (AB, J_{AB} = 8 Hz, 2H, $CH_{2\ NBD}$). ^{13}C {^{1}H} NMR (125 MHz, $CDCl_3$): δ = 215.5 (d, $^{1}J_{Rh\text{-}C}$ = 53 Hz, Rh-$C_{carbene}$), 136.6 (C_{qPh}), 128.8, 128.1, 127.7 (CH_{Ph}), 81.0 (CH_{NBD}), 63.5 (CH_{NBD}), 54.7 (CH_2Ph), 50.9 ($CH_{2\ NBD}$), 48.8 (CH_{NBD}) and 48.0 ppm (NCH_2CH_2N). Electrospray MS (20 V): *m/z* = 445.2 [M - Cl]$^{+}$. Anal. Calcd. for $C_{24}H_{26}N_2ClRh$ (mol wt. 480.84): C, 59.95; H, 5.45; N, 5.83. Found: C, 59.54; H, 5.70; N, 5.72.

Synthesis of 21I

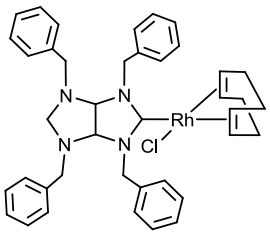

A mixture of 2,4,6,8-tetrabenzyl-2,4,6,8-tetraazabicyclo[3.3.0]octane (**I**H4, 285 mg, 0.6 mmol), $[RhCl(COD)]_2$ (150 mg, 0.3 mmol) and 1,5-cyclooctadiene (330 μL, 3 mmol) was refluxed in deoxygenated acetonitrile overnight. After this time, the volatile components were removed under vacuum. The crude solid was dissolved in CH_2Cl_2 and purified by column chromatography. Elution with CH_2Cl_2/hexane (9:1) afforded a yellow band that contained compound **21I**. Compound **21I** was precipitated in a mixture of CH_2Cl_2/hexanes to give a yellow solid. Yield: 285 mg (65 %). ^{1}H NMR (300 MHz, $CDCl_3$): δ = 7.45-7.22 (m, 20H, CH_{Ph}), 6.46 (d, $^2J_{H\text{-}H}$ = 14 Hz, 2H, CH_2Ph), 5.09 (m, 2H, CH_{COD}), 4.56 (s, 2H, CH_{ring}) 4.49 (d, $^2J_{H,H}$ = 14 Hz, 2H, CH_2Ph), 3.74, 3.62 (AB, J_{AB} = 13.5 Hz, 4H, CH_2Ph), 3.46 (AB, J_{AB} = 9.9 Hz, 1H, $CH_{2\ ring}$), 3.41 (m, 2H, CH_{COD}), 3.32 (AB, J_{AB} = 9.9 Hz, 1H, $CH_{2\ ring}$), 2.41 (m, 4H, $CH_{2\ COD}$) and 1.98 ppm (m, 4H, CH_{COD}). ^{13}C {^{1}H} NMR (125 MHz, $CDCl_3$): δ = 214.0 (d, $^1J_{Rh\text{-}C}$ = 47 Hz, Rh-$C_{carbene}$), 138.8, 135.7 (Cq_{Ph}), 129.1, 128.6, 128.3, 127.6, 127.3 (CH_{Ph}), 100.2 (CH_{COD}), 81.2 (CH_{ring}), 69.0 ($CH_{2\ ring}$), 57.5 (CH_2Ph), 52.6 (CH_{COD}), 52.3 (CH_2Ph), 32.9 and 28.7 ppm ($CH_{2\ COD}$). Electrospray MS (10 V): *m/z* = 683 [M - Cl]$^+$. Anal.Calcd.for $C_{40}H_{44}N_4ClRh$ (mol wt. 719.16): C, 66.80; H, 6.17; N, 7.79. Found: C, 66.60; H, 6.24; N, 7.60.

Synthesis of 22I:

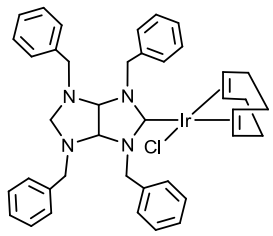

A mixture of 2,4,6,8-tetrabenzyl-2,4,6,8-tetraazabicyclo[3.3.0]octane (**I**H4, 212 mg, 0.45 mmol), $[IrCl(COD)]_2$ (150 mg, 0.22 mmol) and 1,5-cyclooctadiene (278 μL, 2.25 mmol) was refluxed in deoxygenated acetonitrile overnight. After this time, the volatile components were removed under vacuum. The crude solid was dissolved in CH_2Cl_2 and purified by column chromatography. Elution with CH_2Cl_2/hexane (9:1) afforded a yellow band that contained compound **22I**.

Compound **22I** was precipitated in a mixture of CH_2Cl_2/hexanes to give a yellow solid. Yield: 200 mg (55 %). A full-assignment of the ^{13}C NMR spectra of **22I** was carried out with the aid of HSQC NMR experiment (Figure 5.4). ^1H NMR (500 MHz, $CDCl_3$): δ = 7.38-7.23 (m, 20H, CH_{Ph}), 6.27 (d, $^2J_{H,H}$ = 14.0 Hz, 2H, CH_2Ph), 4.65 (m, 2H, CH_{COD}), 4.61 (s, 2H, CH_{ring}), 4.41 (d, $^2J_{H-H}$ = 14.5 Hz, 2H, CH_2Ph), 3.82, 3.65 (AB, J_{AB} = 15 Hz, 4H, CH_2Ph), 3.50, 3.43 (AB, J_{AB} = 10 Hz, 1H, $CH_{2\ ring}$), 3.04 (m, 2H, CH_{COD}), 2.24, 1.78 and 1.69 ppm (m, 10H, $CH_{2\ COD}$). ^{13}C {^1H} NMR (75 MHz, $CDCl_3$): δ = 207.7 (Ir-$C_{carbene}$), 138.8, 135.2 (Cq_{Ph}), 128.9, 128.6, 128.3, 127.6, 127.5 (CH_{Ph}), 86.3 (CH_{COD}), 81.4 (CH_{ring}), 69.3 ($CH_{2\ ring}$), 57.5 (CH_2Ph), 52.9 (CH_{COD}), 52.1 (CH_2Ph), 33.4 and 29.3 ppm ($CH_{2\ COD}$). Electrospray MS (20V): *m/z* = 773 $[M - Cl]^+$, 814 $[M - Cl + CH_3CN]^+$. Anal. calcd. for $C_{40}H_{44}N_4ClIr$ (mol wt. 808.47): C, 59.42; H, 5.49; N, 6.93. Found: C, 59.58; H, 5.04; N, 6.91.

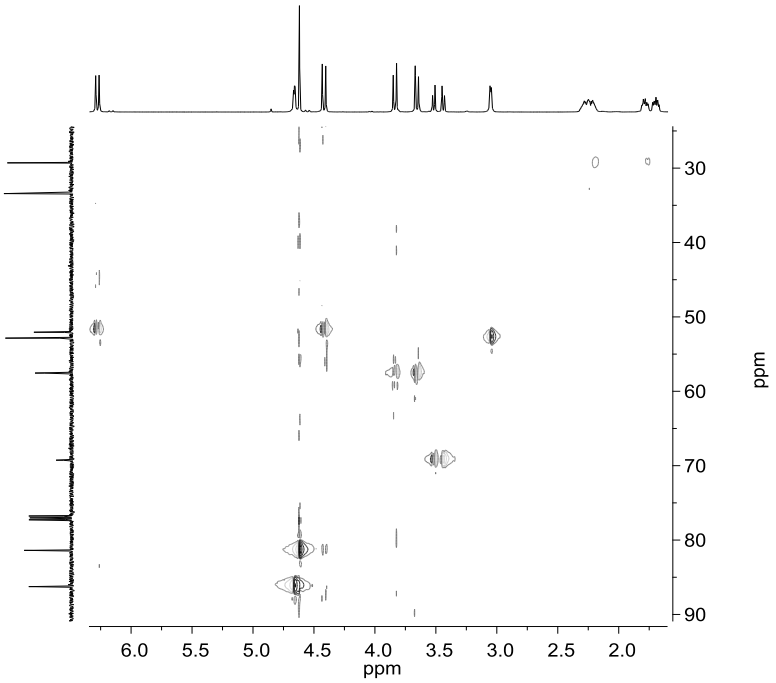

Figure 5.4 ^{13}C HSQC NMR (^1H, 500 MHz and ^{13}C, 125 MHz) of **22I**

Synthesis of 23I:

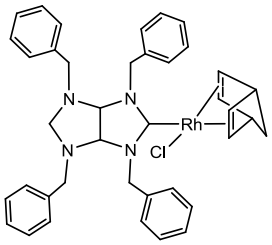

A mixture of 2,4,6,8-tetrabenzyl-2,4,6,8-tetraazabicyclo [3.3.0]octane (**I**H4, 285 mg, 0.6 mmol), $[RhCl(NBD)]_2$ (150 mg, 0.3 mmol) and 2,5-norbornadiene (311 μL, 3 mmol) was refluxed in deoxygenated acetonitrile overnight. After this time, the volatile components were removed under vacuum. The crude solid was dissolved in CH_2Cl_2 and purified by column chromatography. Elution with CH_2Cl_2/hexane (9:1) afforded a yellow band that contained compound **23I**. After the addition of hexanes, a yellow solid precipitated. The solid so obtained contained a mixture of complexes **23I'** and **23I''**. Yield: 71 mg (80%). Electrospray MS (10 V): *m/z* = 667 $[M - Cl]^+$. Anal. calcd. for $C_{39}H_{40}N_4ClRh$ (mol wt. 702.2): C, 66.62; H, 5.73; N, 7.97. Found: C, 66.58; H, 6.00; N, 7.80.

Table 5.1 Spectroscopic characterization of **23I**

^{1}H NMR (500 MHz, $CDCl_3$)	δ (**23I'**) (ppm)	δ (**23I''**) (ppm)	^{13}C {^{1}H} NMR (75 MHz, $CDCl_3$)	δ (**23I'**) (ppm)	δ (**23I''**) (ppm)
CH_{Ph}	7.37-7.04		Rh-C_{imid}, d, J_{Rh-C} = 52.5 Hz	217.1	216.8
CH_2Ph d, $^2J_{H,H}$ = 15 Hz	6.34, 4.50	6.37, 4.61	Cq_{Ph}	138.7 – 136.2	
CH_{NBD}	4.92	4.86	CH_{Ph}	129.1 – 127.3	
CH_{ring}	4.54	4.71	CH_{NBD}	81.8, 57.6	81.2, 58.1
CH_2Ph	3.83, 3.65	3.84, 3.64	CH_{ring}	81.7	81.4
CH_{NBD}	3.74	3.65	$CH_{2\ ring}$	69.8	69.6
$CH_{2\ ring}$	3.48, 3.28	3.88, 3.50	$CH_{2\ NBD}$	63.5	63.5
CH_{NBD}	3.44		CH_2Ph	52.4, 50.8	52.0, 51.1
$CH_{2\ NBD}$	1.41, 1.34	1.26	CH_{NBD}	48.0	48.7

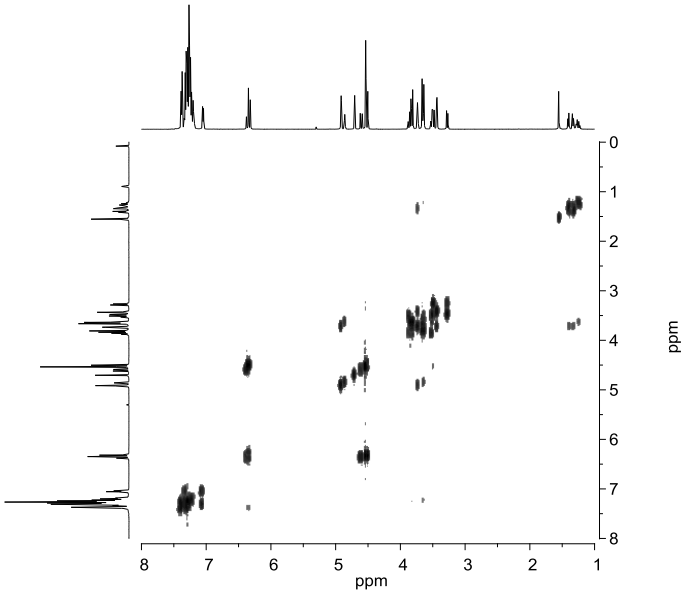

Figure 5.5 COSY NMR (^{1}H, 500 MHz) of **23I**

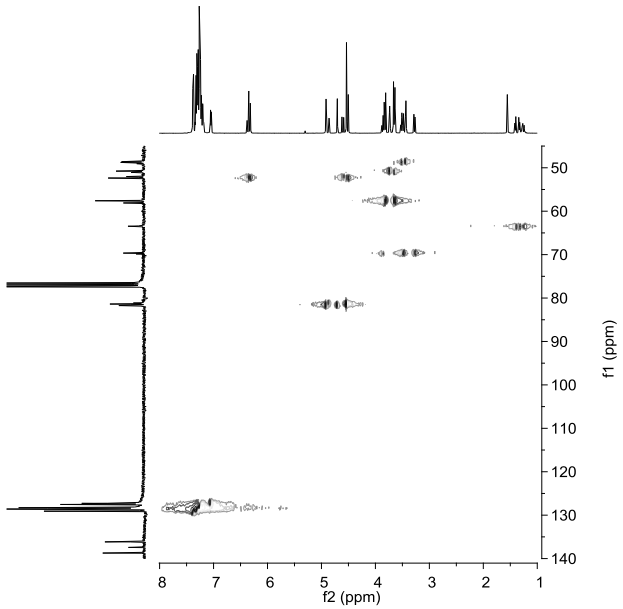

Figure 5.6 ^{13}C HSQC NMR (^{1}H, 500 MHz and ^{13}C, 125 MHz) of **23I**

Synthesis of 24I:

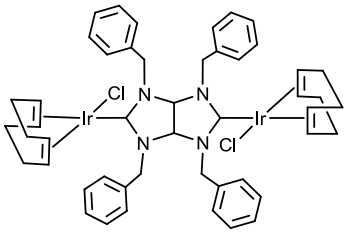

A mixture of 2,4,6,8-tetrabenzyl-2,4,6,8-tetraazabicyclo [3.3.0]octane (**I**H4, 142 mg, 0.3 mmol), $[IrCl(COD)]_2$ (200 mg, 0.3 mmol) and 1,5-cyclooctadiene (186 μL, 1.5 mmol) was refluxed in dry toluene for 48h. After this time, the volatile components were removed under vacuum. The crude solid was dissolved in CH_2Cl_2 and purified by column chromatography. Elution with CH_2Cl_2/hexane (9:1) afforded a yellow band that contained compound **24I**. Compound **24I** was precipitated in a mixture of CH_2Cl_2/hexane to give a yellow solid. Yield: 209 mg (61 %). ^{1}H NMR (500 MHz, $CDCl_3$): δ = 7.30-7.22 (m, 20H, CH_{Ph}), 6.04 (d, $^2J_{H,H}$ = 16 Hz, 4H, CH_2Ph), 4.98 (s, 2H, CH_{ring}), 4.67 (d, $^2J_{H\text{-}H}$ = 13 Hz, 4H, CH_2Ph), 4.66 (m, 4H, CH_{COD}), 2.94 (m, 4H, CH_{COD}), 2.12 (m, 8H, $CH_{2\ COD}$), 1.77 (m, 4H, CH_{COD}) and 1.69 ppm (m, 4H, $CH_{2\ COD}$). ^{13}C {^{1}H} NMR (75 MHz, $CDCl_3$): δ = 211.2 (Ir-$C_{carbene}$), 134.5 (Cq_{Ph}), 129.0, 128.2, 127.9 (CH_{Ph}), 88.6 (CH_{COD}) 78.9 (CH_{ring}), 54.0 (CH_2Ph), 53.3 (CH_{COD}), 33.3 and 29.0 ppm ($CH_{2\ COD}$). Electrospray MS (20 V): *m/z* = 1106.8 [M - Cl]$^+$. Anal. calcd. for $C_{48}H_{54}N_4Cl_2Ir_2$ (mol wt. 1142.3): C, 50.47; H, 4.76; N, 4.90. Found: C, 50.67; H, 4.94; N, 4.72.

Synthesis of 25I

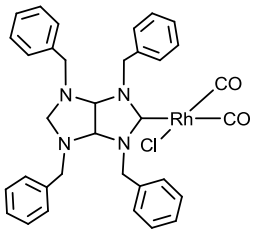

CO gas (1 atm, 10 mL/min) was passed through a solution of complex **21I** (50 mg) in dichloromethane (15 mL) for 20 minutes at 0ºC. After this time, the solution was concentrated under reduced pressure. After the addition of hexanes, a light yellow solid precipitated. The solid obtained contained a mixture of complexes, **25I'** and **25I''**. Yield 40 mg (80%). IR (KBr): 2077 ($\nu_{C=O}$), 1995 ($\nu_{C=O}$) cm^{-1}. Electrospray MS (5 V): *m/z* = 631 [M - Cl]$^+$. Anal. calcd. for $C_{34}H_{32}N_4ClO_2Rh$ (mol wt. 667.00): C, 61.22; H, 4.84; N, 8.40. Found: C, 61.14; H, 4.48; N, 8.23.

Table 5.2 Spectroscopic characterization of **25I**

^{1}H NMR (500 MHz, $CDCl_3$)	δ (**25I'**) (ppm)	δ (**25I''**) (ppm)	^{13}C {^{1}H} NMR (75 MHz, $CDCl_3$)	δ (**25I'**) (ppm)	δ (**25I''**) (ppm)
CH_{Ph}	7.32-7.02		$Rh\text{-}C_{carbene}$ d, $^{1}J_{Rh\text{-}C}$= 40 Hz	203.5	202.7
CH_2Ph d, $^{2}J_{H\text{-}H}$ = 15 Hz	5.70, 4.49	5.59, 4.54	$Rh\text{-}C_{CO}$ d, $^{1}J_{Rh\text{-}C}$ = 75 Hz	185.5, 183.1	185.5, 182.3
CH_{ring}	4.84	4.79	Cq_{Ph}	138.5, 135.8	138.4, 135.3
$CH_{2\ ring}$	4.03, 3.67	3.66-3.63	CH_{Ph}	128.9-127.7	
CH_2Ph	3.94, 3.77	3.87, 3.72	CH_{ring}	82.3	82.6
			$CH_{2\ ring}$	70.8	69.8
			CH_2Ph	58.6, 52.0	58.3, 52.6

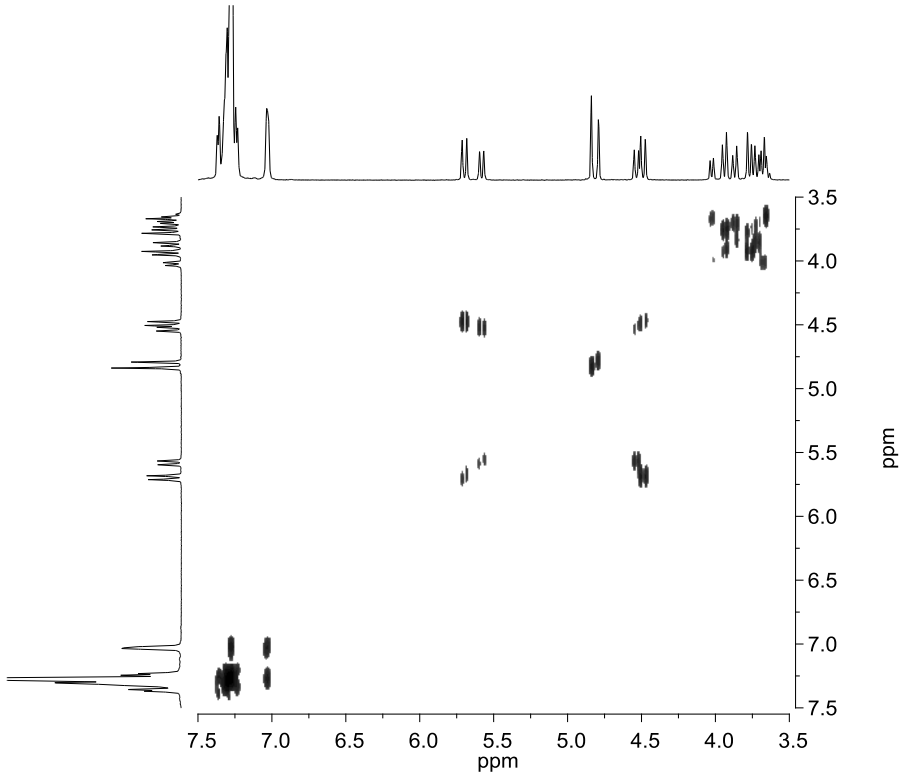

Figure 5.7 COSY NMR (^{1}H, 500 MHz) of **25I**

Synthesis of 26I

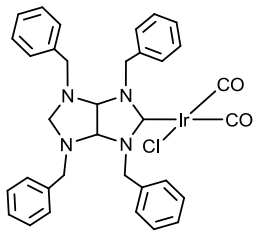

CO gas (1 atm, 10 mL/min) was passed through a solution of compound **26I** (50 mg) in dichloromethane (10 mL) for 20 minutes at 0ºC. The solution was concentrated under reduced pressure, and hexanes were added to get a light yellow solid. The solid so obtained contained a mixture of compounds, **26I'** and **26I''**. Yield 35 mg (75%). IR (KBr): 2063 ($\nu_{C=O}$), 1978 ($\nu_{C=O}$) cm^{-1}. Electrospray MS (20 V): m/z = 721[M - Cl]$^+$. Anal. calcd. for $C_{34}H_{32}N_4ClO_2Ir$ (mol wt. 756.31): C, 53.99; H, 4.23; N, 7.41. Found: 53.97; H, 4.45; N, 7.21.

Table 5.3 Spectroscopic characterization of **26I**

^{1}H NMR (500 MHz, $CDCl_3$)	δ (**26I'**) (ppm)	δ (**26I''**) (ppm)	^{13}C {^{1}H} NMR (125 MHz, $CDCl_3$)	δ (**26I'**) (ppm)	δ (**26I''**) (ppm)
CH_{Ph}	7.25-6.94		Ir-$C_{carbene}$	199.5	198.5
CH_2 Ph d, $^2J_{H,H}$ = 15 Hz	5.69, 4.32	5.66, 4.39	Ir-CO	181.5, 168.6	181.3, 168.0
CH_{ring}	4.75	4.71	C_{qPh}	138.4, 135.5	138.3, 135.0
$CH_{2\ ring}$	3.94, 3.70	3.72-3.67	CH_{Ph}	128.8-127.7	
CH_2Ph	3.88, 3.70	3.78, 3.70	CH_{ring}	82.2	82.5
			$CH_{2\ ring}$	70.9	69.8
			CH_2Ph	58.7, 51.9	58.4, 52.3

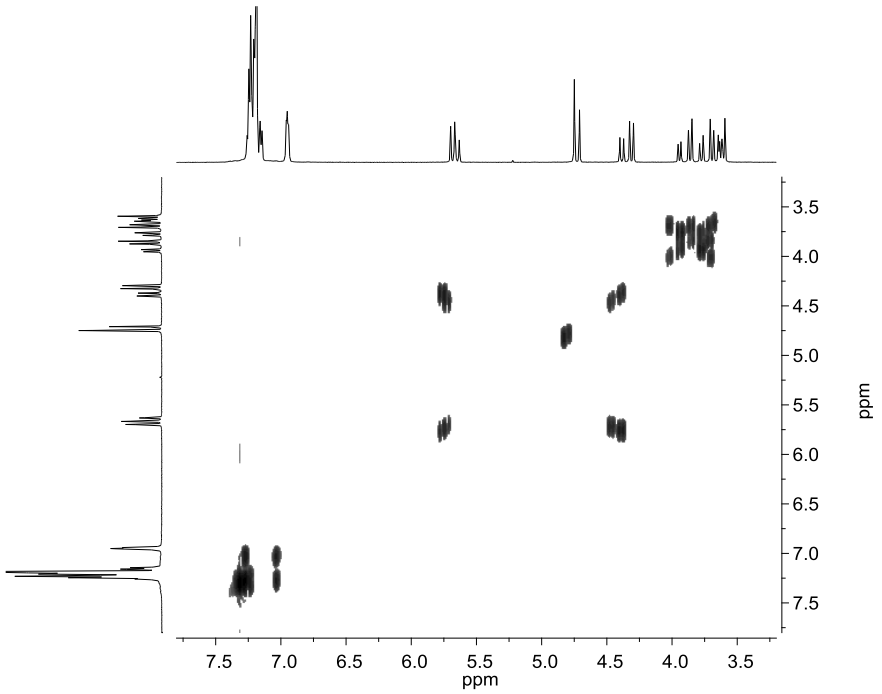

Figure 5.8 COSY NMR (^{1}H, 500 MHz) of **25I**

Synthesis of 27I

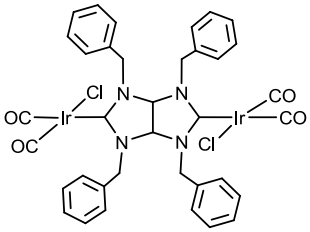

CO gas (1 atm, 10 mL/min) was passed through a solution of compound **24I** (40 mg) in dichloromethane (15 mL) for 20 minutes at 0ºC. The solution was concentrated under reduced pressure, and hexanes were added to get a light yellow solid. The solid so obtained contained a mixture of complexes, **27I'**, **27I''** and **27I'''**. Yield 19 mg (71 %). IR (KBr): 2071 ($\nu_{C=O}$), 1986 ($\nu_{C=O}$) cm^{-1}. Electrospray MS (20 V): *m/z* = 1002.5 [M - Cl]$^+$. Anal. calcd. for $C_{36}H_{30}N_4Cl_2O_4Ir_2$ (mol wt. 1037.99): C, 41.66; H, 2.91; N, 5.40. Found: C, 41.87; H, 3.21; N, 5.00.

Table 5.4 Spectroscopic characterization of **27I**

^{1}H NMR (500 MHz, $CDCl_3$)	δ (**27I'**) (ppm)	δ (**27I''**) (ppm)	δ (**27I'''**) (ppm)
CH_{Ph}		7.46-7.11	
CH_2Ph (d, $^2J_{H,H}$ = 15 Hz)	5.36, 4.84	5.65, 5.51, 4.80, 4.69	5.89, 4.56
CH_{ring}	5.51	5.50	5.49
^{13}C {^{1}H} NMR (125 MHz, $CDCl_3$)	δ (**27I'**) (ppm)	δ (**27I''**) (ppm)	δ (**27I'''**) (ppm)
Ir-$C_{carbene}$	204.3	203.4	Non detected
Ir-CO	180.2, 167.2	180.2, 167.8	
Cq_{Ph}	133.9	133.6	
CH_{Ph}	129.5-127.1		
CH_{ring}	81.4	80.4	
CH_2Ph	53.7	53.7	

Synthesis of 28I

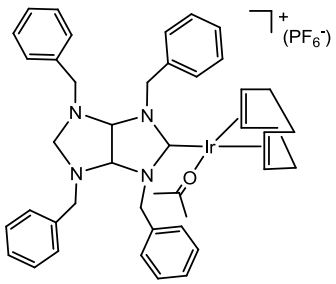

A mixture of **22I** (100 mg, 0.12 mmol) and $AgPF_6$ (32 mg, 0.12 mmol) were stirred in acetone (5mL) at room temperature under the exclusion of light. The resulting suspension was cooled in the fridge during 5 h. The precipitate was filtered and the solution was concentrated under reduced pressure. Diethyl ether was added to get a yellow solid. The solid was washed with diethyl ether several times and dried in vacuum to give **28I** in 62% yield. **28I** was only characterized by ^{1}H NMR. ^{1}H NMR (300 MHz, $(CD_3)_2CO$): δ = 7.37-7.06 (m, 20H, CH_{Ph}), 6.09 (d, $^2J_{H,H}$ = 12 Hz, 2H, CH_2Ph), 5.08 (s, 2H, CH_{ring}), 4.72 (d, $^2J_{H,H}$ = 12 Hz, 2H, CH_2Ph), 4.42 (m, 2H, CH_{COD}), 4.06, 3.88 (AB, J_{AB} = 12 Hz, 4H, CH_2Ph), 3.72, 3.65 (AB, J_{AB} = 10 Hz, 2H, $CH_{2\ ring}$), 2.41 (m, 2H, CH_{COD}), 2.32 (m, 4H, $CH_{2\ COD}$) and 1.79 ppm (m, 4H, CH_{2COD}).

Synthes is of 29I

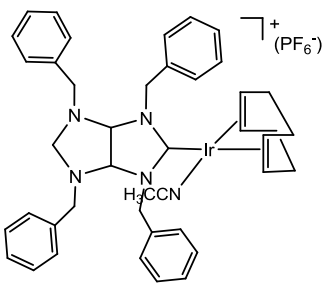

28I (16 mg, 0.016 mmol) was dissolved in 0.5mL of $CDCl_3$ in an NMR tube. Drops of CH_3CN were added and the mixture was stirred during 1 hour. **29I** was not isolated and it was only characterized by ^1H NMR. ^1H NMR (300 MHz, $CDCl_3$): δ = 7.31-7.01 (m, 20H, CH_{Ph}), 5.39 (d, $^2J_{H,H}$ = 15 Hz, 2H, CH_2Ph), 5.07 (s, 2H, CH_{ring}), 4.45 (d, $^2J_{H,H}$ = 14.5 Hz, 2H, CH_2Ph), 4.26 (m, 2H, CH_{COD}), 3.83, 3.65 (AB, J_{AB} = 12 Hz, 4H, CH_2Ph), 3.61 (AB, J_{AB} = 10 Hz, 1H, $CH_{2\ ring}$), 3.50 (m, 2H, CH_{COD}), 3.42 (AB, J_{AB} = 10 Hz, 1H, $CH_{2\ ring}$), 2.14 (m, 4H, $CH_{2\ COD}$), 2.11 (s, 3H, $NCCH_3$) and 1.80 ppm (m, 4H, $CH_{2\ COD}$).

Synthesis of 30I

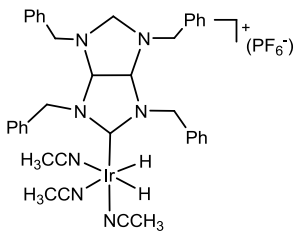

A mixture of **28I** (100 mg, 0.10 mmol) and CH_3CN (16 µL, 0.30 mmol) in $CDCl_3$ (2 mL) was introduced in a reactor. The mixture was stirred under 10 mbar of hydrogen pressure during 30 minutes. The solution was cannulated directly to an NMR tube for its characterization. **30I** was not isolated and it was only characterized by ^1H NMR. ^1H NMR (300 MHz, $CDCl_3$): δ = 7.32-7.18 (m, 20H, CH_{Ph}), 5.73 (d, $^2J_{H,H}$ = 15 Hz, 2H, CH_2Ph), 4.85 (s, 2H, CH_{ring}), 4.34 (d, $^2J_{H,H}$ = 15 Hz, 2H, CH_2Ph), 3.87 (AB, J_{AB} = 12 Hz, 2H, CH_2Ph), 3.72-3.67 (m, 2H, CH_2Ph and 2H, $CH_{2\ ring}$), 2.37 (s, 3H, $NCCH_3$), 1.73 (s, 6H, $NCCH_3$) and -22.15 ppm (s, 2H, Ir-H).

5.2.5 Synthesis of bis-NHC complexes of Rh(I) and Ir(I)

Compound 31J

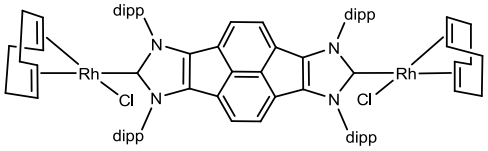

In a Schlenck tube, the bisimidazolium-pyracene chloride salt (50 mg, 0.05 mmol) was dissolved in dry toluene. *t*BuOK (17 mg, 0.15 mmol) and $[RhCl(COD)]_2$ (25 mg, 0.05 mmol) were subsequently added. The reaction mixture was stirred during 4h at room temperature. The green solution was filtered and the solvent was removed under vacuum. The pure sample of **31J** was obtained after column chromatography eluting with a mixture dichloromethane/acetone 95:5. Compound **31J** was precipitated from a mixture dichloromethane/hexane. Yield: 42 mg (61%). ^{1}H NMR (300 MHz, $CDCl_3$): δ = 7.45 (t, $^3J_{H,H}$ = 7.80 Hz, 4H, CH-Ar_{dipp}), 7.28 (d, $^3J_{H,H}$ = 7.80 Hz, 8H, CH-Ar_{dipp}), 5.32 (s, 4H, CH-$Ar_{pyracene}$), 4.56 (bs, 4H, CH_{COD}), 3.27 (bs, 4H, $CH_{isop\ dipp}$), 3.26 (bs, 4H, CH_{COD}), 1.73 (bs, 4H, $CH_{2\ COD}$), 1.47 (bs, 8H, $CH_{2\ COD}$), 1.35 (d, $^3J_{H,H}$ = 6.3 Hz, 24H, $CH_{3\ isop\text{-}dipp}$), 1.35 (bs, 8H, $CH_{2\ COD}$) and 1.03 ppm (d, $^3J_{H,H}$ = 6.8 Hz, 24H, $CH_{3\ isop\ dipp}$). $^{13}C\{^1H\}$ NMR (75 MHz, $CDCl_3$): δ = 195.9 (d, $^1J_{Rh\text{-}C}$ =52.50 Hz, Rh-$C_{carbene}$), 146.8 (Cq-Ar_{dipp}), 144.2, 135.7 ($Cq_{pyracene}$), 134.2 (Cq-Ar_{dipp}), 130.6 ($Cq_{pyracene}$), 130.1, 124.4 (CH-Ar_{dipp}), 121.9 ($CH_{pyracene}$), 97.0, 67.0 (CH_{COD}), 32.7 ($CH_{2\ COD}$), 28.9 ($CH_{isop\ dipp}$), 28.3 ($CH_{2\ COD}$), 26.1 and 24.1 ppm ($CH_{3\ isop\ dipp}$). Electrospray MS: *m*/*z* = 1317 $[M - 2Cl]^{2+}$. Electrospray MS: *m*/*z* 1353.6 $[M - Cl]^+$. Anal. calcd. for $C_{80}H_{96}N_4Cl_2Rh_2$ (mol wt. 1388.5): C, 69.11; H, 9.96; N, 4.06. Found: C, 68.77; H, 10.2; N, 4.20.

Compound 32J

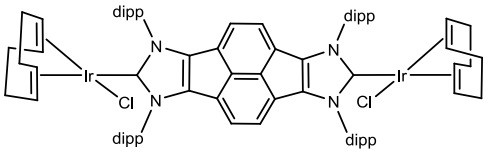

In a Schlenck tube, the bisimidazolium-pyracene chloride salt (50 mg, 0.05 mmol) was dissolved in dry toluene. *t*BuOK (17 mg, 0.15 mmol) and $[IrCl(COD)]_2$ (34 mg, 0.05 mmol) were subsequently added and the reaction mixture was stirred during 4 h at room temperature. The green solution was filtered and the solvent was removed

under vacuum. The clean product was obtained after column chromatography eluting with a mixture dichloromethane/hexane 95:5. The entitled compound was precipitated from a mixture dichloromethane/hexane. Yield: 45 mg (58 %). ^{1}H NMR (500 MHz, $CDCl_3$): δ = 7.42 (t, $^{3}J_{H,H}$ =12.5 Hz, 4H, CH-Ar_{dipp}), 7.25 (d, $^{3}J_{H,H}$ =10 Hz, 8H, CH-Ar_{dipp}), 5.28 (s, 4H, CH-$Ar_{pyracene}$), 4.23 (bs, 4H, CH_{COD}), 3.35 (bs, 4H, $CH_{isop\ dipp}$), 2.94 (bs, 4H, CH_{COD}), 1.60, 1.48 (bs, 8H, $CH_{2\ COD}$), 1.34 (d, $^{3}J_{H,H}$ = 10 Hz, 12H, $CH_{3\ isop\ dipp}$), 1.30, 1.18 (bs, 8H, $CH_{2\ COD}$) and 1.07 ppm (d, $^{3}J_{H,H}$ = 10 Hz, 12H, $CH_{3\ isop\ dipp}$).^{13}C{^{1}H} NMR (125 MHz, $CDCl_3$): δ = 191.5 (Ir-$C_{carbene}$), 146.4 (Cq-Ar_{dipp}), 143.6, 135.5 ($Cq_{pyracene}$), 133.9 (Cq-Ar_{dipp}), 130.9 ($Cq_{pyracene}$), 130.0, 124.1 (CH-Ar_{dipp}), 121.8 ($CH_{pyracene}$), 83.9, 50.7 (CH_{COD}), 33.42 ($CH_{2\ COD}$), 28.8 ($CH_{isop\ dipp}$), 28.6 ($CH_{2\ COD}$) and 25.9 and 23.8 ppm ($CH_{3\ isop\ dipp}$). Electrospray MS: *m*/*z* = 1534.1 $[M - Cl]^{+}$. Anal. calcd. for $C_{80}H_{96}N_4Cl_2Ir_2$ (mol wt. 1569.6): C, 61.24; H, 6.17; N, 3.57. Found: C, 62.01; H, 6.31; N, 3.25.

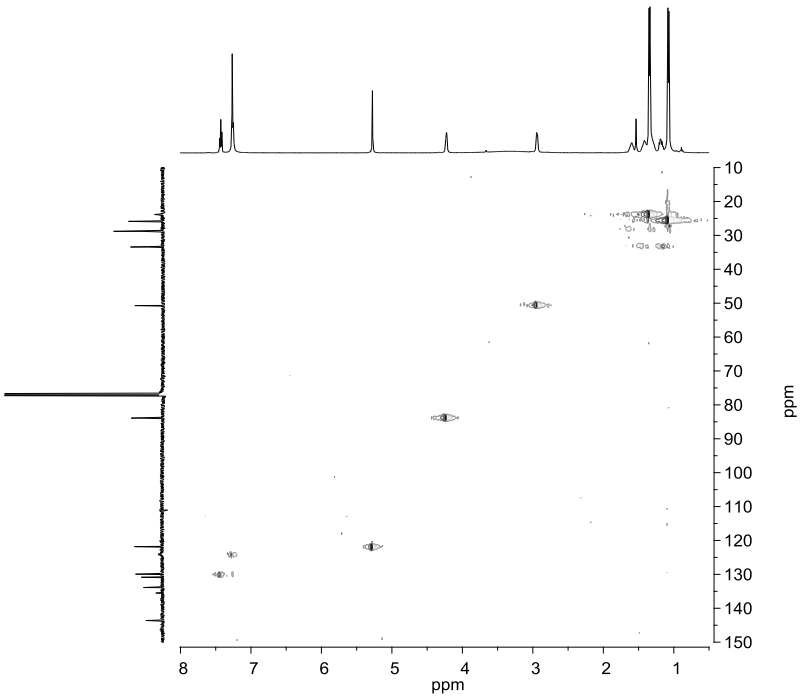

Figure 5.9 ^{13}C HSQC NMR (^{1}H, 500 MHz and ^{13}C, 125 MHz) of **32J**

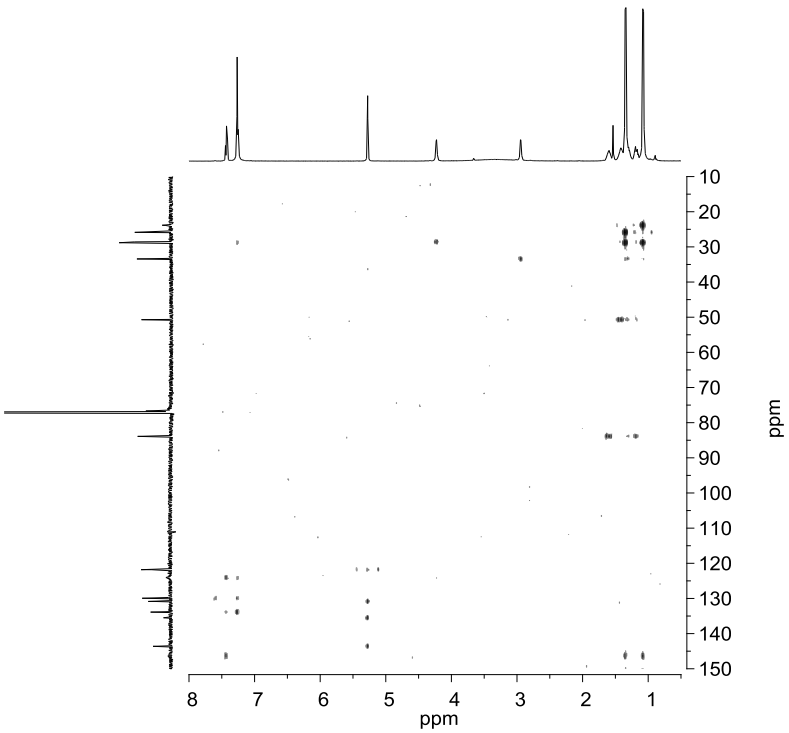

Figure 5.10 ^{13}C HMBC NMR (^{1}H, 500 MHz and ^{13}C, 125 MHz) of **32J**

Compound 33J

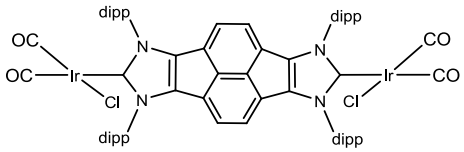

CO gas (1 atm, 10 mL/min) was passed through a solution of complex **33J** (30 mg, 0.02 mmol) in dichloromethane (15 mL) for 20 minutes at 0ºC. After this time, the solution was concentrated under reduced pressure. After the addition of hexanes, a light green solid precipitated. Yield: 24 mg (80 %). ^{1}H NMR (500 MHz, CD_2Cl_2): δ = 7.44 (t, $^{3}J_{H,H}$ =12.5 Hz, 4H, CH-Ar$_{dipp}$), 7.25 (d, $^{3}J_{H,H}$ =10 Hz, 8H, CH-Ar$_{dipp}$), 5.45 (s, 4H, CH-Ar$_{pyracene}$), 3.05 (sept, 8H, CH$_{isop\ dipp}$), 1.27 (d, $^{3}J_{H,H}$ = 5 Hz, 12H, CH$_{3\ isop\ dipp}$) and 0.99 ppm (d, $^{3}J_{H,H}$ = 5 Hz, 12H, CH$_{3\ isop\text{-}dipp}$). ^{13}C{^{1}H} NMR (125 MHz, CD_2Cl_2): δ = 183.3 (CO), 179.4 (C$_{imid}$-Ir), 168.4 (CO), 145.8 (Cq-Ar$_{dipp}$), 143.8, 134.9 (Cq$_{pyracene}$), 132.6 (Cq-Ar$_{dipp}$), 130.8 (Cq$_{pyracene}$), 130.0 (CH-Ar$_{dipp}$), 124.6 (CH-Ar$_{dipp}$), 122.7 (CH$_{pyracene}$), 28.9 (CH$_{isop\ dipp}$),

25.3 ($CH_{2\ COD}$), 23.2 and 23.8 ppm ($CH_{3\ isop\ dipp}$). IR (KBr): 2054 ($\nu_{C=O}$), 1968 ($\nu_{C=O}$) cm^{-1}. Electrospray MS: *m*/*z* = 1433.1 $[M - Cl]^+$. Anal. calcd. for $C_{68}H_{78}N_4Cl_2Ir_2O_4$ (mol wt. 1468.5): C, 55.53; H, 5.35; N, 3.81. Found: C, 55.31; H, 5.21; N, 3.29.

5.3 Catalytic experiments

5.3.1 Catalytic experiments using 'Ru(η^6-arene)(NHC)' complexes

β-Alkylation of secondary alcohols with primary alcohols

The reaction was carried out with secondary alcohol (1 mmol), primary alcohol (1 mmol), the ruthenium complex (0.01 mmol) and KOH (1 mmol) in toluene (0.3 mL) at 110ºC. The reaction was monitored by ^1H NMR spectroscopy by introducing aliquots of the reacting solution in an NMR tube with 0.5 mL of $CDCl_3$. The evolution was determined by integration of the signals corresponding to the protons of the reactives and the products. The products of the catalytic experiments were identified according to previously reported spectroscopic data, 1,3-diphenyl-1-propanol and 1,3-diphenyl-1-propanone,[17] 1-phenyl-1-hexanol and 1-phenyl-1-hexanone,[17] 3-(3-chlorophenyl-1-penyl-1-propanol) and 3-(3-chlorophenyl-1-penyl-1-propanone),[18] 3-(4-chlorophenyl-1-penyl-1-propanol) and 3-(4-chlorophenyl-1-penyl-1-propanone)[18] and 1-phenyl-3-octanol.[19]

Oxidation and oxidative couplings

Catalytic oxidation of alcohols

A mixture of the alcohol (0.2 mmol) and the ruthenium complex (0.01 mmol) was refluxed in toluene (2 mL). The reaction mixture was analyzed by ^1H NMR spectroscopy, by introducing aliquots of the reacting solution in an NMR tube with 0.5 mL of $CDCl_3$. Hexamethylbenzene (0.033 mmol) was used in all cases as internal standard in order to determine conversions and yields. The products were identified comparing with commercially available samples (benzaldehyde, acetophenone,

phenylacetaldehyde, octanal, 4-nitrobenzaldehyde, 4-chlorobenzaldehyde, 2-chlorobenzaldehyde, 4-bromobenzaldehyde, p-tolualdehyde, and 4-methoxybenzaldehyde).

Oxidative homo-coupling of amines to form imines

A mixture of the amine (0.2 mmol) and the ruthenium complex (0.01 mmol) was heated in toluene (2 mL) to 150ºC in a thick-walled glass tube fitted with a Teflon cap. The evolution of the reaction was analyzed by ^{1}H NMR spectroscopy, by introducing aliquots of the reacting solution in an NMR tube with 0.5 mL of $CDCl_3$. Decane (0.2 mmol) was used as internal standard. The products were identified according to commercially available samples (N-benzylidenebenzylamine) or previously reported spectroscopic data (N-hexylidenehexylamine,[20] N-butylidenebutylamine[21] and N-(4-chlorobenzylidene)-4-chlorobenzylamine).[22]

Formation of Amides

A mixture of alcohol (0.2 mmol), amine (0.8 mmol), NaH (0.04 mmol), and the ruthenium complex (0.01 mmol) was refluxed in toluene (2 mL). The reaction mixture was analyzed by ^{1}H NMR spectroscopy, by introducing aliquots of the reacting solution in an NMR tube with 0.5 mL of $CDCl_3$. Hexamethylbenzene (0.033 mmol) was used as internal standard. The products were identified according to previously reported spectroscopic data, (N-benzylphenylacetamide, N-benzylbenzamide and N-hexylbenzamide).[23]

Dimerization of phenylacetylene

The reaction was carried out with phenylacetylene (0.3 mmol), the ruthenium complex (0.015 mmol) and Et_3N (0.075 mmol) in CD_3CN (0.3 mL) at 70ºC. The reaction was monitored by ^{1}H NMR spectroscopy, by introducing aliquots of the reacting solution in an NMR tube with 0.5 mL of $CDCl_3$. The evolution was determined by integration, using ferrocene as internal standard. The generated products were identified according to previously reported spectroscopic data, (*E*)-1,4-

diphenyl-1-buten-3-yne and (*E*)-1,4-diphenyl-1-buten-3-yne, 1,3,5-triphenylbenzene and 1,2,4-triphenylbenzene.[24]

Arylation of arylpyridines

Arylation of 2-phenylpyridine

The ruthenium complex (0.025 mmol) and KOAc (0.05 mmol) were stirred in NMP (2 mL) at room temperature in a thick-walled glass tube for 1 h. Then 2-phenylpyridine (0.5 mmol), Ar-X (1.25 mmol) and K_2CO_3 (1.50 mmol) were subsequently added. The resulting mixture was stirred at 120ºC. H_2O and EtOAc were added to the warm reaction mixture. The organic phase was dried with Na_2SO_4 and concentrated under vacuum. The remaining residue was purified by column chromatography on silica gel (hexanes/EtOAc mixture) to yield the corresponding *ortho*-arylated products. Yields and ratios were determined by ^{1}H NMR spectroscopy and by GC analyses using anisole (0.5 mmol) as internal standard. The products were identified according to previously reported spectroscopic data, 2-(2-phenyl)phenylpyridine and 2-(2,6-diphenyl)phenylpyridine,[25] 2-(2,6-di-*p*-methylphenyl)phenylpyridine, [25] 2-(2-*p*-methoxy phenyl)phenylpyridine and 2-(2,6-di-*p*-methoxyphenyl)phenylpyridine,[26] 2-(2-pyridin-3-yl)phenylpyridine and 2-(2,6-dipyridin-3-yl)phenylpyridine,[27] 2-(2-pyridin-2-yl)phenylpyridine and 2-(2,6-dipyridin-2-yl)phenylpyridine.[25]

2-(2,6-di-*p*-butylphenyl)phenylpyridine: ^{1}H NMR (300 MHz, $CDCl_3$): δ = 8.31 (d, $^3J_{H,H}$ =4.50 Hz, 1H), 7.44 (m, 3H), 7.29 (m, 1H), 6.97 (m, 8H), 6.88 (m, 2 H), 2.53 (t, $^3J_{H,H}$ = 7.65 Hz, 4H), 1.55 (m, 4H), 1.31 (m, 4H) and 0.91 ppm (t, $^3J_{H,H}$ = 7.35 Hz, 6H); ^{13}C{^{1}H} NMR (75 MHz, $CDCl_3$): δ = 148.6 (CH), 142.1 (Cq), 141.0 (Cq), 139.1 (CH), 134.5 (CH), 129.7 (CH), 129.5 (CH), 128.3 (Cq), 127.9 (CH), 127.1 (Cq), 120.9 (Cq), 35.4 (CH_2), 33.6 (CH_2), 22.5 (CH_2) and 14.1 ppm (CH_3).

Arylation of benzo[*h*]quinoline

KOAc (0.05 mmol) and the ruthenium complex (0.025 mmol) were stirred in NMP (2 mL) at room temperature in a thick-walled glass tube for 1 h. Then benzo[*h*]quinoline (0.5 mmol), Ar-X (0.75 mmol) and K_2CO_3 (1 mmol) were added. The resulting mixture was stirred at 120ºC. H_2O and EtOAc were added to the warm reaction mixture. The organic phase was dried with Na_2SO_4 and concentrated under vacuum. The remaining residue was purified by column chromatography on silica gel (hexanes/EtOAc mixture) to yield the monoarylated product. Yields and ratios were determined by ^{1}H NMR spectroscopy and by GC analysis using anisole (0.5 mmol) as internal standard. The products were identified according to previously reported spectroscopic data, 10-phenylbenzo[*h*]quinoline and 10-*p*-methylphenylbenzo[*h*]quinoline.[25]

Arylation of N-phenylpyrazole

KOAc (0.05 mmol) and the ruthenium complex (0.025 mmol) were stirred in NMP (2 mL) at room temperature in thick-walled glass tube for 1 h. Then N-phenylpyrazole (0.5 mmol), chlorobenzene (1.25 mmol) and K_2CO_3 (1.50 mmol) were added. The resulting mixture was stirred at 120ºC. H_2O and EtOAc were added to the warm reaction mixture. The organic phase was dried with Na_2SO_4 and concentrated under vacuum. The remaining residue was purified by column chromatography on silica gel (hexanes/EtOAc mixture) to yield the corresponding *ortho*-arylated products. Conversions were determined by ^{1}H NMR spectroscopy and by GC analyses using anisole (0.5 mmol) as internal standard. Product was identified according to previously reported spectroscopic data, 2-(2,6-diphenyl)phenylpyrazole.[28]

Hydrogen/deuterium exchange

A mixture of the substrate (0.5 mmol) and the ruthenium complex (0.025 mmol) in MeOH-d_4, was heated at 120ºC in a thick-walled glass tube fitted with a Teflon cap. At the desired reaction times, aliquots were extracted from the reaction vessel and added to an NMR tube with 0.5 mL of $CDCl_3$

5.3.2 Catalytic experiments using 'IrCp*(NHC)' complexes

Catalytic dehydrogenation of alcohols

A mixture of benzylalcohol or 1-phenylethanol (0.4 mmol), the iridium complex (0.02 mmol) and Cs_2CO_3 (0.08 mmol) was refluxed in toluene (1 mL) for 24 h. The reaction mixture was analyzed by ^{1}H NMR spectroscopy and the products were identified by comparison with the commercially available products, benzaldehyde and acetophenone.

Homo-coupling of alcohols

A mixture of alcohol (0.4 mmol), the iridium complex (0.004 mmol), silver triflate (0.012 mmol) and toluene-d_8 (200 μL) was heated at 110ºC in a thick-walled glass tube fitted with a Teflon cap. The reaction mixture was analyzed by ^{1}H NMR spectroscopy. Products were identified according to commercially available samples: dihexyl ether, dibutyl ether, and dodecyl ether.

Cross-coupling of alcohols and amines

Etherification of benzylalcohol with primary and secondary alcohols

A mixture of benzylalcohol (0.4 mmol), alkylating alcohol (2.0 mmol), the iridium complex (0.004 mmol) and silver triflate (0.012 mmol) was heated at 110ºC or 130ºC in a thick-walled glass tube fitted with a Teflon cap. The reaction mixture was analyzed by ^{1}H NMR spectroscopy, by introducing aliquots of the reacting solution in an NMR tube with 0.5 mL of $CDCl_3$. The generated products were identified according to commercially available samples (benzyl methyl ether, benzyl ethyl ether, benzyl butyl ether, benzyl hexyl ether, benzyl dodecyl ether, dibenzyl ether, allyl benzyl ether, and benzyl isopropyl ether) or previously reported spectroscopic data (benzyl cyclohexyl ether).[29] For the isolation of the products, the crude was extracted with dichloromethane and filtrated through a pad of Celite. The solvent was removed under vacuum, and the crude oil purified by column chromatography on silica gel using hexanes as eluent.

N-alkylation of aromatic amines with aliphatic amines

A mixture of aliphatic amine (0.2 mmol), aromatic amine (0.4 mmol), the iridium complex (0.01 or 0.004 mmol), silver triflate (0.03 or 0.012 mmol) and toluene-d_8 (200 µL) was heated at 150ºC in a thick-walled glass tube fitted with a Teflon cap. The reaction mixture was analyzed by ^{1}H NMR spectroscopy, by introducing aliquots of the reacting solution inside an NMR tube with 0.5 mL of $CDCl_3$. 1,3,5-trimethoxybenzene (10 mol %) was used in all cases as an internal standard in order to determine conversions and yields. The alkylated products were identified according to previously reported spectroscopic data: N-hexylaniline,[30] N-hexyl-4-methylaniline,[31] N-hexyl-2-methylaniline, [31] N-hexyl-2,4,6-trimethylaniline, [31] 4-fluoro-N-hexylaniline, [31] 4-chloro-N-hexylaniline, [31] N-hexyl-4-methoxyaniline, [31] N-benzylaniline,[32] N-cyclohexylaniline, [32] N-dodecylaniline,[33] N-cyclohexyl-2-methylaniline, [33] N-dodecyl-2-methylaniline, [33] and N-benzyl-2-methylaniline.[34] For the isolation of the products, the crude was filtered through a pad of Celite and the solvent removed under vacuum. The crude alkyl aryl amine product was purified by column chromatography on silica gel using hexanes as eluent.

N-alkylation of primary amines with alcohols

A mixture of alcohol (1.0 or 2.0 mmol), primary amine (0.2 mmol), the iridium complex (0.01 mmol) and silver triflate (0.03 mmol) was heated at 110ºC in a thick-walled glass tube fitted with a Teflon cap. The reaction mixture was analyzed by ^{1}H NMR spectroscopy, by introducing aliquots of the reacting solution inside an NMR tube with 0.5 mL of $CDCl_3$. 1,3,5-trimethoxybenzene (10 mol %) was used in all cases as an internal standard in order to determine conversions and yields. Products were identified according to commercially available samples (N-benzyl-*tert*-butylamine and dibenzylamine) or previously reported spectroscopic data, N-benzylidenebenzylamine,[35] N-benzyl-*n*-butylamine,[36] N,N'-di-*n*-butylbenzylamine,[36] N-hexyl-1-phenethylamine,[37] N-benzyl-1-phenethylamine,[35] and N-cyclohexyl-1-phenetylamine.[38] For the isolation of the products, the crude was extracted with

dichloromethane and filtrated through a pad of Celite. The solvent was removed under vacuum, and the crude solid purified by flash chromatography on silica gel using hexanes as eluent.

Functionalization of arenes

Benzylation of arenes with alcohols and ethers

A mixture of benzylating agent (1 mmol), arene (5 or 10 mmol), the iridium complex (0.01 or 0.001 mmol) and silver triflate (0.03 or 0.003 mmol) was heated at 110ºC in a thick-walled glass tube fitted with a Teflon cap. The reaction mixture was analysed by ^{1}H NMR spectroscopy, by introducing aliquots of the reacting solution inside an NMR tube with 0.5 mL of $CDCl_3$. The yields were calculated based on the amount of arene.

Benzylation of arenes with styrene derivates

A mixture of styrene derivative (1 mmol), arene (5 mmol), iridium complex (0.01 or 0.001 mmol) and silver triflate (0.03 or 0.003 mmol) was heated at 110ºC in a thick-walled glass tube fitted with a Teflon cap. The reaction mixture was analysed by ^{1}H NMR spectroscopy, by introducing aliquots of the reacting solution in an NMR tube with 0.5 mL of $CDCl_3$ and yields calculated based on the amount of arene. The benzylated arenes were identified according to previously reported spectroscopic data: 2- and 4-(methylphenyl) phenylmethane,[39] 2- and 4-(methoxyphenyl)phenylmethane,[40] diphenylmethane,[40] 2,3- and 3,4-(dimethylphenyl)phenylmethane,[40] 2,5-(dimethylphenyl)phenylmethane,[40] 1-methyl-2-(1-phenylethyl)benzene and 1-methyl-4-(1-phenylethyl)benzene,[41] 1-methoxy-2-(1-phenylethyl)benzene and 1-methoxy-4-(1-phenylethyl)benzene,[41] 1,4-dimethyl-2-(1-phenylethyl)benzene,[41] 2- and 4-(1-phenylethyl)phenol,[41] 1-chloro-4-(1-(2-methoxyphenyl)ethyl)benzene and 1-chloro-4-(1-(4-methoxyphenyl)ethyl)benzene,[41] 1-(2-methoxyphenyl)-1,2,3,4-tetrahydronaphthalene and 1-(4-methoxyphenyl)-1,2,3,4-tetrahydronaphthalene,[41] 1-(2-methoxyphenyl)-2,3-dihydro-1H-indene and 1-(4-methoxyphenyl)-2,3-dihydro-1H-indene.[41]

Benzylation of aniline derivates with styrene

A mixture of styrene (1 mmol), aniline derivative (5 mmol), the iridium complex (0.01 mmol) and silver triflate (0.03 mmol) was heated at 150ºC in a thick-walled glass tube fitted with a Teflon cap. The reaction mixture was analysed by ^{1}H NMR spectroscopy, by introducing aliquots of the reacting solution in an NMR tube with 0.5 mL of $CDCl_3$ and yields calculated based on the amount of arene. The products were identified according to previously reported spectroscopic data: 2-(1-phenylethyl)benzenamine and 4-(1-phenylethyl)benzenamine,[42] N-(1-phenylethyl)aniline,[43] 2-methyl-6-(1-phenylethyl)benzenamine and 2-methyl-4-(1-phenylethyl)benzenamine,[44] α-methyl-N-(2-methylphenyl)-benzenemethanamine,[45] 4-methyl-2-(1-phenylethyl)benzenamine, α-methyl-N-(4-methylphenyl)-benzenemethanamine, 4-fluoro-2-(1-phenylethyl)benzanamine and N-(4-fluorophenyl)-α-methyl-benzenemethanamine,[46] 4-chloro-2-(1-phenylethyl)benzanamine[44] and N-(4-chlorophenyl)-α-methyl-benzenemethanamine,[47] 4-methoxy-2-(1-phenylethyl)benzanamine[46] and N-(4-methoxyphenyl)-α-methyl-benzenemethanamine.[45]

Tandem reaction: Transfer hydrogenation and benzylation of arenes

A mixture of benzylating agent (1 mmol), anisole (10 mmol), *i*PrOH (1.5 mmol), the iridium complex (0.01 mmol) and silver triflate (0.03 mmol) was heated at 110ºC in a thick-walled glass tube fitted with a Teflon cap. The reaction mixture was analysed by ^{1}H NMR spectroscopy, by introducing aliquots of the reacting solution inside an NMR tube with 0.5 mL of $CDCl_3$ and yields calculated based on the amount of arene.

5.4 Determination of the kinetic isotopic effect (KIE)

5.4.1 Determination of the kinetic isotopic effect (KIE) for the arylation of 2-phenylpyirine

The reaction was carried out in the same manner as described for the arylation of 2-phenylpyridine reaction. Two sets of reactions were carried out in a parallel manner; 2-phenylpyridine and 2-phenylpyridine-d_2 were reacted with chlorobenzene under the optimized conditions. At the desired times, aliquots were extracted from the reaction vessel and analysed by GC using anisole as internal standard.

Table 5.5 Arylation of 2-phenylpyridine and 2-phenylpyridine-d_2 with chlorobenzene using **3B**

Entry	t (minutes)	2-phenylpyridine Conv.(%)	2-phenylpyridine-d_2 Conv.(%)
1	0	0	0
2	20	15	30
3	40	25	42
4	60	33	51
5	80	39	60
6	110	46	67
7	130	52	71

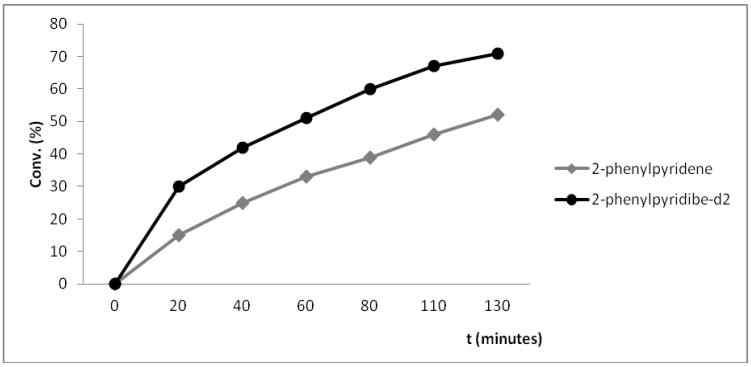

Figure 5.11 Reaction profiles for the arylation of 2-phenylpyridine and 2-phenylpyridine-d_2 with chlorobenzene using **3B**. KIE = k_H/k_D = 0.46

5.4.2 Determination of the kinetic isotopic effect (KIE) for benzo[*h*]quinoline

Two sets of reactions were carried out in a parallel manner, benzo[*h*]quinoline and benzo[*h*]quinoline-*d* were reacted with chlorobenzene under the optimized conditions. At the desired times, aliquots were extracted from the reaction vessel and analysed by GC using anisole as internal standard.

Table 5.6 Arylation of benzo[*h*]quinoline and benzo[*h*]quinoline-*d* with chlorobenzene using **3B**

Entry	t (minutes)	benzo[*h*]quinoline Conv. (%)	benzo[*h*]quinoline-*d* Conv. (%)
1	0	0	0
2	20	27	36
3	40	365	45
4	60	43	50
5	80	46	56
6	110	48	60
7	140	50	62

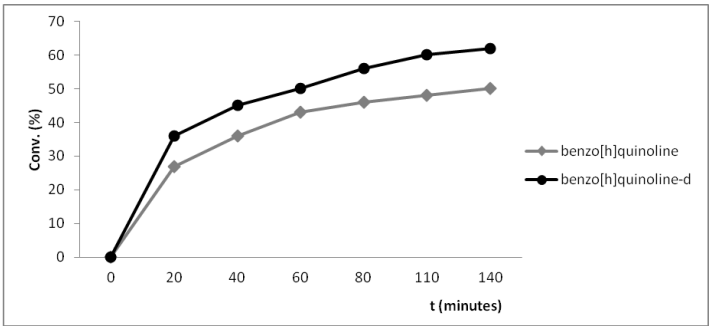

Figure 5.12 Reaction profiles for the arylation of benzo[*h*]quinoline and benzo[*h*]quinoline-*d* with chlorobenzene using **3B**. KIE = k_H/k_D = 0.43

5.5 Reaction of imidazolidines with metal dimers

$[IrCp^*Cl_2]_2$ (1 equiv) and **H**H2 (2 equiv) were placed together in an NMR tube and dissolved in CD_3CN (0.5 mL). A dark precipitate of $[IrCp^*(\mu\text{-}H)Cl]_2$ immediately appeared. The reaction quantitatively afforded the di-μ-hydrido complex and the corresponding azolium salt [**H**H]Cl after five minutes. The total conversion of the amine into [**H**H]Cl was corroborated by ^1H NMR spectroscopy using anisole as internal standard. The spectroscopic data of [**H**H]Cl is in agreement with those reported in the literature.[48] The black solid so formed was separated and redissolved in CD_2Cl_2 and its spectroscopic data compared to those reported in the literature for $[IrCp^*(\mu\text{-}H)Cl]_2$,[49] showing complete agreement.

5.6 X-Ray Diffraction

Single crystals were obtained mainly by slow diffusion of a mixture of solvents and evaporation to dryness. They were mounted on a glass fiber in a random orientation. Data collection was performed at room temperature on a Siemens Smart CCD diffractometer using graphite-monochromated Mo KR radiation (λ=0.71073Å) with a nominal crystal to detector distance of 4.0 cm. Space group assignment was based on systematic absences, E statistics, and successful refinement of the structure. The

structure was solved by direct methods with the aid of successive difference Fourier maps and was refined using the SHELXTL 6.1 software package.[50] All non-hydrogen atoms were refined anisotropically. Hydrogen atoms were assigned to ideal positions and refined using a riding model. The diffraction frames were integrated using the SAINT package.[51]

Table 5.7 Structural parameters, register conditions and refinement for **8E** and **9F**

Parameter	**Complex 8E**	**Complex 9F**
Empirical formula	$C_{21}H_{26}Cl_2N_2Ru$	$C_{14}H_{22}Cl_2N_2Ru$
Formula weight	478.42	402.31
Temperature/K	298	298
Crystal system	orthorhombic	monoclinic
Space group	$Pna2_1$	$P2_1/c$
a/Å	14.5949(5)	14.2961(17)
b/Å	10.8530(4)	7.0647(9)
c/Å	26.1994(9)	16.3109(19)
α/°	90.00	90.00
β/°	90.00	92.052(3)
γ/°	90.00	90.00
Volume/Å^3	4149.9(3)	1646.3(3)
Z	4	4
ρ_{calc} (mg/mm^3)	1.531	1.746
Absorption coefficient (mm^{-1})	1.020	1.040
Reflections collected	10295	10295
Goodness-of-fit on F^2	1.022	1.022
R_1	0.0827	0.0827
wR_2	0.0973	0.0973

Table 5.8 Structural parameters, register conditions and refinement for **22I** and **23I**

Parameter	**Complex 22I**	**Complex 23I**
Empirical formula	$C_{40}H_{42}ClIrN_4$	$C_{39}H_{40}ClN_4Rh$
Formula weight	806.43	703.11
Temperature/K	571(2)	571(2)
Crystal system	monoclinic	triclinic
Space group	$P2_1/c$	P-1
a/Å	15.8306(6)	13.598(2)
b/Å	17.2949(6)	15.521(2)
c/Å	14.8871(5)	15.893(2)
α/°	90.00	90.03(2)
β/°	118.0450(10)	101.599(4)
γ/°	90.00	90.050(10)
Volume/$Å^3$	3597.3(2)	3285.8(9)
Z	4	4
ρ_{calc} (mg/mm^3)	1.489	1.421
Absorption coefficient (mm^{-1})	3.819	0.635
Reflections collected	24411	22785
Goodness-of-fit on F^2	1.146	1.024
R_1	0.0624	0.0741
wR_2	0.1092	0.1136

Table 5.9 Structural parameters, register conditions and refinement for **24I** and **31I**

Parameter	**Complex 24I**	**Complex 31I**
Empirical formula	$C_{54}H_{68}Cl_2Ir_2N_4$	$C_{83}H_{100}F_{12}Ir_2N_{14}O_2P_2$
Formula weight	1228.42	2000.11
Temperature/K	842(2)	446(2)
Crystal system	monoclinic	triclinic
Space group	$P2_1/n$	P-1
a/Å	11.5423(7)	16.310(2)
b/Å	14.0943(9)	16.787(2)
c/Å	30.8140(19)	19.003(3)
α/°	90.00	65.091(2)
β/°	94.282(2)	70.349(2)
γ/°	90.00	66.795(2)
Volume/Å^3	4998.8(5)	4245.7(10)
Z	4	2
ρ_{calc} (mg/mm^3)	1.632	1.565
Absorption coefficient (mm^{-1})	5.465	3.250
Reflections collected	33816	42830
Goodness-of-fit on F^2	0.931	0.935
R_1	0.0722	0.0987
wR_2	0.1434	0.1404

Table 5. 10 Structural parameters, register conditions and refinement for **32J**

Parameter	**Complex 32J**
Empirical formula	$C_{84}H_{100}Cl_{14}N_4Rh_2$
Formula weight	1867.80
Temperature/K	566(2)
Crystal system	monoclinic
Space group	$P2_1/n$
a/Å	18.8621(4)
b/Å	13.8228(3)
c/Å	18.8523(5)
α/°	90.00
β/°	113.389(3)
γ/°	90.00
Volume/Å^3	4511.43(19)
Z	2
ρ_{calc} (mg/mm^3)	1.375
Absorption coefficient (mm^{-1})	3.250
Reflections collected	26996
Goodness-of-fit on F^2	1.060
R_1	0.1127
wR_2	0.1760

5.7 References

(1) Bennett, M. A.; Smith, A. K. *J. Chem. Soc.-Dalton Trans.* **1974**, 233.

(2) Bennett, M. A.; Huang, T. N.; Matheson, T. W.; Smith, A. K. *Inorg. Synth.* **1982**, *21*, 74.

(3) Melchart, M.; Habtemariam, A.; Novakova, O.; Moggach, S. A.; Fabbiani, F. P. A.; Parsons, S.; Brabec, V.; Sadler, P. J. *Inorg. Chem.* **2007**, *46*, 8950.

(4) Ball, R. G.; Graham, W. A. G.; Heinekey, D. M.; Hoyano, J. K.; McMaster, A. D.; Mattson, B. M.; Michel, S. T. *Inorg. Chem.* **1990**, *29*, 2023.

(5) Komiya, S., *Synthesis of Organometallic Compounds. A Practical Guide.* ed.; Wiley: 1997.

(6) Giordano, G.; Crabtree, R. H. *Inorg. Synth.* **1990**, *28*, 88.

(7) Abel, E. W.; Bennett, M. A.; Wilkinson, G. *J. Chem. Soc.* **1959**, 3178.

(8) Sala, A.; Ferrario, F.; Rizzi, E.; Catinella, S.; Traldi, P. *Rapid Commun. Mass Spectrom.* **1992**, *6*, 388.

(9) Ricciardi, F.; Romanchick, W. A.; Joullie, M. M. *J. Polym. Sci. Pol. Chem.* **1983**, *21*, 1475.

(10) Kocher, C.; Herrmann, W. A. *J. Organomet. Chem.* **1997**, *532*, 261.

(11) Lambert, J. B.; Huseland, D. E.; Wang, G. T. *Synthesis* **1986**, 657.

(12) Nielsen, A. T.; Nissan, R. A.; Chafin, A. P.; Gilardi, R. D.; George, C. F. *J. Org. Chem.* **1992**, *57*, 6756.

(13) Herrmann, W. A.; Elison, M.; Fischer, J.; Kocher, C.; Artus, G. R. J. *Chem.-Eur. J.* **1996**, *2*, 772.

(14) Mercs, L.; Neels, A.; Albrecht, M. *Dalton Trans.* **2008**, 5570.

(15) Corberan, R.; Sanau, M.; Peris, E. *J. Am. Chem. Soc.* **2006**, *128*, 3974.

(16) Viciano, M.; Feliz, M.; Corberan, R.; Mata, J. A.; Clot, E.; Peris, E. *Organometallics* **2007**, *26*, 5304.

(17) Fujita, K.; Asai, C.; Yamaguchi, T.; Hanasaka, F.; Yamaguchi, R. *Org. Lett.* **2005**, *7*, 4017.

(18) Martinez, R.; Ramon, D. J.; Yus, M. *Tetrahedron* **2006**, *62*, 8982.

(19) Martinez, R.; Ramon, D. J.; Yus, M. *Tetrahedron* **2006**, *62*, 8988.

(20) Gnanaprakasam, B.; Zhang, J.; Milstein, D. *Angew. Chem. Int. Ed.* **2010**, *49*, 1468.

(21) Bailey, P. S.; Carter, T. P.; Southwic.Lm *J. Org. Chem.* **1972**, *37*, 2997.

(22) Kodama, S.; Yoshida, J.; Nomoto, A.; Ueta, Y.; Yano, S.; Ueshima, M.; Ogawa, A. *Tetrahedron Lett.* **2010**, *51*, 2450.

(23) Muthaiah, S.; Ghosh, S. C.; Jee, J. E.; Chen, C.; Zhang, J.; Hong, S. H. *J. Org. Chem.* **2010**, *75*, 3002.

(24) Daniels, M.; Kirss, R. U. *J. Organomet. Chem.* **2007**, *692*, 1716.

(25) Oi, S.; Fukita, S.; Hirata, N.; Watanuki, N.; Miyano, S.; Inoue, Y. *Org. Lett.* **2001**, *3*, 2579.

(26) Ackermann, L. *Org. Lett.* **2005**, *7*, 3123.

(27) Oi, S.; Funayama, R.; Hattori, T.; Inoue, Y. *Tetrahedron* **2008**, *64*, 6051.

(28) Kim, M.; Kwak, J.; Chang, S. *Angew. Chem. Int. Ed.* **2009**, *48*, 8935.

(29) Sassaman, M. B.; Kotian, K. D.; Prakash, G. K. S.; Olah, G. A. *J. Org. Chem.* **1987**, *52*, 4314.

(30) Byun, E.; Hong, B.; De Castro, K. A.; Lim, M.; Rhee, H. *J. Org. Chem.* **2007**, *72*, 9815.

(31) Hollmann, D.; Bahn, S.; Tillack, A.; Beller, M. *Chem. Commun.* **2008**, 3199.

(32) Fujita, K. I.; Enoki, Y.; Yamaguchi, R. *Tetrahedron* **2008**, *64*, 1943.

(33) Li, J.; Cui, M.; Yu, A.; Wu, Y. *J. Organomet. Chem.* **2007**, *692*, 3732.

(34) Lai, R. Y.; Lee, C. I.; Liu, S. T. *Tetrahedron* **2008**, *64*, 1213.

(35) Blackburn, L.; Taylor, R. J. K. *Org. Lett.* **2001**, *3*, 1637.

(36) Salvatore, R. N.; Nagle, A. S.; Jung, K. W. *J. Org. Chem.* **2002**, *67*, 674.

(37) Johansson, A.; Abrahamsson, P.; Davidsson, O. *Tetrahedron-Asymmetry* **2003**, *14*, 1261.

(38) Ranu, B. C.; Majee, A.; Sarkar, A. *J. Org. Chem.* **1998**, *63*, 370.

(39) Podder, S.; Roy, S. *Tetrahedron* **2007**, *63*, 9146.

(40) Sun, H. B.; Li, B.; Chen, S.; Li, J.; Hua, R. *Tetrahedron* **2007**, *63*, 10185.

(41) Rueping, M.; Nachtsheim, B. J.; Scheidt, T. *Org. Lett.* **2006**, *8*, 3717.

(42) Marcsekova, K.; Doye, S. *Synthesis-Stuttgart* **2007**, 145.

(43) Kawakami, T.; Sugimoto, T.; Shibata, I.; Baba, A.; Matsuda, H.; Sonoda, N. *J. Org. Chem.* **1995**, *60*, 2677.

(44) Babu, N. S.; Reddy, K. M.; Prasad, P. S. S.; Suryanarayana, I.; Lingaiah, N. *Tetrahedron Lett.* **2007**, *48*, 7642.

(45) Kawatsura, M.; Hartwig, J. F. *J. Am. Chem. Soc.* **2000**, *122*, 9546.

(46) Beller, M.; Thiel, O. R.; Trauthwein, H. *Synlett* **1999**, 243.

(47) Suwa, T.; Sugiyama, E.; Shibata, I.; Baba, A. *Synthesis-Stuttgart* **2000**, 789.

(48) Caterina, M. C.; Figueroa, M. A.; Perillo, I. A.; Salerno, A. *Heterocycles* **2006**, *68*, 701.

(49) Jiang, B.; Feng, Y.; Ison, E. A. *J. Am. Chem. Soc.* **2008**, *130*, 14462.

(50) Sheldrick, G. M., *SHELXTL, version 6.1, Bruker AXS, Inc*. ed.; Madison, WI, 2000.

(51) *SAINT, Bruker Analytical X-ray System, version 5.0*. ed.; Madison, WI, 1998.

Chapter 6

Catalizadores multifuncionales de Ru, Ir y Rh con ligandos NHC en procesos de activación de enlaces C-H

En aplicación de la normativa de estudios de doctorado sobre la elaboración de Tesis Doctorales según el programa RD 99/2011, por la que se establece que: la Tesis Doctoral escrita en una lengua diferente del valenciano o del castellano, en el momento de ser depositada, debe contener un apartado suficientemente amplio en una de estas dos lenguas, y debe formar parte de la encuadernación de la tesis; el siguiente capítulo contiene un resumen en castellano del trabajo recogido en la presente Tesis Doctoral.

6.1 Introducción

6.1.1 Carbenos N-heterocíclicos

La versatilidad de los ligandos de tipo carbeno N-heterocíclico (NHC) junto a la fácil preparación de sus precursores (normalmente sales de azolio), han permitido diseñar una gran variedad de topologías y formas de coordinación. Junto a los ligandos NHC más utilizados, imidazol-2-ilidenos, se ha desarrollado una amplia variedad de ligandos NHC con propiedades electrónicas y estéricas muy diferentes.[1-2] A continuación, se incluye una breve reseña de los cuatro tipos de ligandos NHC que se han empleado en el desarrollo de esta Tesis Doctoral: imidazol-2-ilidenos, imidazol-4-ilidenos, pirazol-3-ilidenos y 1,2,3-triazol-4-ilidenos.

Los imidazolilidenos, normalmente, se coordinan al metal por la posición C2 (imidazol-2-ilidenos o *normal*-NHC, Esquema 6.1). Hasta hace poco más de una década, se consideraba que esta era la única posición de coordinación ya que la activación del enlace C(2)-H debería estar siempre favorecida al ser ésta la posición más ácida. En 2001, Crabtree y colaboradores describieron el primer ligando NHC coordinado a través de la posición C4 (imidazol-4-ilidenos o *abnormal*-NHC, Esquema 6.1).[3] A este nuevo tipo de coordinación se le conoce por el término inglés *abnormal-NHC* (*a*NHC), que hace referencia a su carácter inusual. Que se produzca este tipo de coordinación depende de varios factores como la naturaleza del

contraanión de la sal de imidazolio precursora,[4] los grupos N-alquílicos[5] o el disolvente empleado en la reacción.[6]

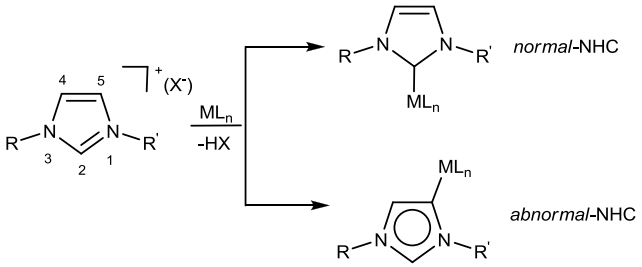

Esquema 6.1

Actualmente existen muchos ejemplos de este tipo de coordinación a diferentes metales de transición como Pd, Rh, Ir, Ru, etc.[7] El estudio de las frecuencias de vibración de ligandos carbonilo en compuestos de Ir(I)-NHC, permitió al mismo grupo de investigación observar que los ligandos *a*NHC son más dadores-σ que sus análogos coordinados a través del C2 (imidazol-2-ilidenos).[8]

Sherer y colaboradores llevaron a cabo estudios teóricos con carbenos de tipo pirazol-3-ilideno (Esquema 6.2) utilizando compuestos de $Cr(CO)_5$.[9] Este estudio concluyó que, al igual que los *a*NHC, los ligandos pirazolilideno son más dadores-σ que los ligandos imidazol-2-ilidenos. Posiblemente, esta mayor capacidad dadora-σ se debe a efectos inductivos, ya que en las posiciones adyacentes al carbeno hay un único átomo de nitrógeno, a diferencia de lo que ocurre en ligandos imidazol-2-ilideno. Asimismo, la acidez del C(3)-H es menor que la posición C(2)-H en sales de imidazolio. En la actualidad, los pocos ejemplos de complejos con ligandos de tipo pirazolilideno, se refieren a algunos complejos de Cr y Mo,[10] Rh,[11-12] Pd,[13] Cu,[14] Fe[15] y Au.[16]

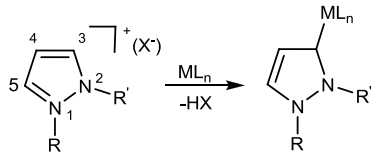

Esquema 6.2

Con el objetivo de ampliar la familia de ligandos *a*NHC o carbenos mesoiónicos,[17] Albrecht y colaboradores describieron la síntesis de carbenos tipo 1,2,3-triazolilideno.[18] Este tipo de ligando ha sido coordinado a diferentes metales como Ag, Rh, Ir, Ru y Pd (Esquema 6.3).[18-19]

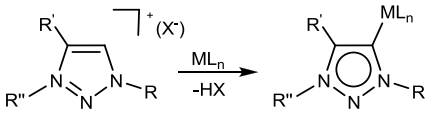

Esquema 6.3

Los estudios de frecuencias de vibración de ligandos carbonilo en compuestos de Ir(I) con 1,2,3-triazolilideno, indicaron que estos ligandos son más dadores-σ que los ligandos imidazol-2-ilideno.[18]

Cálculos DFT llevados a cabo por el Prof. Gusev describen las propiedades electrón-dadoras y estéricas de un grupo de NHCs.[20] Este estudio proporcionó una serie de valores TEP (Parámetros Electrónicos de Tolman) para un gran grupo de diferentes NHCs. Si observamos los valores TEP de carbenos similares a los descritos anteriormente, los carbenos tipo imidazol-2-ilidenos presentan valores de TEP más elevados que carbenos tipo imidazol-4-ilidenos, pirazol-3-ilidenos y 1,2,3-triazol-4-ilidenos, implicando que la capacidad electrón-dadora de estos ligandos es menor (Figura 6.1).

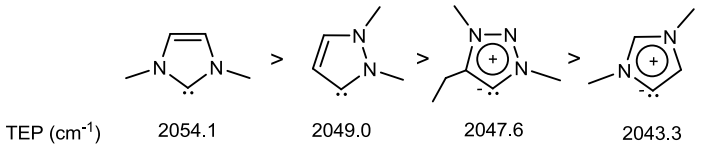

Figura 6.1 Valores TEP de una serie de NHCs

En el trabajo de investigación destinado al desarrollo de esta Tesis Doctoral, además de estudiar la capacidad coordinativa de ligandos mono-NHC nos hemos interesado en el diseño y coordinación de ligandos bis-NHC. La mayoría de los ligandos bis-NHC que podemos encontrar en la bibliografía han sido diseñados para coordinarse a un único metal en forma quelato[21] o *pinza*.[22-23] Sin embargo, el diseño de ligandos bis-NHC que actúen como puente entre dos fragmentos metálicos es de gran interés, [24-25] puesto que permite la obtención de estructuras dimetálicas con las que se podrían lograr nuevos avances en el desarrollo de materiales electrónicos.[26] En este sentido, Bielawski y colaboradores, prepararon una serie de ligandos benzobis(imidazolilideno) que permiten su coordinación a dos centros metálicos. Esta forma de coordinación sitúa a ambos centros metálicos en una orientación opuesta en cada cara del ligando (**6.1**, Figura 6.2). En atención a este tipo de coordinación, a este tipo de ligando se le llama *Janus-Head*, en referencia a la similitud con el dios romano Jano.[26-27] En este contexto, el ligando 1,2,4-trimetiltriazol-di-ilideno (al que llamamos comúnmente *ditz*) es mucho más simple y también puede actuar como puente entre dos centros metálicos (**6.2**, Figura 6.2). [28] Durante los últimos años, nuestro grupo de investigación ha demostrado el extraordinario potencial de este ligando. En particular, se han preparado compuestos homo-[29, 30] y hetero-dimetálicos[29, 31] con el ligando *ditz* lo que ha permitido estudiar su actividad catalítica en procesos tándem en los que cada metal está implicado en una reacción distinta.

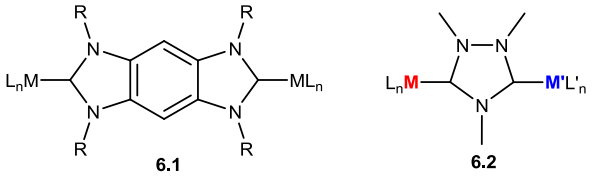

Figura 6.2

6.1.2 Propiedades catalíticas

Los ligandos NHC han atraído un gran interés debido principalmente a su uso en el diseño de catalizadores homogéneos. En los últimos años, se ha descrito un elevado número de aplicaciones catalíticas de compuestos metálicos con ligandos NHC. Estas propiedades catalíticas han sido recogidas en diferentes artículos de revisión.[1, 21-22, 32]

En numerosas ocasiones, se ha relacionado la actividad de un catalizador en procesos de activación de enlaces C-H, con la capacidad electrón-dadora de sus ligandos.[33] Conectando con este hecho, y aprovechando la elevada basicidad de los NHCs, los compuestos con NHCs han sido utilizados en procesos catalíticos que implican la activación de enlaces C-H. Durante esta Tesis Doctoral hemos centrado nuestro interés principalmente en aquellos procesos catalíticos que transcurren a través de un mecanismo de *"préstamo de hidrógeno"*, conocidos más habitualmente por el término inglés *borrowing-hydrogen*, y en la activación C-H de arilpiridinas y arenos.

6.1.2.1 Procesos tipo *borrowing-hydrogen*

Lejos de constituir una única reacción química, los procesos catalíticos englobados bajo el término "*borrowing-hydrogen"* constituyen un amplio abanico de reacciones en las que el nexo común lo determina la intermediación de un catalizador que sirve como transportador de hidrógeno entre un par de sustratos (Esquema 6.4).[34, 35]

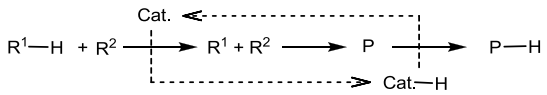

Esquema 6.4

En una reacción típica de *borrowing-hydrogen* se produce la oxidación de un sustrato, normalmente un alcohol (o una amina), por un catalizador metálico que 'toma prestado' dos átomos de hidrógeno. Dependiendo de que el alcohol sea primario o secundario, se generará un aldehído o una cetona, respectivamente. Estos compuestos de carbonilo pueden sufrir una amplia gama de transformaciones ya que pueden

reaccionar *in situ* para dar iminas, alquenos y compuestos de carbonilo funcionalizados. El catalizador metálico, que había tomado prestado el hidrógeno, lo 'devuelve' al nuevo compuesto, produciendo su reducción. Estos procesos catalíticos cumplen el principio de Economía Atómica ya que, normalmente, todos los átomos de los sustratos aparecen en los productos o, como máximo, el único subproducto obtenido es H_2O o NH_3, por lo que se consideran procesos que contribuyen a la química verde.

Este tipo de reacciones facilita el acceso a una amplia variedad de moléculas orgánicas siendo los productos obtenidos, principalmente, alcoholes y aminas, sustancias muy valiosas para la obtención de fármacos de elevado interés para el sector industrial.

6.1.2.2 Activación C-H de arilpiridinas y arenos

Los métodos tradicionales para la formación de nuevos enlaces C-C suponen el empleo de cantidades equimolares de agentes organometálicos. En los últimos años, han aparecido nuevas alternativas para la funcionalización de enlaces C-H catalizadas por metales en las que las condiciones de reacción son mucho más suaves.[36] Por ejemplo, en la bencilación de arenos, el uso de haluros de bencilo como agentes bencilantes es muy perjudicial desde el punto de vista medioambiental. En los últimos años el uso de alcoholes,[37] acetatos[38] o estirenos[39] como agentes bencilantes ha aumentado, permitiendo llevar a cabo estas reacciones en condiciones de reacción mucho más suaves. De la misma forma, tradicionalmente la arilación de arilpiridinas supone el uso de materiales de partida caros y difíciles de sintetizar. Recientemente, el uso de catalizadores de paladio ha permitido usar materiales más baratos y fáciles de conseguir.[40]

6.2 Objetivos de la investigación

El objeto de estudio de esta Tesis Doctoral es la obtención y caracterización de nuevos complejos metálicos con diferentes ligandos del tipo carbeno N-heterocíclico (NHC), el estudio de sus patrones de reactividad y la exploración de sus propiedades catalíticas en procesos donde el uso de los nuevos compuestos pueda aportar una importante mejora. Los objetivos concretos pueden dividirse en los siguientes puntos:

- Síntesis de una serie de sales de azolio precursoras de ligandos N-heterocíclicos de tipo monocarbeno y su coordinación a $[RuCl_2(\eta^6\text{-areno})]_2$ e $[IrCp^*Cl_2]_2$.
- Evaluación de las propiedades catalíticas de los compuestos obtenidos en reacciones de activación de enlaces C-H gobernadas por procesos tipo *borrowing-hydrogen*, y en reacciones de funcionalización de arenos y arilpiridinas.
- Desarrollo de nuevas estrategias de metalación para la obtención de compuestos dimetálicos con ligandos bis-NHC que actúen como puente entre los dos centros metálicos.

6.3 Discusión de Resultados

En este apartado se van a presentar y discutir los resultados obtenidos en relación a los objetivos que se han planteado.

6.3.1 Síntesis de compuestos 'Ru(η^6-areno)(NHC)' e 'IrCp*(NHC)'

El Esquema 6.5 muestra las diferentes sales precursoras de los ligandos NHC que han sido empleadas. Las sales de imidazolio [**A**H]I,[41] [**B**H]I[42] y [**D**H]I[43] y la sal de pirazolio [**F**H]I[11] han sido previamente descritas en la bibliografía, mientras que, las sales de imidazolio [**C**H]I y [**E**H]I y la sal de triazolio [**G**H]I se han sintetizado y caracterizado, por primera vez, a lo largo del trabajo de investigación que se presenta.

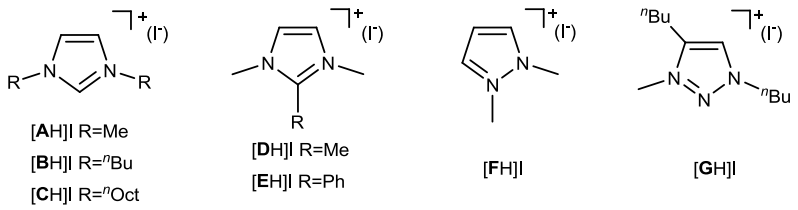

Esquema 6.5 Sales precursoras de los ligandos NHC

Las sales de azolio que muestra el esquema generan ligandos NHC con propiedades electrónicas diferentes.[20, 44] A partir de estas sales se han obtenido carbenos imidazolilideno coordinados por la posición C2 (*normal*-NHC, **A**, **B** y **C**) y por la posición C4 ó C5 (*abnormal*-NHC, **D** y **E**), carbenos de tipo pirazolilideno (**F**) y de tipo triazolilideno (**G**). La elección de los ligandos mencionados nos permitió evaluar cómo influye la capacidad dadora-σ de éstos en la actividad catalítica de los compuestos que los contienen.

6.3.1.1 Síntesis de compuestos tipo 'Ru(η^6-areno)(NHC)'

En primer lugar, obtuvimos una serie de complejos de tipo 'Ru(η^6-areno)(NHC)' (Esquema 6.6) empleando diferentes estrategias de metalación. El uso de tres ligandos η^6-areno diferentes (*p*-cimeno, hexametilbenceno y metilbenzoato), y diferentes

ligandos NHC, nos pareció una buena elección para la modificación de las propiedades electrónicas y estéricas de los complejos.

Principalmente se han empleado dos estrategias de metalación diferentes: la desprotonación de la sal de azolio mediante un exceso de base débil y la transmetalación a partir de complejos de Ag(I)-NHC. El siguiente esquema ilustra los complejos de tipo 'Ru(η^6-areno)(NHC) preparados:

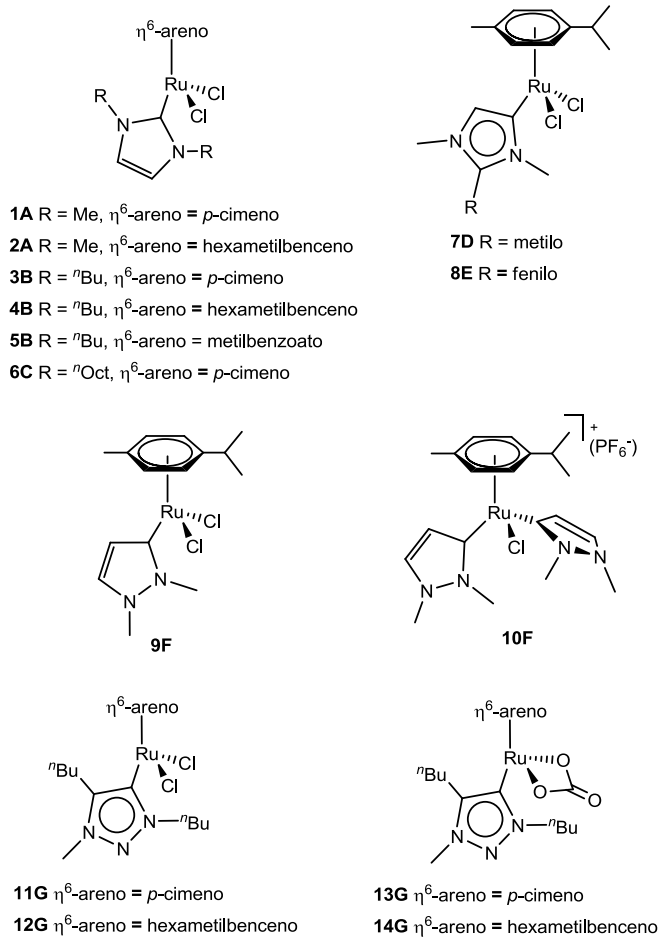

Esquema 6.6 Complejos de tipo 'Ru(η^6-areno)(NHC)' sintetizados

La síntesis del compuesto **1A** está descrita en la bibliografía,[24] sin embargo se preparó empleando una metodología distinta. Los compuestos **1A** y **2A** se obtuvieron según el

procedimiento que muestra el Esquema 6.7, haciendo reaccionar la sal de imidazolio [**A**H]I con $[RuCl_2(p\text{-cimeno})]_2$ o $[RuCl_2(CMe_6)]_2$ en acetonitrilo, en presencia de un exceso de Cs_2CO_3.

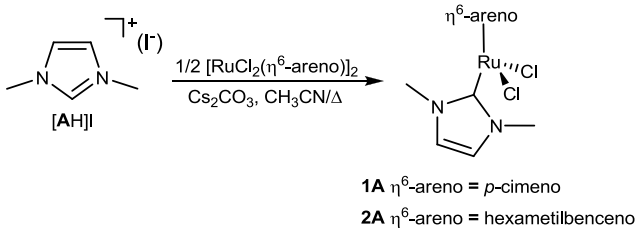

Esquema 6.7 Síntesis de **1A** y **2A**

La coordinación a Ru(II) del resto de ligandos se llevó a cabo empleando una estrategia de metalación diferente. El carbeno derivado de la sal de azolio se coordinó a Ru mediante transmetalación a partir del correspondiente carbeno de Ag(I). Mientras la síntesis del compuesto **3B** está descrita en la bibliografía,[45] el resto de complejos, **4B**, **5B**, **6C**, **7D**, **8E**, **9F**, **10F**, **11G** y **12G** se han sintetizado y caracterizado por primera vez. El Esquema 6.8 muestra la síntesis de los compuestos **3B**, **4B** y **5B**. Los complejos **13G** y **14G** fueron sintetizados a partir de **11G** y **12G**, respectivamente, sustituyendo los ligandos cloro por un ligando carbonato.

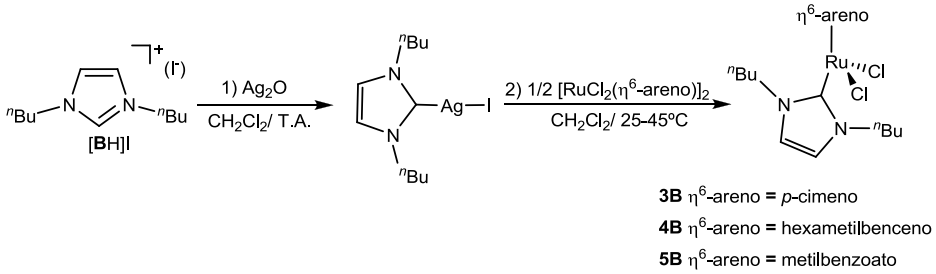

Esquema 6.8 Síntesis de **3B**, **4B** y **5B**

6.3.1.2 Síntesis de compuestos tipo 'IrCp*(NHC)'

Al igual que muchos de los compuestos de Ru(II) descritos anteriormente, los compuestos tipo 'IrCp*(NHC)' mostrados en el Esquema 6.9 fueron sintetizados mediante transmetalación a partir de los correspondientes carbenos de plata.

Mientras que la síntesis de los compuestos **15B**[46] y **16D**[47] ha sido previamente descrita en la bibliografía, el complejo **17F** se ha sintetizado y caracterizado, por primera vez, a lo largo del trabajo de investigación que se presenta.

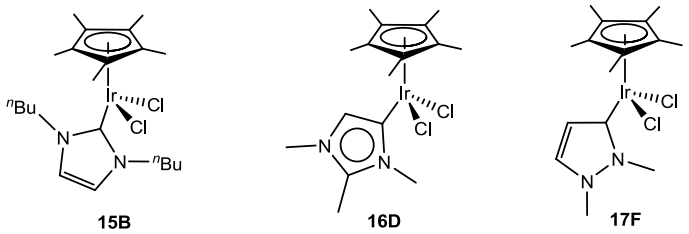

Esquema 6.9 Complejos de tipo 'IrCp*(NHC)' sintetizados

Como muestra el Esquema 6.10, el compuesto **17F** se obtuvo haciendo reaccionar la sal de pyrazolio [**F**H]I con Ag_2O a temperatura ambiente. El compuesto de Ag(I)-NHC generado se hizo reaccionar *in situ* con $[IrCp^*Cl_2]_2$ calentando la mezcla de reacción a reflujo.

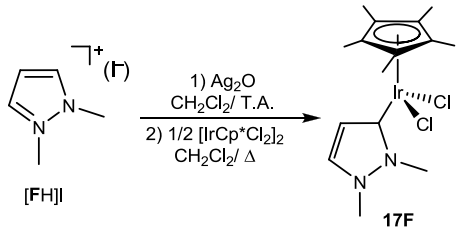

Esquema 6.10 Síntesis de **17F**

Las nuevas sales de azolio y los nuevos compuestos metálicos de Ru(II) e Ir(III) descritos en esta sección han sido caracterizados por espectroscopia de RMN y masas y por análisis elemental. Las estructuras moleculares de los compuestos **8E**, **9F** y **12G** han sido confirmadas mediante Difracción de Rayos X (DRX) sobre monocristal.

6.3.2 Aplicaciones catalíticas

Con el fin de evaluar las propiedades catalíticas de los complejos preparados en el apartado anterior, decidimos emplearlos en reacciones de activación C-H típicamente catalizadas por compuestos de Ru(II) e Ir(III).

Esta sección se divide en dos apartados que recogen los resultados catalíticos al emplear compuestos de tipo 'Ru(η^6-areno)(NHC)' e 'IrCp*(NHC)', respectivamente**.**

6.3.2.1 Actividad catalítica de compuestos tipo 'Ru(η^6-areno)(NHC)'

Como indicamos con detalle a continuación, los compuestos de Ru(II) descritos han mostrado elevada actividad en:

Procesos tipo *borrowing-hydrogen*:

a) β-Alquilación de alcoholes secundarios con alcoholes primarios
b) Oxidación y acoplamientos oxidativos
   b.1) Oxidación de alcoholes y aminas
   b.2) Formación de amidas a partir de aminas y alcoholes

Otros procesos de activación C-H:

c) Dimerización de fenilacetileno
d) Arilación y deuteración de arilpiridinas

a) β-Alquilación de alcoholes secundarios con alcoholes primarios

Tradicionalmente, la β-alquilación de alcoholes secundarios se realizaba a través de procesos complicados, utilizando una gran cantidad de disolventes y de agentes alquilantes muy reactivos. Fujita y colaboradores[48] optimizaron las condiciones de esta reacción diseñando un proceso catalítico, asimilable a escala industrial, en el que los subproductos son mínimos, no nocivos y además se evita la necesidad de añadir a la reacción un aceptor de hidrógeno. Los catalizadores metálicos más empleados para este tipo de reacción son compuestos de 'Cp*Ir(III)'[49] y arenos de Ru(II).[50]

Teniendo en cuenta los ejemplos descritos por Fujita, evaluamos la actividad catalítica de los compuestos de Ru(II) en esta reacción. La reacción fue llevada a cabo en condiciones de máxima Economía Atómica, es decir, intentando que todos los materiales utilizados como reactivos se incorporen a los productos. Así, tal y como muestra el Esquema 6.11, se hizo reaccionar una mezcla equimolar de alcohol primario, alcohol secundario y una base (KOH), en presencia de 1 mol% de catalizador en tolueno a 110ºC.

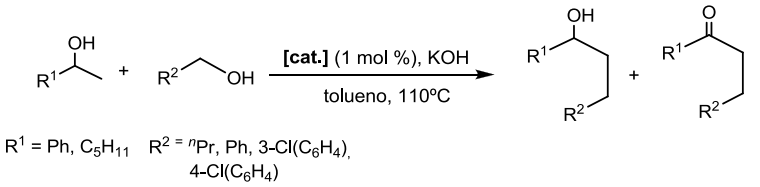

Esquema 6.11 β-Alquilación de alcoholes secundarios con alcoholes primarios

La reacción puede dar lugar a dos productos, al alcohol alquilado y/o la cetona alquilada. La reacción se llevó a cabo utilizando 2-feniletanol y 2-heptanol como alcoholes secundarios y cuatro alcoholes primarios diferentes (butanol, 3-clorobencilalcohol, bencilalcohol y 4-clorobencilalcohol), empleando los catalizadores **1A**, **7D**, **8E**, **9F** y **10F** (Esquema 6.12).

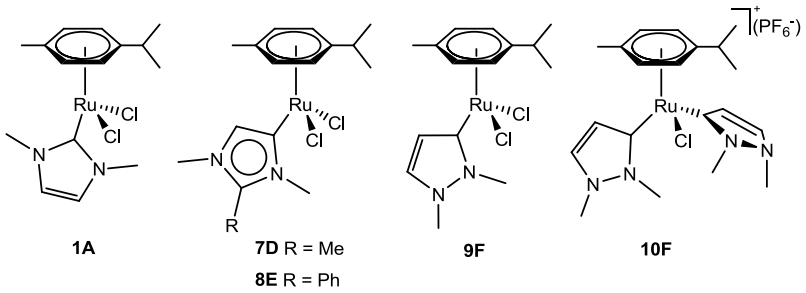

Esquema 6.12 Catalizadores empleados en la β-alquilación de alcoholes secundarios

Los resultados obtenidos nos permitieron concluir que el compuesto catiónico **10F** es el más activo, ya que facilita conversiones muy elevadas en tiempos de reacción cortos (8-10h, con una carga de catalizador de 1 mol %, a una temperatura de 110ºC). El compuesto **9F** también mostró elevada actividad con rendimientos superiores al

95% en tiempos muy similares (8-13h, en las mismas condiciones de reacción). Los complejos **7D** y **8E** proporcionaron conversiones altas, aunque empleando tiempos de reacción más largos. Entre estos dos últimos complejos, **7D** mostró actividades superiores en casi todos los casos. Por último, el complejo coordinado por la posición C2 (**1A**) fue el menos activo, proporcionando rendimientos moderados en tiempos de reacción largos (20-24h). Para la mayor parte de los sustratos estudiados, el proceso fue muy selectivo hacia la formación del alcohol alquilado, siendo la formación de la cetona muy minoritaria.

Los resultados catalíticos obtenidos sugieren que existe una relación entre la actividad catalítica y la capacidad dadora del ligando NHC. Así, observamos que aquellos ligandos más dadores-σ (*a*NHC y pirazolilidenos) confieren mayor actividad a los compuestos metálicos que forman. Estudios recientes han demostrado que los ligandos pirazolilidenos son menos dadores-σ que los imidazolilidenos coordinados de forma *abnormal*.[20] Sin embargo, aquellos complejos con ligandos pirazolilidenos (**9F** y **10F**) proporcionaron los mejores resultados catalíticos. Este comportamiento podría explicarse atendiendo a factores estéricos ya que en **9F** y **10F** el metal presenta una menor congestión estérica.

b) Oxidación y acoplamientos oxidativos

b.1) Oxidación de alcoholes y aminas

El hecho de que un catalizador sea efectivo en la oxidación de alcoholes o aminas puede ser un indicio de su actividad en reacciones que implican procesos de *borrowing-hydrogen* puesto que, como hemos comentado en la introducción de esta sección, la oxidación de estos sustratos es el primer paso en reacciones gobernadas por estos procesos.

Se estudió la actividad catalítica de los compuestos **11G**-**14G** y **3B** en la oxidación de alcoholes y aminas (Esquema 6.13). El catalizador **11G** fue el más activo en la reacción de oxidación de bencilalcohol para formar la correspondiente especie carbonilada.

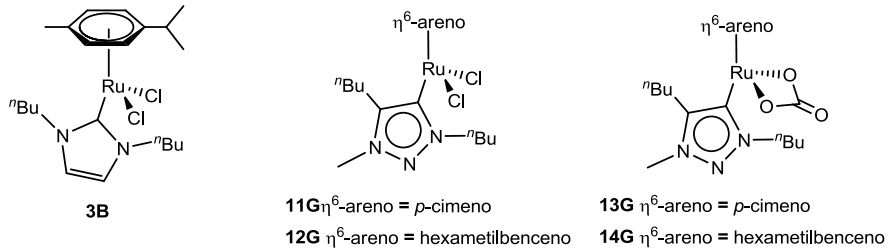

Esquema 6.13 Catalizadores empleados en la oxidación de alcoholes y aminas

Se obtuvieron rendimientos muy elevados al emplear otros alcoholes como 1-feniletanol o derivados de bencilalcohol. Estas reacciones se llevaron a cabo a reflujo de tolueno con un cantidad fija de catalizador (5 mol %), empleando hexametilbenceno como estándar interno (Esquema 6.14).

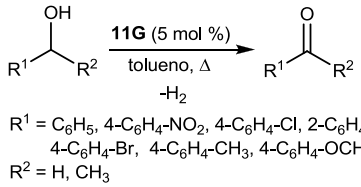

Esquema 6.14 Oxidación de alcoholes

La reacción de acoplamiento oxidativo de aminas para la obtención de iminas también es un método respetuoso con el medio ambiente ya que el único subproducto es amoniaco. En esta reacción, el catalizador **3B** fue el más activo. Como indica el Esquema 6.15, la reacción se llevó a cabo empleando varias aminas primarias, en tolueno y una cantidad fija de catalizador (5 mol %).

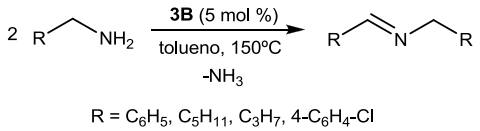

Esquema 6.15 Oxidación de aminas

b.2) Formación de amidas a partir de aminas y alcoholes

Las amidas son un grupo funcional muy importante en péptidos y en gran número de polímeros, así como en productos farmacéuticos y naturales.[51] Milstein y

colaboradores desarrollaron un catalizador de rutenio con un ligando *pinza* hemilábil muy efectivo en la formación de amidas. La reacción descrita por este grupo consiste en la acetilación directa de aminas primarias con una cantidad equimolar de alcohol para producir la amida e hidrógeno.[52] Tras el trabajo pionero de Milstein, varios grupos han descrito catalizadores tipo M-NHC efectivos en la misma reacción.[53]

El hecho de que nuestros catalizadores fueran activos en la deshidrogención oxidativa de alcoholes y aminas, nos hizo pensar que tal vez también lo serían en la formación de amidas. Como muestra el Esquema 6.16, la reacción se llevó a cabo en tolueno a 150ºC y con una cantidad fija de catalizador (5 mol %), en presencia de NaH.

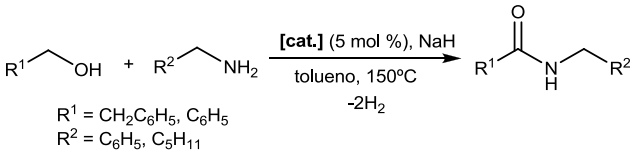

Esquema 6.16 Formación de amidas a partir de alcoholes y aminas

Entre los complejos elegidos para este estudio (**11G**, **12G** y **3B**), **3B** resultó el más activo. Los rendimientos alcanzados fueron en todos los casos superiores al 95%, empleando tiempos de reacción entre 15 y 20h.

Como hemos podido observar, el complejo **11G** que contiene un ligando triazolilideno presenta mayor actividad en la oxidación de alcoholes que su análogo que contiene un ligando imidazol-2-ilideno (**3B**), mientras que este comportamiento se invierte cuando se trata de la oxidación de aminas y de la formación de amidas.

c) Dimerizacion de fenilacetileno

Los compuestos metálicos **1A**, **7D**, **8E**, **9F**, y **10F**, junto al dímero metálico $[RuCl_2(p\text{-cimeno})]_2$, fueron empleados en la reacción de dimerización de fenilacetileno. Entre los posibles productos de esta reacción se encuentran los productos de dimerización (**a** y **b**), aunque también pueden observarse los productos de ciclotrimerización (**c**). La

reacción se llevó a cabo con fenilacetileno y una cantidad fija de catalizador (5 mol %) en acetonitrilo-d_3 a 70ºC, en presencia de NEt_3 durante 8h (Esquema 6.17).

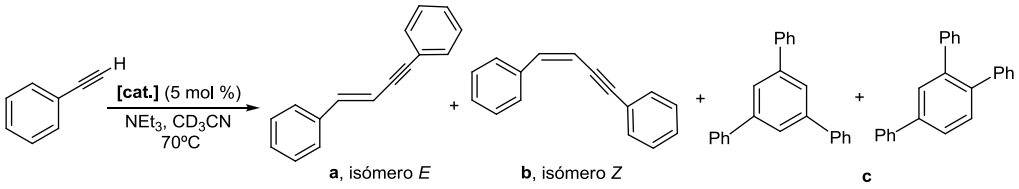

Esquema 6.17 Dimerización de fenilacetileno

Los resultados catalíticos indicaron que los catalizadores de Ru(II) que contienen ligandos NHC dan lugar a los productos de dimerización en un intervalo de rendimientos del 20-42%, con una selectividad moderada hacia el isómero *E*. La actividad catalítica de estos compuestos es comparable a la observada para otros compuestos de Ru(II) descritos en la bibliografía.[54] En cambio, al emplear $[RuCl_2(p\text{-cimeno})]_2$ los únicos productos de reacción fueron los de ciclotrimerización. A la vista de estos resultados, podemos decir que la introducción de ligandos básicos NHC facilita parcialmente que se produzca la dimerización frente a la ciclotrimerización.

d) Arilación y deuteración de fenilpiridinas

d.1) Arilación de arilpiridinas

En los últimos años, se le ha dado un nuevo enfoque a la reacción de arilación de arenos que implica la arilación de arenos no funcionalizados con haluros de arilo, mediante la activación de un enlace C-H. En uno de los primeros ejemplos de formación catalítica de enlaces C-C a partir de una activación C-H, Murai demostró que la presencia de un heteroátomo en el sustrato podía funcionar como agente orientador de la selectividad del proceso.[55] A partir de este trabajo pionero, han sido numerosos los artículos que se han basado en esta idea simple para facilitar la activación selectiva de un gran número de sustratos.[35, 56] Con estos antecedentes en mente, nos propusimos evaluar la actividad de algunos de los compuestos de Ru(II) preparados en la arilación de N-heterociclos.

En primer lugar se estudió la actividad de los complejos **1A-2A**, **3B-5B** y **6C** (Esquema 6.18) junto a los dímeros $[RuCl_2(p\text{-cimeno})]_2$ y $[RuCl_2(CMe)_6]_2$ y un complejo de Ru(II) con un ligando fosfina, en la reacción de arilación de fenilpiridina empleando clorobenceno.

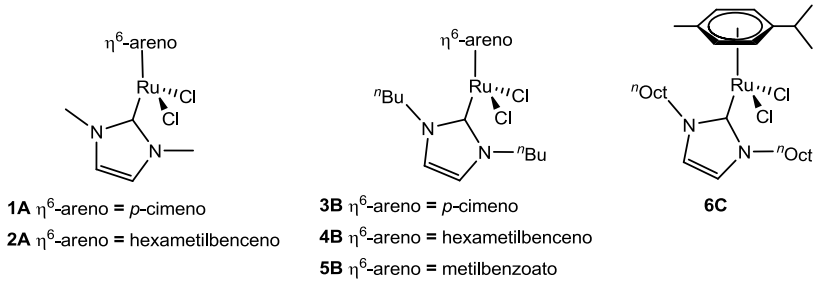

Esquema 6.18 Catalizadores empleados en la arilación de arilpiridinas

Una vez más, el estudio concluyó que el catalizador **3B** es el más activo en la reacción. Así, **3B** se utilizó como catalizador en la arilación de tres sustratos (2-fenilpiridina, benzo[*h*]quinolina y N-fenilpirazol) con diferentes agentes arilantes. El catalizador (5 mol %) se trató inicialmente con KOAc y la reacción se llevó a cabo en NMP a 120ºC en presencia de K_2CO_3 (Esquema 6.19).

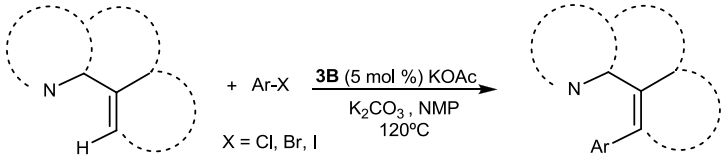

Esquema 6.19 Arilación de arilpiridinas

3B resultó muy eficaz en la arilación de las diferentes arilpiridinas. En particular, empleando clorobenceno los rendimientos fueron superiores al 90%.

d.2) Deuteración de arilpiridinas

El mecanismo de arilación de arilpiridinas implica la regioselectividad de la activación del enlace C-H. Con esto en mente, pensamos que el catalizador **3B** debía también ser activo en la deuteración de arilpiridinas en esta misma posición.

La reacción se llevó a cabo con seis arilpiridinas diferentes en presencia de MeOH-d_4 a 120ºC con una cantidad fija de catalizador (mol %). **3B** presentó una gran eficacia en todos los casos. Por ejemplo, en la deuteración de benzo[*h*]quinolina la conversión fue completa a las 5 horas. La Figura 6.3 muestra los espectros de ^{1}H RMN a tiempo inicial y transcurridas 5 horas. Como se puede apreciar, la señal correspondiente al protón de la posición C-10 desaparece casi por completo.

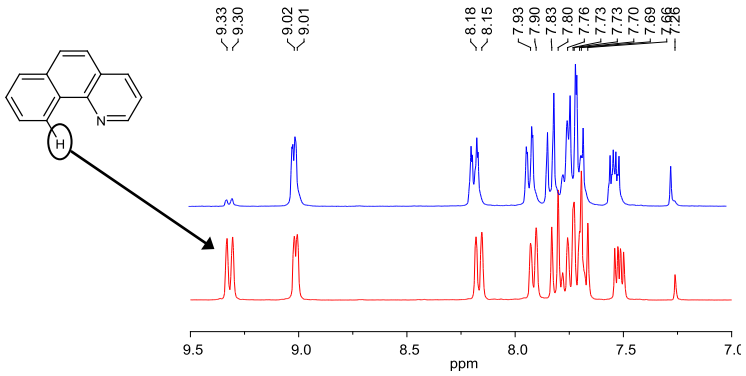

Figura 6.3 Espectro de ^{1}H RMN de la reacción de deuteración de benzo[*h*]quinolina a tiempo inicial (rojo) y después de 5h (azul)

La posibilidad de obtener moléculas orgánicas deuteradas selectivamente, nos permitió estudiar la velocidad de la reacción de arilación de arilpiridinas con diferente marcaje isotópico.

En este sentido, se monitorizó la reacción de arilación de benzo[*h*]quinolina y benzo[*h*]quinolina-*d* con clorobenceno empleando las mismas condiciones que las descritas en el apartado d.1) como muestra el Esquema 6.20.

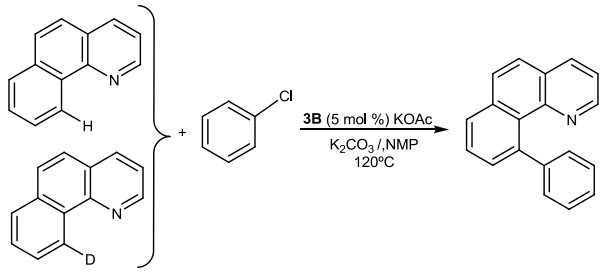

Esquema 6.20 Arilación de benzo[*h*]quinolina y benzo[*h*]quinolina-*d* con clorobenceno

La Figura 6.4 muestra la representación gráfica de la conversión hacia el producto de arilación de benzo[*h*]quinolina (azul) y de benzo[*h*]quinolina-*d* (rojo) frente al tiempo. De esta forma, se pudo calcular el efecto isotópico cinético (EIC=k_H/k_D).

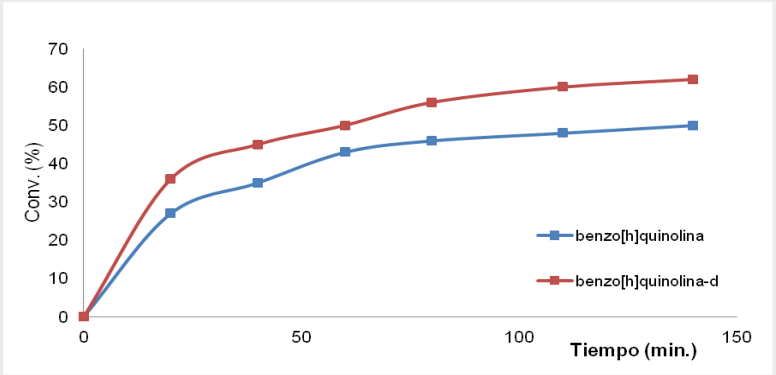

Figura 6.4 Monitorización de la reacción de arilación de benzo[*h*]quinolina y benzo[*h*]quinolina-*d* con clorobenceno.

Sorprendentemente, el valor del EIC es menor que uno (0.43), es decir, se trata de un efecto isotópico cinético inverso, el sustrato deuterado reacciona más rápido que el no deuterado. Esta observación indica que el paso limitante de la reacción no es la abstracción del protón del enlace C-H, lo que justificaría que la reacción de deuteración pueda tener lugar en ausencia de base.

6.3.2.2 Actividad catalítica de compuestos tipo 'IrCp*(NHC)'

Nos propusimos el estudio de la actividad catalítica de los compuestos tipo 'IrCp*(NHC)' en las siguientes reacciones:

Procesos tipo *borrowing-hydrogen*:

a) Acoplamiento cruzado de alcoholes y aminas

a.1) Eterificación de bencilalcohol con alcoholes primarios y secundarios

a.2) N-Alquilación de anilinas con aminas

a.3) N-Alquilación de aminas primarias con alcoholes

Otros procesos de activación C-H:

b) Funcionalización de arenos

c) Reacción tándem: Transferencia de hidrógeno y bencilación de arenos

a) Acoplamiento cruzado de alcoholes y aminas

Dependiendo de las condiciones de reacción empleadas, los compuestos tipo 'IrCp*(NHC)' descritos en esta Tesis son activos en la deshidrogenación de alcoholes para dar las correspondientes especies carboniladas, o en el auto-acoplamiento de alcoholes para formar éteres. Basándonos en estas dos observaciones y en nuestros estudios previos de transferencia de hidrógeno,[49, 57-58] pensamos que estos compuestos debían ser activos en reacciones de acoplamiento de alcoholes y aminas, en sus tres posibles combinaciones.

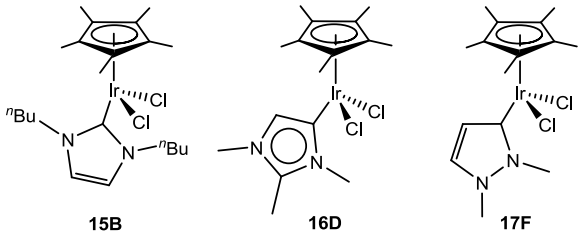

Esquema 6.21 Catalizadores de 'IrCp*(NHC)'

Con el objetivo de comparar la actividad de los compuestos de Ir(III) preparados (**15B**, **16D** y **17F**, Esquema 6.21) y del precursor $[IrCp^*Cl_2]_2$, se llevaron a cabo las reacciones de acoplamiento cruzado de alcoholes y aminas que muestra el Esquema 6.22. Todas las reacciones se llevaron a cabo en presencia de un pequeño exceso de AgOTf respecto al catalizador para formar *in situ* la especie catalíticamente activa.

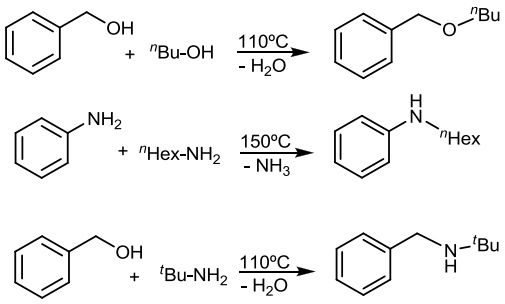

Esquema 6.22 Reacciones de acoplamiento cruzado de alcoholes y aminas

Los cuatro catalizadores resultaron muy activos en las tres reacciones, pero el catalizador **15B** fue el más activo en todos los casos. Cabe mencionar que el compuesto $[IrCp^*Cl_2]_2$ en presencia de AgOTf es activo en estas reacciones, aunque su actividad es notablemente menor que la mostrada por **15B**.

A la vista de estos resultados, se decidió ampliar el número de sustratos de las diferentes reacciones de acoplamiento cruzado de alcoholes y aminas utilizando el catalizador **15B**. En algunos casos, se comparó la actividad de **15B** con la del catalizador de Shvo (Figura 6.5), conocido por su actividad en numerosos procesos de tipo *borrowing-hydrogen*.[59, 60]

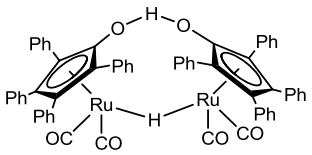

Figura 6.5 Catalizador de Shvo

a.1) Eterificación de bencilalcohol con alcoholes primarios y secundarios

El acoplamiento de bencilalcohol con alcoholes primarios y secundarios puede dar lugar a diferentes productos, tal y como muestra el Esquema 6.23. Las reacciones se llevaron a cabo con un exceso de alcohol primario o secundario utilizando 1 mol % de catalizador **15B**, en ausencia de disolvente y a diferentes temperaturas (110ºC y 130ºC).

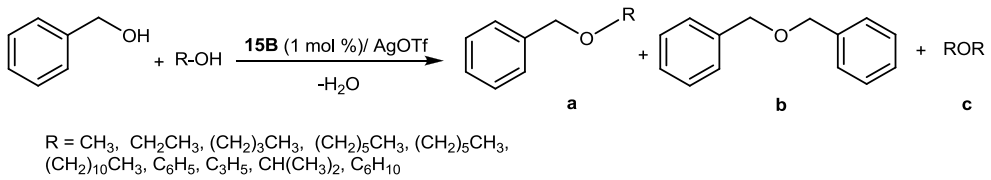

Esquema 6.23 Eterificación de bencilalcohol con alcoholes primarios y secundarios

El catalizador **15B**, en presencia de AgOTf, resultó ser más activo en esta reacción que compuestos metálicos recientemente publicados.[61, 62] En particular, al emplear **15B** se obtuvieron rendimientos más elevados hacia la formación del éter asimétrico que al utilizar el catalizador $[ReBr(CO)_5]$,[62] un resultado que es aún más destacable si se considera que las reacciones se llevaron a cabo a temperaturas más bajas en tiempos de reacción más cortos. Cabe destacar que en todos los casos el producto mayoritario fue el de acoplamiento cruzado.

a.2) N-Alquilación de anilinas con aminas alifáticas

Las reacciones se llevaron a cabo con un exceso de amina aromática respecto a la amina alifática empleando un 5 mol % de **15B** en tolueno-d_8 y a 150ºC (Esquema 6.24). **15B** resultó ser un catalizador muy activo en la N-alquilación de anilinas con una gran variedad de aminas alifáticas.

Se decidió realizar estos mismos ensayos catalíticos empleando el catalizador de Shvo, ya que Beller y colaboradores habían demostrado su elevada actividad en este tipo de reacciones.[59] Las conversiones conseguidas por el catalizador de Shvo fueron muy similares a las alcanzadas por el catalizador **15B** en las mismas condiciones.

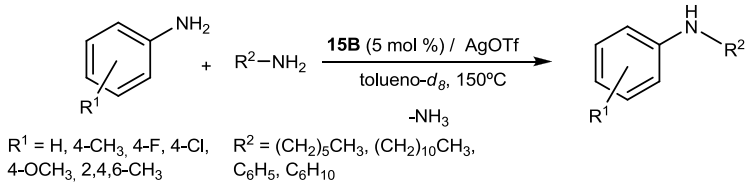

Esquema 6.24 N-Alquilación de anilinas con aminas alifáticas

a.3) N-Alquilación de aminas primarias con alcoholes primarios y secundarios

Finalmente, se estudió la N-alquilación de aminas primarias con alcoholes primarios y secundarios. Esta reacción puede dar lugar a la formación de aminas secundarias y/o terciarias (**a** y **b**, respectivamente en el Esquema 6.25). La reacción se llevó a cabo con un exceso de alcohol respecto a la amina, empleando un 5 mol % de catalizador en ausencia de disolvente a 110ºC (Esquema 6.25).

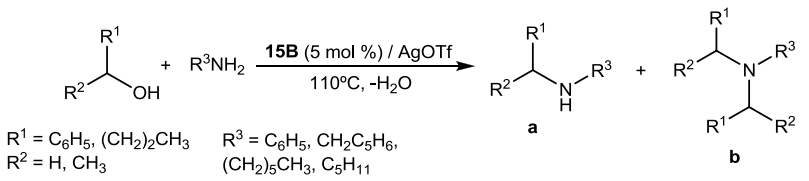

Esquema 6.25 N-Alquilación de aminas primarias con alcoholes primarios y secundarios

Las conversiones obtenidas fueron muy elevadas en todas las combinaciones de aminas y alcoholes. La selectividad hacia la amina secundaria (**a**) o terciaria (**b**) depende de los sustratos empleados. Cabe destacar que al emplear bencilalcohol y bencilamina como sustratos, observamos conversión completa hacia la amina terciaria, resultados que contrastan con los encontrados en la bibliografía. Los estudios catalíticos llevados a cabo por Fujita y colaboradores, empleando como catalizador el dímero de $[IrCp^*Cl_2]_2$, habían demostrado una conversión completa hacia la amina secundaria.[63] Al emplear el catalizador de Shvo, también se observó únicamente la formación de la amina secundaria.

Resumiendo, el catalizador **15B** presentó elevada actividad en diferentes reacciones de acoplamiento cruzado empleando como sustratos aminas y alcoholes, y sólo el catalizador de Shvo muestra una actividad similar. Las reacciones que hemos estudiado se han llevado a cabo en ausencia de base, fosfina, o cualquier otro aditivo, lo que no sólo simplifica el proceso de reacción sino que también proporciona una química más limpia.

b) Funcionalización de arenos

Los compuestos de 'IrCp*(NHC)' también demostraron elevada actividad catalítica en reacciones de funcionalización de arenos. Como en el apartado anterior (acoplamiento de alcoholes y aminas), fue necesario añadir un pequeño exceso de AgOTf para formar *in situ* la especie activa. Una vez más, el catalizador **15B** resultó ser el más activo, así que se decidió ampliar el número de sustratos para verificar su versatilidad catalítica.

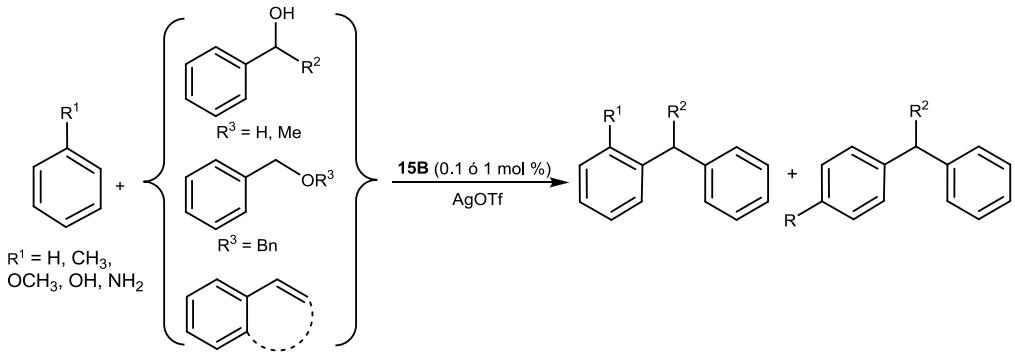

Esquema 6.26 Funcionalización de arenos empleando alcoholes, éteres y estirenos

Se emplearon diferentes agentes bencilantes (bencilalcohol, feniletanol, dibenciléter y derivados de estireno) y una amplia variedad de arenos. La reacciones se llevaron a cabo a 110ºC con 1 ó 0.1 mol % de catalizador respecto al agente bencilante y un gran exceso de areno (10 ó 5 equivalentes); de este modo, no hizo falta añadir disolvente (Esquema 6.26). **15B** resultó muy efectivo en la bencilación de arenos empleando los diferentes agentes bencilantes elegidos. Cabe destacar la diferencia de selectividades al utilizar uno u otro agente bencilante. Por ejemplo, en la bencilación de anisol empleando 1-feniletanol la selectividad hacia el producto bencilado en la posición *para* (*o*:*p* 10:90) es mayor que al emplear bencilalcohol (*o*:*p* 35:65). Este hecho puede ser debido al mayor impedimento estérico que provoca el sustrato 1-feniletanol, de forma que la formación del producto *para* está más favorecida.

c) Catálisis tándem: Transferencia de hidrógeno y bencilación de arenos

Aprovechando la extraordinaria versatilidad catalítica del compuesto **15B**, nos propusimos diseñar una reacción tándem en la que un catalizador estándar de Friedel-Crafts no sería activo. En este sentido, se llevó a cabo la reacción de bencilación de anisol empleando benzaldehído o acetofenona, en presencia de **15B** e *i*-PrOH (Esquema 6.27). En primer lugar, tendría lugar la reducción del grupo carbonilo empleando *i*-PrOH en condiciones de transferencia de hidrógeno, generando acetona y el alcohol correspondiente. En el segundo paso de la reacción, el alcohol generado actuaría como agente bencilante, dando lugar a los productos de bencilación *orto* y *para* (Esquema 6.27).

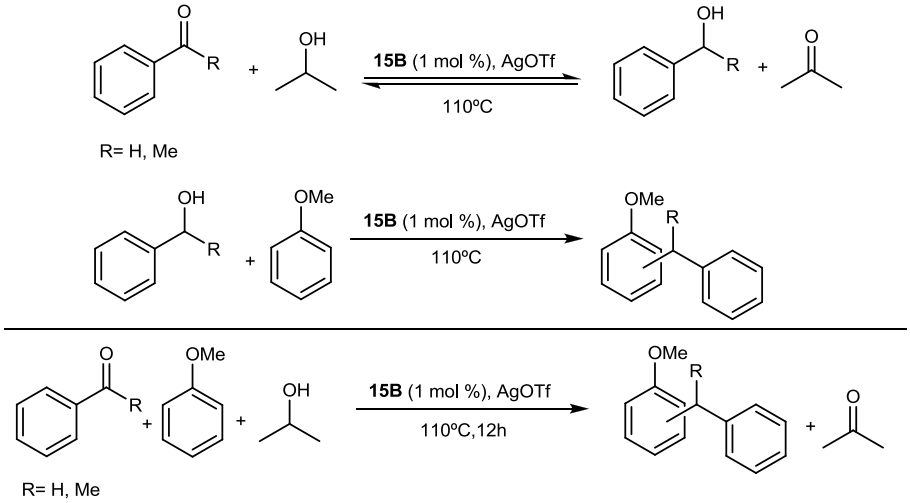

Esquema 6.27 Reacción tándem

El compuesto **15B** es capaz de catalizar ambas reacciones, dando lugar a los productos de bencilación de anisol de manera casi cuantitativa tras 12h de reacción. Cabe destacar que fueron suficientes 1.5 equivalentes de *i*-PrOH para promover la reducción del grupo carbonilo del aldehído o cetona. La irreversibilidad del segundo paso de la reacción hace que el *i*PrOH se consuma en el primer paso, en virtud del principio de Le Châtelier.

Así pues, aprovechando que **15B** es también un excelente catalizador de transferencia de hidrógeno,[58] se ha podido llevar a cabo una reacción tándem sin precedentes que permite extender el número de posibles agentes bencilantes a cetonas y aldehídos, aumentando, por tanto, el número de agentes capaces de producir la funcionalización de arenos.

En general, los ensayos catalíticos se siguieron por RMN de ^{1}H empleando en muchos casos un estándar interno como anisol o hexametilbenceno. El avance de la reacción se evaluó comparando las señales correspondientes a los sustratos iniciales con las señales correspondientes a los productos. En el caso de la arilación de arilpiridinas, la reacción se monitorizó por cromatografía de gases empleando también un estándar interno. Se cogieron alícuotas a diferentes tiempos de reacción, observando cómo las señales de los sustratos desaparecen en el espectro de GC y las nuevas señales de los productos aparecen.

6.3.3 Síntesis de compuestos de Rh(I) e Ir(I) con ligandos bis-NHC

Durante esta Tesis Doctoral, además de interesarnos por la síntesis y reactividad de compuestos que contienen ligandos monocarbeno, también hemos centrado nuestro interés en la síntesis de compuestos que contienen ligandos biscarbeno. Los ligandos bis-NHC que hemos diseñado van a actuar como puente entre dos centros metálicos dando lugar a compuestos bimetálicos que se orientan de manera facialmente opuesta.

Con el fin de sintetizar compuestos bimetálicos con nuevas topologías, hemos empleado dos formas de coordinación diferentes. La primera de ellas implica la doble activación C-H del grupo $C(sp^3)$-H_2 de una bis-imidazolidina, una alternativa al uso de sales de azolio. La segunda familia de compuestos se obtuvo a partir una sal de bis-imidazolio preparada a partir de un imino-piraceno descrito en la bibliografía.

6.3.3.1 Obtención de complejos con ligandos NHC mediante la doble activación C-H del grupo $C(sp^3)$-H_2 de N-heterociclos neutros

En la bibliografía podemos encontrar un único ejemplo en el que se sintetizan complejos tipo M-NHC por activación C-H del grupo Csp^3-H_2 de N-heterociclos neutros.[64] Con el fin de evaluar si este método era general para la obtención de complejos con ligandos NHC, se hizo reaccionar la imidazolidina **H**H2 con diferentes precursores metálicos de Rh e Ir. La reacción se llevó a cabo a reflujo de acetonitrilo durante 12h (Esquema 6.28). Los compuestos obtenidos se purificaron mediante cromatografía de columna. Observamos que fue necesaria la adición de un exceso de diolefina para obtener rendimientos superiores al 50%. Este hecho se debe a que el 1,5-ciclootadieno (para **18H** y **19H**) y el 2,5-norbornadieno (para **20H**) están actuando como aceptores de una molécula de H_2. El análisis mediante cromatografía de gases de los productos de reacción confirmó la presencia de cicloocteno y norborneno, respectivamente, además las cantidades observadas de mono-olefinas están en concordancia con los rendimientos obtenidos.

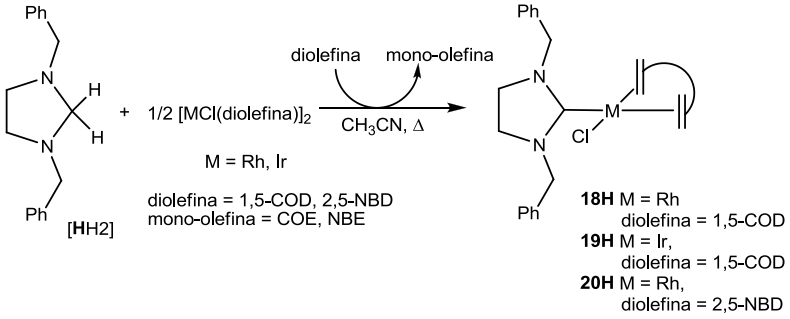

Esquema 6.28 Síntesis de **18H**, **19H** y **20H**

Teniendo en cuenta estos resultados, pensamos que esta nueva metodología podría ser adecuada para la obtención de complejos con ligandos NHC cuyas sales de imidazolio precursoras no sean accesibles. Así, llevamos a cabo la reacción de la bis-imidazolidina **IH4** con los precursores $[MCl(diolefina)]_2$ (M = Ir, Rh; diolefina = COD, NBD) en idénticas condiciones a las indicadas previamente. Como se observa en el Esquema 6.29, se obtuvieron las correspondientes especies monometaladas **21I-**

23I. Cuando la reacción se llevó a cabo a reflujo de tolueno y añadiendo un equivalente de $[IrCl(COD)]_2$, fue posible obtener el compuesto dimetálico de Ir(I) **24I**. El complejo dimetálico **24I** también pudo obtenerse a partir del monometálico **22I**, tal y como muestra el Esquema 6.29.

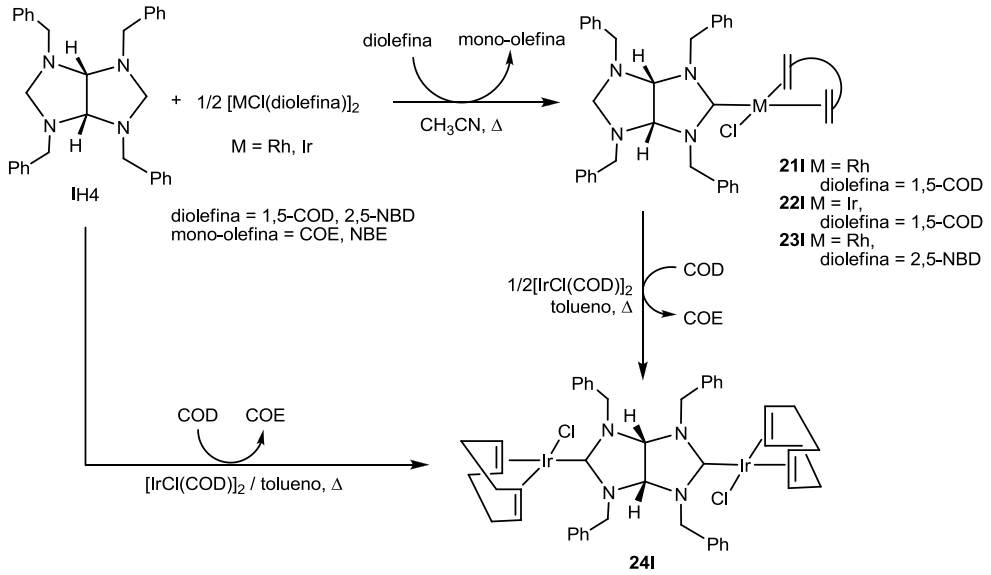

Esquema 6.29 Síntesis de **21I-24I**

Los derivados de carbonilo de los complejos **21I**, **22I** y **24I** fueron obtenidos de manera sencilla haciendo pasar una corriente de CO sobre una disolución del compuesto en diclorometano, como muestran el Esquema 6.30 y el Esquema 6.31.

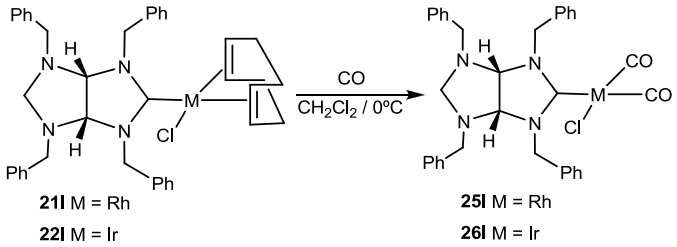

Esquema 6.30 Síntesis de **25I** y **26I**

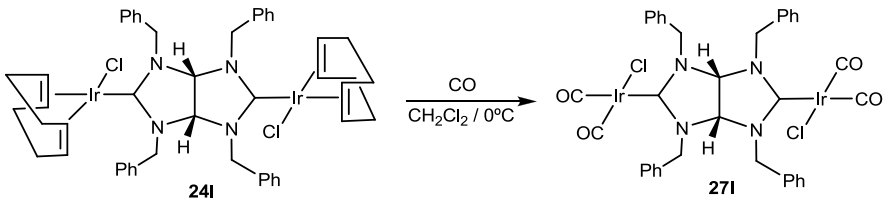

Esquema 6.31 Síntesis de **27I**

Las frecuencias de vibración de los ligandos CO en el espectro de IR para los compuestos **25I** y **26I** aparecieron a 2077 y 1995 cm^{-1} y a 2063 y 1978 cm^{-1}, respectivamente. Estos valores son próximos a los descritos en la literatura para compuestos de Rh(I)[65] e Ir(I)[66] con ligandos monocarbenos tipo imidazol-2-ilideno e imidazolin-2-ilideno. Los valores observados para el compuesto bimetálico **27I** (2071 y 1986 cm^{-1}) indican que la doble coordinación del ligando disminuye la capacidad dadora-σ del carbeno respecto al compuesto de Ir monocoordinado.

Resumiendo, se han sintetizado una serie de compuestos a partir de biciclos neutros por la doble activación C-H de un grupo $C(sp^3)H_2$. Las reacciones fueron llevadas a cabo en presencia de diolefinas que actúan como aceptores de hidrógeno. Este método permitió la obtención de nuevos compuestos metálicos con arquitecturas sofisticadas.

6.3.3.2 Síntesis de nuevos complejos bis-NHC a partir de sales de bis-imidazolio

Con la finalidad de aumentar el número de ligandos bis-NHC que puedan actuar como puente entre dos centros metálicos, pensamos que el ligando tetraquis(imino)piraceno (TIP, Esquema 6.32) podría ser un buen precursor. El ligando TIP, descrito por Cowley y colaboradores, presenta un comportamiento redox muy interesante para el diseño de dispositivos electrónicos modulares y la comprensión de procesos bioquímicos.[67]

La sal de bis-imidazolio [H**J**H]$(Cl)_2$ se obtuvo al hacer reaccionar el ligando TIP con cloro(metoxi)metano a 100ºC con un rendimiento del 65%. La reacción de [H**J**H]$(Cl)_2$ con $[MCl(COD)]_2$ (M = Rh, Ir) en tolueno a temperatura ambiente y en

presencia de *t*BuOK, dio lugar a los compuestos bimetálicos **31J** y **32J** (Esquema 6.32). Estos compuestos fueron purificados mediante cromatografía de columna.

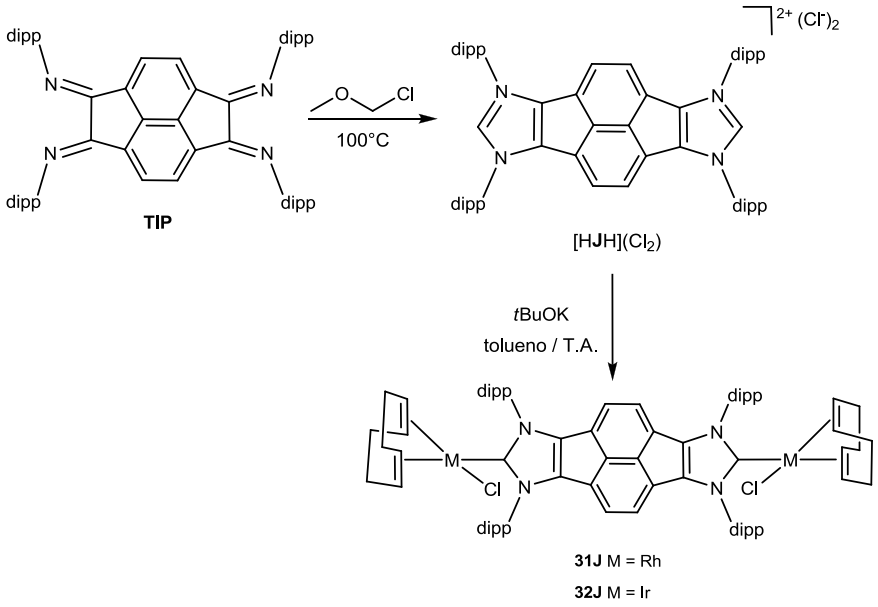

Esquema 6.32 Síntesis de [H**J**H](Cl_2), **31J** y **32J**

El derivado carbonilado de **32J** se obtuvo haciendo pasar una corriente de CO sobre una disolución de **32J** en diclorometano a 0ºC, tal y como muestra el Esquema 6.33.

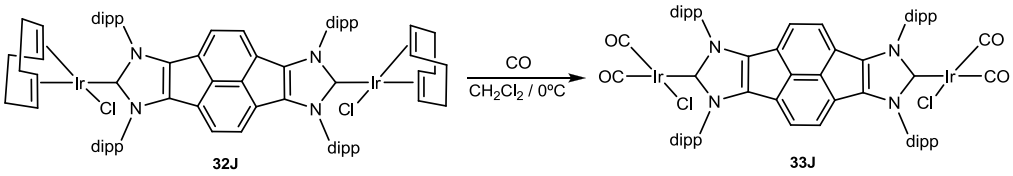

Esquema 6.33 Síntesis de **33J**

Las frecuencias de vibración de los ligandos CO en el espectro de IR para el compuesto **33J** aparecieron a 1968 y 2054 cm^{-1}. Estos valores son próximos a los descritos en la literatura para el compuesto de Ir(I) con el ligando monocarbeno IPr(BIAN) siendo BIAN el grupo bis(imino)acenafteno.[68]

Los nuevos compuestos metálicos de Rh(I) e Ir(I) descritos en esta sección han sido caracterizados por espectroscopia de RMN y masas y por análisis elemental. Las estructuras moleculares de los compuestos **22I**, **23I**, **24I** y **31J** han sido confirmadas mediante Difracción de Rayos X (DRX) sobre monocristal.

6.4 Conclusiones

Durante esta Tesis Doctoral se han obtenido una serie de complejos sencillos de 'Ru(η^6-areno)(NHC)' y de 'IrCp*(NHC), donde NHC se refiere a ligandos carbeno N-heterocíclico de tipo imidazolilideno *normal* y *abnormal*, pirazolilideno y triazolilideno.

Estos compuestos han sido utilizados en una gran variedad de reacciones catalíticas, permitiéndonos establecer bases razonables para estudiar la relación estructura-propiedades catalíticas de los sistemas utilizados. En general, hemos observado que los compuestos empleados presentan propiedades catalíticas extraordinarias, en comparación con otros catalizadores tradicionales utilizados para las mismas transformaciones. Las reacciones seleccionadas para el estudio de la actividad de los complejos de Ru(II) e Ir(III) fueron, principalmente, reacciones gobernadas por procesos de *borrowing-hydrogen* y reacciones que implican la activación C-H de arilpiridinas y arenos.

En muchas de las reacciones estudiadas, los catalizadores **3B** y **15B** han presentado las mejores actividades. Estos dos complejos contienen un ligando 1,3-di-*n*-butilimidazol-2-ilideno.

Por último, se han sintetizado dos nuevas familias de complejos con ligandos NHC ditópicos. Se han empleado dos estrategias de metalación en la preparación de los compuestos con ligandos bis-NHC. En particular, una de estas estrategias es muy novedosa puesto que implica la doble activación C-H de un grupo $C(sp^3)H_2$.

La posibilidad de preparar complejos homo-dimetálicos sugiere que pronto podremos encontrar la vía para sintetizar especies hetero-dimetálicas. Por nuestra experiencia, estos complejos suelen ser potencialmente útiles para el diseño de nuevos procesos catalíticos tándem.

6.5 Referencias

(1) Poyatos, M.; Mata, J. A.; Peris, E. *Chem. Rev.* **2009**, *109*, 3677.

(2) Schuster, O.; Yang, L. R.; Raubenheimer, H. G.; Albrecht, M. *Chem. Rev.* **2009**, *109*, 3445; Kuhl, O. *Coord. Chem. Rev.* **2009**, *253*, 2481; de Fremont, P.; Marion, N.; Nolan, S. P. *Coord. Chem. Rev.* **2009**, *253*, 862.

(3) Grundemann, S.; Kovacevic, A.; Albrecht, M.; Faller, J. W.; Crabtree, R. H. *Chem. Commun.* **2001**, 2274.

(4) Kovacevic, A.; Grundemann, S.; Miecznikowski, J. R.; Clot, E.; Eisenstein, O.; Crabtree, R. H. *Chem. Commun.* **2002**, 2580; Appelhans, L. N.; Zuccaccia, D.; Kovacevic, A.; Chianese, A. R.; Miecznikowski, J. R.; Macchioni, A.; Clot, E.; Eisenstein, O.; Crabtree, R. H. *J. Am. Chem. Soc.* **2005**, *127*, 16299; Baya, M.; Eguillor, B.; Esteruelas, M. A.; Olivan, M.; Onate, E. *Organometallics* **2007**, *26*, 6556.

(5) Grundemann, S.; Kovacevic, A.; Albrecht, M.; Faller, J. W.; Crabtree, R. H. *J. Am. Chem. Soc.* **2002**, *124*, 10473; Eguillor, B.; Esteruelas, M. A.; Olivan, M.; Puerta, M. *Organometallics* **2008**, *27*, 445; Cavallo, L.; Correa, A.; Costabile, C.; Jacobsen, H. *J. Organomet. Chem.* **2005**, *690*, 5407.

(6) Kovacevic, A.; Meadows, K. R.; Counts, M.; Arthur, D. J. *Inorg. Chim. Acta* **2011**, *373*, 259.

(7) Arnold, P. L.; Pearson, S. *Coord. Chem. Rev.* **2007**, *251*, 596; Kruger, A.; Albrecht, M. *Aust. J. Chem.* **2011**, *64*, 1113; Poulain, A.; Iglesias, M.; Albrecht, M. *Curr. Org. Chem.* **2011**, *15*, 3325; Krueger, A.; Albrecht, M. *Aust. J. Chem.* **2011**, *64*, 1113.

(8) Chianese, A. R.; Kovacevic, A.; Zeglis, B. M.; Faller, J. W.; Crabtree, R. H. *Organometallics* **2004**, *23*, 2461; Song, G. Y.; Zhang, Y.; Li, X. W. *Organometallics* **2008**, *27*, 1936; Leuthausser, S.; Schwarz, D.; Plenio, H. *Chem.-Eur. J.* **2007**, *13*, 7195; Kelly, R. A.; Clavier, H.; Giudice, S.; Scott, N. M.; Stevens, E. D.; Bordner, J.; Samardjiev, I.; Hoff, C. D.; Cavallo, L.; Nolan, S. P. *Organometallics* **2008**, *27*, 202.

(9) Tafipolsky, M.; Scherer, W.; Ofele, K.; Artus, G.; Pedersen, B.; Herrmann, W. A.; McGrady, G. S. *J. Am. Chem. Soc.* **2002**, *124*, 5865.

(10) Ofele, K.; Roos, E.; Herberhold, M. *Z.Naturforsch.(B)* **1976**, *31*, 1070.

(11) Kocher, C.; Herrmann, W. A. *J. Organomet. Chem.* **1997**, *532*, 261.

(12) Herrmann, W. A.; Schutz, J.; Frey, G. D.; Herdtweck, E. *Organometallics* **2006**, *25*, 2437.

(13) Han, Y.; Huynh, H. V.; Tan, G. K. *Organometallics* **2007**, *26*, 6581; Han, Y.; Huynh, H. V. *Chem. Commun.* **2007**, 1089.

(14) Raubenheimer, H. G.; Desmet, M.; Lindeque, L. *J. Chem. Res.-S* **1995**, 184.

(15) Raubenheimer, H. G.; Desmet, M.; Olivier, P.; Kruger, G. J. *J. Chem. Soc.-Dalton Trans.* **1996**, 4431.

(16) Kessler, F.; Szesni, N.; Maass, C.; Hohberger, C.; Weibert, B.; Fischer, H. *J. Organomet. Chem.* **2007**, *692*, 3005.

(17) Guisado-Barrios, G.; Bouffard, J.; Donnadieu, B.; Bertrand, G. *Angew. Chem. Int. Ed.* **2010**, *49*, 4759.

(18) Mathew, P.; Neels, A.; Albrecht, M. *J. Am. Chem. Soc.* **2008**, *130*, 13534.

(19) Poulain, A.; Canseco-Gonzalez, D.; Hynes-Roche, R.; Muller-Bunz, H.; Schuster, O.; Stoeckli-Evans, H.; Neels, A.; Albrecht, M. *Organometallics* **2011**, *30*, 1021.

(20) Gusev, D. G. *Organometallics* **2009**, *28*, 6458.

(21) Mata, J. A.; Poyatos, M.; Peris, E. *Coord. Chem. Rev.* **2007**, *251*, 841.

(22) Pugh, D.; Danopoulos, A. A. *Coord. Chem. Rev.* **2007**, *251*, 610.

(23) Peris, E.; Crabtree, R. H. *Coord. Chem. Rev.* **2004**, *248*, 2239.

(24) Herrmann, W. A.; Elison, M.; Fischer, J.; Kocher, C.; Artus, G. R. J. *Chem.-Eur. J.* **1996**, *2*, 772.

(25) Simons, R. S.; Custer, P.; Tessier, C. A.; Youngs, W. J. *Organometallics* **2003**, *22*, 1979; Chiu, P. L.; Chen, C. Y.; Zeng, J. Y.; Lu, C. Y.; Lee, H. M. *J. Organomet. Chem.* **2005**, *690*, 1682; Wang, X.; Liu, S.; Weng, L.-H.; Jin, G.-X. *Chemistry* **2007**, *13*, 188; Mercs, L.; Neels, A.; Stoeckli-Evans, H.; Albrecht, M. *Inorg. Chem.* **2011**, *50*, 8188; Su, G.; Huo, X. K.; Jin, G. X. *J. Organomet. Chem.* **2011**, *696*, 533.

(26) Williams, K. A.; Boydston, A. J.; Bielawski, C. W. *Chem. Soc. Rev.* **2007**, *36*, 729.

(27) Boydston, A. J.; Williams, K. A.; Bielawski, C. W. *J. Am. Chem. Soc.* **2005**, *127*, 12496; Khramov, D. M.; Boydston, A. J.; Bielawski, C. W. *Angew. Chem. Int. Ed.* **2006**, *45*, 6186; Boydston, A. J.; Rice, J. D.; Sanderson, M. D.; Dykhno, O. L.; Bielawski, C. W. *Organometallics* **2006**, *25*, 6087; Boydston, A. J.; Bielawski, C. W. *Dalton Trans.* **2006**, 4073.

(28) Guerret, O.; Sole, S.; Gornitzka, H.; Teichert, M.; Trinquier, G.; Bertrand, G. *J. Am. Chem. Soc.* **1997**, *119*, 6668.

(29) Mas-Marza, E.; Mata, J. A.; Peris, E. *Angew. Chem. Int. Ed.* **2007**, *46*, 3729; Zanardi, A.; Corberan, R.; Mata, J. A.; Peris, E. *Organometallics* **2008**, *27*, 3570.

(30) Zanardi, A.; Mata, J. A.; Peris, E. *Organometallics* **2009**, *28*, 4335.

(31) Zanardi, A.; Mata, J. A.; Peris, E. *J. Am. Chem. Soc.* **2009**, *131*, 14531; Zanardi, A.; Mata, J. A.; Peris, E. *Chem. Eur. J.* **2010**, *16*, 13109 ; Zanardi, A.; Mata, J. A.; Peris, E. *Chem.-Eur. J.* **2010**, *16*, 10502.

(32) Corberan, R.; Mas-Marza, E.; Peris, E. *Eur. J. Inorg. Chem.* **2009**, 1700; Normand, A. T.; Cavell, K. J. *Eur. J. Inorg. Chem.* **2008**, 2781; Diez-Gonzalez, S.; Marion, N.; Nolan, S. P. *Chem. Rev.* **2009**, *109*, 3612; Mata, J. A.; Poyatos, M. *Curr. Org. Chem.* **2011**, *15*, 3309.

(33) Bourissou, D.; Guerret, O.; Gabbai, F. P.; Bertrand, G. *Chem. Rev.* **2000**, *100*, 39; Dragutan, V.; Dragutan, I.; Delaude, L.; Demonceau, A. *Coord. Chem. Rev.* **2007**, *251*, 765.

(34) Hamid, M.; Slatford, P. A.; Williams, J. M. J. *Adv. Synth. Catal.* **2007**, *349*, 1555; Guillena, G.; Ramon, D. J.; Yus, M. *Angew. Chem. Int. Ed.* **2007**, *46*, 2358; Guillena, G.; Ramon, D. J.; Yus, M. *Chem. Rev.* **2010**, *110*, 1611.

(35) Dobereiner, G. E.; Crabtree, R. H. *Chem. Rev.* **2010**, *110*, 681.

(36) Alberico, D.; Scott, M. E.; Lautens, M. *Chem. Rev.* **2007**, *107*, 174; Seregin, I. V.; Gevorgyan, V. *Chem. Soc. Rev.* **2007**, *36*, 1173; Giri, R.; Shi, B. F.; Engle, K. M.; Maugel, N.; Yu, J. Q. *Chem. Soc. Rev.* **2009**, *38*, 3242; Ackermann, L.; Novak, P. *Org. Lett.* **2009**, *11*, 4966; Lyons, T. W.; Sanford, M. S. *Chem. Rev.* **2010**, *110*, 1147.

(37) Sun, H. B.; Li, B.; Chen, S.; Li, J.; Hua, R. *Tetrahedron* **2007**, *63*, 10185; Podder, S.; Choudhury, J.; Roy, S. *J. Org. Chem.* **2007**, *72*, 3129.

(38) Mertins, K.; Lovel, I.; Kischel, J.; Zapf, A.; Beller, M. *Adv. Synth. Catal.* **2006**, *348*, 691; Mertins, K.; Iovel, I.; Kischel, J.; Zapf, A.; Beller, M. *Angew. Chem. Int. Ed.* **2005**, *44*, 238; Iovel, I.; Mertins, K.; Kischel, J.; Zapf, A.; Beller, M. *Angew. Chem. Int. Ed.* **2005**, *44*, 3913.

(39) Rueping, M.; Nachtsheim, B. J.; Scheidt, T. *Org. Lett.* **2006**, *8*, 3717.

(40) Daugulis, O.; Zaitsev, V. G. *Angew. Chem. Int. Ed.* **2005**, *44*, 4046; Ackermann, L.; Althammer, A.; Fenner, S. *Angew. Chem. Int. Ed.* **2009**, *48*, 201.

(41) Herrmann, W. A.; Kocher, C.; Goossen, L. J.; Artus, G. R. J. *Chem.-Eur. J.* **1996**, *2*, 1627.

(42) Sala, A.; Ferrario, F.; Rizzi, E.; Catinella, S.; Traldi, P. *Rapid Commun. Mass Spectrom.* **1992**, *6*, 388.

(43) Ricciardi, F.; Romanchick, W. A.; Joullie, M. M. *J. Polym. Sci. Pol. Chem.* **1983**, *21*, 1475.

(44) Fuerstner, A.; Alcarazo, M.; Krause, H.; Lehmann, C. W. *J. Am. Chem. Soc.* **2007**, *129*, 12676.

(45) Mercs, L.; Neels, A.; Albrecht, M. *Dalton Trans.* **2008**, 5570.

(46) Corberan, R.; Sanau, M.; Peris, E. *J. Am. Chem. Soc.* **2006**, *128*, 3974.

(47) Viciano, M.; Feliz, M.; Corberan, R.; Mata, J. A.; Clot, E.; Peris, E. *Organometallics* **2007**, *26*, 5304.

(48) Fujita, K.; Asai, C.; Yamaguchi, T.; Hanasaka, F.; Yamaguchi, R. *Org. Lett.* **2005**, *7*, 4017.

(49) da Costa, A. P.; Viciano, M.; Sanau, M.; Merino, S.; Tejeda, J.; Peris, E.; Royo, B. *Organometallics* **2008**, *27*, 1305.

(50) Viciano, M.; Sanau, M.; Peris, E. *Organometallics* **2007**, *26*, 6050.

(51) Cupido, T.; Tulla-Puche, J.; Spengler, J.; Albericio, F. *Curr. Op. Drug Discov. Devel.* **2007**, *10*, 768.

(52) Gunanathan, C.; Ben-David, Y.; Milstein, D. *Science* **2007**, *317*, 790.

(53) Nordstrom, L. U.; Vogt, H.; Madsen, R. *J. Am. Chem. Soc.* **2008**, *130*, 17672; Ghosh, S. C.; Muthaiah, S.; Zhang, Y.; Xu, X. Y.; Hong, S. H. *Adv. Synth. Catal.* **2009**, *351*, 2643; Zhang, Y.; Chen, C.; Ghosh, S. C.; Li, Y. X.; Hong, S. H. *Organometallics* **2010**, *29*, 1374; Ghosh, S. C.; Hong, S. H. *Eur. J. Org. Chem.* **2010**, 4266; Dam, J. H.; Osztrovszky, G.; Nordstrom, L. U.; Madsen, R. *Chem.-Eur. J.* **2010**, *16*, 6820.

(54) Bassetti, M.; Marini, S.; Diaz, J.; Gamasa, M. P.; Gimeno, J.; Rodriguez-Alvarez, Y.; Garcia-Granda, S. *Organometallics* **2002**, *21*, 4815; Bassetti, M.; Pasquini, C.; Raneri, A.; Rosato, D. *J. Org. Chem.* **2007**, *72*, 4558; Jenkins, H. A.; Klempner, M. J.; Prokopchuk, E. M.; Puddephatt, R. J. *Inorg. Chim. Acta* **2003**, *352*, 72.

(55) Kakiuchi, F.; Murai, S. *Acc. Chem. Res.* **2002**, *35*, 826.

(56) Benhamou, L.; Wolf, J.; Cesar, V.; Labande, A.; Poli, R.; Lugan, N.; Lavigne, G. *Organometallics* **2009**, *28*, 6981; Colby, D. A.; Bergman, R. G.; Ellman, J. A. *Chem. Rev.* **2010**, *110*, 624.

(57) Corberan, R.; Sanau, M.; Peris, E. *Organometallics* **2006**, *25*, 4002.

(58) Corberan, R.; Peris, E. *Organometallics* **2008**, *27*, 1954.

(59) Hollmann, D.; Bahn, S.; Tillack, A.; Beller, M. *Chem. Comm.* **2008**, 3199; Hollmann, D.; Bahn, S.; Tillack, A.; Beller, M. *Angew. Chem., Int. Ed.* **2007**, *46*, 8291.

(60) Hollmann, D.; Tillack, A.; Michalik, D.; Jackstell, R.; Beller, M. *Chem. Asian J.* **2007**, *2*, 403.

(61) Cuenca, A. B.; Mancha, G.; Asensio, G.; Medio-Simon, M. *Chem.Eur. J.* **2008**, *14*, 1518; Corma, A.; Renz, M. *Angew. Chem., Int. Ed.* **2007**, *46*, 298; Saburi, H.; Tanaka, S.; Kitamura, M. *Angew. Chem., Int. Ed.* **2005**, *44*, 1730.

(62) Liu, Y.; Hua, R. M.; Sun, H. B.; Qiu, X. Q. *Organometallics* **2005**, *24*, 2819.

(63) Fujita, K. I.; Enoki, Y.; Yamaguchi, R. *Tetrahedron* **2008**, *64*, 1943.

(64) Coalter, J. N.; Ferrando, G.; Caulton, K. G. *New J. Chem.* **2000**, *24*, 835; Ho, V. M.; Watson, L. A.; Huffman, J. C.; Caulton, K. G. *New J. Chem.* **2003**, *27*, 1446.

(65) Denk, K.; Sirsch, P.; Herrmann, W. A. *J. Organomet. Chem.* **2002**, *649*, 219.

(66) Chang, Y. H.; Fu, C. F.; Liu, Y. H.; Peng, S. M.; Chen, J. T.; Liu, S. T. *Dalton Trans.* **2009**, 861.

(67) Vasudevan, K. V.; Findlater, M.; Cowley, A. H. *Chem. Commun.* **2008**, 1918; Vasudevan, K. V.; Vargas-Baca, I.; Cowley, A. H. *Angew. Chem. Int. Ed.* **2009**, *48*, 8369; Vasudevan, K. V.; Cowley, A. H. *New J. Chem.* **2011**, *35*, 2043.

(68) Vasudevan, K. V.; Butorac, R. R.; Abernethy, C. D.; Cowley, A. H. *Dalton Trans.* **2010**, *39*, 7401.